UNIVERSITÀ DEGLI STUDI DI VERONA DIPARTIMENTO DI BIOTECNOLOGIE

DOTTORATO DI RICERCA IN BIOTECNOLOGIE

CICLO XXIX

Handling light safely: The function of higher plants antenna systems analyzed by reverse genetic

S.S.D. BIO/04 FISIOLOGIA VEGETALE

Coordinatore: Ch.mo Prof. Massimo Delledonne

Tutor: Prof. Luca Dall'Osto

Dottorando: Mauro Bressan

Summary

According to the forecasts of human population rise, climate global changes and arable lands availability, the actual world food production rates risk to be inadequate and therefore need to be increased. Strategies such as breeding to improve harvest index or boosting fertilizers and water usage is likely to be unsustainable. Model predictions suggest that key factor for improving crop productivity will be the increase in biomass yield. However, classical breeding strategies have targeted traits other than the rate of leaf photosynthesis, leading into no significant improvement in light-to-biomass conversion efficiency per unit ground area in the major crops, efficiency which indeed remains inherently low. Among the factors which contribute to this low photosynthetic rate in plants, is the management of light: in the natural environment, irradiance undergoes continuous, sharp fluctuations and easily becomes limiting or exceeds the capacity of plants to use it for assimilation. Plants have a number of mechanisms that switch off assimilation to prevent the deleterious effects of prolonged or repeated exposure to over-excitation, thus preserving plant fitness. However, safeguard of the system is paid in term of losses of CO_2 fixation. Recent evidence confirmed that optimization of these processes improves ability of plants to assimilate carbon over long time periods, thus opening the way to genetic manipulation of photoprotection mechanisms. Therefore, further advances in understanding the processes and the physiology of these mechanisms are urgent in the prospective of improving light use efficiency of crops.

In this thesis, I study the major photoprotective mechanisms active in the light-harvesting moieties of higher plants, at the molecular level.

Photosynthetic carbon dioxide assimilation underpins the survivor of life forms on Earth by providing O_2 and essential food and fuel. The primary step in this process is the conversion of sunlight into chemical energy, driven by multi-subunit, pigment-protein complexes of the chloroplast. Among them, Photosystem (PS) I and II mediate light harvesting and funnel excitation energy toward photochemical reactions. Both photosystems are surrounded by an antenna system which enhances both light-harvesting in limiting light and dissipation of excess excited states in saturating light. However, the two PSs have evolved different strategies in order to balance absorption *vs*. dissipation of sunlight within their antenna (LHC) systems. Despite recent advances in the comprehension of these mechanisms on a molecular level, knowledge is still limited.

This thesis

The aim of this thesis is to understand the molecular basis of the mechanisms regulating light harvesting and photoprotection in higher plants. Avoiding photoinhibition in the ever-changing environment has shaped different mechanisms regulating photosynthesis in PSI and PSII, aimed at preventing the formation of ^{3}Chl* and reactive oxygen species in excess light. These events occur in the antenna moieties of PSs, large and complex systems composed of several LHC subunits, which coordinate chlorophylls and carotenoids, and assemble with the core units to form megacomplexes. Identification of molecular basis for photoprotection is complex due to the high number of gene products involved: many hypothesis have been based on measurements *in vitro*, which however might not reflect *in vivo* phenomena. Therefore, to obtain a thorough understanding of the photoprotective response in higher plants, we applied a reverse genetic approach to the model plant *Arabidopsis thaliana*. We were able to obtain mutants having supercomplexes with reduced antenna size or altered chromophores composition. By combining all the obtained information we were able to provide a comprehensive picture of the light harvesting properties and of the dissipative dynamics in the entire PSII supercomplex. Further, we investigated, a peculiar spectroscopic features of PSI antenna, namely the red chlorophylls, and how modulation of these components affect *in vivo* the photosynthetic efficiency.

In **chapter 1**, we reviewed the current knowledge on biogenesis of light-harvesting complexes. LHC form an array of pigment-proteins embedded in the thylakoid membrane, which transfer light energy to the reaction center of photosystems. Evolution generated a wide group of antenna proteins, which optimized photosynthesis for the most different environmental conditions. In particular, we focused the review paper on LHC gene expression, import into chloroplast, targeting to the thylakoids, and regulation of both assembly into supercomplexes and turnover rate. The main function of LHCs is to harvest photon energy, and transfer excitation energy to the reaction center. In addition LHC catalyze photoprotective reactions by the dissipation of excess energy absorbed. The transcription of lhc genes is strongly regulates by the light. Thus mRNAs encoding antenna subunits undergo circadian rhythms with up-regulation in light-limiting conditions and repression under excess light condition. LHC proteins are synthesized on cytosol ribosomes, and include an N-terminal transit peptide for

addressing the protein to the chloroplast through TOC and TIC translocons machinery. LHC in the stroma is captured by cpSRP, which mediate targeting of the polypeptide into thylakoids. Turnover rate of antenna subunits is highly regulated under different environmental conditions. E.g. during photoacclimatory response to excess light, a strong decrease in the level of Lhc is detected. These changes are not coupled to any significant change of lhcb gene transcription, and were thus attributed to a post-transcriptional regulatory mechanism. However, despite major efforts in identifying the proteases involved in the degradation of the apoproteins, the regulatory details of this process remain obscure.

Large antenna systems favor energy supply in low light conditions such as dawn, sunset and shaded canopies, yet they cause excess excitation beyond the maximal capacity for photochemical reactions under excess light, leading to ROS production and photoinhibition. Within the photosynthetic machinery, PSII have been indicated as the primary target of photoinhibition. Land colonization exacerbated the inherent photosensitizer property of chlorophylls, since brought increased light intensity, O_2 concentration and favored the probability of rapid light changes within canopies. Avoiding photoinhibition in the ever-changing environment has likely shaped mechanisms that regulate PSII quantum efficiency preventing ROS production. These set of inducible mechanisms, collectively referred to as NPQ (Non-Photochemical Quenching), facilitate heat dissipation of the chlorophyll excited state energy. Under full sunlight, NPQ converts as much as 80% of absorbed photons into heat. Several evidence suggest that the site of quenching is located within the peripheral antenna system of the PSII, however knowledge on (i) the interacting partners of LHC, and (ii) the localization of the quenching site(s) within the antenna of PSII, is limited. Moreover, a number of different mechanisms have been proposed, e.g. energy transfer to a lutein quencher in trimers, formation of a zeaxanthin radical cation in monomers.

In **chapter 2** we studied the role of distinct members of the PSII peripheral antenna in triggering NPQ, by a reverse genetic approach. The PSII outer antenna is composed by the major, trimeric antenna LHCII and by the minor, monomeric antenna complexes CP24, CP26 and CP29. We have isolated and characterized an *Arabidopsis* mutant lacking all monomeric antennae of PSII, called *NoM*. Its NPQ induction rate was substantially slower than the wild type. Further, we introduced the *npq1, lut2* and

npq4 mutations, preventing, respectively, Zea and Lut synthesis or PSBS accumulation, and found that lack of monomeric antennae substantially changed the xanthophyll-dependence of the residual NPQ activity, implying the fast- and slow-activated components contributing to NPQ in wild type were catalyzed respectively by monomeric and trimeric components of the PSII antenna system. A carotenoid radical cation signal was detected in wild type, while lost in the mutant. Therefore, we concluded that NPQ is catalyzed by two independent mechanisms with the fastest activated response catalyzed within monomeric LHC proteins depending on the formation of radical cation. Trimeric LHCII was responsible for the slowly activated quenching component, which does not depend on lutein nor on charge transfer events, while zeaxanthin was essential.

In **chapter 3** we move to the PSI and investigated the differential roles of carotenes and xanthophylls in PSI photoprotection. Carotenes and xanthophylls, the two classes of carotenoids in plants, function as accessory pigments in photosynthesis. Moreover, they act as strong antioxidants, thus protecting photosynthetic membranes from photoxidation under excess light conditions. Indeed, carotenes and xanthophylls bound to photosynthetic complexes mediate (i) de-excitation of chlorophyll singlets, (ii) quenching of chlorophyll triplets and (iii) detoxification of ROS. PSI-LHCI coordinates β-Carotene in both the core complex and light-harvesting system (LHCI), while xanthophylls lutein and violaxanthin bind exclusively to antenna subunit, and under excess light zeaxanthin is accumulated upon de-epoxidation of violaxanthin. We functionally dissected the xanthophyll and carotene dependent photoprotection mechanism of PSI, to gain a deeper insights on the pigment-protein interactions which optimize PSI photoprotection capacity. Indeed, while PSII has been identified as the main target of photooxidative damage, PSI is considered to be less sensitive to photoinhibition and its photoprotection was less investigated. To this aim, we analyzed the Arabidopsis mutants *szl1*, with a carotene content lower than that of the wild type, and *npq1*, with suppressed zeaxanthin formation. When exposed to excess light, the szl1 genotype displayed PSI photoinhibition stronger than that of wild-type plants, while removing zeaxanthin had no such effect, suggesting that β-carotene is crucial in controlling chlorophyll triplet formation. Accordingly, fluorescence-detected magnetic resonance analysis showed an increase in the yield of chlorophyll triplets in β-carotene-depleted complexes, and a greater singlet oxygen release was measured in β-carotene depleted LHCI. We conclude that β-carotene molecules bound to the LHCI system elicits a protective response, consisting of a reduction in the yield of harmful triplet excited states, while accumulation of zeaxanthin plays a minor role in

restoring phototolerance. Former results suggested a crucial role of the interaction between LHCI and β-carotene in PSI photoprotection, thus we further studied the peripheral antenna system of PSI.

In vascular plant, the outer antenna of PSI is composed by four polypeptides (Lhca1-Lhca4). Within LHC superfamily, Lhcas display peculiar spectroscopic properties, including “red spectral forms” which originates from Chl with energies lower than P700, and whose biological role is still a matter of debate. However, the high degree of conservation of LHCI system within higher plants suggests a specific function in the acclimation to the natural environment. In **chapter 4** the LHCI system was studied by isolating an *Arabidopsis thaliana* mutant devoid of the whole LHCI system *(ΔLhca)*, and by characterizing its performance in photosynthesis and photoprotection. We found that PSI absorption cross-section was smaller in the mutant: as a consequence, the redox balance of the photosynthetic electron chain was affected, yielding into a more reduced PQ than the wild type. *ΔLhca* plants alleviate the imbalance in the excitation energy between PSI and PSII by greatly enhancing the formation of PSI-LHCII supercomplexes, however despite such a compensating response, the mutant was unable to restore a normal growth rate. Thus, we investigated whether LHCI and LHCII are functionally equivalent when bound to PSI, and found that the excitation energy transfer efficiency was not altered by the substitution of LHCI with LHCII in PSI complex. Rather, a significant reduction in the absorption cross-section was observed, likely because the LHCII trimer (42 Chls) cannot fully compensate for the missing LHCI (57 Chls).

We further analyzed the photosynthetic phenotype of *ΔLhca* plants while acclimating to different light regimes, as described in **chapter 5**. When exposed to constant, excess light, the mutant did not enhance photooxidation with respect to wild type plants. Instead, under fluctuating light conditions, in mutant plants both the growth rate and the redox balance were strongly impaired, to a level that the great enhancement of state II transition cannot entirely compensate. We conclude that the reduced photosynthetic yield of this genotype has a dual origin: (1) enhancement in PSI absorption cross-section, upon LHCII binding, can not compensate for the missing LHCI; moreover, (2) the overall range of wavelength absorbed by the PSI-LHCII complex is narrower than that provided by LHCI and its red chlorophylls. Since LHCII absorbs the same wavelengths when bound to PSI or PSII, the PSI antenna of *ΔLhca* is more “shaded” by the abundant PSII-LHCII antenna system. It means that a PSI

endowed with red-spectral forms plays a crucial role in optimizing the photosynthetic electron flow by outcompeting LHCII in harvesting far-red light.

Although *ΔLhca* plants compensate for LHCI depletion by enhancing LHCII binding to PSI, it turned out into a contrasting physiological *vs.* biochemical state transition phenotypes. Indeed, while LHCII binding to PSI was greatly increased as shown by biochemical measurements, chlorophyll fluorescence analysis suggested a reduced capacity for LHCII fluorescence quenching by PSI in the mutant. To elucidate the reasons for discrepancy, in **chapter 6** we further characterized state transition in *ΔLhca* plants. While STN7 kinase was found fully active in the mutant, both topology and lateral heterogeneity of thylakoids was affected by lack of LHCI, yielding into higher LHCII content in stromal membranes respect to the wild type, as revealed by electron microscopy and biochemical analysis. This affected the overall fluorescence yield of thylakoid domains already in state I and minimized changes in RT fluorescence yield when LHCII does connect to PSI reaction center. It comes that interpretation of chlorophyll fluorescence analysis of state transitions becomes problematic when applied to mutants whose thylakoid architecture is significantly modified respect to wild type.

Introduction

1.1 Oxygenic photosynthesis

In plants, green algae and cyanobacteria, oxygenic photosynthesis is the process which catalyzes the conversion of sunlight into chemical energy. Most of the Earth's living systems are powered by this process, which supplies the reducing equivalents necessary to fix carbon dioxide to organic molecules, creating biomass, food and fuel. Ultimately, this process determines the composition of our atmosphere and underpin the survival of all life on our planet. Photosynthesis is a redox reaction that uses water as an electron donor, and yields into carbon dioxide (CO_2) fixation to sugars and molecular oxygen (O_2) evolution as by-product. The overall equation of the photosynthetic reaction is the following:

$$nH_2O + nCO_2 + light \rightarrow (CH_2O)n + nO_2$$

Photosynthesis takes place in three stages, which include (1) light harvesting and excitation energy transfer, (2) electron-transfer reactions aimed to generate proton motive force, chemical energy (ATP) and reducing power(NADPH), and (3) use of ATP and NADPH to fuel synthesis of organic compounds from CO_2 by means of Calvin cycle reactions of carbon fixation (Figure 1).

The whole process can be separated into light and dark phases. This classification is based on the dependence of reactions from solar energy: the first strictly requires light, while the latter occurs also in the dark, as long as ATP and NADPH are available.

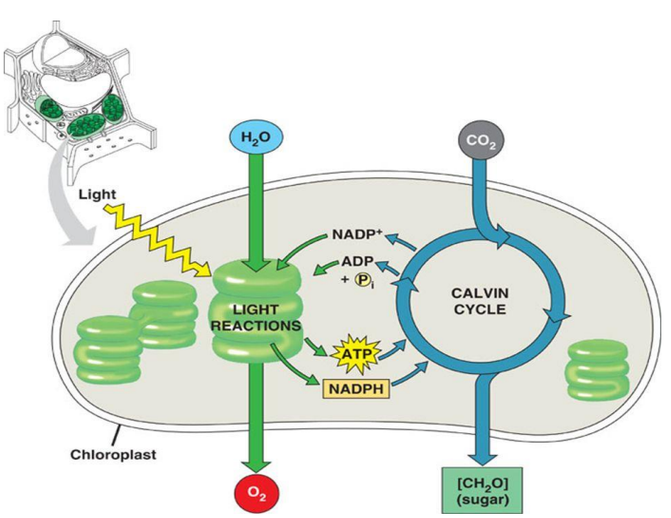

Figure 1.Schematic representation of light and dark phases in photosynthesis

In the light phase, photosynthetically active radiation (PAR) is absorbed and converted into chemical energy and reducing power , according to the equations:

$$ADP + Pi + energy \rightarrow ATP$$

$$2\ NADP^{+} + 2\ H_2O + light \rightarrow 2\ NADPH + O_2 + 2H^{+}$$

During the dark phase, both ATP and NADPH sustain CO_2 fixation into glyceraldehyde-3-phosphate (GAP), which is then used for the synthesis of a wide range of compounds of the cellular metabolism (Nelson and Ben-Shem, 2004). The process of the dark reactions is summarized by the following equation:

$$3CO_2 + 9ATP + 6NADH \rightarrow GAP + 9ADP + 8Pi + 6NADP^{+}$$

1.1.1 Chloroplast

In photosynthetic eukaryotes, reactions of both light and dark phases occur in organelles called chloroplasts. The chloroplast is surrounded by two membranes, together called *envelope*, which includes the outer membrane, highly permeable, and the inner membrane containing specific transporters for metabolites and protein transfer between cytoplasm and chloroplasts. The envelope membranes separate a compartment called stroma, which contains all the enzymes that catalyze the dark phase reactions. A third membranes system, the thylakoids, is found in the stroma and it defines another compartment, the *lumen* (Figure 2)

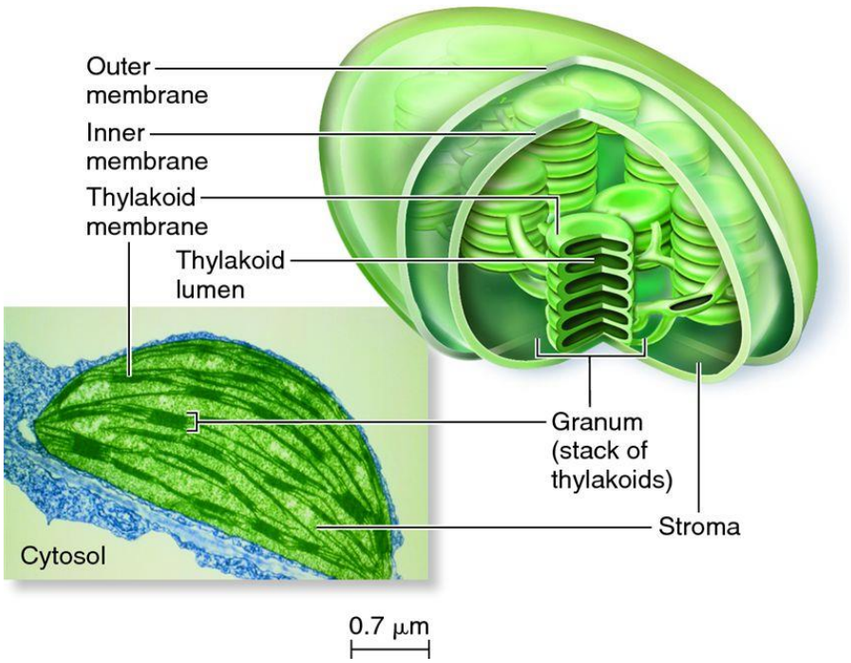

Figure 2. Transmission electron micrograph and schematic structure reconstruction of a chloroplast.

The thylakoid system consists of stacks of flat vescicles which form the *grana*, and long interconnecting stromal thylakoids which linked different grana, called *stroma lamellae* (Barber, 1980). In higher plants, there are about one hundred chloroplasts per cell, each including its own genome, transcriptional and translational machineries.

1.1.2 The light phase

Protein complexes which carry out the light reactions of photosynthesis are embedded into thylakoid membranes, and include Photosystem II (PSII) , Photosystem I (PSI), cytochrome b_6f complex (Cyt-b_6f) and ATP synthase (ATPase). These complexes are not evenly distributed throughout thylakoids: PSII resides mainly in grana membranes and is segregated from PSI, which is almost exclusively localized in the stroma lamellae; Cyt-b_6f is distributed in grana and grana margins, ATPase localizes predominantly in the stroma lamellae (Figure 3).

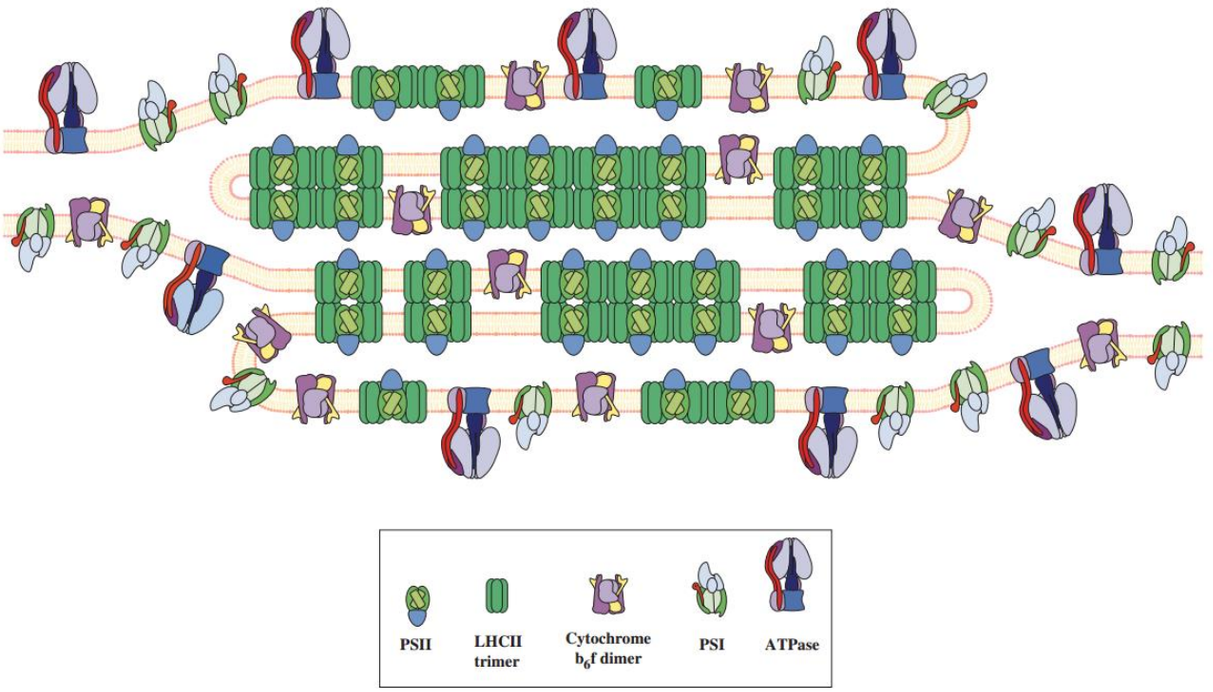

Figure 3. Lateral heterogeneity of protein complexes in thylakoid membranes of higher plants (Allen and Forsberg, 2001).

Each photosystem binds antenna pigments, namely chlorophylls (Chl) and carotenoids (Car), which absorb light and funnel the excitation energy to a reaction center (RC). The two photosystems (PS) work in series and use light energy to catalyze water oxidation and electron transfer to $NADP^+$; during the electron transport hydrogen ions are pumped into the thylakoid lumen, thus the redox energy is converted into a trans-thylakoid proton gradient. ATP synthase exploits such a proton motive force to generate ATP, thanks to the hydrogen ions that flow back out in the stroma (Figure 4).

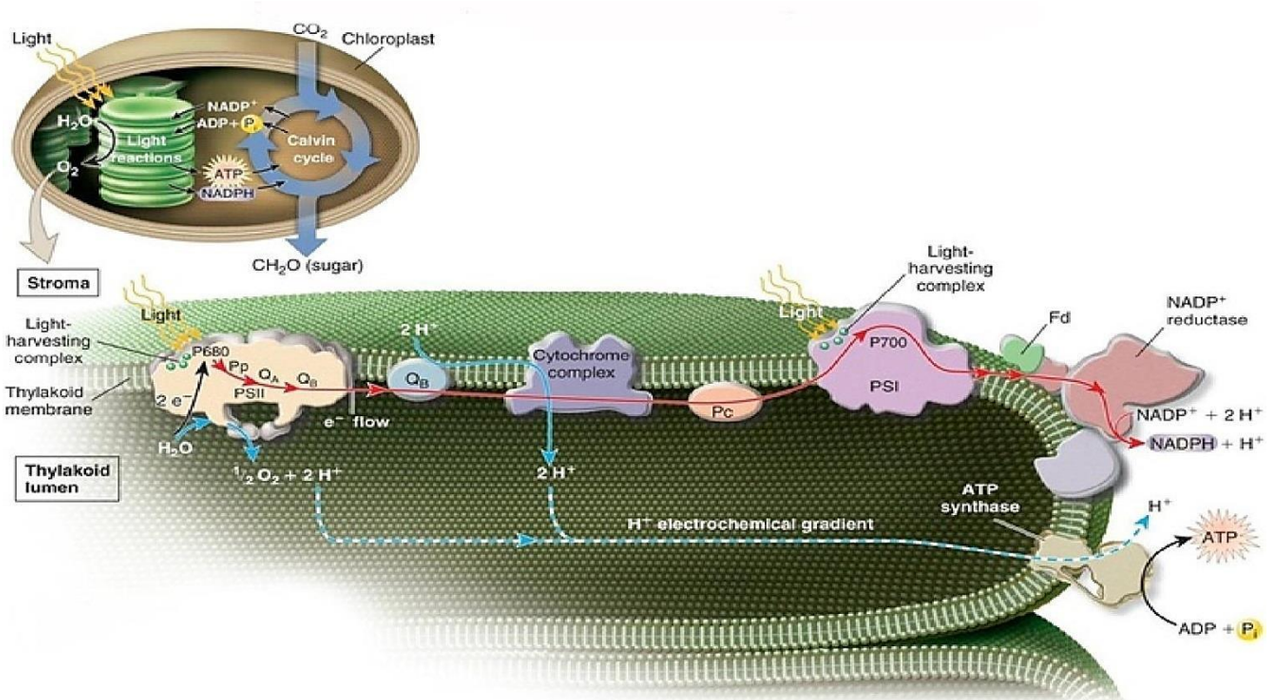

Figure 4. The light phase of photosynthesis. A schematic organization of the major protein complexes involved in light harvesting and electron transport in thylakoid membranes is shown. PSII, photosystem II; Cytochrome complex, Cytochrome b_6f; PSI, photosystem I; QB, plastoquinone/plastoquinol ;PC, plastocyanin; FD, ferredoxin.

Within each photosystem, hundreds of antenna pigments absorb light energy and then transmit it by inductive resonance from one chromophore to the next, finally to the RC through a mechanism called "Forster's transfer". The energy transfer requires that pigment molecules are in close contact with each other. This is an energetically down-hill reaction, and energy is thus preferentially transferred from chlorophyll *b* (λmax≈647 nm) to chlorophyll *a* (λmax≈663 nm). Energy that has been captured by the RC induces the simultaneous excitation of pairs of special Chl *a* molecules, the primary electron donor labeled as P680 (in PSII) and P700 (in PSI). It originates the translocation of an electron across the membrane through a series of cofactors (Figure 5).

The first chemical step happens within only a few picoseconds upon receiving the first energy quantum (Figure 5), then excited P680* loses an electron to pheophytin (Pheo), producing oxidized P680 ($P680^+$) and reduced Pheo ($Pheo^-$) in PSII, followed by electron transfer steps from Pheo to a plastoquinone (PQ) molecule at the Q_A-site. The missing electron on $P680^+$ is recovered, through the oxidation of a tyrosine residue also referred to as Yz.

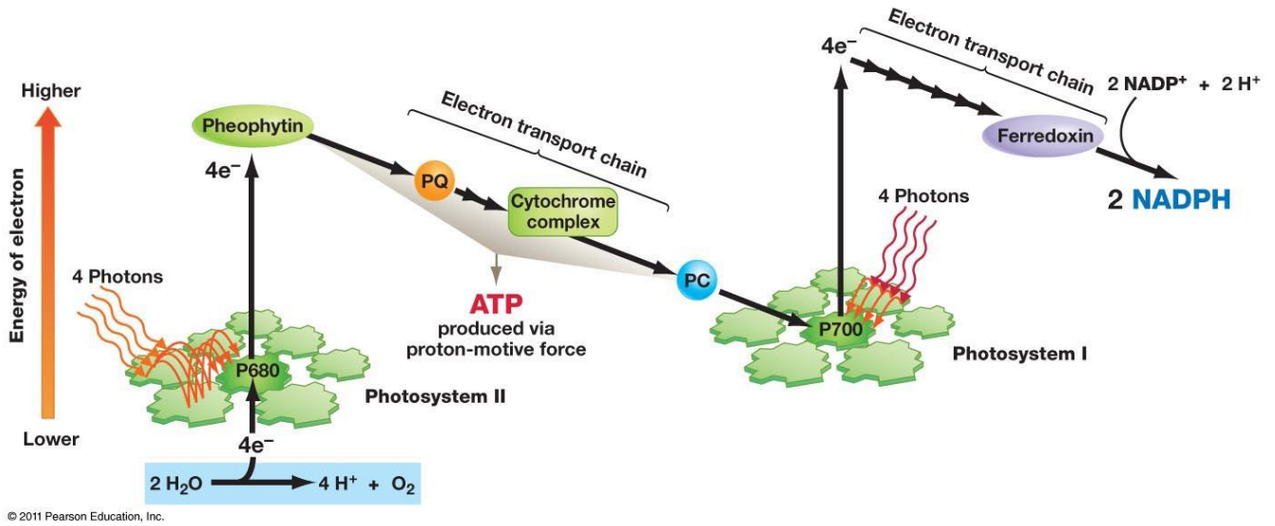

Figure 5. The two photosystems act in series, as described in the so called Z-scheme of Bendall and Hill. Cofactors involved in electron translocation between H_2O and $NADP^+$ are indicated.

Yz extracts an electron from a cluster of four manganese atoms (OEC, oxygen-evolving complex), which binds two substrate water molecules. Upon four consecutive events of charge separation of P680, the manganese cluster accumulates a total of four oxidizing equivalents, which are used to oxidize two water molecules leading to the formation of O_2, the release of protons in the inner thylakoid space and the return of manganese cluster to the reduced state. The electron on Q_A is then transferred to the PQ at the Q_B-site, which works as a two-electron acceptor and becomes fully reduced and protonated after two photochemical turnovers of the RC. The reduced plastoquinone (plastoquinol, PQH2) then unbinds from the PSII and diffuses in the hydrophobic core of the membrane, after which an oxidized PQ molecule finds its way to the Q_B-binding site and the process is repeated. Because the QB-site is near the outer aqueous phase, the protons added to PQ during its reduction are taken from the outside of the membrane, the stroma. Electrons are passed from PQH2 to a membrane-bound Cyt-b_6f, concomitant with the release of two protons to the luminal side of the membrane. The Cyt-b_6f then transfers one electron to a mobile carrier in the thylakoid lumen called plastocyanin (PC), which serves as electron donor to PSI RC P700. Upon photon absorption by PSI, a charge separation occurs with the electron transfer through a Chl and a bound quinone (Q_A) to a set of 4Fe-4S clusters. From these clusters, the electron is used to reduce ferredoxin on the stromal side. Two ferredoxin molecules can reduce $NADP^+$ to NADPH, via the flavoprotein ferredoxin-$NADP^+$ oxidoreductase.

1.1.3 The dark phase

Photosynthesis is a way of using CO_2 to synthesize organic molecules, which contain many C-H bonds and are highly reduced compared with CO_2. The dark phase of photosynthesis includes a series of reactions (Figure 6), overall indicated as Calvin-Benson cycle (Benson and Calvin, 1950): through these reactions, atmospheric CO_2 is reduced to carbohydrates, using the chemical energy (ATP and NADPH) produced during the light reactions (Figure 4). The Calvin cycle allows the synthesis of one GAP each three CO_2 molecules and the regeneration of Ribulose-5-phosphate (Ru5P) to preserve the cyclic character of the process.

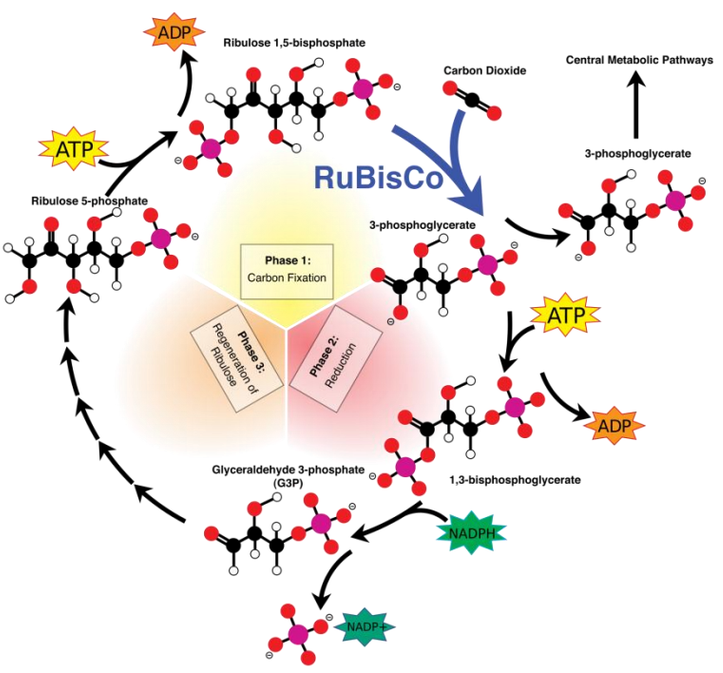

Figure 6. Enzymatic steps involved in Calvin-Benson cycle.

1.2 Photosynthetic pigments in higher plants

In higher plants, pigments responsible for absorption of PAR, charge separation and energy transfer toward the reaction center are coordinated on the photosystems. Photosynthetic pigments can be divided into two main classes of compounds: chlorophylls and carotenoids.

1.2.1 Chlorophylls

The chlorophyll molecule consists of a central magnesium atom surrounded by a porphyrin ring (a cyclic tetrapyrrole); a long carbon–hydrogen side chain, known as phytol chain, is attached to the ring. Chlorophyll occurs in several distinct forms: chlorophylls *a* and *b* are the major types found in higher plants and green algae; chlorophylls *c* and *d* are found, often with Chl *a*, in different red algae, while bacteriochlorophylls occurs in photosynthetic bacteria. Different chlorophylls are distinguished from their substitutions, e.g. Chl *a* e *b* differ in a substituent in the second pyrrole ring, being a methyl for the former, an aldehyde for the latter (Figure 7).

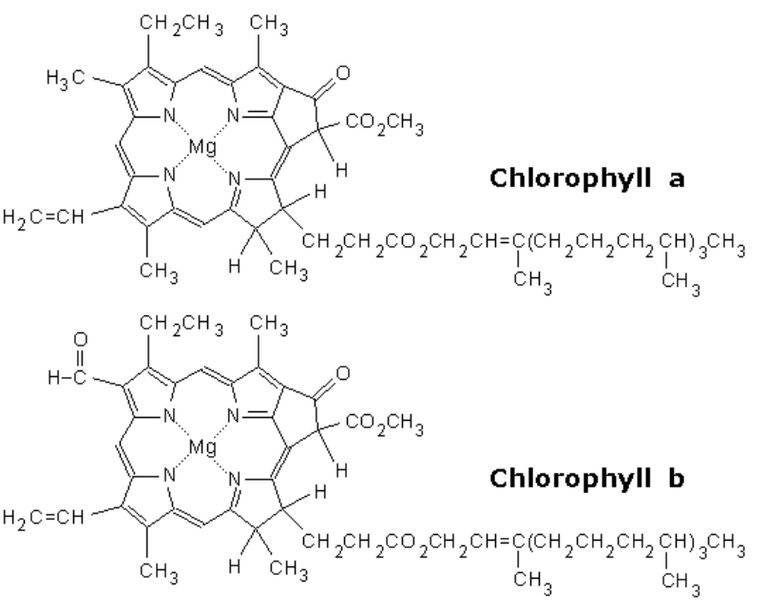

Figure 7.Structure of chlorophyll a and b.

The characteristic ability of Chls to absorb light in the visible region is due to the high number of conjugated double bonds present in these molecules. The Chls absorption spectrum has two main components: the Soret transition in the blue region and the Q_y transition in the red part of the spectrum. The Q_y transition is the red-most band, which peaks around 640-670 nm, respectively in Chl *b* and Chl *a* in organic solvent (Figure 8). It corresponds to the transition of an electron from S_0 to S_1 (the first excited state). The Soret band corresponds to transitions to higher states. Its maximum is around 430 and 460 nm for Chl *a* and Chl *b*, respectively. A latest absorption band of the spectrum is the weak Q_x transition that appears around 580-640 nm and is partly masked by the Q_y vibronic

transitions. It corresponds to the transition from a ground state (S_0) electron to the second excited state (S_2).

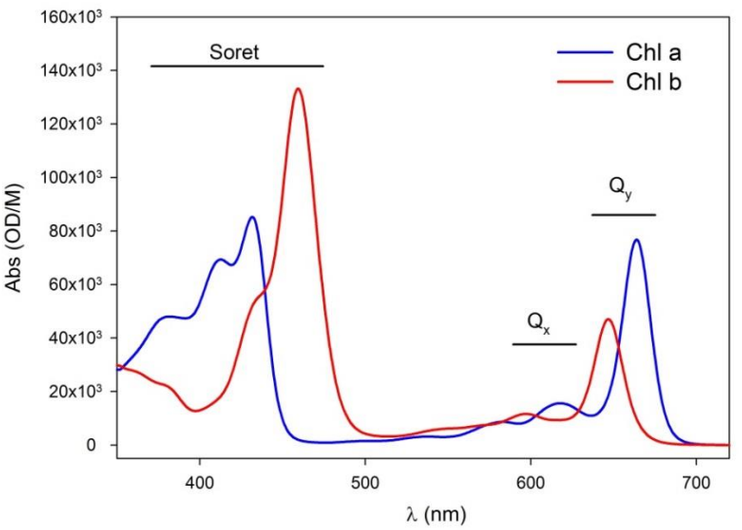

Figure 8.Chlorophyll a and b absorption spectra in acetone 80%.

1.2.2 Light harvesting and excitation energy transfer

Higher plants possess an intricate light-harvesting antenna system for effective capture of photons and excitation energy transfer (EET) to the reaction centers of both Photosystems I and II. For the energy transfer, at least two molecules are needed, an excited donor (D) and an acceptor (A) in its ground state. The excitation transfer between two pigments has two contributions corresponding to a direct Coulomb term (Förster, 1948) and an electron exchange term (Dexter, 1953) (Figure 9).

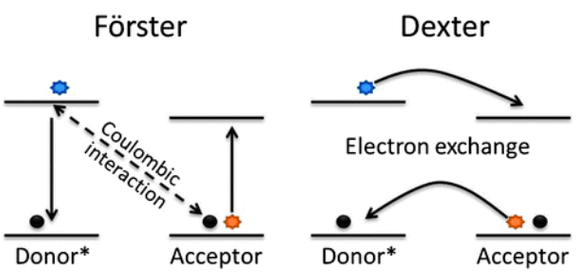

Figure 9 Schematic illustrations of Förster resonance energy transfer and Dexter electron-exchange energy transfer.

The electron exchange mechanism is based on the exchange of an electron between the excited donor molecule (D) and an acceptor molecule (A) (Dexter, 1953). When the molecular orbitals of these molecules are almost overlapping and the interaction energy between them is high, then an excited electron can be transferred to the empty higher energy level of the molecule A, the electron in the ground state of the molecule A is simultaneously moved to fill the "electron hole" of molecule D.

If the distance between A and D is too large for the superimposition of the respective molecular orbitals and if the transition is not forbidden, the coulomb contribution becomes dominant. In this case the interaction between A and D can be described as a dipole-dipole interaction (Pearlstein, 1982). The dipole-dipole interaction can be strong (the excitation energy is distributed on the donor and the acceptor molecule) or weak (the excitation energy is localized on either of the molecules).

The excitation energy between chlorophylls is probably transferred according to the weak dipole-dipole interaction (Förster, 1965). According to Förster, three parameters control such an excitation energy (or exciton) transfer:

(i) the energy levels of the electron transitions of both D and A molecules (namely, the degree of superposition of the fluorescence emission spectrum of the donor and the absorption spectrum of the acceptor)

(ii) the distance between molecules D and A

(iii) the orientation of the dipole moments of D and A molecules.

In a typical network of chlorophylls within light-harvesting systems, the distance between a pair of chlorophylls is generally (large) such that the exchange term is negligible; thus, the coupling is dominated by the Coulomb term. The protein environment influences the orientation and the optical characteristics of the chlorophylls, slightly changing the energy levels inside the chromophores. Because of the Stokes shift, the fluorescence band of a pigment absorbing at the shorter wavelengths overlaps the absorption band of a pigment absorbing at longer wavelengths, but not vice versa. Consequently, energy transfer occurs in only one direction, and most of the energy is channeled towards the Chl *a* molecule with the lowest energy, that is localized in the reaction center.

1.2.3 Carotenoids

Carotenoids (Car) are poly-isoprenoid compounds which contain 40 carbon atoms, all are derivative from the biosynthetic pathway of terpenoids. Car are among the most widespread of all natural pigments and fulfil a variety of functions, including an essential roles in organisms performing oxygenic photosynthesis. Structurally, carotenoids of the thylakoids take the form of a polyene hydrocarbon chain which is terminated by rings, and may or may not have additional oxygen atoms attached. They are split into two classes, xanthophylls (which contain oxygen) and carotenes (which are purely hydrocarbons, and contain no oxygen). The double carbon-carbon bonds interact with each other in a process called conjugation, and the π-electrons delocalization in the conjugated double bonds system leads to the light absorption in the visible range 400-500 nm (Figure 10).

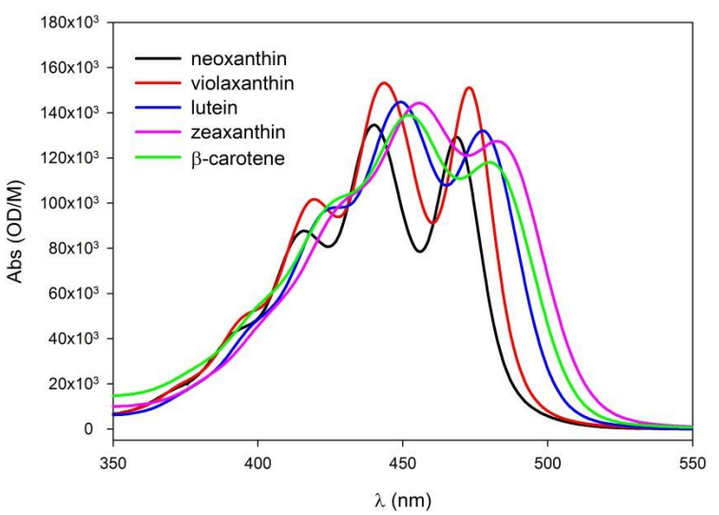

Figure 10. Absorption spectra of principal higher plants carotenoids in acetone 80%.

When Cars absorb light, electrons are transferred from the ground state S_0 to the second excited singlet state S_2; this strongly dipole-dipole transition is responsible for the characteristic absorption spectrum. The first excited singlet state S_1 cannot be populated from the ground state by photon absorption, due to symmetry reasons.

In higher plants the most abundant carotenoids associated with thylakoid membranes are the α- and β-Carotene (α-Car, β-Car) and the xanthophylls Lutein (Lut), Violaxanthin (Vio), Neoxanthin (Neo) and Zeaxanthin (Zea). Into the thylakoids, they can be found as a free pool or as non-covalently bound to the photosystems, probably involving hydrophobic interactions.

Carotenoids are built from the 5-carbon compound isopentenyl diphosphate (IPP), then the condensation of 8 IPP molecules by phytoene synthase produces phytoene (Figure 11).

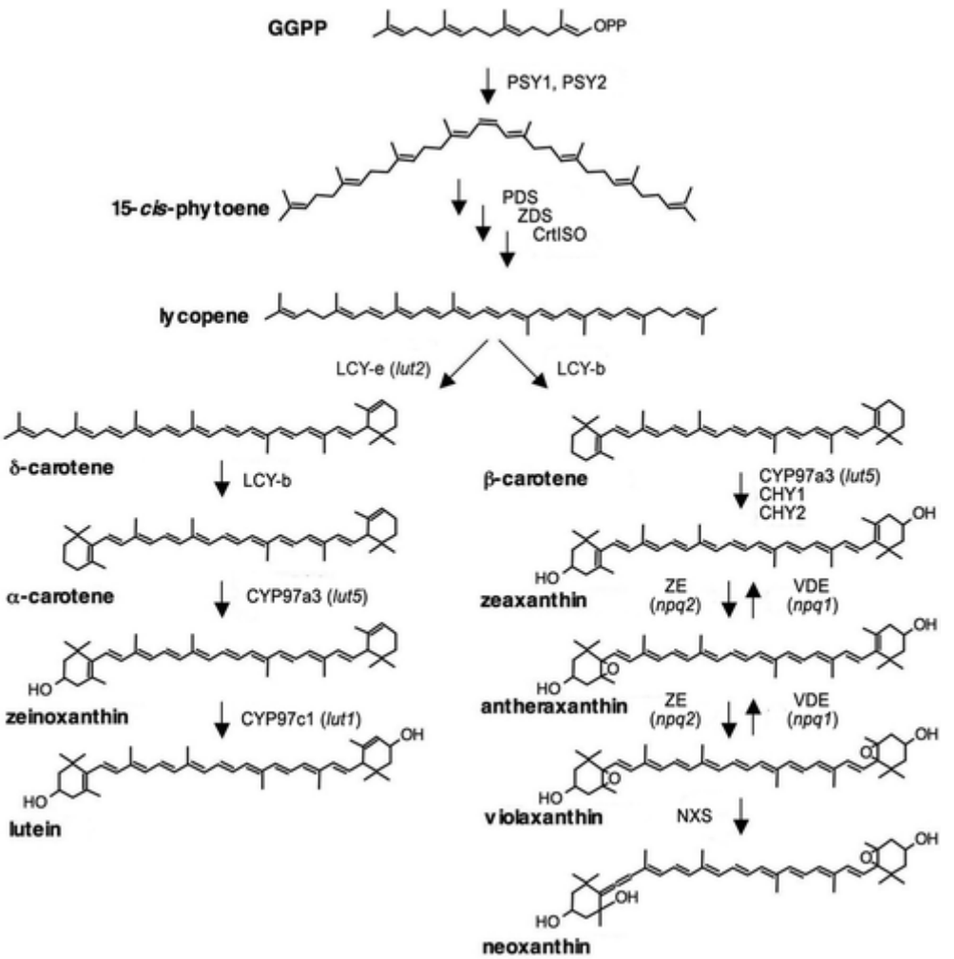

Figure 11. Biosynthetic pathway of carotenoids in A. thaliana, showing the enzymes controlling each step: lycopene β-cyclase (LCY-b), lycopene ε-cyclase (LCY-e), β-carotene hydroxylase (CYP97A3), ε–β-carotene hydroxylase (CYP97C1), β-carotene hydroxylase 1 and 2 (CHY1 and CHY2, respectively), Zea epoxidase (ZEP), Vio deepoxidase (VDE), and neoxanthin synthase (NXS). The names of Arabidopsis knockout mutants are given in brackets.

Phytoene is reduces to lycopene by phytoene desaturase, at this point the biosynthesis process splits into two branches: one leads to the formation of α-Car and Lut, while the other to β-Car, Zea, Vio and Neo (Pogson et al., 1996). The cyclization of the ends of the lycopene polyene chain is the first branch point in the pathway and results in the production of carotenes either with either one β- and one ε-ring (α-Car), or with two β- rings (β-Car). Zea is epoxidated twice to make Vio, which can be subsequently modified to make Neo. In *Arabidopsis* four enzymes provide for Chls hydrogenation: CHY1 and CHY2, two non-heme di-iron monoxygenase which catalyze the hydroxylation of β-ring only, and CYP97A3 (LUT5) and CYP97C1 (LUT1), two heme-containing cytochrome P450 hydroxylases which preferentially catalyze the hydroxylation of β and ε ring, respectively. Composition of carotenoids in the thylakoids is not constant, rather it rapidly changes according to the intensity of incident light, or during the acclimation to long-term stress (Demmig-Adams et al., 1989).

Three xanthophylls, namely Vio, antheraxanthin and Zea, take part to the so-called cycle of xanthophylls, which consists of a reversible light-dependent de-epoxidation of Vio in Zea via the intermediate antheraxanthin (Figure 12).

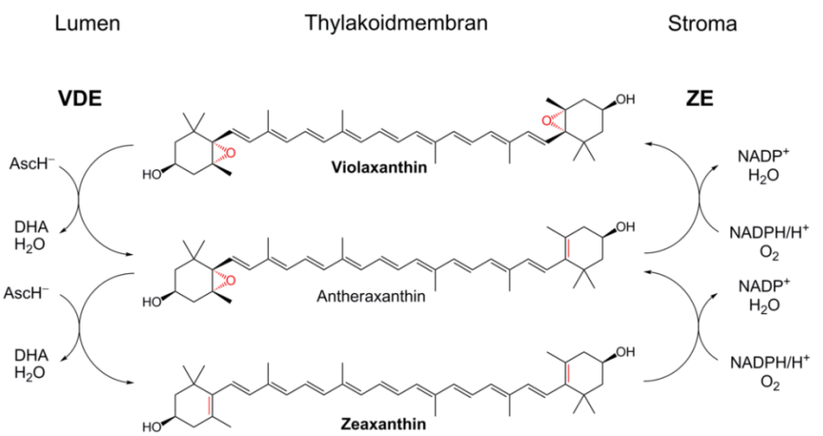

Figure 12. The xanthophyll cycle. Schematic representation of reactions and enzymes involved in the cycle.

This process is catalyzed by violaxanthin de-epoxidase (VDE) (Yamamoto and Kamite, 1972), a lumenal enzyme activated by lumen acidification (Gilmore and Yamamoto, 1992), which occur when a leaf is treated with an excess of light: that condition saturates the electron transport capacity and induce the increase of the transmembrane proton gradient. The enzyme zeaxanthin epoxidase (ZE), located in stromal side of the thylakoid membranes and constitutively activated (Bouvier et al., 1996),

catalyzes the epoxidation reaction which completes the cycle. The xanthophylls cycle is a key component in the activation of several photo-protection mechanisms as thermal energy dissipation of excess excitation energy (NPQ) (Niyogi, 1999; Holt et al., 2005), this point will be discussed in detail in the thesis.

1.3 The light absorbing units: organization and function of PSII and PSI supramolecular complexes

Photosystems are multi-protein supercomplexes which carry out the primary events of photosynthesis, namely light absorption and charge separation. Both PSI and PSII are composed by 2 functional domains: (a) the core complex involved in light harvesting, charge separation and electron transport, and (b) the peripheral antenna system, which enlarges the light harvesting capacity of the PS and mediates excitation energy transfer to RC. The different subunits which constitute the core complex are encoded by genes denominated *Psa* and *Psb*, respectively for PSI and PSII; some of them are localized in the plastid genome and encode for the major subunits of PSI core (PsaA, PsaB) and PSII core (D1, D2, CP43, CP47). Their sequences have been highly conserved during evolution both in bacteria and eukaryotic organisms. The peripheral antenna system includes polypeptides belonging to multigene family LHC (light-harvesting complex), all these genes being nuclear encoded and denominated Lhca and Lhcb, respectively for the antenna proteins of PSI and PSII (Jansson, 1999). Unlike the core complex subunits, both structure and composition of LHC subunits can vary greatly among different photosynthetic organisms, reflecting the light environments in which these organisms have evolved and the need for different strategies aimed at the management of PAR absorption.

1.3.1 PSII core complex

Within the PSII, defined as a water-plastoquinone oxidoreductase, absorption of four light quanta trigger water splitting into molecular oxygen and reducing equivalents. PSII core complex, the domain where the primary photochemistry takes place (Figure 13), is composed by four large intrinsic subunits (D1, D2, CP43 and CP47), twelve low-molecular-mass intrinsic subunits (PsbE, PsbF, PsbH,

PsbI, PsbJ, PsbK, PsbL, PsbM, PsbTc, PsbW, PsbX and PsbZ), and four extrinsic subunits attached on the luminal surface (PsbO, PsbP, PsbQ and PsbTn) (Shi et al., 2012; Wei et al., 2016).

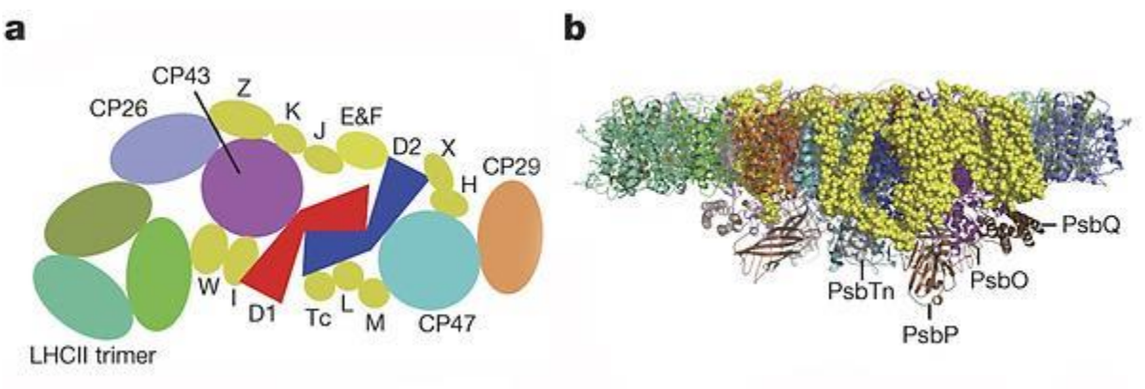

Figure 13. (A) Schematic model for PSII and (B) 3D crystal structure of PSII core complex (Wei et al., 2016)

Surrounding the four major core subunits, the low-molecular mass intrinsic subunits form a discontinuous belt-like structure around the core. Such a small subunits participate in stabilizing both the core complex (PsbK, PsbJ, PsbE, PsbF and PsbX) and its dimeric state (PsbTc, PsbL and PsbM), , mediating the interactions of peripheral antennae with the core (PsbW, PsbZ and PsbH) and binding of cytochrome b_{559} (PsbE and PsbF). Binding sites of the four extrinsic subunits, namely PsbO, PsbP, PsbQ and PsbTn, are located on the luminal side of the core complexThree of these subunits (PsbO, PsbP, PsbQ) compose the oxygen evolving complexes (OEC), while PsbTn function is unknown (Zouni et al., 2001; Umena et al., 2011).

1.3.2 PSII peripheral antenna system

All PSII antennae are Chl *a/b*- and xanthophyll-binding proteins. They fulfils the role of light-harvesting for PSII, transferring it in a highly efficient manner to the RC where primary photochemistry takes place. Another important function of LHC complexes for plant life will be discussed in detail in the thesis and concern their role in photoprotective mechanisms in excess light conditions. Indeed, LHCII are involved in a number of mechanisms established by plants during short-term and long-term stress that causes over-excitation of PSII and generation of harmful reactive excited states. The PSII outer

antenna system is composed by one copy each of three monomeric (minor) antennae CP29 (Lhcb4), CP26 (Lhcb5) and CP24 (Lhcb6) (Bassi et al., 1996), and at least four copies of the major trimeric antenna complex LHCII (Thornber et al., 1967; Caffarri et al., 2009). Homologous genes Lhcb1, Lhcb2 and Lhcb3 encode members of the heterotrimeric LHCII complex, which is the most abundant light-harvesting complex of higher plants. In *Arabidopsis thaliana*, Lhcb1 is encoded by 5 genes. The mature proteins encoded by *Lhcb1.1*, *Lhcb1.2* and *Lhcb1.3* are identical, whereas the Lhcb1.4 and Lhcb1.5 proteins are divergent but almost identical to each other. Lhcb2 is encoded by 3 genes, arisen as a result of recent gene duplication. The mature proteins expressed by *Lhcb2.1* and *Lhcb2.2* are identical, while Lhcb2.3 differs by only few amino acids with respect to the other two. Lhcb3 is encoded by a single gene, as well as the minor antennae Lhcb5 and Lhcb6 , while Lhcb4 is encoded by three highly conserved genes. *Lhcb4.1* and *Lhcb4.2* are similarly expressed, while the level of *Lhcb4.3* messenger is 20 times lower under control conditions (Jansson, 1999) and Lhcb4.3 protein is not present in detectable amount into thylakoids (Klimmek et al., 2006; de Bianchi et al., 2011b). The major antenna LHCII (Figure 14) includes heterotrimers composed by the gene products Lhcb1, Lhcb2 and Lhcb3, however their polypeptide composition is not equimolar, being Lhcb1 found in larger amount (Caffarri et al., 2004; Dekker and Boekema, 2005).

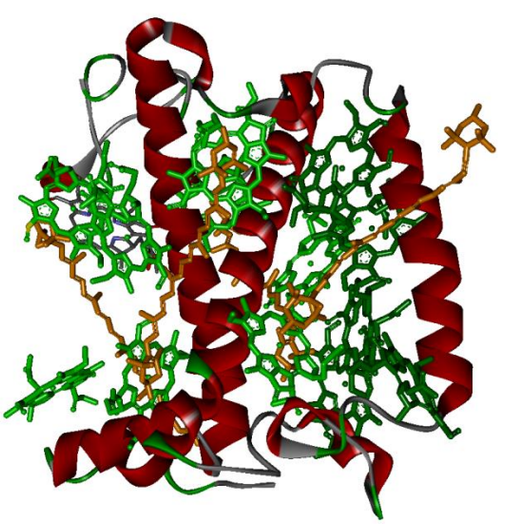

Figure 14. Cryo-electron microscopy model of LHCII. For clarity, the Chl phytyl chains are not shown. Green, Chl a; dark green, Chl b; orange, xanthophylls (Wei et al., 2016).

Crystal structure of LHCII has been resolved (Liu et al., 2004). Each monomer is constituted of 3 transmembrane domains with α-helix conformation (helices A, B and C). The N-terminal is fully hydrophilic, thus protrudes into the stroma space, instead the C-terminal peptides is exposed on the lumenal space. Two amphipathic helixes, named D and E, were found respectively on the C-terminal peptide and in the B-C loop region; both helices lie on the lumenal surface. The basic structural and functional unit of LHCII is the trimer. The whole trimerization region covers the amino-terminal domain, the carboxy terminus, the stromal end of helix B, several hydrophobic residues in helix C and also pigments and lipids bound to these parts of the polypeptide chain. Each monomer binds 14 Chl and 4 xanthophylls. Chlorophylls in LHCII are vertically distributed into two layers within the membrane, each layer lying close to the stromal or lumenal surface of the monomer: a layer of eight Chl surrounds the central helices A and B forming an elliptical ring toward the stromal surface; the remaining six Chl are arranged in a layer close to the lumenal surface, forming two separate clusters of four chlorophylls and a Chl *a*-Chl *a* dimer. Two central Lut molecules are bound in the grooves on both sides of the helices A and B cross-brace, forming the inner L1 and L2 Car binding sites (Caffarri et al., 2001); the polyene chains are firmly fixed in two hydrophobic cavities, providing strong linkage between helices A and B. The third xanthophyll, Neo, is located in the Chl *b*-rich region around helix C, in the binding site N1 (Remelli et al., 1999). The fourth carotenoid is Vio, located in a peripheral site named V1 (Ruban et al., 1999). V1 site is constituted by a hydrophobic pocket at the interface monomer-monomer, formed by several Chls, hydrophobic residues and the PG; part of the xanthophyll is located inside this pocket, while the opposite end group protrudes outside, toward the stromal surface.

CP29, the largest among LHC proteins, is composed by 256-258 amino acids in its mature form in *A. thaliana*. The overall sequence identity between CP29 and LHCII is 34%, but most of the substitutions are conservative, especially in the helix regions. It is a key component for the stability of the PSII-LHCII supercomplex (van Oort et al., 2010). The crystal structure of spinach CP29 has been recently resolved (Pan et al., 2011) and showed 13 Chl binding sites (eight Chls *a*, four Chls *b*, one mixed site) and three species of carotenoids (Lut, Vio and Neo). Each Car molecule occupies a separate site in CP29: Lut in site L1, Vio in site L2, Neo in site N1. Unlike LHCII, CP29 does not bind any pigment at Chls b601 and b605 sites, located at the periphery of the LHCII monomer. Instead, a new Chl-binding site, namely

a615, which is absent in LHCII, has been discovered on the surface of CP29 and close to the corresponding Chl b601 site of LHCII. Regarding the Cars binding sites, CP29 and LHCII show great differences at site L2, which binds Lut in LHCII but Vio in CP29. In addition, CP29 does not contain the V1 Car-binding site, identified at the monomer-monomer interface of the LHCII trimer. The L1 and N1 sites are conserved between CP29 and LHCII.

More recently, the cryo-EM structure of PSII-LHCII-CP29-CP26 supercomplex (Wei et al., 2016) was achieved (Figure 14)and allowed to gain further details on the structure of CP29. The long N-terminal region (87 amino acid residues) of CP29 was unobserved in the previous crystal structure, owing to its high flexibility and proteolysis during crystallization, while the cryo-EM shows that this region forms two motifs with irregular coil structures (motifs I and II) (Figure 15). Motif I (Pro12–Lys41) superposes well with the corresponding N-terminal region of LHCII. A Chl density resembling Chl b601 of LHCII is observed in this region. Motif II (Pro42–Phe87) forms an L-shaped structure containing an approximately 40 Å-long hairpin loop (Pro42–Ser72) running nearly parallel to the stromal surface, and a short hairpin loop (Ala73–Phe87) beneath the long hairpin.

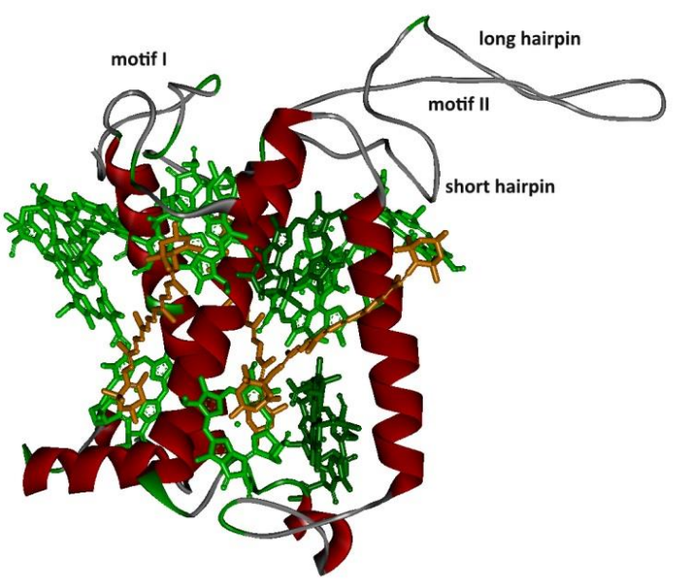

Figure 15. Cryo-electron microscopy model of CP29. For clarity, the Chl phytyl chains are not shown. Green, Chl a; dark green, Chl b; orange, xanthophylls (Wei et al., 2016)

Strikingly, a new Chl-binding site is found attached to the short hairpin in motif II and located at the region facing CP47. This Chl is coordinated by the backbone carbonyl of Leu80 and was tentatively

assigned as Chl *a* with its binding site named 616. Chl a616 in CP29 superposes partly with Chl a617 in Lhca3 and Lhca4 within the PSI–LHCI supercomplex, thus suggesting these pigments may serve similar roles as interfacial Chls facilitating energy transfer between two adjacent LHC complexes.

CP26 is 243 amino acids long in *A. thaliana*, and its sequence shows 48% identity with respect to that of LHCII.In the recent cryo-EM structure of PSII supercomplex, thirteen Chl binding sites and three Car binding sites were observed in CP26. Among them, Chls b601, a604, b607 and b608 were not predicted by the previous functional study (Ballottari et al., 2009). The Cars are assigned as two Lut (sites L1 and L2) and one Neo (site N1). While the site L1 is mainly occupied by Lut, the site L2 can also accept Vio as well as Lut, and the N1 site is selective for Neo (Caffarri et al., 2007).

CP24 is the smallest among LHC proteins (211 amino acids in *A. thaliana*), due to the deletion of a portion of the C-terminal region of the protein, common to the other members of the superfamily. Sequence homology, absorption spectroscopy and pigment analysis of both reconstituted and native complexes, suggest that CP24 coordinates 5 Chl *a*, 5 Chl *b* and 2 xanthophylls (Pagano et al., 1998; Bassi et al., 1996; Passarini et al., 2014). Unlike other Lhcb proteins, CP24 does not bind Neo, indeed the Tyr residue involved in N1 stabilization is absent.

1.3.3 Supramolecular architecture of PSII-LHCII

The supramolecular organization of PSII–LHCII has been studied by electron microscopy (EM) and single particle analysis on heterogeneous preparations obtained directly from mildly solubilized membranes, which allows enrichment of the high molecular weight complexes (Yakushevska et al., 2001; Boekema et al., 1999) (Figure 16). The location of the large core subunits was assigned by cross-linking experiments (Harrer et al., 1998) and confirmed by EM on solubilized membranes of plants lacking individual antenna complexes (Yakushevska et al., 2003).

The larger supercomplex observed in *Arabidopsis thaliana* by EM contains a dimeric core (C_2), two LHCII trimers (trimer S) strongly bound to the complex on the side of CP43 and CP26, and two more trimers, moderately bound (trimer M) in contact with CP29 and CP24. This complex is known as the $C_2S_2M_2$ supercomplex (Dekker and Boekema, 2005). CP24 and Lhcb3 are necessary for binding the trimer M (Kovacs et al. 2006). In the absence of CP26 no bands containing high molecular weight supercomplexes are visible and the amount of the fractions containing the smaller supercomplexes

(C_2S, C_2M, C_2S_2, C_2SM) is extremely reduced (Caffarri et al., 2009). $C_2S_2M_2$ were still detectable in a mutant without CP29, although their amounts were reduced compared with the wild type. In this mutant an empty space was observed within this supercomplex at the CP29 position, implying that the missing protein was not replaced by other LHC subunits (de Bianchi et al., 2011a).

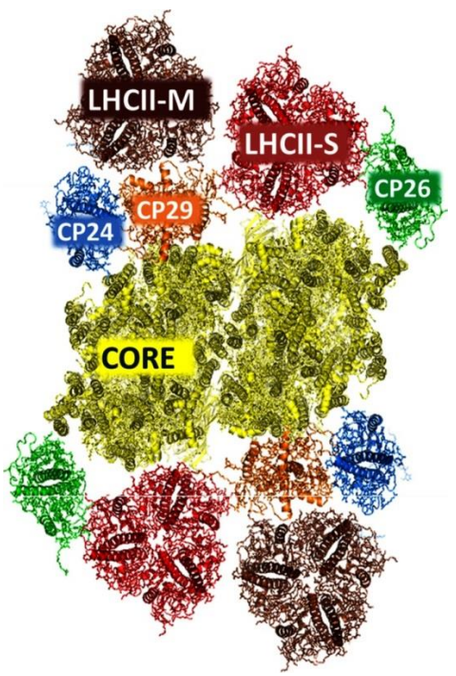

Figure 15. A structural model of $C_2S_2M_2$-type PSII–LHCII supercomplex from higher plants. Model shows the core dimer and the monomeric and trimeric outer antennae (Van Amerongen and Croce, 2013)

More recently, the structure of a 1.1-MDa spinach PSII–LHCII supercomplex has been solved at 3.2 Å resolution through single-particle cryo-EM. The structure confirmed a homodimeric supramolecular system, with one LHCII trimer and one CP26 monomer flanking the side near CP43, and one CP29 monomer associated with CP47 on the other side.

It is worth noting that PSII-LHCII stoichiometry is not static, indeed long-term acclimation to different light regimes is accompanied by a regulation of the amount of LHC proteins: e.g. under high light the amount of LHC is reduced, while the opposite effect is observed under low light, where the PSII core associates with a larger amount of LHCII proteins (Bailey 2001; Ballottari 2007). Biochemical and structural analysis of isolated thylakoids from low-light grown plants (Kouril et al. BBA 2014) showed

that, beside 4 LHCII per PSII core dimer of the $C_2S_2M_2$ supercomplex, other 4 “extra” LHCII can be found, which are not strongly connected to the supercomplex however still lead to relatively good excitation energy transfer.

1.3.5 PSI core complex

Photosystem I of higher plant is a light-dependent plastocyanin-ferredoxin oxidoreductase. Its core complex comprises 15 subunits, denoted PsaA–PsaL, PsaN, PsaO and PsaR (Scheller et al., 2001, Qin 2015), and encoded by both nuclear and plastid genes (Figure 17). PSI core complex coordinates 98 Chls *a* and 22 β-Car molecules.

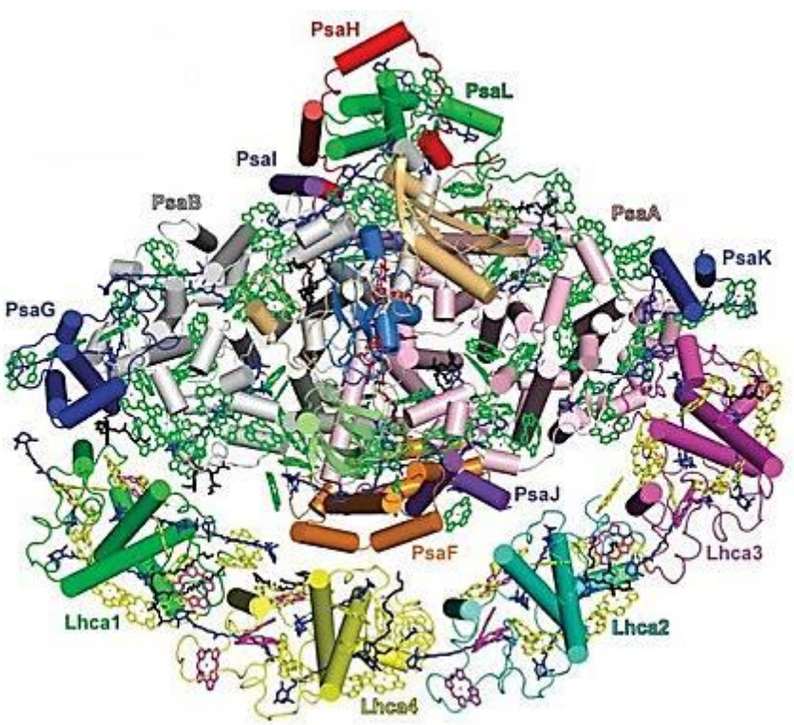

Figure 17. A Schematic model of photosystem I. Subunits organization and overall structure of the PSI-LHCI supercomplex from Pisum sativumat a resolution of 2.8 Å. (Qin et al., 2015).

Only PsaA, B, and C are directly involved in binding the electron transport cofactors: the special pair of Chl *a* P700, A_0 (a Chl *a* molecule), A_1 (a phylloquinone) and three [4Fe–4S] iron–sulfur clusters. The other subunits fulfill different functions: PsaD and PsaE provide the docking site for soluble ferredoxin on the stromal side of the supercomplex (Jordan et al., 2001; Fromme et al., 2001; Ihnatowicz.A. et al., 2004); PsaF and PsaN mediate the interaction with plastocyanin (Haldrup et al., 2000, 1999; Farah et al., 1995); PsaF, PsaK and PsaG are crucial for Lhca binding (Ben Shem et al., 2003; Haldrup et al., 2000) (Jensen et al., 2000, 2002; Varotto et al., 2002) and for stability of the PSI complex; PsaH, PsaI, PsaL, and PsaO form a cluster of integral membrane proteins, placed on one side of the core, interacting with LHCII during state transition.

1.3.6 PSI peripheral antenna

PSI core binds an extended peripheral antenna system (LHCI, light-harvesting complex of PSI), arranged on the side of PsaF/J subunits and composed of four nuclear-encoded light-harvesting proteins (Lhca1-4), each binding Chl *a*, Chl *b* and xanthophylls. One copy each of Lhca1-4 is present per supercomplex (Ballottari et al., 2004) with a molecular mass between 20 and 24 kDa (Fig. 18). Binding of the antenna moiety to the core is strongly cooperative (Morosinotto et al., 2005a), and the minimal building blocks for the antenna system were the heterodimers Lhca1/4 and Lhca2/3 (Wientjes and Croce, 2011). In additions, two more genes, Lhca5 and Lhca6, were identified in the genome of *Arabidopsis* (Jansson, 1999). Lhca5 and Lhca6 encode for subunits highly homologous to the Lhca1-4 proteins, but their expression level is very low in all conditions tested and proteins are present in non-stoichiometric amounts in WT plants (Klimmek et al., 2006). All of the Lhca proteins have three major transmembrane helices, A, B, and C, and an amphipathic helix D at the lumenal side, similar to the structures of light-harvesting complexes of PSII..

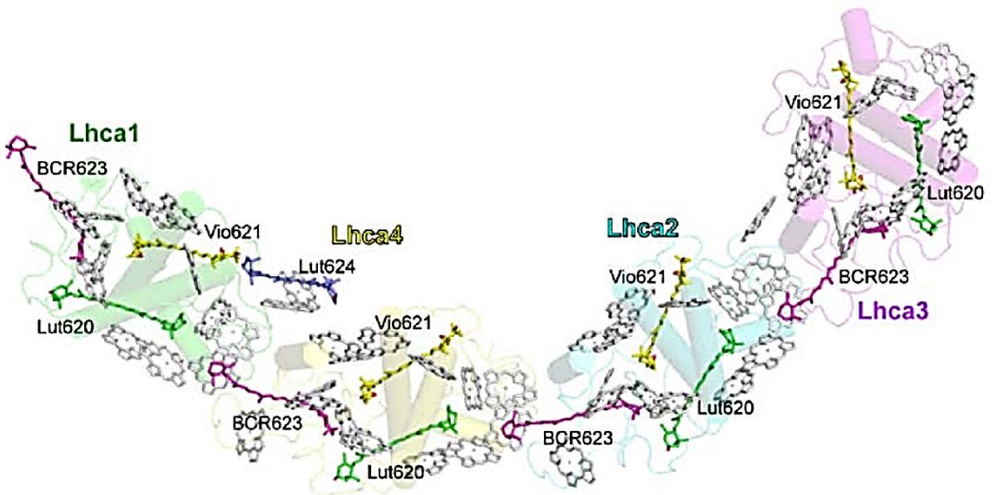

Figure 18. Arrangement of Car in four Lhca subunits. View along the membrane from the stromal side. The three Car binding sites L1 (Lut620), L2 (Vio621) and N1 (β-Car623) in each Lhca were shown in green, yellow and magenta, respectively. Lut624 in the L3 site of Lhca4 was shown in light blue. Chls a were shown in gray and Chls b were shown in orange (Qin et al., 2015).

Recently Qin and co-workers identified 45 Chls *a*, 12 Chls *b*, 4 β-Car, 5 Lut and 4 Vio in the LHCI system. These Chls are distributed into two layers, one close to the stromal and one close to the luminal surface; all Chls *b* are located in helix C or nearby the N-terminal loop, both of which form the interfacial regions of two adjacent Lhca proteins, which suggests these pigments might mediate energy transfer between adjacent Lhca subunits. Each Lhca binds three carotenoids (Lut, Vio and β-Car) at three sites (L1, L2, and N1, respectively), and another Lut (Lut624) binds in between Lhca1 and Lhca4 (Figure 18).

A peculiarity of PSI antenna moiety of higher plant are the so called red spectral forms, that originates from Chls which have absorption maxima at longer wavelengths than P700 (Lam et al., 1984). In *Arabidopsis thaliana*, Lhca4 and Lhca3 showed the red-most emission (735 and 725 nm at 77 K, respectively). The molecular basis of the red spectral forms was studied by mutational analysis and *in vitro* reconstitution into recombinant Lhca complexes.

It was shown that these low-energy absorption forms originate from Chl-Chl excitonic interactions between Chl a603-a609 in Lhca3-4 antenna complexes (Morosinotto et al., 2003)(Figure 19).

The biological functions of the red pigments in the PSI still remain controversial: they might provide an advantage in leaves under a canopy, since they extend the absorption capacity of the complex

toward longer λ, or could mediate the dissipation of excitation energy in excess before being transferred to the RC (Croce et al., 1996; Rivadossi et al., 1999).

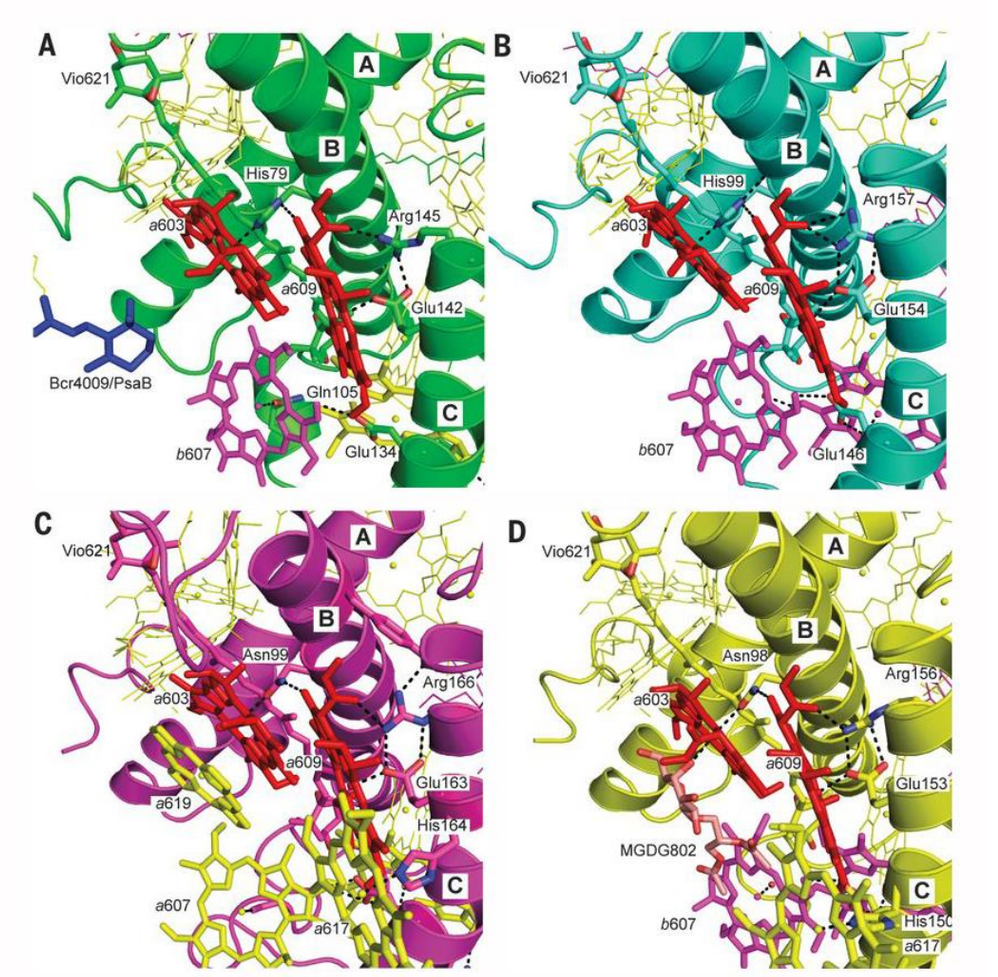

Figure 19. Local environments of the red Chl a603-a609 dimers in LHCI. Lhca proteins: green, Lhca1 (A); cyan, Lhca2(B) ; magenta, Lhca3 (C); yellow, Lhca4 (D).TheChla603-a609 dimers in the four Lhca subunits with their surrounding transmenbrane helices and other cofactors. View is along the membrane from the stromal side (Qin et al., 2015).

1.3.6 Supramolecular architecture of the PSI-LHCI supercomplex

While the PSII supercomplexes are dimeric and bind a variable amount of trimeric LHCII, the PSI supercomplex consists of a monomeric core with single copies of four different LHCI proteins, as recently confirmed by the crystal structure resolved at 2.8 Å (Ben Shem et al., 2004; Qin et al., 2015). Unlike PSII, PSI-LHCI supercomplex is a rigid and stable system, indeed mutants depleted of individual

Lhca showed that missing subunits were not replaced by other LHC (Morosinotto et al., 2005a; Wientjes et al., 2009). While sustained over-excitation triggers the long-term reduction of PSII antenna size (Anderson 1986), the composition of the PSI outer antenna was found to be constant in a number of different light conditions (Ballottari et al., 2007). However, the PSI light harvesting capacity was shown to be tuned to changes in light quality and quantity by recruiting LHCII as additional antenna, in order to balances excitation delivery to PSI and PSII (Allen 1992; Galka et al., 2012). LHCI subunits are arranged on the side of PsaF/J subunits, while LHCII binds to the opposite side (Lunde et al., 2000; Galka et al., 2012) (Figure 20).

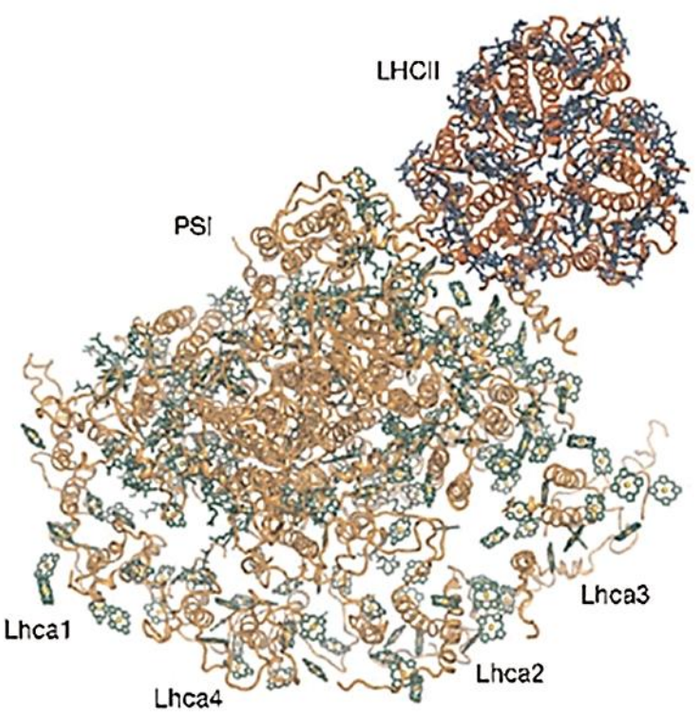

Fig. 20. Models for association of both LHCI and the mobile LHCII antenna in PSI supercomplex (Kargul and Barber, 2008).

1.4 Photoxidative stress and photoprotection mechanisms

1.4.1 Generation of reactive oxygen species

Most days plants experience irradiances that exceed their photosynthetic capacity. Light intensity and spectral quality are highly variable in according to diurnal and seasonal fluctuations in irradiances. Moreover, what constitutes excess light for a leaf depends on environmental conditions, indeed stresses such as cold, drought, salinity and nutrient deficiency can influence and exacerbate EL stress. Environmental conditions might therefore prevent the maintenance of a high capacity for photosynthetic carbon assimilation, thus the amount of energy absorbed by photosystems can become far higher than that used by downstream assimilatory metabolism. This condition yields into over-excitation of the photosynthetic apparatus, and lead to the generation of both potentially dangerous excited states and reactive oxygen species (ROS) (Prasil et al., 1992; Tjus et al., 1998, 2001), which oxidize lipids, proteins and pigments in the immediate vicinity. ROS are continuously generate within the photosynthetic apparatus, and Chls have a crucial role in these events, being able to act as a potent endogenous photosensitizer. Potentially damaging molecules are generated at three major sites in the photosynthetic apparatus, namely LHCII, PSII RC and PSI.

Within PSII antenna, absorption of light causes Chl to enter the singlet excited state (^{1}Chl*). Before excitation energy is trapped by the RC, triplet Chl (^{3}Chl*) can be formed by intersystem crossing, the latter being an inherent physical property of ^{1}Chl*. The yield of ^{3}Chl* formation depends on the [^{1}Chl*] in the antenna, therefore environmental conditions which cause accumulation of excitation energy in the Lhcs, and thereby increase the lifetime of singlet Chl, increase the probability of intersystem crossing. ^{3}Chl* is a long-lived state (~ms timescale) which can react with $^3O_2$ to produce the very reactive singlet oxygen ($^1O_2$), a strong oxidized and the main responsible for the decline in the photochemical efficiency (Tardy and Havaux, 1996).

Even PSII RC can become an important source of ROS: excitation energy trapping involves charge separation and formation of $P680^+$ / Pheo; this radical pair is reversible, and the event of charge recombination can generate triplet P680 (^{3}P680*), while energy exchange between ^{3}P680* and O_2 results in formation of $^1O_2$. (Vass et al., 1992; Aro et al., 1993).

In contrast to $P680^+$, $P700^+$ is less oxidizing and relatively stable, and a very efficient quencher of excitation energy (Dau, 1994), therefore the average lifetime of $^1Chl*$ in the PSI-LHCI is several times shorter than in the PSII-LHCII. However, at the acceptor side of PSI, FD can reduce molecular oxygen to superoxide anion (O_2^-). This short-living specie can be metabolized to hydrogen peroxide (H_2O_2) or hydroxyl radical (OH•), the latter being an extremely aggressive ROS.

1.5 Photoprotection mechanisms

Plants evolved several photoprotective mechanisms aimed at avoiding ROS formation and preventing photoinhibition. These strategies can be divided into two different classes, depending on the time-scale of action, namely short-term and long-term photoprotective mechanisms.

1.5.1.1 Non-Photochemical Quenching (NPQ)

Since production of $^3Chl^*$ is a constitutive property of Chl, and $^3Chl^*$ originates from $^1Chl^*$, plants evolved a rapidly inducible mechanism, termed NPQ (Non-Photochemical Quenching), that allows the harmless thermal dissipation of $^1Chl^*$ in excess within PSII (Frank et al., 2000) in order to prevent ROS production ((Demmig-Adams and Adams, 1992). Activation of NPQ reduce the lifetime of $^1Chl^*$, thus the kinetic of energy dissipation can be monitored *in vivo* as a light-dependent quenching of leaf Chl fluorescence. NPQ is a very efficient process that protects PSII reaction centers from photoinhibition. Different processes contribute to NPQ, which affect fluorescence rise and decay and can be dissected into three major kinetic components: the so-called energy-dependent quenching (qE, half time ~1 min), the intermediate quenching component (qZ/qM, half time ~10-20 min) and the photoinhibitory quenching (qI, half time ~60 min).

1.5.1.2 The energy-dependent quenching component, qE

Absorption of sunlight that saturates plant capacity for photochemistry results in the build-up of a proton gradient across thylakoid membranes and inhibition of ATPase activity due to Pi and ADP shortage. Over-acidification of the lumenal compartment in turn lead to inhibition of key electron

transporters (Cyt b_6f and OEC) thus further reducing the electron transport rates. Lumen acidification also works as a signal of excessive light, that triggers the feedback down-regulation of PSII energy conversion events. The control by lumen pH allows induction or reversal of qE within seconds upon changes in light intensity, namely it is fast enough to cope with natural fluctuations in irradiance (Muller et al., 2001). The requirement for low lumen pH is evidenced by the inhibition of qE by ionophores such as nigericin, which collapses ΔpH and prevents qE activation (Shikanai et al., 1999). The lumenal acidification which trigger qE promotes at least two events, namely activation of the xanthophyll cycle (Adams et al., 1996) and protonation of specific lumen-exposed residues of PSII subunits (Horton et al., 1992). It has been hypothesized that protonation (i) induces a conformational change of specific LHC toward a dissipative state, and (ii) activates a binding site for Zea in the LHC moiety, which ultimately open a dissipative channel within the PSII outer antenna (Ma et al., 2003; Holt et al., 2004).

Signal transduction of lumen over-acidification involves the PSII subunit PsbS in higher plants, as shown by the qE-null phenotype of *npq4-1* mutant of Arabidopsis, devoid of PsbS (Li et al., 2000). PsbS belongs to the LHC protein superfamily, has four transmembrane helices and does not bind pigments (Dominici et al., 2002); therefore, quenching reactions must be located into interacting pigment-binding subunits of PSII, located together with PsbS in grana partitions. PsbS senses the ΔpH through two symmetrically arranged, lumen-exposed, glutamates (Glu-122 and Glu-226). Mutating one or the other of these two glutamates inhibits the PsbS function in qE of 50%, whereas the PSBS-E122Q/E226Q double mutant lacks qE response. The exact localization of PsbS within grana stacks is still not defined: PsbS is not a component of the purified C_2S_2 complex (Nield et al., 2000) and cannot be accommodated in the $C_2S_2M_2$ complex (Dekker and Boekema, 2005), the latter being consistent with biochemical analysis of purified $C_2S_2M_2$ supercomplexes (Caffarri et al., 2009). Recent results (Sacharz et al., 2017) showed that PsbS specifically interact with the antenna system: in the presence of ΔpH alone, PsbS is found to be mainly associated with the trimeric LHCII, while a combination of ΔpH and Zea increases the proportion of PsbS bound to the monomeric antenna complexes .

LHCB proteins appear to be ideal candidates for shielding the quenching sites. The *ch1* mutant of *A. thaliana*, in which folding of LHC proteins is impaired due to the lacks Chl *b*, exhibits a strongly reduced capacity for qE (Andrews et al., 1995). The role of individual LHCs in the quenching reactions has been investigated by reverse genetics. Down-regulation of Lhcb1 yields into a lower qE, while

either down-regulation Lhcb2 or knockout of Lhcb3 did not significantly affect quenching kinetics (Andersson et al., 2003; Pietrzykowska et al., 2014).

qE response was impaired in both CP24 and CP29 knockout plants (de Bianchi et al., 2008; Andersson et al., 2001). However, depletion of a single Lhcb subunit did not completely abolish qE, implying redundancy within the subfamily members.

Additional open questions concern the biophysical mechanism(s) by which the quenching reaction are catalyzed. Proposals include (i) Chl-Chl interactions, acting as quenchers (Muller et al., 2010; Wahadoszamen et al., 2012; Kell et al., 2014); (ii) formation of short-living Chl-xanthophyll excited states, which serve as traps for ^{1}Chl* (Ruban et al., 2007; Bode et al., 2009; van Oort et al., 2015); (iii) charge transfer events in a Chl *a*–Zea heterodimer, followed by charge recombination at the ground state (Holt et al., 2005). Interaction between Chl *a* and Zea might be promoted by different biochemical events, such as a conformational change caused by the interaction PsbS-CP29 (Ahn et al., 2008) or PsbS-LHCII, forming a Zea–PsbS complex at the interface (Barros et al., 2009a; Barros et al., 2009b). Quenching response was also proposed to originate from an event of LHCII aggregation (Pascal et al., 2005; Ruban et al., 2007); this suggestion was supported by the evidence that low energy states emitting at ~700 nm can be induced in isolated LHCB complexes upon induction of aggregation *in vitro* (Ruban et al., 1994; Müller et al., 2010) and that similar fluorescence changes can be observed also *in vivo* in high-light treated leaves (Ruban et al., 2007).

1.5.1.3 The slow phases of NPQ induction, qI and qM/qZ

According to kinetics of rise in the light and decay in darkness, NPQ can be dissected in three major kinetic components, namely qE, qZ/qM and qI. The middle phase of quenching induction was originally attributed to the event of state transitions , the mechanism which balances the excitation pressure between PSII and PSI through a reversible migration of LHCII between PSs (Haldrup et al., 2001). However, the *stn7* mutant of Arabidopsis is unable to activate state transition and still retains the middle phase of quenching. Further analysis showed that the intermediate quenching component correlates with both (i) the conversion of Vio into Zea, and (ii) the photorelocation response of chloroplast, therefore has been designated as qZ/qM (Nilkens et al., 2010; Cazzaniga et al., 2013). Photoinhibitory quenching, or qI, is commonly associated with the damage of the D1 protein that leads to photoinhibition and to a lower photosynthetic capacity (Aro et al., 1993). The term qI is used for all NPQ processes relaxing with far slower kinetics than the trans-thylakoid pH gradient, and thus

comprises all processes contributing to the light-induced inactivation and damaging of PSII in the long term.

1.5.1.4 State1-state2 transitions

State transitions are a short-term adaptation mechanism mediated by the reversible phosphorylation of the main light-harvesting complex protein (LHCII) and its migration between photosystem I (PSI) and photosystem II (PSII) (Rochaix, 2007) (Figure 21). PSII and PSI hold pigments systems with distinct absorption characteristics and a distinct action spectrum, indeed PSI has a broad absorption peak in the far-red region, whereas PSII has strong absorption in the blue and red, but not in the far-red region. Since the two photosystems are connected in series, plants need to constantly balance their excitation levels to ensure optimal efficiency of electron flow under different quality and quantity light conditions (Jennings and Zucchelli, 1986).

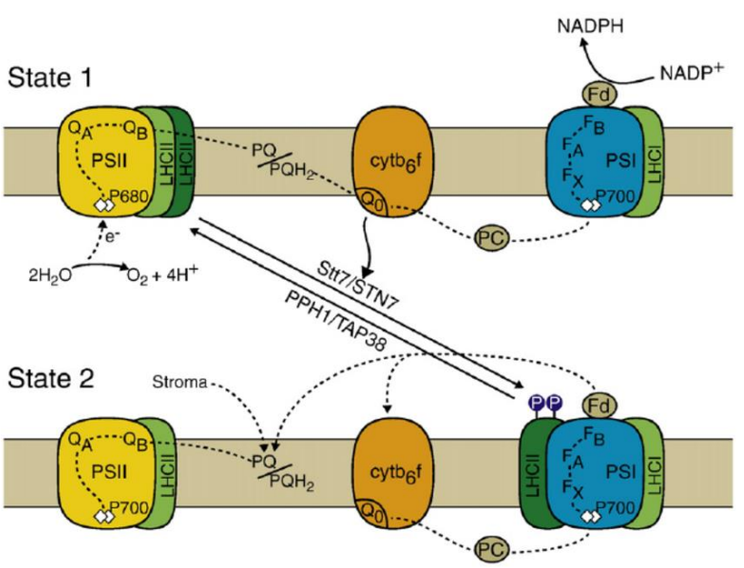

Figure 21. Schematic representation of state I – state II transitions, with complexes and enzymes involved (http://www.molbio.unige.ch/eng/researchgroups/rochaix/objectives).

Under conditions that promote a preferential excitation of PSII, the redox state of the PQ pool becomes more reduced; binding of PQH_2 to the Q_0 site of the Cyt-b_6f leads to a conformational

change of this complex that activates a kinase called STN7 (Zito et al., 1999; Pesaresi et al.). STN7 kinase is responsible for the phosphorylation of LHCII (Bellafiore et al., 2005). The phosphorylation at the N-terminus of LHCII causes a conformational change that lowers the affinity of LHCII for PSII while increase its affinity for PSI (Nilsson et al., 1997). A preferential excitation of PSI leads to the oxidation of the PQ pool, inactivation of the kinase and dephosphorylation of LHCII by TAP38/PPH1 protein phosphatases, upon which LHCII migrates back to PSII (Shapiguzov et al., 2010).

1.5.2 Long-term photoprotective mechanisms

When plants experience sustained over-excitation of the photosynthetic apparatus, photoprotective mechanisms are activated on long-term scale. E.g. one of these mechanisms involve adjustment of light-harvesting antenna size, as effect of changes in Lhc gene expression or Lhc protein degradation (Maxwell et al., 1995). Increase in capacity for photosynthetic electron transport and CO2 fixation rate can be achieved during acclimation. In some overwintering evergreen plants, that undergo prolonged cold-stress conditions, mechanisms of sustained thermal dissipation of excess photons have been described (Gilmore and Ball., 2001). These mechanisms involve the regulation of both nuclear and chloroplast gene expression. In *A. thaliana*, such a regulation is mediated by photoreceptors such as cryptochrome (Ruckle et al., 2007), or through biochemical and metabolic signals such as the plastoquinone redox state (Pfannschmidt et al., 1999), the perception of ROS (op den Camp et al., 2003), the release of carotenoids oxidation products (Ramel 2012), the redox state of the glutathione pool and the ATP/ADP ratio (Walters, 2004).

Adams, W.W., Demmig-Adams, B., Barker, D.H., and Kiley, S. (1996). Carotenoids and photosystem II characteristics of upper and lower halves of leaves acclimated to high light. Aust.J.Plant Physiol. **23**: 669–677.

Allen, J.F. and Forsberg, J. (2001). Molecular recognition in thylakoid structure and function. Trends Plant Sci. **6**: 317–326.

Van Amerongen, H. and Croce, R. (2013). Light harvesting in photosystem II. Photosynth. Res.

Andersson, J., Walters, R.G., Horton, P., and Jansson, S. (2001). Antisense inhibition of the photosynthetic antenna proteins CP29 and CP26: implications for the mechanism of protective energy dissipation. Plant Cell **13**: 1193–204.

Andersson, J., Wentworth, M., Walters, R.G., Howard, C.A., Ruban, A. V, Horton, P., and Jansson, S. (2003). Absence of the Lhcb1 and Lhcb2 proteins of the light-harvesting complex of photosystem II - effects on photosynthesis, grana stacking and fitness. Plant J. **35**: 350–61.

Andrews, J.R., Fryer, M.J., and Baker, N.R. (1995). Consequences of LHC II deficiency for photosynthetic regulation in chlorina mutants of barley. Photosynth. Res. **44**: 81–91.

Aro, E.-M., Virgin, I., and Andersson, B. (1993). Photoinhibition of Photosystem II - inactivation, protein damage and turnover. Biochim.Biophys.Acta **1143**: 113–134.

Ballottari, M., Govoni, C., Caffarri, S., and Morosinotto, T. (2004). Stoichiometry of LHCI antenna polypeptides and characterization of gap and linker pigments in higher plants Photosystem I. Eur. J. Biochem. **271**: 4659–65.

Ballottari, M., Mozzo, M., Croce, R., Morosinotto, T., and Bassi, R. (2009). Occupancy and functional architecture of the pigment binding sites of photosystem II antenna complex Lhcb5. J. Biol. Chem. **284**: 8103–8113.

Barber, J. (1980). Membrane surface charges and potentials in relation to photosynthesis. Biochim.Biophys.Acta **594**: 253–308.

Bassi, R., Giuffra, E., Croce, R., Dainese, P., and Bergantino, E. (1996). Biochemistry and molecular biology of pigment binding proteins. **NATO ASI s**: 41–63.

Bellafiore, S., Barneche, F., Peltier, G., and Rochaix, J.-D. (2005). State transitions and light adaptation require

chloroplast thylakoid protein kinase STN7. Nature **433**: 892–895.

Benson, A.A. and Calvin, M. (1950). Carbon Dioxide Fixation by Green Plants. Annu. Rev. Plant Physiol. Plant Mol. Biol. **1**: 25–42.

de Bianchi, S., Betterle, N., Kouril, R., Cazzaniga, S., Boekema, E., Bassi, R., and Dall'Osto, L. (2011a). Arabidopsis mutants deleted in the light-harvesting protein Lhcb4 have a disrupted Photosystem II macrostructure and are defective in photoprotection. Plant Cell **23**: 2659–2679.

de Bianchi, S., Betterle, N., Kouril, R., Cazzaniga, S., Boekema, E., Bassi, R., and Dall'Osto, L. (2011b). Arabidopsis Mutants Deleted in the Light-Harvesting Protein Lhcb4 Have a Disrupted Photosystem II Macrostructure and Are Defective in Photoprotection. Plant Cell **23**: 2659–2679.

de Bianchi, S., Dall'Osto, L., Tognon, G., Morosinotto, T., and Bassi, R. (2008). Minor Antenna Proteins CP24 and CP26 Affect the Interactions between Photosystem II Subunits and the Electron Transport Rate in Grana Membranes of Arabidopsis. PLANT CELL ONLINE **20**: 1012–1028.

Boekema, E.J., van Roon, H., van Breemen, J.F., and Dekker, J.P. (1999). Supramolecular organization of photosystem II and its light-harvesting antenna in partially solubilized photosystem II membranes. Eur.J.Biochem. **266**: 444–452.

Bouvier, F., d'Harlingue, A., Hugueney, P., Marin, E., Marion-Poll, A., and Camara, B. (1996). Xanthophyll biosynthesis. Cloning, expression, functional reconstitution, and regulation of beta-cyclohexenyl carotenoid epoxidase from pepper (Capsicum annuum). J. Biol. Chem. **271**: 28861–7.

Caffarri, S., Croce, R., Breton, J., and Bassi, R. (2001). The major antenna complex of photosystem II has a xanthophyll binding site not involved in light harvesting. J.Biol.Chem. **276**: 35924–35933.

Caffarri, S., Croce, R., Cattivelli, L., and Bassi, R. (2004). A look within LHCII: differential analysis of the Lhcb1-3 complexes building the major trimeric antenna complex of higher-plant photosynthesis. Biochemistry **43**: 9467–76.

Caffarri, S., Kouril, R., Kereiche, S., Boekema, E.J., and Croce, R. (2009). Functional architecture of higher plant photosystem II supercomplexes. EMBO J. **28**: 3052–3063.

Caffarri, S., Passarini, F., Bassi, R., and Croce, R. (2007). A specific binding site for neoxanthin in the monomeric antenna proteins CP26 and CP29 of Photosystem II. FEBS Lett. **581**: 4704–4710.

Cazzaniga, S., Dall'Osto, L., Kong, S.G., Wada, M., and Bassi, R. (2013). Interaction between avoidance of photon absorption, excess energy dissipation and zeaxanthin synthesis against photooxidative stress in Arabidopsis. Plant J.

Croce, R., Zucchelli, G., Garlaschi, F.M., Bassi, R., and Jennings, R.C. (1996). Excited state equilibration in the photosystem I -light - harvesting I complex: P700 is almost isoenergetic with its antenna. Biochemistry **35**: 8572–8579.

Dau, H. (1994). Molecular mechanisms and quantitative models of variable photosystem II fluorescence. Photochem.Photobiol. **60**: 1–23.

Dekker, J.P. and Boekema, E.J. (2005). Supramolecular organization of thylakoid membrane proteins in green plants. Biochim.Biophys.Acta **1706**: 12–39.

Demmig-Adams, B. and Adams, W.W. (1992). Photoprotection and other responses of plants to high light stress. Ann.Rev.Plant Physiol.Plant Mol.Biol. **43**: 599–626.

Dexter, D.L. (1953). A Theory of Sensitized Luminescence in Solids. J. Chem. Phys. **21**: 836–850.

Dominici, P., Caffarri, S., Armenante, F., Ceoldo, S., Crimi, M., and Bassi, R. (2002). Biochemical properties of the PsbS subunit of photosystem II either purified from chloroplast or recombinant. J.Biol.Chem. **277**: 22750–22758.

Farah, J., Rappaport, F., Choquet, Y., Joliot, P., and Rochaix, J.D. (1995). Isolation of a psaF-deficient mutant of Chlamydomonas reinhardtii: efficient interaction of plastocyanin with the photosystem I reaction center is mediated by the PsaF subunit. EMBO J. **14**: 4976–4984.

Förster, T. (1965). Delocalized Excitation and Excitation Transfer - Theodor Förster - Google Books.

Förster, T. (1948). Zwischenmolekulare Energiewanderung und Fluoreszenz. Ann. Phys. **437**: 55–75.

Frank, H.A., Bautista, J.A., Josue, J.S., and Young, A.J. (2000). Mechanism of nonphotochemical quenching in green plants: Energies of the lowest excited singlet states of violaxanthin and zeaxanthin. Biochemistry **39**: 2831–2837.

Fromme, P., Jordan, P., and Krauss, N. (2001). Structure of photosystem I. Biochim.Biophys.Acta **1507**: 5–31.

Galka, P., Santabarbara, S., Khuong, T.T.H., Degand, H., Morsomme, P., Jennings, R.C., Boekema, E.J., and Caffarri, S. (2012). Functional analyses of the plant photosystem I-light-harvesting complex II

supercomplex reveal that light-harvesting complex II loosely bound to photosystem II is a very efficient antenna for photosystem I in state II. Plant Cell **24**: 2963–78.

Gilmore, A.M. and Yamamoto, H.Y. (1992). Dark induction of zeaxanthin-dependent nonphotochemical fluorescence quenching mediated by ATP. Proc.Natl.Acad.Sci.USA **89**: 1899–1903.

Haldrup, A., Jensen, P.E., Lunde, C., and Scheller, H. V (2001). Balance of power: a view of the mechanism of photosynthetic state transitions. Trends Plant Sci. **6**: 301–5.

Haldrup, A., Naver, H., and Scheller, H. V (1999). The interaction between plastocyanin and photosystem I is inefficient in transgenic Arabidopsis plants lacking the PSI-N subunit of photosystem I. Plant J. **17**: 689–698.

Haldrup, A., Simpson, D.J., and Scheller, H. V (2000). Down-regulation of the PSI-F subunit of photosystem I (PSI) in Arabidopsis thaliana. The PSI-F subunit is essential for photoautotrophic growth and contributes to antenna function. J.Biol.Chem. **275**: 31211–31218.

Harrer, R., Bassi, R., Testi, M.G., and Sch[illegible]**er, C.** (1998). Nearest-neighbor analysis of a photosystem II complex from Marchantia polymorpha L.(liverwort), which contains reaction center and antenna proteins. Eur.J.Biochem. **255**: 196–205.

Holt, N.E., Fleming, G.R., and Niyogi, K.K. (2004). Toward an understanding of the mechanism of nonphotochemical quenching in green plants. Biochemistry **43**: 8281–8289.

Holt, N.E., Zigmantas, D., Valkunas, L., Li, X.P., Niyogi, K.K., and Fleming, G.R. (2005). Carotenoid cation formation and the regulation of photosynthetic light harvesting. Science (80-.). **307**: 433–436.

Horton, P., Ruban, A. V, and Walters, R.G. (1992). Delta pH-dependent control of chloroplast light harvesting by binding of DCCD to LHCII. Res. Photosynth. **9**: 311–314.

Ihnatowicz.A., Pesaresi, P., Varotto, C., Richly, E., Schneider, A., Jahns, P., Salamini, F., and Leister, D. (2004). Mutants for photosystem I subunit D of Arabidopsis thaliana: effects on photosynthesis, photosystem I stability and expression of nuclear genes for chloroplast functions. Plant J. **37**: 8396–8852.

Jansson, S. (1999). A guide to the Lhc genes and their relatives in Arabidopsis/IT>. Trends Plant Sci. **4**: 236–240.

Jennings, R.C. and Zucchelli, G. (1986). Studies on thylakoid phosphorylation and noncyclic electron transport. Arch. Biochem. Biophys. **246**: 108–13.

Jensen, P.E., Gilpin, M., Knoetzel, J., and Scheller, H. V (2000). The PSI-K subunit of photosystem I is involved in the interaction between light-harvesting complex I and the photosystem I reaction center core. J. Biol. Chem. **275**: 24701–8.

Jensen, P.E., Rosgaard, L., Knoetzel, J., and Scheller, H. V (2002). Photosystem I activity is increased in the absence of the PSI-G subunit. J.Biol.Chem. **277**: 2798–2803.

Jordan, P., Fromme, P., Witt, H.T., Klukas, O., Saenger, W., and Krauss, N. (2001). Three-dimensional structure of cyanobacterial photosystem I at 2.5 A resolution. Nature **411**: 909–917.

Kargul, J. and Barber, J. (2008). Photosynthetic acclimation: Structural reorganisation of light harvesting antenna - role of redox-dependent phosphorylation of major and minor chlorophyll a/b binding proteins. FEBS J. **275**: 1056–1068.

Klimmek, F., Sjodin, A., Noutsos, C., Leister, D., and Jansson, S. (2006). Abundantly and rarely expressed Lhc protein genes exhibit distinct regulation patterns in plants. Plant Physiol **140**: 793–804.

Lam, E., Ortiz, W., Mayfield, S., and Malkin, R. (1984). Isolation and characterization of a light-harvesting chlorophyll a/b protein complex associated with photosystem I. Plant Physiol. **74**: 650–655.

Li, X.P., Bjorkman, O., Shih, C., Grossman, A.R., Rosenquist, M., Jansson, S., and Niyogi, K.K. (2000). A pigment-binding protein essential for regulation of photosynthetic light harvesting. Nature **403**: 391–395.

Liu, Z., Yan, H., Wang, K., Kuang, T., Zhang, J., Gui, L., An, X., and Chang, W. (2004). Crystal structure of spinach major light-harvesting complex at 2.72 A resolution. Nature **428**: 287–92.

Lunde, C., Jensen, P.E., Haldrup, A., Knoetzel, J., and Scheller, H. V (2000). The PSI-H subunit of photosystem I is essential for state transitions in plant photosynthesis. Nature **408**: 613–615.

Ma, Y.Z., Holt, N.E., Li, X.P., Niyogi, K.K., and Fleming, G.R. (2003). Evidence for direct carotenoid involvement in the regulation of photosynthetic light harvesting. Proc.Natl.Acad.Sci.U.S.A **100**: 4377–4382.

Morosinotto, T., Breton, J., Bassi, R., and Croce, R. (2003). The nature of a chlorophyll ligand in Lhca proteins determines the far red fluorescence emission typical of photosystem I. J. Biol. Chem. **278**: 49223–9.

Müller, M.G., Lambrev, P., Reus, M., Wientjes, E., Croce, R., and Holzwarth, A.R. (2010). Singlet Energy Dissipation in the Photosystem II Light-Harvesting Complex Does Not Involve Energy Transfer to Carotenoids. ChemPhysChem **11**: 1289–1296.

Muller, P., Li, X.P., and Niyogi, K.K. (2001). Non-photochemical quenching. A response to excess light energy. Plant Physiol **125**: 1558–1566.

Nelson, N. and Ben-Shem, A. (2004). The complex architecture of oxygenic photosynthesis. Nat. Rev. Mol. Cell Biol. **5**: 971–82.

Nield, J., Funk, C., and Barber, J. (2000). Supermolecular structure of photosystem II and location of the PsbS protein. Philos. Trans. R. Soc. Lond. B. Biol. Sci. **355**: 1337–44.

Nilkens, M., Kress, E., Lambrev, P., Miloslavina, Y., Müller, M., Holzwarth, A.R., and Jahns, P. (2010). Identification of a slowly inducible zeaxanthin-dependent component of non-photochemical quenching of chlorophyll fluorescence generated under steady-state conditions in Arabidopsis. Biochim. Biophys. Acta - Bioenerg. **1797**: 466–475.

Nilsson, A., Stys, D., Drakenberg, T., Spangfort, M.D., Forsén, S., and Allen, J.F. (1997). Phosphorylation controls the three-dimensional structure of plant light harvesting complex II. J. Biol. Chem. **272**: 18350–7.

Niyogi, K.K. (1999). PHOTOPROTECTION REVISITED: Genetic and Molecular Approaches. Annu. Rev. Plant Physiol. Plant Mol. Biol. **50**: 333–359.

van Oort, B., Alberts, M., de Bianchi, S., Dall'Osto, L., Bassi, R., Trinkunas, G., Croce, R., and Van Amerongen, H. (2010). Effect of antenna-depletion in Photosystem II on excitation energy transfer in Arabidopsis thaliana. Biophys. J. **98**: 922–931.

Pagano, A., Cinque, G., and Bassi, R. (1998). In vitro reconstitution of the recombinant photosystem II light-harvesting complex CP24 and its spectroscopic characterization. J. Biol. Chem. **273**: 17154–65.

Pan, X., Li, M., Wan, T., Wang, L., Jia, C., Hou, Z., Zhao, X., Zhang, J., and Chang, W. (2011). Structural insights into energy regulation of light-harvesting complex CP29 from spinach. Nat.Struct.Mol.Biol. **18**: 309–315.

Pascal, A.A., Liu, Z., Broess, K., van Oort, B., van Amerongen, H., Wang, C., Horton, P., Robert, B., Chang, W., and Ruban, A. (2005). Molecular basis of photoprotection and control of photosynthetic light-harvesting. Nature **436**: 134–7.

Passarini, F., Xu, P., Caffarri, S., Hille, J., and Croce, R. (2014). Towards in vivo mutation analysis: Knock-out of specific chlorophylls bound to the light-harvesting complexes of Arabidopsis thaliana — The case of CP24 (Lhcb6). Biochim. Biophys. Acta - Bioenerg. **1837**: 1500–1506.

Pearlstein, R.M. (1982). EXCITON MIGRATION AND TRAPPING IN PHOTOSYNTHESIS. Photochem. Photobiol. **35**: 835–844.

Pesaresi, W.P., Hertle, A., Pribil, M., Kleine, T., Wagner, R., Strissel, H., Ihnatowicz, A., Bonardi, V., Scharfenberg, M., Schneider, A., Pfannschmidt, T., and Leister, D. Arabidopsis STN7 Kinase Provides a Link between Short-and Long-Term Photosynthetic Acclimation.

Pietrzykowska, M., Suorsa, M., Semchonok, D.A., Tikkanen, M., Boekema, E.J., Aro, E.-M., and Jansson, S. (2014). The light-harvesting chlorophyll a/b binding proteins Lhcb1 and Lhcb2 play complementary roles during state transitions in Arabidopsis. Plant Cell **26**: 3646–60.

Pogson, B., McDonald, K.A., Truong, M., Britton, G., and DellaPenna, D. (1996). Arabidopsis carotenoid mutants demonstrate that lutein is not essential for photosynthesis in higher plants. Plant Cell **8**: 1627–1639.

Prasil, O., Adir, N., and Ohad, I. (1992). Dynamics of photosystem II: Mechanism of photoinhibition and recovery processes. In The Photosystems: Stucture, Function and Molecular Biology, J. Barber, ed (Elsevier: Amsterdam), pp. 295–348.

Qin, X., Suga, M., Kuang, T., and Shen, J.-R. (2015). Structural basis for energy transfer pathways in the plant PSI-LHCI supercomplex. Science (80-.). **348**.

Remelli, R., Varotto, C., Sandona, D., Croce, R., and Bassi, R. (1999). Chlorophyll binding to monomeric light-harvesting complex. A mutation analysis of chromophore-binding residues. J.Biol.Chem. **274**: 33510–33521.

Rivadossi, A., Zucchelli, G., Garlaschi, F.M., and Jennings, R.C. (1999). The importance of PSI chlorophyll red forms in light-harvesting by leaves. Photosynt.Res. **60**: 209–215.

Rochaix, J.D. (2007). Role of thylakoid protein kinases in photosynthetic acclimation. FEBS Lett.

Ruban, A. V., Berera, R., Ilioaia, C., van Stokkum, I.H.M., Kennis, J.T.M., Pascal, A.A., van Amerongen, H., Robert, B., Horton, P., and van Grondelle, R. (2007). Identification of a mechanism of photoprotective energy dissipation in higher plants. Nature **450**: 575–578.

Ruban, A. V., Young, A., and Horton, P. (1994). Modulation of chlorophyll fluorescence quenching in isolated light harvesting complex of Photosystem II. Biochim. Biophys. Acta - Bioenerg. **1186**: 123–127.

Ruban, A. V, Lee, P.J., Wentworth, M., Young, A.J., and Horton, P. (1999). Determination of the stoichiometry and strength of binding of xanthophylls to the photosystem II light harvesting complexes. J.Biol.Chem. **274**: 10458–10465.

Ruckle, M.E., DeMarco, S.M., and Larkin, R.M. (2007). Plastid Signals Remodel Light Signaling Networks and Are Essential for Efficient Chloroplast Biogenesis in Arabidopsis. PLANT CELL ONLINE **19**: 3944–3960.

Sacharz, J., Giovagnetti, V., Ungerer, P., Mastroianni, G., and Ruban, A. V (2017). The xanthophyll cycle affects reversible interactions between PsbS and light-harvesting complex II to control non-photochemical quenching. Nat. plants **3**: 16225.

Shapiguzov, A., Ingelsson, B., Samol, I., Andres, C., Kessler, F., Rochaix, J.-D., Vener, A. V, and Goldschmidt-Clermont, M. (2010). The PPH1 phosphatase is specifically involved in LHCII dephosphorylation and state transitions in Arabidopsis. Proc. Natl. Acad. Sci. U. S. A. **107**: 4782–7.

Ben Shem, A., Frolow, F., and Nelson, N. (2003). Crystal structure of plant photosystem I. Nature **426**: 630–635.

Ben Shem, A., Frolow, F., and Nelson, N. (2004). Light-harvesting features revealed by the structure of plant Photosystem I. Photosynth. Res. **81**: 239–250.

Shi, L.X., Hall, M., Funk, C., and Schröder, W.P. (2012). Photosystem II, a growing complex: Updates on newly discovered components and low molecular mass proteins. Biochim. Biophys. Acta - Bioenerg. **1817**: 13–25.

Shikanai, T., Munekage, Y., Shimizu, K., Endo, T., and Hashimoto, T. (1999). Identification and characterization of Arabidopsis mutants with reduced quenching of chlorophyll fluorescence. Plant Cell Physiol. **40**: 1134–1142.

Tardy, F. and Havaux, M. (1996). Photosynthesis, chlorophyll fluorescence, light-harvesting system and photoinhibition resistance of a zeaxanthin- accumulating mutant of Arabidopsis thaliana. J.Photochem.Photobiol.B **34**: 87–94.

Thornber, J.P., Stewart, J.C., Hatton, M.W.C., and Bailey, J.L. (1967). Studies on the Nature of Chloroplast Lamellae. 11. Chemical Composition and Further Physical Properties of. **1**.

Tjus, S.E., Moller, B.L., and Scheller, H. V (1998). Photosystem I is an early target of photoinhibition in barley illuminated at chilling temperatures. Plant Physiol **116**: 755–764.

Tjus, S.E., Scheller, H. V, Andersson, B., and Moller, B.L. (2001). Active oxygen produced during selective excitation of photosystem I is damaging not only to photosystem I, but also to photosystem II. Plant Physiol **125**: 2007–2015.

Umena, Y., Kawakami, K., Shen, J.-R., and Kamiya, N. (2011). Crystal structure of oxygen-evolving photosystem II at a resolution of 1.9 Å. Nature **473**: 55–60.

Varotto, C., Pesaresi, P., Jahns, P., Lessnick, A., Tizzano, M., Schiavon, F., Salamini, F., and Leister, D. (2002). Single and double knockouts of the genes for photosystem I subunits G, K, and H of Arabidopsis. Effects on photosystem I composition, photosynthetic electron flow, and state transitions. Plant Physiol. **129**: 616–624.

Vass, I., Styring, S., Hundal, T., Koivuniemi, A., Aro, E.-M., and Andersson, B. (1992). Reversible and irreversible intermediates during photoinhibition of photosystem II: Stable reduced QA species promote chlorophyll triplet formation. Proc.Natl.Acad.Sci.USA **89**: 1408–1412.

Walters, R.G. (2004). Towards an understanding of photosynthetic acclimation. J. Exp. Bot. **56**: 435–447.

Wei, X., Su, X., Cao, P., Liu, X., Chang, W., Li, M., Zhang, X., and Liu, Z. (2016). Structure of spinach photosystem II–LHCII supercomplex at 3.2 Å resolution. Nature **534**: 69–74.

Wientjes, E. and Croce, R. (2011). The light-harvesting complexes of higher-plant Photosystem I: Lhca1/4 and Lhca2/3 form two red-emitting heterodimers. Biochem. J. **433**: 477–85.

Yakushevska, A.E., Jensen, P.E., Keegstra, W., van Roon, H., Scheller, H. V, Boekema, E.J., and Dekker, J.P. (2001). Supermolecular organization of photosystem II and its associated light-harvesting antenna in Arabidopsis thaliana. Eur.J.Biochem. **268**: 6020–6028.

Yakushevska, A.E., Keegstra, W., Boekema, E.J., Dekker, J.P., Andersson, J., Jansson, S., Ruban, A. V, and Horton, P. (2003). The structure of photosystem II in Arabidopsis: localization of the CP26 and CP29 antenna complexes. Biochemistry **42**: 608–613.

Yamamoto, H.Y. and Kamite, L. (1972). The effects of dithiothreitol on violaxanthin deepoxidation and absorbance changes in the 500nm region. Biochim.Biophys.Acta **267**: 538–543.

Zito, F., Finazzi, G., Delosme, R., Nitschke, W., Picot, D., and Wollman, F.A. (1999). The Qo site of cytochrome b6f complexes controls the activation of the LHCII kinase. EMBO J. **18**: 2961–9.

Zouni, A., Witt, H.T., Kern, J., Fromme, P., Krauss, N., Saenger, W., and Orth, P. (2001). Crystal structure of photosystem II from Synechococcus elongatus at 3.8 A resolution. Nature **409**: 739–43.

Chapter 1

Biogenesis of light harvesting proteins

This chapter was published in

Biochimica et Biophysica Acta, vol 1847861–871 (2015)

Biochimica et Biophysica Acta 1847 (2015) 861–871

Contents lists available at ScienceDirect

Biochimica et Biophysica Acta

journal homepage: www.elsevier.com/locate/bbabio

Review

Biogenesis of light harvesting proteins☆

Luca Dall'Osto, Mauro Bressan, Roberto Bassi *

Dipartimento di Biotecnologie, Università di Verona, 37134 Verona, Italy

ARTICLE INFO

Article history:
Received 5 December 2014
Received in revised form 4 February 2015
Accepted 7 February 2015
Available online 14 February 2015

Keywords:
Photosynthesis
Light-harvesting complex
Thylakoid membrane
lhc gene expression
LHC turnover
LHC targeting and assembly

ABSTRACT

The LHC family includes nuclear-encoded, integral thylakoid membrane proteins, most of which coordinate chlorophyll and xanthophyll chromophores. By assembling with the core complexes of both photosystems, LHCs form a flexible peripheral moiety for enhancing light-harvesting cross-section, regulating its efficiency and providing protection against photo-oxidative stress. Upon its first appearance, LHC proteins underwent evolutionary diversification into a large protein family with a complex genetic redundancy. Such differentiation appears as a crucial event in the adaptation of photosynthetic organisms to changing environmental conditions and land colonization. The structure of photosystems, including nuclear- and chloroplast-encoded subunits, presented the cell with a number of challenges for the control of the light harvesting function. Indeed, LHC-encoding messages are translated in the cytosol, and pre-proteins imported into the chloroplast, processed to their mature size and targeted to the thylakoids where are assembled with chromophores. Thus, a tight coordination between nuclear and plastid gene expression, in response to environmental stimuli, is required to adjust LHC composition during photoacclimation. In recent years, remarkable progress has been achieved in elucidating structure, function and regulatory pathways involving LHCs; however, a number of molecular details still await elucidation. In this review, we will provide an overview on the current knowledge on LHC biogenesis, ranging from organization of pigment–protein complexes to the modulation of gene expression, import and targeting to the photosynthetic membranes, and regulation of LHC assembly and turnover. Genes controlling these events are potential candidate for biotechnological applications aimed at optimizing light use efficiency of photosynthetic organisms. This article is part of a Special Issue entitled: Chloroplast biogenesis.

1. Introduction

Light harvesting is a fundamental step of primary productivity, and the light use efficiency has indeed been identified as a critical factor for biomass and biofuel production in photoautotrophs [1–3]. In the past decade, progress has been made in elucidating both structural and functional bases of light harvesting, and investigation into regulation of antenna protein assembly, turnover and relative abundance, has been an area of considerable interest.

In the photosynthetic apparatus, excitation energy is rapidly transferred among chlorophylls (Chls) to a reaction center (RC), where the occurrence of charge separation events fuels electron transport chain and leads to water oxidation and $NADP^+$ reduction, and catalyzes the generation of a trans-thylakoid protonmotive force and the synthesis of ATP [4]. Within the photosynthetic machinery, a remarkably high quantum efficiency is achieved by the protein scaffold of photosystems (PSs), which keep the Chls at the right geometry and distance, thus avoiding concentration quenching while favoring excitonic interactions and fast energy transfer [5]. Photosystems I and II are membrane-integral, multisubunit pigment–protein complexes, main actors in the light energy conversion process. Both PSs are composed by a core-complex containing the RC, and by an array of membrane-embedded light-harvesting complexes (LHCs), a modular antenna system surrounding the core. All these structural elements together form a so-called supercomplex [6]. Within thylakoid membranes, PSII is located in the region of stacked membrane disks called grana, while PSI is mainly found in the stromatic lamellae, unappressed regions which connect grana stacks [7]. See [8] for a somehow different view.

Evolution generated a wide group of photoautotrophs, ranging from cyanobacteria to higher plants, which optimized photosynthesis for the most diverse environmental conditions occurring together with the enlargement of LHC protein super-family [9], in contrast with the high conservation in the subunits of the PSI and PSII core complexes [10]. Members of the LHC superfamily comprise about 40% of the protein content in the thylakoid membrane and, together, make the most abundant membrane protein on earth. They all share structural motifs with membrane-spanning regions hosting closely spaced and conserved Chl binding residues [11]. As a result LHC subunits have a lower protein/pigment mass ratio (~2) with respect to the core complex or

☆ This article is part of a Special Issue entitled: Chloroplast biogenesis.

* Corresponding author at: Dipartimento di Biotecnologie, Università di Verona, Strada Le Grazie 15, 37134 Verona, Italy. Tel.: +39 045 8027916; fax: +39 045 8027929.
E-mail address: roberto.bassi@univr.it (R. Bassi).

http://dx.doi.org/10.1016/j.bbabio.2015.02.009
0005-2728/

either photosystems (>3), and far lower than non-LHC antenna complexes such as phycobilisomes, which appeared earlier in evolution and were then outclassed by LHCs [12–14].

Besides extending the absorption capacity of the RC supercomplexes, LHC antenna systems regulate PS photochemical efficiency and provide enhanced level of photoprotection. Indeed, while the efficiency of energy conversion is maximal under constant, moderate irradiances, photosynthesis is hampered when the concentration of Chl singlet excited states (^{1}Chl*) in the photosynthetic machinery exceeds the capacity for photochemical quenching [15]. In these conditions the probability for Chl triplet (^{3}Chl*) formation increases leading to release of singlet oxygen ($^1O_2$) [16]. Molecular safety systems are built in LHC proteins which catalyze detoxification of $^1O_2$ [17,18] or prevent its formation by downregulating ^{1}Chl* lifetime [19]. The evolutionary selection of LHCs more efficient in the activation of photoprotective responses has likely been crucial during transition from aquatic to aerial environment in which a concomitant increase in O_2 concentration leads to a higher risk of $^1O_2$ formation and photoxidative damage [13]. The formation of eukaryotic plastids was followed by the diversification of LHC on multiple isoforms, thus leading to a genetic complexity within a conserved supramolecular assembly, whose evolutionary importance emerges by considering that individual gene products are tuned to a different balance between light harvesting and photoprotection capacity [20].

2. LHC: molecular architecture, localization, function

The first structure of a light-harvesting complex obtained by X-ray crystallography was that of trimeric LHCII, the major light-harvesting complex of plants encoded by *lhcb1–3* genes [21,22]. This complex has three membrane-spanning helices (named A, B and C), connected by both stroma- and lumen-exposed loops, and two amphipathic helices (D and E) exposed to the lumenal surface (Fig. 1A). Each monomer binds 4 xanthophylls, 8 Chl *a* and 6 Chl *b* molecules, and two different lipids, phosphatidyl glycerol and digalactosyl diacyl glycerol. More recently, the 2.8 Å resolution structure of the monomeric antenna CP29 (Lhcb4) from spinach was published [23]. The CP29 structure, based on the three membrane-spanning regions and the two amphipathic helices exposed on the lumen surface, revealed great similarities with a LHCII monomer [24]. This protein contains binding sites for 13 Chls and 3 xanthophylls.

In green algae and plants, PSII and PSI are the supramolecular complexes which coordinate the LHC subunits and catalyze the photosynthetic light reactions. The largest PSII supercomplexes purified from plants [6,25] are composed of a dimeric core (C2), surrounded by the nuclear-encoded, outer antenna system which includes four trimeric LHCII, and two copies each of the monomeric antennae CP29, CP26 (Lhcb5) and CP24 (Lhcb6) [26,27]. CP29 and CP26, located nearby the core, mediate the binding of the so-called LHCII-S (strongly-bound, named by their susceptibility to detachment by detergents) [28], while the monomeric subunit CP24 and a trimeric LHCII-M (moderately-bound) enlarge the light harvesting capacity of the complex (Fig. 1B). In green algae, major LHCII components diversified independently with respect to those of higher plants: in *Chlamydomonas reinhardtii*, subunits of trimeric LHCII are encoded by nine Lhcbm genes, called Lhcbm1–m6, m8, m9 and m11 [29], while CP24 orthologs were not detected. The C2S2M2 is the most abundant PSII supercomplex in thylakoid membranes of *Arabidopsis*, either grown in low or high light conditions [6]. The abundance in trimeric LHCII is higher in low light than in excess light (EL) conditions. In both conditions the stoichiometry of trimeric LHCII per monomeric PSII core is higher than two [30,31], suggesting that additional trimers, loosely-bound (LHCII-L) exist that are lost during purification of supercomplexes.

Core complex of PSI is also endowed with a peripheral antenna system called LHCI (light-harvesting complex of PSI), of four antenna proteins (Lhca1–4), one copy per supercomplex [32] (Fig. 1C). Binding of the antenna moiety to the core is strongly cooperative [33] with the Lhca1/4 and Lhca2/3 heterodimers being the minimal building blocks [34]. The composition of the peripheral antenna was found constant irrespective from light conditions [35]. Lhcas were not interchangeable, indeed missing subunits could not be replaced by others in *Arabidopsis* mutants disrupted in individual *lhca* genes [33,36]. In addition to *lhca1–4*, two additional genes, *lhca5* and *lhca6*, were identified in the genome of *Arabidopsis* [11], which encode subunits highly homologous to Lhca1–4, and yet are found in sub-stoichiometric amounts with respect to PSI RC [37]. Consistently, Lhca5 was found to replace missing Lhca4 in a small fraction of PSI supercomplexes [38] and to mediate interaction between PSI and the NADH dehydrogenase-like complex (NDH), forming the supercomplex which drives PSI cyclic electron transport [39,40]. The study of the PSI–LHCI supercomplex in organisms other than higher plants showed differences in the organization [41]. In *C. reinhardtii*, nine Lhca gene products [29] were found to participate to large PSI supercomplexes [42].

Besides the typical three-helix type members, the LHC super-family includes other proteins which share sequence similarity with the former and yet carry significant differences, namely PsbS, LhcSR and the light-harvesting-like (LIL) proteins.

PSBS is a four-helix protein present in all land plants [43], which is essential for the photoprotective mechanism of Excess Energy Dissipation (EED) [44,45] and the EL-dependent reorganization of LHC antenna system within PSII [46,47]. Interestingly, psbS genes are present in many green algae, including *C. reinhardtii*, but the protein was not accumulated in the chloroplast [48], suggesting that this sequence might have a different function in lower organisms.

LHCSR is also essential for EED [49], but in green algae and mosses, while plants lack orthologs. In *C. reinhardtii*, LHCSR has been first described as a stress-related protein, whose transcripts accumulate in response to EL conditions [49,50] as a component of an early photoprotective type [51,52].

LIL [11,37] proteins which are found in both plants and algae differ in their number of transmembrane segments: the three-helix early light-inducible proteins (ELIPs), the one-helix proteins (OHPs) and the stress-enhanced proteins (SEPs) are likely involved in photoprotection rather than in light harvesting [53,54]. Although these subunits are not constitutive components of PSs, biochemical evidences suggest that they can establish weak interactions with PSs [55]. Their mode of action was proposed to include regulation of pigment biosynthesis [56] and/or scavenging of reactive oxygen species (ROS) [57].

The main function of LHCs is to harvest photon energy, delocalize excitons for significant time lengths (ns) and transfer excitation energy to the RCs to drive electron transport [5,58]. Besides light absorption, remarkable properties of the LHC proteins are the ability (i) to actively regulate PSII quantum efficiency and (ii) to catalyze photoprotective reactions (Fig. 2). Fluctuations of light intensity, temperature, nutrients and water availability on a daily as well as seasonal basis yield into changes of excitation pressure on PSII, by affecting the capacity for photochemical quenching of ^{1}Chl* [15] and to increased $^1O_2$ release [59,60]. Activation of photoprotective safety systems is thus mandatory in order to either scavenge ROS or limit their release [61]. LHC subunits have key roles in these processes. Lhcb proteins are ideal candidates for a role in down-regulation of ^{1}Chl* lifetime through the process of EED, that safely dissipates excitation energy in excess [19]: indeed, the depletion of LHC proteins is obtained in *ch1* mutants, and leads to depletion of EED [62] and to a dramatic increase in photosensitivity [18,63]. Xanthophylls bound to the LHC proteins protect the complex against $^1O_2$ formation, by either quenching ^{3}Chl* or directly scavenging $^1O_2$ [64–66]. Additional LHC-dependent regulation is the lateral migration of phosphorylated LHCII trimers, triggered by PQ over-reduction, to stroma-exposed membranes where they connect to PSI, balancing excitation distribution of PSs via the so called state I–state II transition (ST) [67,68]. In *C. reinhardtii*, the amplitude of ST is far larger than in higher plants, possibly due to phosphorylation of CP26 and CP29 in addition to that of LHCII. This appears to dissociate PSII supercomplexes since CP29, CP26 and LHCII trimers were all found to become associated to the PSI–LHCI

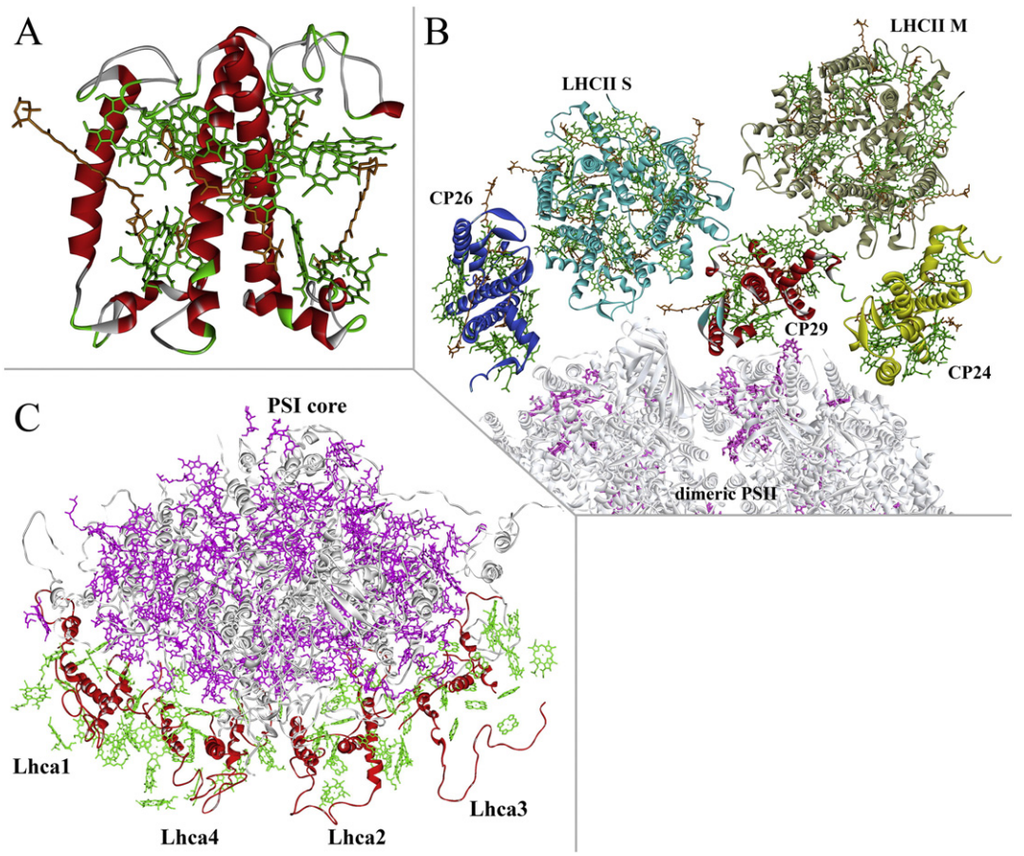

Fig. 1. Model of the structure of (A) monomeric LHCII, side view, (B) photosystem II supercomplex C2S2M2 and (C) photosystem I supercomplex, top view. The C2S2M2 model has been assembled using the crystal structures of monomeric antenna CP29 and trimeric LHCII [21,23], the cyanobacterial PSII core [185], and the plant PSI–LHCI supercomplex [186]. For the monomeric antennas CP26 and CP24, the structure of CP29 has been used. Color legend for the supercomplexes: core complexes, silver; LHCII-M, gray; LHCII-S, cyano; CP29, red; CP24, yellow; CP26, blue; LHCI, red; Chls of core complex, violet; Chls of LHC, green; and xanthophylls, orange. For clarity, the phytol chains of the Chls have been hidden.

under conditions promoting ST [69–71]. The idea of a simple balance between PSs was recently challenged by the finding that the increase in PSI antenna size is much smaller than expected in the assumption that all LHCII disconnected from PSII actually becomes an antenna for PSI [72]. Long-term photoacclimatory responses consist into the stoichiometric reduction of the trimeric LHCII complement, relieving chronic over-excitation on the PSII [73].

3. Biogenesis of LHC: expression, import, membrane insertion and assembly with chromophores

Long-term acclimatory responses in plants and algae allow for a feedback to environmental changes occurring on a time-scale of hours to days [37,74–76]. Such responses include the stoichiometric regulation of PSI/PSII ratio, and the adjustment of antenna size to PS's ability of using excitation energy from harvested photons [35,77]. Regulation of light-harvesting requires fine-tuning in response to environmental cues: indeed, expression of antenna proteins is regulated on multiple levels from mRNA transcription to protein degradation. Acclimation requires the coordinated expression of genetic information located in both nuclear and plastid genomes. In the case of LHC, mRNAs are translated in the cytosol, and precursors are then imported into the chloroplast, addressed to the photosynthetic membrane, folded with chromophores and assembled with the plastid-encoded subunits of the core complex [78] (Fig. 3).

Light strongly regulates transcription of *lhc* genes depending on phytochrome activity. Thus mRNAs encoding antenna subunits undergo circadian as well as shorter term fluctuations [79] with up-regulation in light-limiting conditions and repression in EL. There is evidence of a blue light-dependent mechanism which regulates photoacclimation in algae [80,81] most of which do not have phytochromes, while the importance of photoreceptors in sensing and responding to EL by transcriptional regulation appears negligible in higher plants [82].

Since the different components of PSs are encoded by distinct genomes, matching stoichiometric balance with environmental stimuli requires a concerted gene expression. Coupling light sensing and regulation of *lhc* gene expression involves the so-called retrograde (plastid to nucleus) signals, for which multiple pathways have been proposed [83]. A direct correlation has been reported between level of *lhc* gene transcription and protein accumulation level [37,84–86]. Response to environmental cues involves fast (<1 h) transcriptional regulation, and analysis of expression patterns allowed to identify associations of gene products which participate to the same molecular pathways. However, a number of contrasting results have questioned a major role of *lhc* gene transcriptional regulation in the long term acclimatory response: algal cells grown under limiting CO_2, a condition which severely overexcites PSII, underwent no significant changes in the level of LHCBM mRNAs [87]; the prompt down-regulation of *lhc* gene transcription by EL exposure is relieved within 24 h under EL treatment and does not lead to any decrease of the corresponding gene products [85,88], implying the action of other regulatory mechanisms.

A comparison between transcriptomic and proteomic dataset highlighted a major role of post-transcriptional control of LHC content in barley [89]. In *Arabidopsis*, light intensity strongly affected global translation by cytoplasmic ribosomes, and differentially regulates specific transcripts within the LHC superfamily [90]. A link between *lhc* message translation in the cytosol and photosynthetic

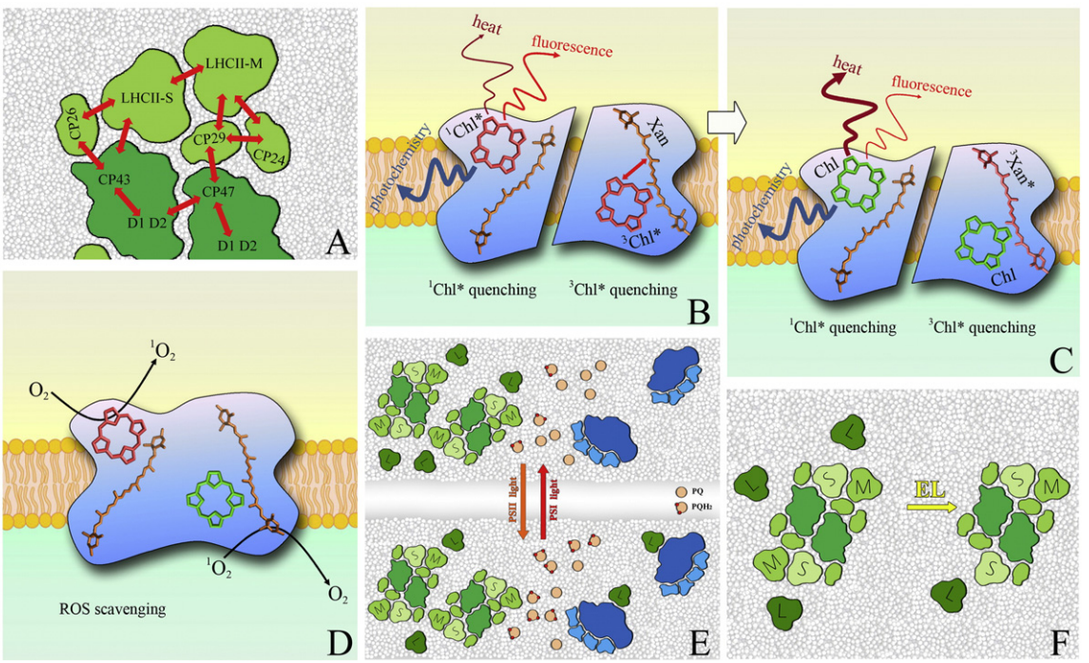

Fig. 2. Functional roles of LHC proteins. (A) Excitation energy transfer: connectivity among antennae and with the core subunits is represented according to [187]. (B, C) Regulation of ^{1}Chl* and ^{3}Chl* de-excitation: conformational changes of LHC to a dissipative state decrease ^{1}Chl* lifetime and promote thermal dissipation of excitation energy in excess; while, zeaxanthin binding to LHC modulates ^{3}Chl* formation in vivo. Both processes lower the yield of potentially dangerous Chl excited states on the complexes, thus preventing ROS formation. (D) ROS scavenging: xanthophylls preserve PSII from photoinactivation and protect membrane lipids from oxidation, being particularly active against singlet oxygen; photoprotection capacity of xanthophylls is enhanced upon binding to LHC. (E, F) Lateral migration of phosphorylated LHCII balances excitation delivery between PSII (green) and PSI (blue) via the so called state I–state II transition (E), while the EL-induced reduction of Lhcb stoichiometry is a long-term photoacclimatory response, aimed at counteracting prolonged over-excitation on the PSII (F). PSII:LHC supercomplexes are depicted according to [30,188].

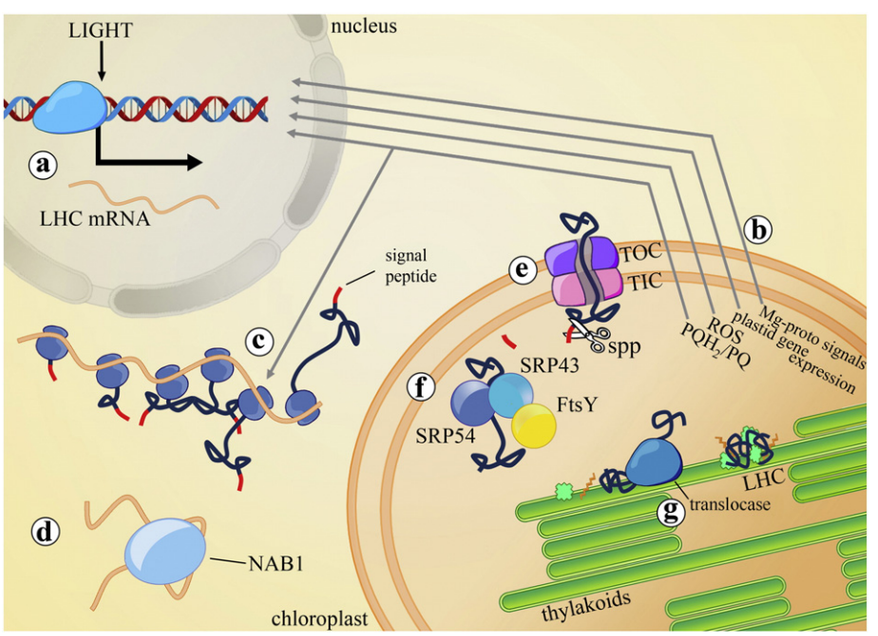

Fig. 3. Life cycle of a LHC. The diagram displays an overview of regulatory events and co-ordination between the nucleus, cytoplasm and chloroplast, which overall adjust LHC expression, import in the organelles and insertion into the photosynthetic membrane. (a) Environmental signals such as circadian rhythm and diurnal fluctuation of lights regulate *lhc* gene transcription. (b) Upon sensing environmental stimuli, chloroplasts communicate their functional status to the nucleus. A number of pathways have been involved in the regulatory signaling of photosynthetic gene expression; PQ redox state and plastid gene expression affect Lhcb transcription. (c) The redox state of PQ pool is linked to post-transcriptional regulation of *lhc* gene expression. (d) In *C. reinhardtii*, the cytosolic RNA-binding protein NAB1 interacts with specific Lhcbm transcripts, leading to translational repression. (e) TOC and TIC, translocons of the envelope membrane, mediate translocation of LHC precursor in the stroma and cleavage of the signal peptide. (f) LHC in the stroma is captured by the dimeric cpSRP; interaction with the SRP receptor cpFtsY brings LHC to the Alb3/Alb4 translocases, which mediate the co-translational targeting of the polypeptide into the thylakoids. (g) In the photosynthetic membrane, pigment binding might proceed by a self-assembly or by means of a folding machinery. Further details are discussed in the text.

activity was observed in seedlings treated with DCMU, an inhibitor of the photosynthetic electron transport: DCMU impaired light-dependent translational induction while did not affect the up-regulation of Lhcb transcripts upon dark to light transition [91]. In *C. reinhardtii*, analysis of polysomal profile upon photoacclimation to EL revealed translational repression of specific LhcbM [76]. NAB1, a cytosolic RNA-binding protein lacking in a *Chlamydomonas* mutant affected on photoacclimation, modulates LhcbM composition by selectively interacting with specific *lhcbm* transcripts [92], which are sequestrated in sub-polysomal mRNA–ribonucleoprotein complexes thus leading to translational repression. Activity of the repressor was regulated through Arg methylation [93] and thiol modification [94], and is thus linked to the redox condition of the cytosol, which in turn is reliant on the photosynthetic electron transport rate. However, many details on the regulation of photosynthetic gene expression still remain elusive, as well as the identity of the retrograde signals which modulate nuclear gene expression to the status of the plastid. Also in *Chlamydomonas*, plastoquinone (PQ) redox state affects expression of several *lhcbm* genes, whose transcription is repressed upon exposure to EL [85]. This is consistent with the redox state of plastoquinol (PQH_2) being the rate-limiting step of photosynthetic electron transport and thus reflects the balance between photon absorption and energy utilization by downstream reactions. In plants, the role of PQ redox state in regulating *lhc* gene transcription is controversial [95,96]. However, in barley [89] redox state of PQ was found to control post-transcriptional regulation of *lhc* genes [89]. Additional pathways have been involved in the regulatory signaling of photosynthetic gene transcription including intermediates of tetrapyrrole biosynthesis, ROS [97], coupling to plastid gene expression [98], secondary metabolites [99] and carotenoid oxidation products [100].

LHC proteins are synthesized on cytosolic ribosomes, in the form of precursors carrying an N-terminal transit peptide for addressing to the protein import machinery of the chloroplast. The latter is a multiprotein complex of the envelope membrane composed by the TOC and TIC translocons [101,102], respectively inserted in the outer and inner envelope membranes, which mediates precursor translocation towards the plastid stroma compartment [103]. Once in the stroma, transit peptide is taken away by the stromal processing peptidase (spp), then the mature LHC polypeptides are targeted and integrated into the thylakoids following a SRP-dependent pathway [104]. TOC34, one of the three subunits forming the core complex of TOC, is encoded by a single gene in *Chlamydomonas* [105], while two paralogs in *Arabidopsis* (AtTOC33, AtTOC34) form functionally different TOC translocons [106]; AtTOC33 depletion led to an impaired assembly of the photosynthetic machinery, and that subunit was proposed as the preferential pathway for import of LHC proteins [107]. The main pathway by which LHC subunits are targeted to the thylakoid membranes involves identification and capture by a plastidic signal recognition particle (cpSRP), a heterodimeric protein complex comprised of cpSRP54 and cpSRP43 [108]. Binding of LHC polypeptide to the cpSRP involves a conserved sequence motif, called L18, which is localized in between helices A and C [109]. Once assembled, this complex interacts with cpFtsY, homologous to the bacterial SRP receptor, which bring LHCs to the Alb3/Alb4 translocases [110]. The latter catalyze the GTP-dependent, co-translational targeting of the polypeptide into the thylakoids, which together with pigment binding yields into a functional light-harvesting complex [108,111].

Mutations affecting components of cpSRP targeting pathway lead to a phenotype of truncated Chl antenna size. *Chlamydomonas tla3* mutant, which exhibited a 90% reduction in the Lhcb complement per PSII RC, was deleted in a gene homolog to the cpSRP43 [112]. *Arabidopsis* mutant plants devoid of both 43- and 54-kDa subunits of the cpSRP had severely impaired accumulation of LHCs in thylakoids although still viable [113]. Interestingly, retention of the different LHCs was uneven: some (Lhca1, Lhcb3) were completely missing, while others (Lhcb1, Lhcb6) were in part retained or even enriched with respect to WT plants (Lhcb4). The maintenance of functional LHC targeting to the thylakoids, even in plants in which cpSRP pathway was missing, suggests that more than one targeting mechanism is active. Indeed, evidence for a second pathway in the import step can be postulated based on evidences in *Chlamydomonas* [114] and in *Arabidopsis* [115]. Association between TIC and chlorophyllide *a* oxygenase (CAO) was suggested to be required for Lhcb1 and Lhcb4 import, with CAO participating to Chl *b* supply to the nascent LHC complexes, before it was delivered to thylakoids via fusion of vesicles budding from the inner envelope membrane [116]. Based on a dual location of CAO, in the inner envelope and thylakoid membranes, the existence of two different import/assembly pathways (cpSRP- and CAO-dependent) for LHCs has been suggested. However, *Arabidopsis* mutant lacking CAO activity [117] showed that Chl *b* depletion did not affect import of LHC precursors, processing to mature form and insertion into thylakoids. Regardless of whether LHC polypeptide accumulation, folding and binding of pigment take place in the inner envelope or in the thylakoid membranes, it is clear that our knowledge on molecular mechanisms for LHC targeting is still poor.

cpSRP is proposed to maintain the antenna complex in an unfolded form devoid of pigments prior to delivery to the membrane [118]. Pigment binding is mandatory for LHC stability into thylakoids; indeed, apoproteins do not accumulate in the absence of chromophores [119]. Little is known on how chlorophylls and xanthophylls are provided to the nascent complexes.

Hoober et al. [114] proposed that LHCII assembly takes place in the inner envelope of the chloroplast and consists of 4 steps: (i) partial LHC insertion until a stop-transfer region within the B helix enters the membrane; (ii) binding of Chl molecules which allows the LHC complex to reach a stable conformation and be retained in the membrane; (iii) insertion of helix A and C domains in the membrane; and (iv) further pigment binding and fixing of the ion bridges between helices A and B, yielding into a fully assembled LHC pigment–protein. Alternatively, it has suggested that assembly of LHCs in the thylakoids requires translocation of both the luminal loop and the hydrophilic C terminus across the membrane. Both these models still await experimental confirmation. It is still possible that LHC insertion and folding with pigments is a spontaneous process following ALB3/4 catalyzed steps. This is suggested by the possibility of obtaining in vitro pigment–protein complexes, indistinguishable from those purified from chloroplasts, from its apoprotein and chromophores [120,121]. The possibility of step-triggering the folding process by sequential addition of individual chromophores has been exploited to track LHC folding dynamics by time-resolved spectroscopy experiments, which have monitored the establishment of excitation energy transfer between Chls *a* and *b* [122] or from Chls to an acceptor dye [123] in the nascent complex. These experiments showed that pigment binding and building of the protein secondary structure are closely coupled events and occur with the same kinetics. In particular, folding of LHCII in vitro occurred into a faster step (10–60 s) followed by a slower process requiring several minutes [124] (Fig. 4). The fast phase was attributed to Chl *a* binding, whereas slow binding events were dependent on Chl *b* binding [123]. Time-resolved circular dichroism spectroscopy showed the formation of α-helices during both phases [125]. Double electron resonance spectroscopy, which measures the distances between two spin label pairs, was recently used to gain insights into LHCII folding [126]. Results showed that achievement of the tertiary structure, through the formation of ion bridges between helices A and B, and binding of the last pigments, were late steps in LHCII folding, which strengthen the complex and enabled molecular interactions with partners in the photosystem.

Although this unique property of LHC proteins is consistent with self-assembly [127], it must be considered that folding in vitro occurs at very high pigment concentration, while it appears unlikely that Chl molecules can freely diffuse in thylakoids without yielding dangerous photochemical reactions [60]. Since individual LHCs showed a highly reproducible pigment composition in vivo [128–132], the question arises how such a specificity is maintained for at least ten distinct antenna proteins that

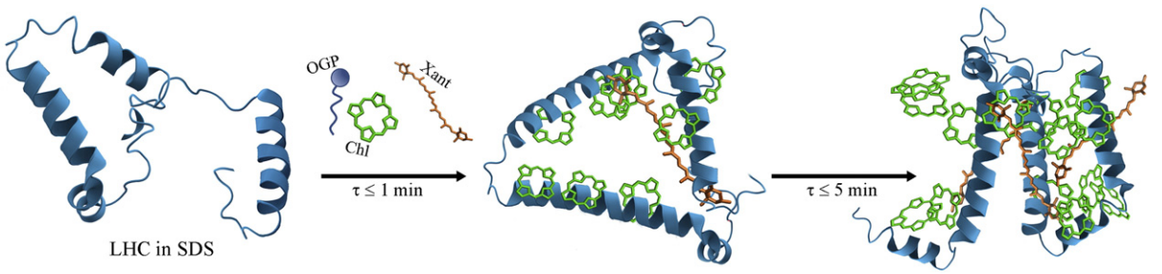

Fig. 4. In vitro folding dynamic of LHCII. The model proposed by [126] is displayed. Upon mixing LHCII apoprotein with pigments, folding was shown to occur in two phases. Both phases are triggered by pigment binding, and correspond to acquisition of complete secondary ($\tau_1 \leq 1$ min) and tertiary ($\tau_2 \leq 5$ min) structures, respectively. Abbreviations: SDS, sodium dodecyl sulfate; OGP, octyl β-D-glucopyranoside; Chl, chlorophylls; and Xant, xanthophylls.

are assembled in close proximity, i.e. with a similar accessibility to chromophores. Whether a pigment delivery step mediated by a specific carrier is involved, or if LHC folding occurs coupled to the final steps of pigment biosynthesis [133,134] is unknown, since no mutants impaired in such a function have been identified so far. The integral membrane complexes Alb3/Alb4 are needed for the accumulation of LHC in the thylakoids [110]. Thus, in the hypothesis that assembly with pigments proceeds under the control of a folding machinery, Alb3/Alb4 appears as potential components of such a still unknown putative assembling supercomplex.

4. Role of chromophores in the biogenesis of LHCs

Chlorophylls and xanthophylls are structural elements of LHCs, and have been shown to be essential for pigment–protein folding in vitro [135]. In vivo, the assembly of LHC apoproteins with their cofactors is a checkpoint in the modulation of LHC abundance, which interacts with transcriptional and translational regulatory networks. Indeed, no LHC proteins accumulate in the absence of pigment synthesis [136,137] and stoichiometric adjustment of the photosynthetic subunits requires a coordinated biosynthesis of apoproteins and chromophores [138].

In particular, Chls *a* and *b* are both required for stabilization of the apoproteins and assembly of the majority of antenna complexes in higher plants [139]; this is consistent with the evidence that lack of Chl *b* in *ch1* mutant of *Arabidopsis* yielded into near-complete depletion in LHCs [18,62]. Instead, lack of Chl *b* does not impair LHC assembly in the green alga *C. reinhardtii* [140]. Marine photoautotrophs evolved a variety of Chl species [141,142] while land plants all have Chls *a* and *b* as the only light harvesting porphyrins, both being needed for LHC biogenesis, thus suggesting a specific function in folding for each. While the universal role of Chl *a* in the photochemistry is well established, it is interesting to assess whether Chl *b* has a regulative role for LHC biogenesis besides the enhancement of light-harvesting cross-section.

Crystal structure of plant LHCs showed distinct and specific Chl *b* binding sites [21], thus suggesting that Chl distribution is regulated by their binding affinity. In vivo changes in the Chl *a*/*b* ratio of antenna complexes by irradiance during growth have never been reported in WT plants. However, the Chl *a*/*b* ratio of thylakoids has been altered by impairing the Chl *b* metabolism through the overexpression of a cyanobacterial CAO gene in *Arabidopsis* [143] leading to an increased Chl *b* abundance and a higher LHCII content with respect to WT. This led to the hypothesis that CAO activity (i) determines the rate of Chl *b* biosynthesis and (ii) regulates LHC biogenesis and light acclimation [144]. Indeed, acclimation of WT plants to either low- or high-light involves modulation of both CAO activity [145] and Chl *b* content, which leads to changes in PSII antenna size. The mechanism responsible to such a Chl *b*-dependent accumulation of LHCs is still unknown, although Tanaka and Tanaka [144] hypothesized that LHCII does not acquire a proper conformation below a minimal Chl *b* threshold, making it a better substrate for proteases. Whether this hypothetical mechanism is actually important in vivo and how it is interfaced with regulation of *lhc* gene transcription/translation regulation in the cytoplasm, is still to be assessed.

LHC chromophores also include the xanthophylls lutein, neoxanthin and violaxanthin. The latter is exchanged with zeaxanthin (Zea) which is only synthesized upon EL exposure. In vitro reconstitution analyses revealed xanthophyll binding sites with high specificity [121]. In vivo, however, xanthophyll binding site appears to be more promiscuous as judged by the observation that xanthophyll biosynthesis mutants showed little modifications of Chl to Car ratio and LHC abundance with respect to WT plants [65,66,146,147].

Exception to this pattern is Zea, the only xanthophyll in the *npq2 lut2 Arabidopsis* mutant which, in consequence, undergoes a decrease of PSII antenna size due to a selective destabilization of LHCs [148]; the effect was also observed in the *C. reinhardtii* mutant *npq2 lor1* [149] with similar xanthophyll composition, suggesting that Zea might down-regulate PSII biochemical antenna size. Since Zea binding to LHCs was shown to trigger a conformational change [150], the Zea-binding LHC might become available for proteolysis; this would allow closing the feed-back loop in which overexcitation leads to thylakoid lumen acidification and activation of VDE (violaxanthin de-epoxidase) yielding into accumulation of Zea, which binds to antenna proteins leading to their degradation and decreased lumen acidification, adjusting LHC complement to the average incident light. Even before LHC degradation, Zea binding increases Chl triplet quenching efficiency and ROS scavenging, thus partially relieving photoxidative damage in both PSs [151,152].

The strongest effect on the biogenesis of LHCs comes from limitation in the relative abundance of the total pool of xanthophyll vs carotenes, rather than from changes in composition within the pools. In *Arabidopsis*, combination of mutations of xanthophyll biosynthesis yielded into an eight-fold decrease in xanthophyll/carotenoid ratio with respect to WT [153]. As a consequence, LHCII to PSII core complex stoichiometry was strongly decreased. This was in striking contrast with the case of PSI, where the LHCI to RC ratio was the same as in WT. Decreasing xanthophylls to carotene ratio had a strong effect into the total amount of PSI, which decreased together with xanthophyll abundance till its complete depletion in the xanthophyll-less mutant [137]. Since PSI core only binds β-carotene, while xanthophylls are components of LHCI, the most obvious conclusion is that PSI requires LHCI for its stability. However, this is not the case since *ch1* mutant lacks Lhca proteins and yet has an efficient PSI activity. The lesion in *ch1* leaves the mutant without Chl *b*, while its content in xanthophylls is nearly WT. We conclude that a xanthophyll-dependent coupled mechanism exists for the co-regulation of PSII antenna size and the PSI core complex, which is consistent with the maintenance of a proper redox state of PQ pool. This mechanism appears to be effective in the regulation of both the antenna size with respect to light intensity and PSI to PSII ratio, in an integrated plot (Fig. 5).

The limitation in PSI accumulation was shown to be due to a decreased translation efficiency of PsaA core complex subunit. The connection with xanthophyll availability is still to be elucidated but it is well possible that xanthophylls might affect the activity of the Alb3/4–cpSRP complex, which acts in both PsaA and LHC insertion into the thylakoid

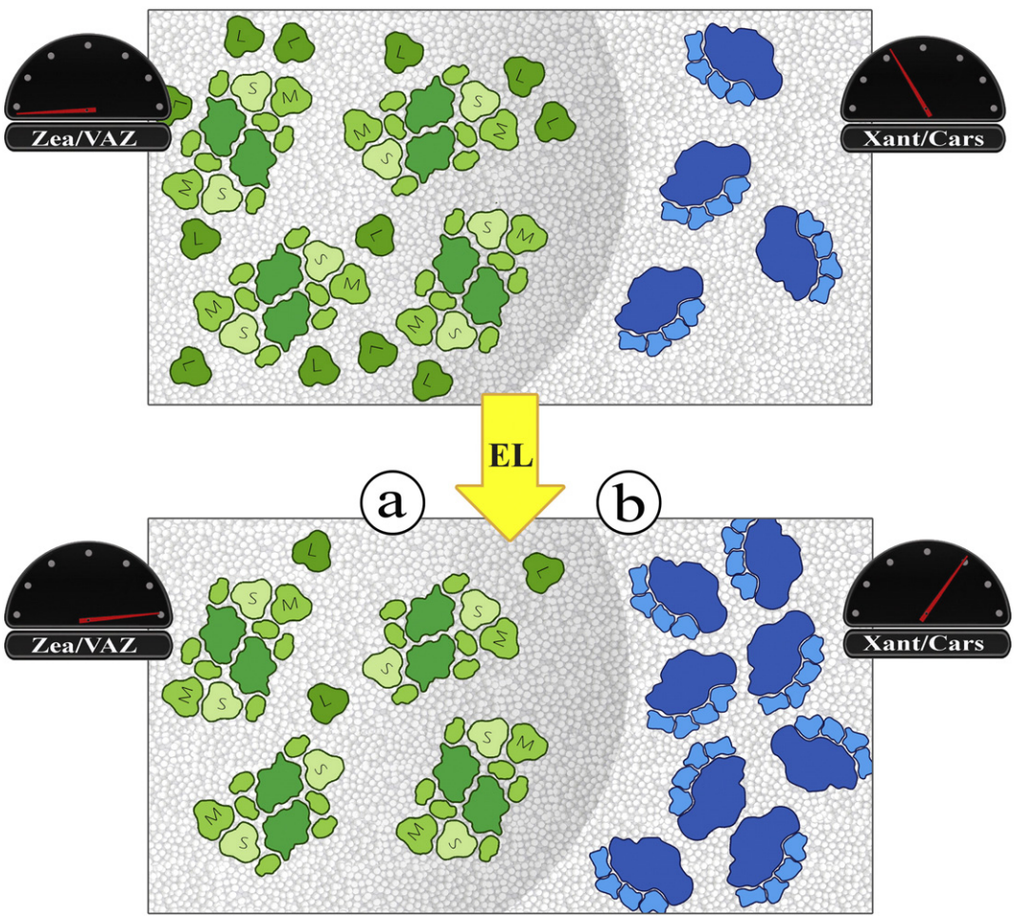

Fig. 5. Scheme of the regulation of PSII antenna size and PSI to PSII ratio as assessed in *Arabidopsis* xanthophyll biosynthesis mutants. (a) Zeaxanthin down-regulates PSII biochemical antenna size: its binding to LHCs triggers a conformational change of the complex, which might become available for proteolysis. (b) The modulation of xanthophyll to carotene ratio in EL would reflect into an adjustment of PSI level. Such a xanthophyll-dependent coupled mechanism, co-regulating PSII antenna size and PSI to PSII ratio, is consistent with the maintenance of a proper redox state of PQ pool. VAZ, violaxanthin + antheraxanthin + zeaxanthin; Xant, xanthophylls.

membrane. Within LHC superfamily, Lhca proteins show a higher affinity for xanthophylls. This effect might be ascribed to the capacity of LHCI of binding small amounts of β-carotene [154], at difference with LHCII.

5. Degradation of LHCs during acclimation and senescence

Despite the paramount importance of intramembrane proteolytic events which take place in the chloroplasts, present knowledge about the identity of proteases involved and the mechanism of their regulation is limited [155]. In particular, even less is known about the proteases involved in the regulation of LHC turnover.

Under low irradiance, turnover of LHCs is very slow, insomuch as being hardly detectable [156]. The half-life of LHCs was determined by short-term labeling in vivo with ^{35}S-methionine, and was found around 10 h in *Lemna minor* [157] and much slower in *Phaseolus vulgaris* [158] since no LHCII degradation was detected within 24 h. However, treatments such as light-to-dark transition, EL conditions or senescence induced by prolonged darkness, speed-up turnover rate of LHCs.

In particular, during photoacclimatory response to EL, a strong decrease in the level of Lhcb polypeptides per PSII RC is detected within a few hours by the application of the stress. These changes are not coupled to any significant change of *lhcb* gene transcription, and were thus attributed to a post-transcriptional regulatory mechanism [90], possibly modulated by the PQ redox state [89]. Another possibility is that regulation of LHC abundance is achieved by tuning turnover rate. Consistent with this idea, EL up-regulates expression of a number of chloroplastic proteases [159]. Up to now, such mechanisms have been mainly investigated in higher plants, and early results suggested that Ser/Cys-type proteolytic enzymes were implicated in LHCII degradation during chloroplast development [160] or participated to the ATP-dependent proteolysis of LHCII upon acclimation to EL [161,162]. The proteolytic enzyme, found associated to the surface of stroma-exposed thylakoid domains, was shown active in degrading de-phosphorylated form of LHCII in vitro. Moreover, a SppA protease was suggested to participate to LHCII degradative regulation [163]. Substrate specificity and mechanism of substrate recognition of EL-induced, thylakoid-bound proteases were studied in vitro by means of wild-type and mutant recombinant LHCII: results showed that the N-terminal domain of the antenna was needed for the protease–substrate recognition, thus suggesting that the degradative event originates at the N-terminal region [164].

More recently, a metalloprotease was identified as responsible for Lhcb1 degradation during chloroplast senescence induced by prolonged darkness [165]; such an enzyme is an integral protein of thylakoids, requires ATP and either Mg^{2+} or Zn^{2+} for activation, and was present even in chloroplasts of illuminated leaves, although in an inactive form. In *Arabidopsis*, a reverse genetic approach allowed to identify FtsH6 as the protease involved in degradation of LHCII, which occurs during photoacclimatory response to EL conditions [166]. In a more recent study [167] a chloroplastic AtFtsH heterocomplex was shown to be involved in stress-dependent degradation of Lhcb1–2–3 apoproteins. In *Arabidopsis* Deg1, a serine-type, thylakoid extrinsic protease, was shown to induce cleavage of the monomeric antennae CP26 and CP29

in response to EL [168,169], while Deg2 triggers degradation of the monomeric antenna CP24 in response to high-temperature and high-light stress [170]. The latter result is consistent with the evidence that CP24 underwent the most rapid decline among the Lhcb complexes during acclimation to EL in *Arabidopsis* [35].

Thus, a number of proteases were shown able to catalyze proteolysis of Lhcb subunits, but the level of redundancy of the system is still unclear. None of the FtsH sequences encoding for chloroplastic proteases were up-regulated in high light [171]. Although degradation of pigment–protein complexes is expected to be a highly regulated process in order to avoid photochemical damage of PSs, a regulatory network for LHC proteolytic activities of the chloroplast has not yet been described.

Monomerization of the major antenna may represent the triggering event of degradative response, indeed the monomeric forms of LHCII are targeted for proteolysis, while the trimeric forms are not [164]. Another possibility is that activation of proteolysis is triggered by the recognition of amino acids on exposed, unfolded region of the target protein, possibly located either at the N-terminal domain [172] or in the luminal loop regions [173]. The chloroplast protein SGR, recently identified by studying a stay-green mutant line in *Oryza sativa* [174], has been associated with the first events of destabilization of the LHC proteins, which are obligatory steps for degradation of Chls and antenna polypeptides [175]. Another possible scenario is that Chl *b* degradation is the first event that precedes and triggers proteolysis [176], this model strengthened by the evidence that FtsH lacks a strong unfoldase activity. However, it is reasonable to assume that initiation of the proteolytic reaction is the rate-limiting step, while the subsequent degradative steps might be very fast, since no degradation products can be detected in vivo once LHC dismantling is triggered by EL or sustained darkness [177].

6. Concluding remarks

During the last decade, considerable progress has been achieved with respect to both molecular and functional characterization of light-harvesting in green algae and plants. Structures of LHCII and CP29 [23] were elucidated at the atomic level, and new insights were gained on the organization and the interactions of PS supercomplexes within the thylakoid membrane [6]. Mutations affecting either the cpSRP-dependent pathway [112] or the cytosolic translation efficiency [94] showed that such mechanisms are target for reducing cellular pigment content and PS antenna size. Therefore, they potentially represent biotechnological strategies for optimizing photosynthetic yield of algal mass culture [3]. A number of studies have led to our present understanding of the photoprotective mechanisms of EED, localized within the LHC moiety [178–181]. Capacity of prompt response to fluctuating light has been predicted to affect canopy photosynthesis by up to 30% [182], thus comprehension of molecular details of thermal dissipation opens the possibility to manipulate light-use efficiency in order to enhance crop productivity [183,184].

By contrast, several aspects of biogenesis of LHC still remain poorly understood. Some of them concern the role of *lhc* expression regulation in the long term photoacclimation. Research on the cross-talk between chloroplast and nucleus in plant cells showed that post-transcriptional control of LHCs is mediated by a signal from the chloroplast, affecting translation in the cytoplasm [90] and whose molecular nature is still unknown. The existence of a retrograde signaling that synchronizes *lhc* gene expression to the status of the chloroplast is largely accepted, but again its molecular identity still remains elusive. Understanding of LHC precursors targeting and insertion in the photosynthetic membranes is still limited with respect to whether assembly of the complete LHC proceeds through a spontaneous folding with recruitment of free chromophores, or involves an assembly supercomplex. Finally, identification and characterization of proteases involved in LHC degradation, and comprehension on how polypeptide and pigment turnover interact with each other, are key steps for understanding the life cycle of antenna proteins.

Evolution has diversified LHCs into a large and diverse group of proteins which, despite only apparent redundancy, were shown to be crucial in adapting to a range of (even extreme) environmental conditions, thus they represent a base of genetic variability which offers perspective for the enhancement of light-to-biomass conversion efficiency, particularly in non-natural environments such as photobioreactors.

Acknowledgements

This work was supported by the Marie Curie Actions — Networks for Initial Training Accliphot (PITN-2012-316427). Because of space constraints, a number of noteworthy publications have not been cited or discussed properly. We apologize to the authors for this lack of completeness.

References

[1] J. Beckmann, F. Lehr, G. Finazzi, B. Hankamer, L. Wobbe, O. Kruse, Improvement of light to biomass conversion by de-regulation of light-harvesting protein translation in *Chlamydomonas reinhardtii*, J. Biotechnol. 142 (2009) 70–77.
[2] P.G. Stephenson, C.M. Moore, M.J. Terry, M.V. Zubkov, T.S. Bibby, Improving photosynthesis for algal biofuels: toward a green revolution, Trends Biotechnol. 29 (2011) 615–623.
[3] S. Cazzaniga, L. Dall'Osto, J. Szaub, L. Scibilia, M. Ballottari, S. Purton, R. Bassi, Domestication of the green alga *Chlorella sorokiniana*: reduction of antenna size improves light-use efficiency in a photobioreactor, Biotechnol. Biofuels 7 (2014) 157.
[4] N. Nelson, C.F. Yocum, Structure and function of photosystems I and II, Annu. Rev. Plant Biol. 57 (2006) 521–565.
[5] H. Van Amerongen, R. Croce, Light-harvesting in photosystem II, Photosynth. Res. 116 (2013) 251–263.
[6] R. Kouril, J.P. Dekker, E.J. Boekema, Supramolecular organization of photosystem II in green plants, Biochim. Biophys. Acta, Bioenerg. 1817 (2012) 2–12.
[7] B. Andersson, J.M. Anderson, Lateral heterogeneity in the distribution of chlorophyll–protein complexes of the thylakoid membranes of spinach chloroplasts, Biochim. Biophys. Acta 593 (1980) 427–440.
[8] M. Suorsa, M. Rantala, R. Danielsson, S. Jarvi, V. Paakkarinen, W.P. Schroder, S. Styring, F. Mamedov, E.-M. Aro, Dark-adapted spinach thylakoid protein heterogeneity offers insights into the photosystem II repair cycle, Biochim. Biophys. Acta 1837 (2014) 1463–1471.
[9] G.E. Hoffman, M.V. Sanchez-Puerta, C.F. Delwiche, Evolution of light-harvesting complex proteins from Chl c-containing algae, BMC Evol. Biol. 11 (2011).
[10] J. Xiong, C.E. Bauer, Complex evolution of photosynthesis, Annu. Rev. Plant Biol. 53 (2002) 503–521.
[11] S. Jansson, A guide to the Lhc genes and their relatives in *Arabidopsis*, Trends Plant Sci. 4 (1999) 236–240.
[12] G.R. Wolfe, F.X. Cunningham, D. Durnford, B.R. Green, E. Gantt, Evidence for a common origin of chloroplasts with light-harvesting complexes of different pigmentation, Nature 367 (1994) 566–568.
[13] J.A.D. Neilson, D.G. Durnford, Structural and functional diversification of the light-harvesting complexes in photosynthetic eukaryotes, Photosynth. Res. 106 (2010) 57–71.
[14] J.A.D. Neilson, D.G. Durnford, Evolutionary distribution of light-harvesting complex-like proteins in photosynthetic eukaryotes, Genome 53 (2010) 68–78.
[15] Z.R. Li, S. Wakao, B.B. Fischer, K.K. Niyogi, Sensing and responding to excess Light, Annu. Rev. Plant Biol. 60 (2009) 239–260.
[16] A. Krieger-Liszkay, C. Fufezan, A. Trebst, Singlet oxygen production in photosystem II and related protection mechanism, Photosynth. Res. 98 (2008) 551–564.
[17] C. Triantaphylides, M. Havaux, Singlet oxygen in plants: production, detoxification and signaling, Trends Plant Sci. 14 (2009) 219–228.
[18] L. Dall'Osto, S. Cazzaniga, M. Havaux, R. Bassi, Enhanced photoprotection by protein-bound vs free xanthophyll pools: a comparative analysis of chlorophyll b and xanthophyll biosynthesis mutants, Mol. Plant 3 (2010) 576–593.
[19] P. Horton, A.V. Ruban, R.G. Walters, Regulation of light harvesting in green plants, Annu. Rev. Plant Physiol. Plant Mol. Biol. 47 (1996) 655–684.
[20] S. Caffarri, S. Frigerio, E. Olivieri, P.G. Righetti, R. Bassi, Differential accumulation of *Lhcb* gene products in thylakoid membranes of *Zea mays* plants grown under contrasting light and temperature conditions, Proteomics 5 (2005) 758–768.
[21] Z. Liu, H. Yan, K. Wang, T. Kuang, J. Zhang, L. Gui, X. An, W. Chang, Crystal structure of spinach major light-harvesting complex at 2.72 A resolution, Nature 428 (2004) 287–292.
[22] R. Standfuss, A.C.T. van Scheltinga, M. Lamborghini, W. Kuhlbrandt, Mechanisms of photoprotection and nonphotochemical quenching in pea light-harvesting complex at 2.5 A resolution, EMBO J. 24 (2005) 919–928.
[23] X. Pan, M. Li, T. Wan, L. Wang, C. Jia, Z. Hou, X. Zhao, J. Zhang, W. Chang, Structural insights into energy regulation of light-harvesting complex CP29 from spinach, Nat. Struct. Mol. Biol. 18 (2011) 309–315.
[24] X. Pan, Z. Liu, M. Li, W. Chang, Architecture and function of plant light-harvesting complexes II, Curr. Opin. Struct. Biol. 23 (2013) 515–525.

[25] S. Caffarri, R. Kouril, S. Kereiche, E.J. Boekema, R. Croce, Functional architecture of higher plant photosystem II supercomplexes, EMBO J. 28 (2009) 3052–3063.
[26] S. de Bianchi, N. Betterle, R. Kouril, S. Cazzaniga, E. Boekema, R. Bassi, L. Dall'Osto, *Arabidopsis* mutants deleted in the light-harvesting protein Lhcb4 have a disrupted photosystem II macrostructure and are defective in photoprotection, Plant Cell 23 (2011) 2659–2679.
[27] S. de Bianchi, L. Dall'Osto, G. Tognon, T. Morosinotto, R. Bassi, Minor antenna proteins CP24 and CP26 affect the interactions between photosystem II subunits and the electron transport rate in grana membranes of *Arabidopsis*, Plant Cell 20 (2008) 1012–1028.
[28] E.J. Boekema, H. van Roon, J.F. van Breemen, J.P. Dekker, Supramolecular organization of photosystem II and its light-harvesting antenna in partially solubilized photosystem II membranes, Eur. J. Biochem. 266 (1999) 444–452.
[29] D. Elrad, A.R. Grossman, A genome's-eye view of the light-harvesting polypeptides of *Chlamydomonas reinhardtii*, Curr. Genet. 45 (2004) 61–75.
[30] R. Kouril, E. Wientjes, J.B. Bultema, R. Croce, E.J. Boekema, High-light vs. low-light: effect of light acclimation on photosystem II composition and organization in *Arabidopsis thaliana*, Biochim. Biophys. Acta, Bioenerg. 1827 (2013) 411–419.
[31] L. Dall'Osto, C. Unlu, S. Cazzaniga, H. Van Amerongen, Disturbed excitation energy transfer in *Arabidopsis thaliana* mutants lacking minor antenna complexes of photosystem II, Biochim. Biophys. Acta 1837 (2014) 1981–1988.
[32] P.E. Jensen, R. Bassi, E.J. Boekema, J.P. Dekker, S. Jansson, D. Leister, C. Robinson, H.V. Scheller, Structure, function and regulation of plant photosystem I, Biochim. Biophys. Acta 1767 (2007) 335–352.
[33] T. Morosinotto, M. Ballottari, F. Klimmek, S. Jansson, R. Bassi, The association of the antenna system to photosystem I in higher plants, J. Biol. Chem. 280 (2005) 31050–31058.
[34] E. Wientjes, R. Croce, The light-harvesting complexes of higher-plant photosystem I: Lhca1/4 and Lhca2/3 form two red-emitting heterodimers, Biochem. J. 433 (2011) 477–485.
[35] M. Ballottari, L. Dall'Osto, T. Morosinotto, R. Bassi, Contrasting behavior of higher plant photosystem I and II antenna systems during acclimation, J. Biol. Chem. 282 (2007) 8947–8958.
[36] F. Klimmek, U. Ganeteg, J.A. Ihalainen, H. van Roon, P.E. Jensen, H.V. Scheller, J.P. Dekker, S. Jansson, The structure of higher plant LHCI: in vivo characterisation and structural interdependence of the Lhca proteins, Biochemistry 44 (2005) 3065–3073.
[37] F. Klimmek, A. Sjodin, C. Noutsos, D. Leister, S. Jansson, Abundantly and rarely expressed Lhc protein genes exhibit distinct regulation patterns in plants, Plant Physiol. 140 (2006) 793–804.
[38] E. Wientjes, G.T. Oostergetel, S. Jansson, E.J. Boekema, R. Croce, The role of Lhca complexes in the supramolecular organization of higher plant photosystem I, J. Biol. Chem. 284 (2009) 7803–7810.
[39] L.W. Peng, Y. Fukao, M. Fujiwara, T. Takami, T. Shikanai, Efficient operation of NAD(P)H dehydrogenase requires supercomplex formation with photosystem I via minor LHCI in *Arabidopsis*, Plant Cell 21 (2009) 3623–3640.
[40] L.W. Peng, T. Shikanai, Supercomplex formation with photosystem I is required for the stabilization of the chloroplast NADH dehydrogenase-like complex in *Arabidopsis*, Plant Physiol. 155 (2011) 1629–1639.
[41] A. Busch, M. Hippler, The structure and function of eukaryotic photosystem I, Biochim. Biophys. Acta, Bioenerg. 1807 (2011) 864–877.
[42] R. Bassi, S.Y. Soen, G. Frank, H. Zuber, J.D. Rochaix, Characterization of chlorophyll-a/b proteins of photosystem-I from *Chlamydomonas-reinhardtii*, J. Biol. Chem. 267 (1992) 25714–25721.
[43] N.P. Schultes, R.B. Peterson, Phylogeny-directed structural analysis of the *Arabidopsis* PsbS protein, Biochem. Biophys. Res. Commun. 355 (2007) 464–470.
[44] X.P. Li, O. Bjorkman, C. Shih, A.R. Grossman, M. Rosenquist, S. Jansson, K.K. Niyogi, A pigment-binding protein essential for regulation of photosynthetic light harvesting, Nature 403 (2000) 391–395.
[45] X.P. Li, P. Muller-Moule, A.M. Gilmore, K.K. Niyogi, PsbS-dependent enhancement of feedback de-excitation protects photosystem II from photoinhibition, Proc. Natl. Acad. Sci. U. S. A. 99 (2002) 15222–15227.
[46] N. Betterle, M. Ballottari, S. Zorzan, S. de Bianchi, S. Cazzaniga, L. Dall'Osto, T. Morosinotto, R. Bassi, Light-induced dissociation of an antenna hetero-oligomer is needed for non-photochemical quenching induction, J. Biol. Chem. 284 (2009) 15255–15266.
[47] M.P. Johnson, T.K. Goral, C.D. Duffy, A.P. Brain, C.W. Mullineaux, A.V. Ruban, Photoprotective energy dissipation involves the reorganization of photosystem II light-harvesting complexes in the grana membranes of spinach chloroplasts, Plant Cell 23 (2011) 1468–1479.
[48] G. Bonente, F. Passarini, S. Cazzaniga, C. Mancone, M.C. Buia, M. Tripodi, R. Bassi, S. Caffarri, The occurrence of the psbS gene product in *Chlamydomonas reinhardtii* and in other photosynthetic organisms and its correlation with energy quenching, Photochem. Photobiol. 84 (2008) 1359–1370.
[49] G. Peers, T.B. Truong, E. Ostendorf, A. Busch, D. Elrad, A.R. Grossman, M. Hippler, K.K. Niyogi, An ancient light-harvesting protein is critical for the regulation of algal photosynthesis, Nature 462 (2009) 518–521.
[50] Z.D. Zhang, J. Shrager, M. Jain, C.W. Chang, O. Vallon, A.R. Grossman, Insights into the survival of *Chlamydomonas reinhardtii* during sulfur starvation based on microarray analysis of gene expression, Eukaryot. Cell 3 (2004) 1331–1348.
[51] A. Alboresi, C. Gerotto, G.M. Giacometti, R. Bassi, T. Morosinotto, *Physcomitrella patens* mutants affected on heat dissipation clarify the evolution of photoprotection mechanisms upon land colonization, Proc. Natl. Acad. Sci. U. S. A. 107 (2010) 11128–11133.
[52] K.K. Niyogi, T.B. Truong, Evolution of flexible non-photochemical quenching mechanisms that regulate light harvesting in oxygenic photosynthesis, Curr. Opin. Plant Biol. 16 (2013) 307–314.
[53] M. Havaux, G. Guedeney, Q.F. He, A.R. Grossman, Elimination of high-light-inducible polypeptides related to eukaryotic chlorophyll a/b–binding proteins results in aberrant photoacclimation in *Synechocystis* PCC6803, Biochim. Biophys. Acta, Bioenerg. 1557 (2003) 21–33.
[54] R. Tanaka, L. Rothberg, S. Oka, A. Takabayashi, M. Shibata, F. Myouga, R. Motohashi, K. Shinozaki, B. Grimm, A. Tanaka, LIL3, a light-harvesting-like protein, plays an essential role in chlorophyll and tocopherol biosynthesis, Proc. Natl. Acad. Sci. U. S. A. 107 (2010) 16721–16725.
[55] U. Andersson, M. Heddad, I. Adamska, Light stress-induced one-helix protein of the chlorophyll a/b-binding family associated with photosystem I, Plant Physiol. 132 (2003) 811–820.
[56] T. Tzvetkova-Chevolleau, F. Franck, A.E. Alawady, L. Dall'Osto, F. Carriere, R. Bassi, B. Grimm, L. Nussaume, M. Havaux, The light stress-induced protein ELIP2 is a regulator of chlorophyll synthesis in *Arabidopsis thaliana*, Plant J. 50 (2007) 795–809.
[57] D. Vavilin, D. Yao, W. Vermaas, Small cab-like proteins retard degradation of photosystem II-associated chlorophyll in *Synechocystis* sp PCC 6803 — kinetic analysis of pigment labeling with N-15 AND C-13, J. Biol. Chem. 282 (2007) 37660–37668.
[58] R. Croce, H. Van Amerongen, Light-harvesting in photosystem I, Photosynth. Res. 116 (2013) 153–166.
[59] J.-P. Chauvet, M. Bazin, R. Santus, In the triplet-triplet energy transfer from chlorophyll to carotene in Triton X 100 micelles, Photochem. Photobiol. 41 (1985) 83–90.
[60] A. Krieger-Liszkay, Singlet oxygen production in photosynthesis, J. Exp. Bot. 56 (2005) 337–346.
[61] K. Asada, The water–water cycle in chloroplasts: scavenging of active oxygens and dissipation of excess photons, Annu. Rev. Plant Physiol. Plant Mol. Biol. 50 (1999) 601–639.
[62] M. Havaux, L. Dall'Osto, R. Bassi, Zeaxanthin has enhanced antioxidant capacity with respect to all other xanthophylls in *Arabidopsis* leaves and functions independent of binding to PSII antennae, Plant Physiol. 145 (2007) 1506–1520.
[63] E.H. Kim, X.P. Li, R. Razeghifard, J.M. Anderson, K.K. Niyogi, B.J. Pogson, W.S. Chow, The multiple roles of light-harvesting chlorophyll a/b–protein complexes define structure and optimize function of *Arabidopsis* chloroplasts: a study using two chlorophyll b-less mutants, Biochim. Biophys. Acta 1787 (2009) 973–984.
[64] M. Mozzo, L. Dall'Osto, R. Hienerwadel, R. Bassi, R. Croce, Photoprotection in the antenna complexes of photosystem II: role of individual xanthophylls in chlorophyll triplet quenching, J. Biol. Chem. 283 (2008) 6184–6192.
[65] L. Dall'Osto, C. Lico, J. Alric, G. Giuliano, M. Havaux, R. Bassi, Lutein is needed for efficient chlorophyll triplet quenching in the major LHCII antenna complex of higher plants and effective photoprotection in vivo under strong light, BMC Plant Biol. 6 (2006) 32.
[66] L. Dall'Osto, S. Cazzaniga, H. North, A. MArion-Poll, R. Bassi, The *Arabidopsis* aba4-1 mutant reveals a specific function for neoxanthin in protection against photoxidative stress, Plant Cell 19 (2007) 1048–1064.
[67] J.F. Allen, Protein phosphorylation in regulation of photosynthesis, Biochim. Biophys. Acta 1098 (1992) 275–335.
[68] P. Galka, S. Santabarbara, T.T.H. Khuong, H. Degand, P. Morsomme, R.C. Jennings, E.J. Boekema, S. Caffarri, Functional analyses of the plant photosystem I–light-harvesting complex II supercomplex reveal that Light-harvesting complex II loosely bound to photosystem II is a very efficient antenna for photosystem I in state II, Plant Cell 24 (2012) 2963–2978.
[69] R. Bassi, F. Rigoni, R. Barbato, G.M. Giacometti, Light-harvesting chlorophyll a/b proteins (LHCII) populations in phosphorylated membranes, Biochim. Biophys. Acta 936 (1988) 29–38.
[70] H. Takahashi, M. Iwai, Y. Takahashi, J. Minagawa, Identification of the mobile light-harvesting complex II polypeptides for state transitions in *Chlamydomonas reinhardtii*, Proc. Natl. Acad. Sci. U. S. A. 103 (2006) 477–482.
[71] R. Tokutsu, M. Iwai, J. Minagawa, CP29, a monomeric light-harvesting complex II protein, is essential for state transitions in *Chlamydomonas reinhardtii*, J. Biol. Chem. 284 (2009) 7777–7782.
[72] C. Unlu, B. Drop, R. Croce, H. Van Amerongen, State transitions in *Chlamydomonas reinhardtii* strongly modulate the functional size of photosystem II but not of photosystem I, Proc. Natl. Acad. Sci. U. S. A. 111 (2014) 3460–3465.
[73] J.M. Anderson, Photoregulation of the composition, function and structure of thylakoid membranes, Annu. Rev. Plant Physiol. 37 (1986) 93–136.
[74] S. Puthiyaveetil, I.M. Ibrahim, J.F. Allen, Oxidation–reduction signalling components in regulatory pathways of state transitions and photosystem stoichiometry adjustment in chloroplasts, Plant Cell Environ. 35 (2012) 347–359.
[75] R. Lucinski, G. Jackowski, The structure, functions and degradation of pigment-binding proteins of photosystem II, Acta Biochim. Pol. 53 (2006) 693–708.
[76] S.M. Mckim, D.G. Durnford, Translational regulation of light-harvesting complex expression during photo acclimation to high-light in *Chlamydomonas reinhardtii*, Plant Physiol. Biochem. 44 (2006) 857–865.
[77] G. Bonente, S. Pippa, S. Castellano, R. Bassi, M. Ballottari, Acclimation of *Chlamydomonas reinhardtii* to different growth irradiances, J. Biol. Chem. 287 (2012) 5833–5847.
[78] J.P. Dekker, E.J. Boekema, Supramolecular organization of thylakoid membrane proteins in green plants, Biochim. Biophys. Acta 1706 (2005) 12–39.
[79] K. Kloppstech, Diurnal and circadian rhythmicity in the expression of light-induced plant nuclear messenger-RNAs, Planta 165 (1985) 502–506.
[80] C.S. Im, S. Eberhard, K.Y. Huang, C.F. Beck, A.R. Grossman, Phototropin involvement in the expression of genes encoding chlorophyll and carotenoid biosynthesis enzymes and LHC apoproteins in *Chlamydomonas reinhardtii*, Plant J. 48 (2006) 1–16.
[81] B. Schellenberger Costa, A. Jungandreas, T. Jakob, W. Weisheit, M. Mittag, C. Wilhelm, Blue light is essential for high light acclimation and photoprotection in the diatom *Phaeodactylum tricornutum*, J. Exp. Bot. 64 (2014) 483–493.

[82] R.G. Walters, J.J. Rogers, F. Shephard, P. Horton, Acclimation of *Arabidopsis thaliana* to the light environment: the role of photoreceptors, Planta 209 (1999) 517–527.
[83] J.D. Woodson, J. Chory, Coordination of gene expression between organellar and nuclear genomes, Nat. Rev. Genet. 9 (2008) 383–395.
[84] M. Piippo, Y. Allahverdiyeva, V. Paakkarinen, U.M. Suoranta, N. Battchikova, E.M. Aro, Chloroplast-mediated regulation of nuclear genes in *Arabidopsis thaliana* in the absence of light stress, Physiol. Genomics 25 (2006) 142–152.
[85] D.G. Durnford, J.A. Price, S.M. Mckim, M.L. Sarchfield, Light-harvesting complex gene expression is controlled by both transcriptional and post-transcriptional mechanisms during photoacclimation in *Chlamydomonas reinhardtii*, Physiol. Plant. 118 (2003) 193–205.
[86] U. Ganeteg, F. Klimmek, S. Jansson, Lhca5 — an LHC-type protein associated with photosystem I, Plant Mol. Biol. 54 (2004) 641–651.
[87] T. Yamano, K. Miura, H. Fukuzawa, Expression analysis of genes associated with the induction of the carbon-concentrating mechanism in *Chlamydomonas reinhardtii*, Plant Physiol. 147 (2008) 340–354.
[88] Y.B. Chen, D.G. Durnford, M. Koblizek, P.G. Falkowski, Plastid regulation of Lhcb1 transcription in the chlorophyte alga *Dunaliella tertiolecta*, Plant Physiol. 136 (2004) 3737–3750.
[89] S. Frigerio, C. Campoli, S. Zorzan, L.I. Fantoni, C. Crosatti, F. Drepper, W. Haehnel, L. Cattivelli, T. Morosinotto, R. Bassi, Photosynthetic antenna size in higher plants is controlled by the plastoquinone redox state at the post-transcriptional rather than transcriptional level, J. Biol. Chem. 282 (2007) 29457–29469.
[90] M. Floris, R. Bassi, C. Robaglia, A. Alboresi, E. Lanet, Post-transcriptional control of light-harvesting genes expression under light stress, Plant Mol. Biol. 82 (2013) 147–154.
[91] M.E. Petracek, L.F. Dickey, S.C. Huber, W.F. Thompson, Light-regulated changes in abundance and polyribosome association of ferredoxin mRNA are dependent on photosynthesis, Plant Cell 9 (2014) 2291–2300.
[92] J.H. Mussgnug, L. Wobbe, I. Elles, C. Claus, M. Hamilton, A. Fink, U. Kahmann, A. Kapazoglou, C.W. Mullineaux, M. Hippler, J. Nickelsen, P.J. Nixon, O. Kruse, NAB1 is an RNA binding protein involved in the light-regulated differential expression of the light-harvesting antenna of *Chlamydomonas reinhardtii*, Plant Cell 17 (2005) 3409–3421.
[93] O. Blifernez, L. Wobbe, K. Niehaus, O. Kruse, Protein arginine methylation modulates light-harvesting antenna translation in *Chlamydomonas reinhardtii*, Plant J. 65 (2011) 119–130.
[94] L. Wobbe, O. Blifernez, C. Schwarz, J.H. Mussgnug, J. Nickelsen, O. Kruse, Cysteine modification of a specific repressor protein controls the translational status of nucleus-encoded LHCII mRNAs in *Chlamydomonas*, Proc. Natl. Acad. Sci. U. S. A. 106 (2009) 13290–13295.
[95] D.-H. Yang, B. Andersson, E.M. Aro, I. Ohad, The redox state of the plastoquinone pool controls the level of the light-harvesting chlorophyll a/b binding protein complex II (LHC II) during photoacclimation — cytochrome b(6)f deficient *Lemna perpusilla* plants are locked in a state of high-light acclimation, Photosynth. Res. 68 (2001) 163–174.
[96] S. Pursiheimo, P. Mulo, E. Rintamaki, E.M. Aro, Coregulation of light-harvesting complex II phosphorylation and lhcb mRNA accumulation in winter rye, Plant J. 26 (2001) 317–327.
[97] V. Fey, R. Wagner, K. Brautigam, T. Pfannschmidt, Photosynthetic redox control of nuclear gene expression, J. Exp. Bot. 56 (2005) 1491–1498.
[98] D. Leister, I. Romani, L. Mittermayr, F. Paieri, E. Fenino, T. Kleine, Identification of target genes and transcription factors implicated in translation-dependent retrograde signaling in *Arabidopsis*, Mol. Plant 7 (2014) 1228–1247.
[99] Y. Xiao, T. Savchenko, E.E. Baidoo, W.E. Chehab, D.M. Hayden, V. Tolstikov, J.A. Corwin, D.J. Kliebenstein, J.D. Keasling, K. Dehesh, Retrograde signaling by the plastidial metabolite MEcPP regulates expression of nuclear stress-response genes, Cell 149 (2012) 1525–1535.
[100] F. Ramel, S. Birtic, C. Ginies, L. Soubigou-Taconnat, C. Triantaphylides, M. Havaux, Carotenoid oxidation products are stress signals that mediate gene responses to singlet oxygen in plants, Proc. Natl. Acad. Sci. U. S. A. 109 (2012) 5535–5540.
[101] C. Andres, B. Agne, F. KEssler, The TOC complex: preprotein gateway to the chloroplast, Biochim. Biophys. Acta 1803 (2010) 715–723.
[102] E. Kovács-Bogdán, J. Soll, B. Bolter, Protein import into chloroplasts: the Tic complex and its regulation, Biochim. Biophys. Acta 1803 (2010) 740–747.
[103] E. Schleiff, T. Becker, Common ground for protein translocation: access control for mitochondria and chloroplasts, Nat. Struct. Mol. Cell. Biol. 12 (2011) 48–59.
[104] D. Schünemann, Structure and function of the chloroplast signal recognition particle, Curr. Genet. 44 (2004) 295–304.
[105] M. Kalanon, G.I. McFadden, The chloroplast protein translocation complexes of *Chlamydomonas reinhardtii*: a bioinformatic comparison of Toc and Tic components in plants, green algae and red algae, Genetics 179 (2008) 95–112.
[106] J. Bauer, K.H. Chen, A. Hiltbunner, E. Wehrli, M. Eugster, D. Schnell, F. KEssler, The major protein import receptor of plastids is essential for chloroplast biogenesis, Nature 403 (2000) 203–207.
[107] S. Kubis, R. Patel, J. Combe, J. Bedard, S. Kovacheva, K. Lilley, A. Biehl, D. Leister, G. Rios, C. Koncz, P. Jarvis, Functional specialization amongst the *Arabidopsis* Toc159 family of chloroplast protein import receptors, Plant Cell 16 (2004) 2059–2077.
[108] T.X. Nguyen, S. Chandrasekar, S. Neher, P. Walter, S.O. Shan, Concerted complex assembly and GTPase activation in the chloroplast signal recognition particle, Biochemistry 50 (2011) 7208–7217.
[109] C.J. Tu, E.C. Peterson, R. Henry, N.E. Hoffman, The L18 domain of light-harvesting chlorophyll proteins binds to chloroplast signal recognition particle 43, J. Biol. Chem. 275 (2000) 13187–13190.
[110] L. Gerdes, T. Bals, E. Klostermann, M. Karl, K. Philippar, M. Hunken, J. Soll, D. Schunemann, A second thylakoid membrane-localized Alb3/Oxal/YidC homologue is involved in proper chloroplast biogenesis in *Arabidopsis thaliana*, J. Biol. Chem. 281 (2006) 16632–16642.
[111] X. Zhang, C. Schaffitzel, N. Ban, S.O. Shan, Multiple conformational switches in a GTPase complex control co-translational protein targeting, Proc. Natl. Acad. Sci. U. S. A. 106 (2009) 1754–1759.
[112] H. Kirst, J.G. Garcia-Cerdan, A. Zurbriggen, T. Ruehle, A. Melis, Truncated photosystem chlorophyll antenna size in the green microalga *Chlamydomonas reinhardtii* upon deletion of the TLA3–CpSRP43 gene, Plant Physiol. 160 (2012) 2251–2260.
[113] C. Hutin, M. Havaux, J.P. Carde, K. Kloppstech, K. Meiherhoff, N. Hoffman, L. Nussaume, Double mutation cpSRP43(−)/cpSRP54(−) is necessary to abolish the cpSRP pathway required for thylakoid targeting of the light-harvesting chlorophyll proteins, Plant J. 29 (2002) 531–543.
[114] J.K. Hoober, L.L. Eggink, M. Chen, Chlorophylls, ligands and assembly of light-harvesting complexes in chloroplasts, Photosynth. Res. 94 (2007) 387–400.
[115] C. Reinbothe, S. Bartsch, L.L. Eggink, J.K. Hoober, J. Brusslan, R. Andrade-Paz, J. Monnet, S. Reinbothe, A role for chlorophyllide a oxygenase in the regulated import and stabilization of light-harvesting chlorophyll a/b proteins, Proc. Natl. Acad. Sci. U. S. A. 103 (2006) 4777–4782.
[116] U.C. Vothknecht, H. Soll, Chloroplast membrane transport: interplay of prokaryotic and eukaryotic traits, Gene 354 (2005) 99–109.
[117] S. Nick, J. Meurer, J. Soll, E. Ankele, Nucleus-encoded light-harvesting chlorophyll a/b proteins are imported normally into chlorophyll b-free chloroplasts of *Arabidopsis*, Mol. Plant 6 (2013) 860–871.
[118] S. Falk, S. Irmgard, cpSRP43 is a novel chaperone specific for light-harvesting chlorophyll a, b-binding proteins, J. Biol. Chem. 285 (2010) 21655–21661.
[119] M.A. Harrison, J.A. Nemson, A. Melis, Assembly and composition of the chlorophyll a–b light-harvesting complex of barley (*Hordeum-vulgare* L) — immunochemical analysis of chlorophyll B-less and chlorophyll B-deficient mutants, Photosynth. Res. 38 (1993) 141–151.
[120] R. Bassi, R. Croce, D. Cugini, D. Sandona, Mutational analysis of a higher plant antenna protein provides identification of chromophores bound into multiple sites, Proc. Natl. Acad. Sci. U. S. A. 96 (1999) 10056–10061.
[121] R. Croce, S. Weiss, R. Bassi, Carotenoid-binding sites of the major light-harvesting complex II of higher plants, J. Biol. Chem. 274 (1999) 29613–29623.
[122] R. Horn, H. Paulsen, Early steps in the assembly of light-harvesting chlorophyll a/b complex — time-resolved fluorescence measurements, J. Biol. Chem. 279 (2004) 44400–44406.
[123] R. Horn, G. Grundmann, H. Paulsen, Consecutive binding of chlorophylls a and b during the assembly in vitro of light-harvesting chlorophyll-a/b protein (LHCIIb), J. Mol. Biol. 366 (2007) 1045–1054.
[124] D. Reinsberg, K. Ottmann, P.J. Booth, H. Paulsen, Effects of chlorophyll a, chlorophyll b, and xanthophylls on the in vitro assembly kinetics of the major light-harvesting chlorophyll a/b complex, LHCIIb, J. Mol. Biol. 308 (2001) 59–67.
[125] R. Horn, H. Paulsen, Folding in vitro of light-harvesting chlorophyll a/b protein is coupled with pigment binding, J. Mol. Biol. 318 (2002) 547–556.
[126] C. Dockter, A. Volkov, C. Bauer, Y. Polyhach, Z. Joly-Lopez, G. Jeschke, H. Paulsen, Refolding of the integral membrane protein light-harvesting complex II monitored by pulse EPR, Proc. Natl. Acad. Sci. U. S. A. 106 (2009) 18485–18490.
[127] F.G. Plumley, G.W. Schmidt, Reconstitution of chloroform a/b light-harvesting complexes: xanthophyll-dependent assembly and energy transfer, Proc. Natl. Acad. Sci. U. S. A. 84 (1987) 146–150.
[128] A. Pagano, G. Cinque, R. Bassi, In vitro reconstitution of the recombinant photosystem II light-harvesting complex CP24 and its spectroscopic characterization, J. Biol. Chem. 273 (1998) 17154–17165.
[129] R. Remelli, C. Varotto, D. Sandona, R. Croce, R. Bassi, Chlorophyll binding to monomeric light-harvesting complex. A mutation analysis of chromophore-binding residues, J. Biol. Chem. 274 (1999) 33510–33521.
[130] R. Croce, G. Canino, F. Ros, R. Bassi, Chromophore organization in the higher-plant photosystem II antenna protein CP26, Biochemistry 41 (2002) 7334–7343.
[131] V.H.R. Schmid, S. Potthast, M. Wiener, V. Bergauer, H. Paulsen, S. Storf, Pigment binding of photosystem I light-harvesting proteins, J. Biol. Chem. 277 (2002) 37307–37314.
[132] A. Wehner, S. Storf, P. Jahns, V.H. Schmid, De-epoxidation of violaxanthin in light-harvesting complex I proteins, J. Biol. Chem. 279 (2004) 26823–26829.
[133] R. Tanaka, A. Tanaka, Tetrapyrrole biosynthesis in higher plants, Annu. Rev. Plant Biol. 58 (2007) 321–346.
[134] D. DellaPenna, B.J. Pogson, Vitamin synthesis in plants: tocopherols and carotenoids, Annu. Rev. Plant Biol. 57 (2006) 711–738.
[135] H. Paulsen, B. Finkenzeller, N. Kuhlein, Pigments induce folding of light-harvesting chlorophyll alpha/beta-binding protein, Eur. J. Biochem. 215 (1993) 809–816.
[136] C. Campoli, S. Caffarri, J.T. Svensson, R. Bassi, A.M. Stanca, L. Cattivelli, C. Crosatti, Parallel pigment and transcriptomic analysis of four barley Albina and Xantha mutants reveals the complex network of the chloroplast-dependent metabolism, Plant Mol. Biol. 71 (2009) 173–191.
[137] L. Dall'Osto, M. Piques, M. Ronzani, B. Molesini, A. Alboresi, S. Cazzaniga, R. Bassi, The *Arabidopsis* nox mutant lacking carotene hydroxylase activity reveals a critical role for xanthophylls in photosystem I biogenesis, Plant Cell 25 (2013) 591–608.
[138] D. Vavilin, D.C. Brune, W. Vermaas, 15N-labeling to determine chlorophyll synthesis and degradation in *Synechocystis* sp. PCC 6803 strains lacking one or both photosystems, Biochim. Biophys. Acta 1708 (2005) 91–101.
[139] F.G. Plumley, G.W. Schmidt, Light-harvesting chlorophyll a/b complexes: interdependent pigment synthesis and protein assembly, Plant Cell 7 (1995) 689–704.
[140] J.E.W. Polle, J.R. Benemann, A. Tanaka, A. Melis, Photosynthetic apparatus organization and function in the wild type and a chlorophyll b-less mutant of *Chlamydomonas reinhardtii*. Dependence on carbon source, Planta 211 (2000) 335–344.

[141] H. Scheer, in: B. Grimm, R.J. Porra, W. Rudiger, H. Scheer (Eds.), An Overview of Chlorophylls and Bacteriochlorophylls: Biochemistry, Biophysics, Functions and Applications, Dordrecht, 2006, pp. 1–26.
[142] M. Chen, M. Schliep, R.D. Willows, Z.-L. Cai, B.A. Neilan, H. Scheer, A red-shifted chlorophyll, Science 329 (2010) 1318–1319.
[143] M. Hirashima, S. Satoh, R. Tanaka, A. Tanaka, Pigment shuffling in antenna systems achieved by expressing prokaryotic chlorophyllide *a* oxygenase in *Arabidopsis*, J. Biol. Chem. 281 (2006) 15385–15393.
[144] R. Tanaka, A. Tanaka, Chlorophyll cycle regulates the construction and destruction of the light-harvesting complexes, Biochim. Biophys. Acta 1807 (2011) 968–976.
[145] Y. Sakuraba, R. Tanaka, A. Yamasato, A. Tanaka, Determination of a chloroplast degron in the regulatory domain of chlorophyllide *a* oxygenase, J. Biol. Chem. 284 (2009) 36689–36699.
[146] L. Dall'Osto, A. Fiore, S. Cazzaniga, G. Giuliano, R. Bassi, Different roles of a- and b-branch xanthophylls in photosystem assembly and photoprotection, J. Biol. Chem. 282 (2007) 35056–35068.
[147] S. Cazzaniga, Z. Li, K.K. Niyogi, R. Bassi, L. Dall'Osto, The *Arabidopsis* szl1 mutant reveals a critical role of β-carotene in photosystem I photoprotection, Plant Physiol. 159 (2012) 1745–1758.
[148] M. Havaux, L. Dall'Osto, S. Cuine, G. Giuliano, R. Bassi, The effect of zeaxanthin as the only xanthophyll on the structure and function of the photosynthetic apparatus in *Arabidopsis thaliana*, J. Biol. Chem. 279 (2004) 13878–13888.
[149] J.E. Polle, K.K. Niyogi, A. Melis, Absence of lutein, violaxanthin and neoxanthin affects the functional chlorophyll antenna size of photosystem-II but not that of photosystem-I in the green alga *Chlamydomonas reinhardtii*, Plant Cell Physiol. 42 (2001) 482–491.
[150] E. Formaggio, G. Cinque, R. Bassi, Functional architecture of the major light-harvesting complex from higher plants, J. Mol. Biol. 314 (2001) 1157–1166.
[151] L. Dall'Osto, N.E. Holt, S. Kaligotla, M. Fuciman, S. Cazzaniga, D. Carbonera, H.A. Frank, J. Alric, R. Bassi, Zeaxanthin protects plant photosynthesis by modulating chlorophyll triplet yield in specific light-harvesting antenna subunits, J. Biol. Chem. 287 (2012) 41820–41834.
[152] M. Ballottari, M.J.P. Alcocer, C. D'Andrea, D. Viola, T.K. Ahn, A. Petrozza, D. Polli, G.R. Fleming, G. Cerullo, R. Bassi, Regulation of photosystem I light harvesting by zeaxanthin, Proc. Natl. Acad. Sci. U. S. A. 111 (2014) E2431–E2438.
[153] A. Fiore, L. Dallosto, S. Cazzaniga, G. Diretto, G. Giuliano, R. Bassi, A quadruple mutant of *Arabidopsis* reveals a β-carotene hydroxylation activity for LUT1/CYP97C1 and a regulatory role of xanthophylls on determination of the PSI/PSII ratio, BMC Plant Biol. 12 (2012).
[154] R. Croce, R. Bassi, The light-harvesting complex of photosystem I: pigment composition and stoichiometry, in: G. Garab (Ed.)Photosynthesis: Mechanisms and Effects, vol. 1, 1998, pp. 421–424.
[155] Z. Adam, Emerging roles for diverse intramembrane proteases in plant biology, Biochim. Biophys. Acta 1828 (2013) 2933–2936.
[156] J. Bennett, Biosynthesis of the light-harvesting chlorophyll a/b protein polypeptide turnover in darkness, Eur. J. Biochem. 118 (1981) 61–70.
[157] J.P. Slovin, E.M. Tobin, Synthesis and turnover of the light-harvesting chlorophyll a/b–protein in *Lemna gibba* grown with intermittent red light: possible translational control, Planta 154 (1982) 465–472.
[158] R. Anastassiou, J.H. Argyroudi-Akoyunoglou, Thylakoid-bound proteolytic activity against LHC II apoprotein in bean, Photosynth. Res. 43 (1995) 241–250.
[159] T. Halperin, O. Ostersetzer, Z. Adam, ATP-dependent association between subunits of Clp protease in pea chloroplasts, Planta 213 (2001) 614–619.
[160] L.A. Tziveleka, J.H. Argyroudi-Akoyunoglou, Implications of a developmental-stage-dependent thylakoid-bound protease in the stabilization of the light-harvesting pigment–protein complex serving photosystem II during thylakoid biogenesis in red kidney bean, Plant Physiol. 117 (1998) 961–970.
[161] M. Lindahl, D.H. Yang, B. Andersson, Regulatory proteolysis of the major light-harvesting chlorophyll a/b protein of photosystem II by a light-induced membrane-associated enzymic system, Eur. J. Biochem. 231 (1995) 503–509.
[162] D.-H. Yang, J. Webster, Z. Adam, M. Lindahl, B. Andersson, Induction of acclimative proteolysis of the light-harvesting chlorophyll a/b protein of photosystem II in response to elevated light intensities, Plant Physiol. 118 (1998) 827–834.
[163] M. Lensch, R.G. Hermann, A. Sokolenko, Identification and characterization of SppA, a novel light-inducible chloroplast protease complex associated with thylakoid membranes, J. Biol. Chem. 276 (2001) 33645–33651.
[164] D.-H. Yang, H. Paulsen, B. Andersson, The N-terminal domain of the light-harvesting chlorophyll a/b–binding protein complex (LHCII) is essential for its acclimative proteolysis, FEBS Lett. 466 (2000) 385–388.
[165] A. Zelisko, G. Jackowski, Senescence-dependent degradation of Lhcb3 is mediated by a thylakoid membrane-bound protease, J. Plant Physiol. 161 (2004) 1157–1170.
[166] A. Zelisko, M. Garcia-Lorenzo, G. Jackowski, S. Jansson, C. Funk, AtFtsH6 is involved in the degradation of the light-harvesting complex II during high-light acclimation and senescence, Proc. Natl. Acad. Sci. U. S. A. 102 (2005) 13699–13704.
[167] R. Lucinski, G. Jackowski, AtFtsH heterocomplex-mediated degradation of apoproteins of the major light harvesting complex of photosystem II (LHCII) in response to stresses, J. Plant Physiol. 170 (2013) 1082–1089.
[168] M. Zienkiewicz, A. Ferenc, W. Wasilewska, E. Romanowska, High light stimulates Deg1-dependent cleavage of the minor LHCII antenna proteins CP26 and CP29 and the PsbS protein in *Arabidopsis thaliana*, Planta 235 (2012) 279–288.
[169] M. Zienkiewicz, N. Kokoszka, I. Baclawska, A. Drozak, E. Romanowska, Light intensity and quality stimulated Deg1-dependent cleavage of PSII components in the chloroplasts of maize, Plant Physiol. Biochem. 67 (2013) 126–136.
[170] R. Lucinski, L. Misztal, S. Samardakiewicz, G. Jackowski, The thylakoid protease Deg2 is involved in stress-related degradation of the photosystem II light-harvesting protein Lhcb6 in *Arabidopsis thaliana*, New Phytol. 192 (2011) 74–86.
[171] A. Zaltsman, A. Feder, Z. Adam, Developmental and light effects on the accumulation of FtsH protease in *Arabidopsis* chloroplasts—implications for thylakoid formation and photosystem II maintenance, Plant J. 42 (2005) 609–617.
[172] P.J. Nixon, M. Barker, M. Boehm, R. de Vries, J. Komenda, FtsH-mediated repair of the photosystem II complex in response to light stress, J. Exp. Bot. 56 (2005) 357–363.
[173] V. Mick, K. Eggert, B. Heinemann, S. Geister, H. Paulsen, Single amino acids in the lumenal loop domain influence the stability of the major light-harvesting chlorophyll a/b complex, Biochemistry 43 (2004) 5467–5473.
[174] S.Y. Park, J.W. Yu, J.-S. Park, J. Li, S.C. Yoo, N.Y. Lee, S.K. Lee, S.W. Jeong, H.S. Seo, H.J. Koh, J.S. Jeon, Y.I. Park, N.C. Paek, The senescence-induced staygreen protein regulates chlorophyll degradation, Plant Cell 19 (2007) 1649–1664.
[175] M. Kusaba, A. Tanaka, R. Tanaka, Stay-green plants: what do they tell us about the molecular mechanism of leaf senescence, Photosynth. Res. 117 (2013) 221–234.
[176] Y. Horie, H. Ito, M. Kusaba, R. Tanaka, A. Tanaka, Participation of chlorophyll b reductase in the initial step of the degradation of light-harvesting chlorophyll a/b–protein complexes in *Arabidopsis*, J. Biol. Chem. 284 (2009) 17449–17456.
[177] M. Kusaba, H. Ito, R. Morita, S. Iida, Y. Sato, M. Fujimoto, S. Kawasaki, R. Tanaka, H. Hirochika, M. Nishimura, A. Tanaka, Rice NON-YELLOW COLORING1 is involved in light-harvesting complex II and grana degradation during leaf senescence, Plant Cell 19 (2007) 1362–1375.
[178] N.E. Holt, D. Zigmantas, L. Valkunas, X.P. Li, K.K. Niyogi, G.R. Fleming, Carotenoid cation formation and the regulation of photosynthetic light harvesting, Science 307 (2005) 433–436.
[179] A.V. Ruban, R. Berera, C. Ilioaia, I.H. van Stokkum, J.T. Kennis, A.A. Pascal, H. Van Amerongen, B. Robert, P. Horton, R. van Grondelle, Identification of a mechanism of photoprotective energy dissipation in higher plants, Nature 450 (2007) 575–578.
[180] T.K. Ahn, T.J. Avenson, M. Ballottari, Y.C. Cheng, K.K. Niyogi, R. Bassi, G.R. Fleming, Architecture of a charge-transfer state regulating light harvesting in a plant antenna protein, Science 320 (2008) 794–797.
[181] S. Bode, C.C. Quentmeier, P.N. Liao, N. Hafi, T. Barros, L. Wilk, F. Bittner, P.J. Walla, On the regulation of photosynthesis by excitonic interactions between carotenoids and chlorophylls, Proc. Natl. Acad. Sci. U. S. A. 106 (2009) 12311–12316.
[182] X.G. Zhu, D.R. Ort, J. Whitmarsh, S.P. Long, The slow reversibility of photosystem II thermal energy dissipation on transfer from high to low light may cause large losses in carbon gain by crop canopies: a theoretical analysis, J. Exp. Bot. 55 (2004) 1167–1175.
[183] E.H. Murchie, M. Pinto, P. Horton, Agriculture and the new challenges for photosynthesis research, New Phytol. 181 (2009) 532–552.
[184] E.H. Murchie, K.K. Niyogi, Manipulation of photoprotection to improve plant photosynthesis, Plant Physiol. 155 (2011) 86–92.
[185] Y. Umena, K. Kawakami, J.R. Shen, N. Kamiya, Crystal structure of oxygen-evolving photosystem II at a resolution of 1.9 A, Nature 473 (2011) 55–60.
[186] A. Amunts, H. Toporik, A. Borovikova, N. Nelson, Structure determination and improved model of plant photosystem I, J. Biol. Chem. 285 (2010) 3478–3486.
[187] S. Caffarri, K. Broess, R. Croce, H. Van Amerongen, Excitation energy transfer and trapping in higher plant photosystem II complexes with different antenna sizes, Biophys. J. 100 (2011) 2094–2103.
[188] E. Wientjes, B. Drop, R. Kouril, E.J. Boekem, R. Croce, During state 1 to state 2 transition in *Arabidopsis thaliana*, the photosystem II supercomplex gets phosphorylated but does not disassemble, J. Biol. Chem. 288 (2013) 32821–32826.

Chapter 2

Two mechanisms for dissipation of excess light in monomeric and trimeric light-harvesting complexes.

This chapter was published in

Nature Plants, Article number: 17033 (2017)

nature plants

ARTICLES

PUBLISHED: 10 APRIL 2017 | VOLUME: 3 | ARTICLE NUMBER: 17033

Two mechanisms for dissipation of excess light in monomeric and trimeric light-harvesting complexes

Luca Dall'Osto[1†], Stefano Cazzaniga[1†], Mauro Bressan[1], David Paleček[2], Karel Žídek[2], Krishna K. Niyogi[3,4], Graham R. Fleming[4,5,6], Donatas Zigmantas[2] and Roberto Bassi[1,7*]

Oxygenic photoautotrophs require mechanisms for rapidly matching the level of chlorophyll excited states from light harvesting with the rate of electron transport from water to carbon dioxide. These photoprotective reactions prevent formation of reactive excited states and photoinhibition. The fastest response to excess illumination is the so-called non-photochemical quenching which, in higher plants, requires the luminal pH sensor PsbS and other yet unidentified components of the photosystem II antenna. Both trimeric light-harvesting complex II (LHCII) and monomeric LHC proteins have been indicated as site(s) of the heat-dissipative reactions. Different mechanisms have been proposed: energy transfer to a lutein quencher in trimers, formation of a zeaxanthin radical cation in monomers. Here, we report on the construction of a mutant lacking all monomeric LHC proteins but retaining LHCII trimers. Its non-photochemical quenching induction rate was substantially slower with respect to the wild type. A carotenoid radical cation signal was detected in the wild type, although it was lost in the mutant. We conclude that non-photochemical quenching is catalysed by two independent mechanisms, with the fastest activated response catalysed within monomeric LHC proteins depending on both zeaxanthin and lutein and on the formation of a radical cation. Trimeric LHCII was responsible for the slowly activated quenching component whereas inclusion in supercomplexes was not required. This latter activity does not depend on lutein nor on charge transfer events, whereas zeaxanthin was essential.

Plants and algae use light as an energy source for carbon dioxide (CO_2) fixation into sugars. Their photosystems are composed of a core complex, where charge separation events fuel electron transport from H_2O to $NADP^+$, and an antenna system, which expands the absorption cross-section. Large antennas favour energy supply in low-light conditions, yet at high-light (HL) intensities they cause excess excitation beyond the maximal capacity for photochemical reactions. Unquenched singlet excited states of chlorophyll (^{1}Chl*) undergo intersystem crossing and the resulting triplets (^{3}Chl*) react with oxygen (O_2) to yield singlet oxygen ($^1O_2$) and photoinhibition. Within the photosynthetic machinery, photosystem II (PSII) and its reaction centre (RC), the special Chl pair P680, have been indicated as the primary target of photoinhibition[1]. Avoiding photoinhibition in the ever-changing environment has likely shaped mechanisms that regulate PSII quantum efficiency[2]. This set of inducible mechanisms, collectively referred to as NPQ (non-photochemical quenching), facilitate heat dissipation of the ^{1}Chl* state energy and can thus be monitored as a light-dependent decrease of Chl fluorescence. Under full sunlight, NPQ converts as much as 80% of absorbed photons into heat, thereby reducing the quantum yield of PSII (reviewed in[3]).

NPQ can be dissected into a number of kinetic components: qE, qZ, qM and qI[4–6]. qE (energy quenching) is the dominant NPQ component, which is rapidly induced (within 20–60 s), is reversible in seconds and is triggered by the over-acidification of the thylakoid membrane. Signal transduction of luminal acidification involves PsbS, through protonation of two lumen-exposed glutamate residues[7]. Since PsbS is an atypical LHC protein, not binding pigments[8,9], quenching reactions must be located in interacting pigment-binding subunits of PSII, located in grana partitions together with PsbS.

PSII is made by a Chl *a*- and β-carotene-binding dimeric core complex[10] surrounded by an antenna system binding Chl *a*, *b* and xanthophylls. Antennas are arranged into an inner layer of mononomeric LHC proteins called CP29, CP26 and CP24 (encoded by the *Lhcb4*, *Lhcb5* and *Lhcb6* genes, respectively) and an outer layer of trimeric LHCII subunits made of *Lhcb1-Lhcb3* gene products[11]. Together, the PSII core and antenna system form supercomplexes[12], whose composition undergoes dynamic changes depending on acclimation to light conditions[13] and NPQ activation[14]. Several lines of evidence suggest that the site of quenching is located within the PSII antenna system: (1) lutein (Lut) and zeaxanthin (Zea), ligands of LHC proteins, are essential for NPQ activity[15]; (2) Chl *b*-less plants lack both LHCs and qE[16] although depletion of PSII core complexes does not affect qE activity[17]; (3) DCCD binding to lumen-exposed protonatable residues of LHCs inhibits qE[18]; (4) quenching induced by aggregation in isolated LHC proteins shares spectroscopic features with qE[19]. Nevertheless, identification of PsbS partners in quenching reactions is complex due to the high number of gene products involved: in *Arabidopsis*, only Lhcb5 and Lhcb6 subunits are encoded by single genes, whereas Lhcb4 and LHCII are encoded, respectively, by three and nine genes[11].

[1]Dipartimento di Biotecnologie, Università di Verona, Strada Le Grazie 15, 37134 Verona, Italy. [2]Department of Chemical Physics, Lund University, Getingevägen 60, Lund S-22241, Sweden. [3]Howard Hughes Medical Institute, Department of Plant and Microbial Biology, University of California, Berkeley 94720-3102, California, USA. [4]Molecular Biophysics and Integrated Bioimaging Division, Lawrence Berkeley National Laboratory, Berkeley 94720, California, USA. [5]Graduate Group in Applied Science and Technology, University of California, Berkeley 94720, California, USA. [6]Department of Chemistry, Hildebrand B77, University of California, Berkeley 94720-1460, California, USA. [7]Consiglio Nazionale delle Ricerche (CNR), Istituto per la Protezione delle Piante (IPP), Via Madonna del Piano 10, 50019 Sesto Fiorentino, Firenze, Italy. †These authors contributed equally to the work. *e-mail: roberto.bassi@univr.it

Also, open questions include the role of Zea, which enhances the amplitude of quenching reactions[20], and the biophysical mechanism(s) by which the quenching reactions are initiated. Proposals include (1) Chl-Chl interactions, yielding into a mixing of charge transfer (CT) states and excitonic states, acting as quenchers[21,22]; (2) formation of short-living Chl-xanthophyll excited states, which serve as traps for ^{1}Chl*[19,23]; (3) CT events in a Chl *a*–Zea heterodimer, followed by charge recombination to the ground state[24,25]. Interaction between Chl *a* and Zea might be promoted by a conformational change from the interaction of protonated PsbS with CP29[26] or between PsbS and LHCII, forming a Zea–PsbS/LHCII complex at the interface[27]. It was also shown that ^{1}Chl* quenching can occur by the formation of a transient Chl^--Lut^+ state[28]. The large number of models for the NPQ mechanism clearly shows that knowledge is limited: many hypotheses are based on measurements *in vitro*, which, although mimicking, might not closely reflect *in vivo* phenomena.

In this work, we isolated and characterized the *Arabidopsis koLhcb4.1 koLhcb4.2 koLhcb5* triple mutant (hereafter referred to as *NoM*), which lacks all monomeric Lhcbs but retains a full trimeric LHCII complement. Further, we introduced the *npq1, lut2* and *npq4* mutations, preventing, respectively, Zea and Lut synthesis or PsbS accumulation. Lack of monomeric antenna complexes delayed substantially the onset of quenching reactions and changed the xanthophyll-dependence of the residual NPQ activity, implying the fast- and slow-activated components contributing to NPQ in wild type were catalysed, respectively, by monomeric and trimeric components of the PSII antenna system.

Results

NoM is a triple knock-out mutant of *Arabidopsis*, lacking all monomeric Lhcb subunits of the PSII. *NoM* plants were obtained by crossing homozygous transfer DNA (T-DNA) mutants carrying insertions in genes encoding *Lhcb4.1*, *Lhcb4.2* and *Lhcb5*, as previously described[29–31]. When grown in a climate chamber for 4 weeks under controlled conditions (150 µmol photons m^{-2} s^{-1}, 23 °C, 8/16 day/night), *NoM* plants showed a significant growth reduction with respect to wild-type plants (Fig. 1 and Table 1). The possibility that such a phenotype was due to the presence of unrelated mutation(s) was ruled out since parental knock-out (KO) mutants were not affected in their growth[29–31]. Moreover, the reduced growth was not due to altered development, since leaf formation rates were similar in the two genotypes (Supplementary Fig. 1a).

Dark-adapted *NoM* plants showed a high Chl fluorescence phenotype: images of minimum Chl fluorescence (F_0) were captured and false-colour images relative to F_0 parameter were generated from the fluorescence data. A far higher emission in the mutant suggested that absorbed light energy was not used for photochemistry as efficiently as in the wild type, thus yielding an enhanced excitation level in the antenna (Fig. 1).

The quantum efficiency of PSII photochemistry was assessed by Chl fluorescence analysis *in vivo*[32]. The ratio of variable to maximum fluorescence (F_v/F_m), that is the maximal photochemical yield of the PSII RC, was 0.57 ± 0.02 in *NoM* versus 0.81 ± 0.01 in wild type (Table 1), indicating partial loss of PSII activity. *NoM* leaves, illuminated at 150 µmol photons m^{-2} s^{-1} for 25 min, showed a significant reduction in both maximal efficiency of PSII photochemistry (F'_v/F'_m) and the efficiency of PSII-harvested light for Q_A reduction (Φ_{PSII}), with respect to wild type. These effects suggest a defective connection of the LHC antenna to the PSII RC, consistent with the increased F_0 level compared to wild type (Table 1 and Fig. 1).

NoM plants grown in control light showed a slight but significant decrease in Chl content per leaf area compared to wild type as well as lower Chl *a*/*b* and Chl/Car ratios (Table 1). In dark-adapted plants, the content of xanthophylls (neoxanthin, Vio and Lut) was higher in *NoM*, whereas the level of β-carotene was unaffected. Synthesis of Zea, induced by exposing plants for 20 min to HL (1,200 µmol photons m^{-2} s^{-1}, 23 °C), was the same in both genotypes (Supplementary Table 1).

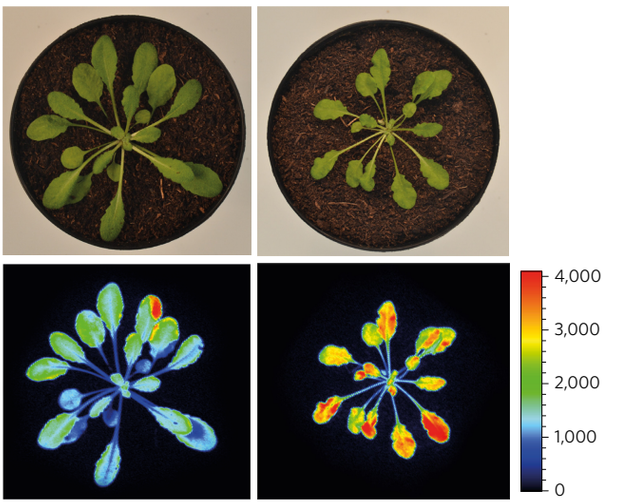

Figure 1 | Phenotype of wild-type and *NoM* plants. Upper panels: plants were grown for 6 weeks at 150 µmol photons m^{-2} s^{-1}, 23 °C, 8/16 h light/dark. Lower panels: imaging of minimal Chl fluorescence (F_0) of wild-type and *NoM* plants. Relative fluorescence is indicated by the colour scale bar (arbitary units).

The SDS–polyacrylamide gel electrophoresis (SDS–PAGE) of thylakoid membrane polypeptides showed that *NoM* plants completely lacked Lhcb4 (Fig. 2a), despite still containing the *Lhcb4.3* gene, in agreement with previous reports that Lhcb4.3 did not accumulate in mutants deleted in both Lhcb4.1 and Lhcb4.2[30]. The band corresponding to Lhcb6 was also missing, because of destabilization in the absence of its docking site CP29[30]. The *NoM* mutant is, thus, lacking all monomeric LHC proteins of PSII.

The organization of pigment-binding complexes was then analysed by non-denaturing PAGE (Fig. 2b). The photosystem I (PSI) formed a single green band at 650 kDa including the core complex and its antenna moiety. In the case of PSII instead, the component pigment–proteins migrated as multiple bands: namely, the monomeric Lhcbs, the trimeric LHCII, the Lhcb4–Lhcb6–LHCII-M complex and the PSII core. The upper region of the gel contained undissociated supercomplexes, which formed multiple green bands according to their different LHC complements. The pattern from *NoM* thylakoids differed in the lack of all PSII supercomplex bands, as well as of the Lhcb4–Lhcb6–LHCII-M complex. The mobility and abundance of PSI-LHCI, PSII core and monomeric Lhcbs were unaffected, whereas the abundance of the trimeric LHCII was enhanced in *NoM* with respect to wild type.

Quantification of pigment-binding proteins by immunotitration (Fig. 2c,d) yielded the same PSI/PSII (PsaA/CP47) ratio for wild type and *NoM* and an increased LHCII/PSII ratio, suggesting the mutant reacted to the lack of monomeric LHCs by over-accumulating (+60%) the trimeric LHCII antenna.

NPQ of chlorophyll fluorescence. We assessed the ability of wild type and *NoM* to undergo quenching of Chl fluorescence upon exposure to HL and analysed the known components of the NPQ mechanism including the abundance of the luminal pH sensor PsbS, the extent of thylakoid lumen acidification and the capacity for Zea synthesis. PsbS was present in both genotypes and its abundance with respect to LHCII was similar in *NoM* versus wild type (Supplementary Fig. 2a). Measuring lumen acidification

Table 1 | Measurement of Chl and Car content, fresh weight and key photosynthetic parameters on leaves of *Arabidopsis* wild type and *NoM*.

	Chl a/b	Chl/Car	µg Chl per cm^2	Fresh weight (g)	F_0/Chl (a.u.)	F_v/F_m	F'_v/F'_m	Φ_{PSII}	P700 max (a.u.)
WT	2.97 ± 0.02	3.85 ± 0.06	22.1 ± 0.8	0.47 ± 0.21	63.8 ± 4.7	0.81 ± 0.01	0.60 ± 0.02	0.48 ± 0.02	3251 ± 234
NoM	2.72 ± 0.06*	3.70 ± 0.06*	19.3 ± 1.3*	0.14 ± 0.04*	177.7 ± 16.3*	0.57 ± 0.02*	0.37 ± 0.04*	0.30 ± 0.04*	1587 ± 196*

PSII function was determined on plants either dark-adapted (F_0/Chl, F_v/F_m) or upon illumination at 150 µmol photons m^{-2} s^{-1} for 25 min in the presence of saturating CO_2 (F'_v/F'_m, Φ_{PSII}), the maximum amount of photo-oxidizable PSI RC (P700 max) on dark-adapted leaves. Symbols and error bars show means ± s.d. ($n > 5$). Values that are significantly different (Student's *t*-test, $P < 0.05$) from the wild type (WT) are marked with an asterisk (*). Car, carotenoids; a.u., arbitrary units.

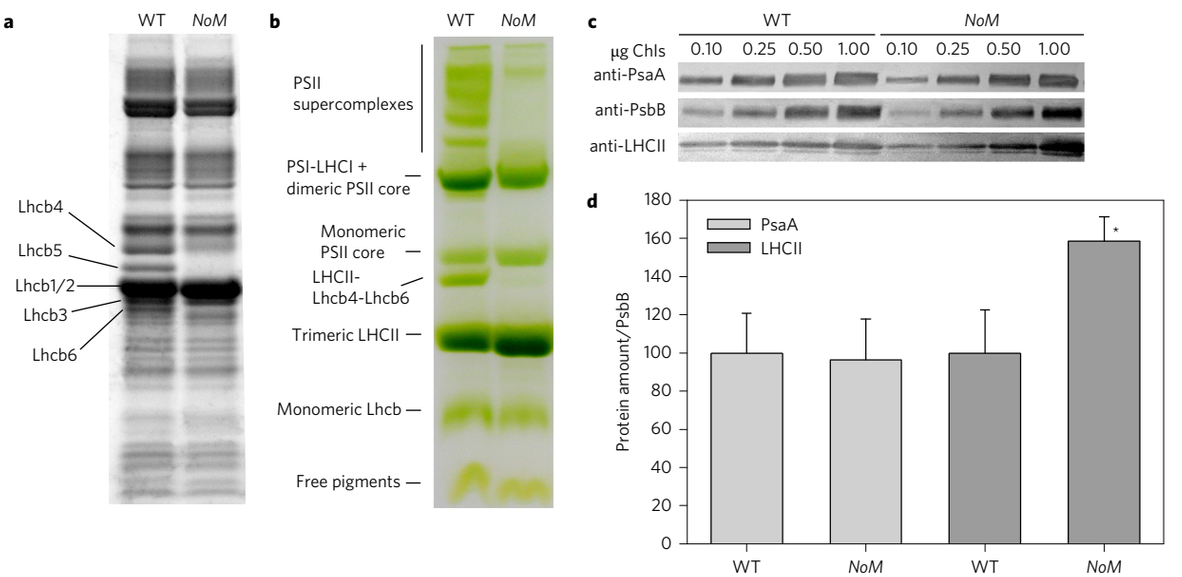

Figure 2 | Biochemical characterization of the *NoM* mutant. a, SDS–PAGE analysis of wild-type (WT) and *NoM* mutant thylakoid proteins performed with the Tris-Tricine buffer system. Selected apoprotein bands are marked. **b**, Thylakoid pigment–protein complexes were separated by non-denaturing Deriphat-PAGE upon solubilization with α-DM (dodecyl-D-maltopyranoside). **c**, Immunoblotting used for the quantification of photosynthetic subunits in the wild-type and mutant thylakoids. Immunoblot analysis was performed with antibodies directed against individual gene products: LHCII subunit, the PSII core subunit PsbB (CP47) and the PSI core subunit (PsaA). Thylakoids corresponding to 0.1, 0.25, 0.5 and 1.0 µg of Chls were loaded for each sample. All samples were loaded on the same SDS–PAGE slab gel. **d**, Results of the immunotitration of thylakoid proteins. Data of PSII antenna subunits were normalized to the core amount, PsbB content and expressed as a percentage of the corresponding wild-type content. Data are expressed as mean ± s.d. ($n = 4$). The significantly different value from wild-type membranes (Student's *t*-test, $P < 0.05$) is marked with an asterisk (*).

from the light-induced quenching of 9-aminoacridine[33] showed that mutant and wild-type chloroplasts had the same ΔpH over a wide range of light intensities (Supplementary Fig. 2b). Consistently, the kinetic of Zea accumulation was the same in both wild-type and *NoM* leaves, and the same de-epoxidation index was measured over different light intensities (Supplementary Fig. 2c,d). These results are consistent with proton-pumping not being affected in *NoM* versus wild-type chloroplasts. Thus, changes in quenching activity are expected to reflect altered efficiency of quenching reactions only.

The NPQ activity of the two genotypes is shown in Fig. 3a. Upon exposure of wild-type plants to saturating irradiance (1,200 µmol photons m^{-2} s^{-1}, 23 °C), NPQ suddenly reached a value of 1.2 in the first minute, followed by a biphasic rise, faster at 1–4 min and then slower, reaching a maximal value of 2.2 upon 12 min of illumination. NPQ of *NoM* underwent an initial rise, followed by a transient decrease. Quenching resumed only after 5 min illumination, after which quenching rapidly rose to 90% of wild-type value at 12 min illumination. This is consistent with three phases of quenching overlapping in wild type: phase 1 (P1, 0–1 min), phase 2 (P2, 1–4 min) and phase 3 (P3, 4–12 min), although P2 is missing in *NoM*. Recovery in the dark was faster and more complete in *NoM* versus wild type. We did not identify a correlation between NPQ amplitude and preflowering growth stages, since similar kinetics of NPQ were measured at different plant ages within the same genotype (Supplementary Fig. 1b).

The initial fast phase P1 of NPQ induction is transient, depends on the trans-thylakoid ΔpH and PsbS and has been proposed to originate in the PSII core complex[34]. The slower kinetic components, P2 and P3, depend on both lumen acidification, Lut and Zea accumulation[15]. In order to further evaluate the modulation of kinetics by Zea, we measured NPQ during two consecutive cycles of HL, separated by a dark relaxation. Zea was synthesized during the first light treatment and was present at the onset of the second illumination period owing to the slow kinetic of the Zea-Viola back-reaction[6]. The resulting kinetics showed that preloading with Zea resulted in a much faster rise of quenching, reaching near maximal amplitude in both genotypes already in P1 with no further increase in P2 and P3. A transient decline of quenching in P2 followed by recovery in P3 was still evident in the mutant trace (Fig. 3b). The kinetic of dark relaxation was still faster than in wild type and the difference increased during the second dark period. Since the kinetic of Zea accumulation was the same in both wild-type and *NoM* leaves (Supplementary Fig. 2c), the differences in quenching kinetics are likely due to differences in the availability of Zea-binding sites. The results of Fig. 3a,b imply that the lack of monomeric LHCs affects NPQ mainly during illumination of dark-adapted leaves. In order to further assess this point, we

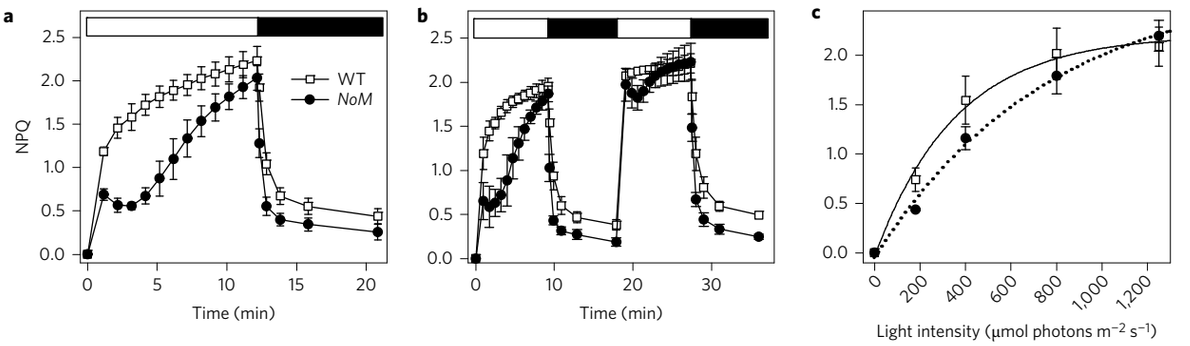

Figure 3 | Kinetics of rise and relaxation of photoprotective energy dissipation. a, Measurements of NPQ kinetics on wild-type (WT) and *NoM* leaves illuminated with 1,200 μmol photons m^{-2} s^{-1}. See Supplementary Fig. 3 for NPQ kinetics of the parental double mutants *koLhb4* and *koLhcb5 Lhcb6*. **b**, NPQ kinetics of wild-type and *NoM* plants during two consecutive periods of illumination with white light (1,200 μmol photons m^{-2} s^{-1}). **c**, Dependence of NPQ amplitude measured at different light intensities. Steady-state photosynthesis was induced by white actinic light; parameters were measured after 25 min of illumination. Symbols and error bars show means ± s.d. ($n > 3$). White and black bars represent light and dark periods.

measured NPQ during steady-state photosynthesis at different light intensities (Fig. 3c), showing that the overall NPQ activity was indeed significantly lower in *NoM* versus wild type at light intensities below 1,000 μmol photons m^{-2} s^{-1}.

In order to verify *in vivo* the differential role of Zea and of other known factors determining NPQ activity, further genetic analysis was undertaken. To this aim, *Arabidopsis NoM* mutants devoid of Zea (*NoM npq1*), Lut (*NoM lut2*) or both (*NoM npq1 lut2*), or lacking the PsbS subunit (*NoM npq4*) were generated. P1 was maintained in the *npq1* and *lut2* mutants, whereas P2 was reduced in *lut2* and both P2 and P3 were reduced in *npq1* with respect to wild type. Contrary to *lut2*, the NPQ kinetic of *NoM lut2* was identical to *NoM* in all components whereas *NoM npq1* retained the P1 component only.

Introducing the *npq1* mutation in wild type and *NoM* had a strong decreasing effect in the NPQ activity of both genotypes (Fig. 4a,b), suggesting Zea-binding to antenna subunits active in NPQ occurred in both genotypes. The effect of introducing the *lut2* mutation was, instead, significant in wild type only (Fig. 4a,b), implying Lut-binding sites active in NPQ were missing in *NoM*. The effect of introducing the double mutation *npq1 lut2* or the *npq4* mutation caused a full depletion of activity in wild-type and *NoM* background (Fig. 4a,b).

The pigment composition of xanthophyll- or PsbS-deficient mutants, in either dark-adapted state or upon 12 min illumination with HL, is shown in Supplementary Table 1. Xanthophyll content was higher in *NoM* mutants with respect to the corresponding genotypes accumulating monomeric LHCs, and β-carotene was the same. Lut was absent in all the *lut2* genotypes, and compensated for by increased Vio. Treatment with HL induced Zea synthesis in *npq4* and *NoM npq4* plants to the same level as in wild type, whereas *lut2* and *NoM lut2* accumulated 2.5-fold more Zea. In *npq1* and *NoM npq1* genotypes, HL did not induce Vio de-epoxidation as in *npq1 lut2* or *NoM npq1 lut2* genotypes. The double illumination experiment (Fig. 4c,d) confirmed that NPQ in the *NoM* mutants was fully dependent on Zea although independent from Lut. This was strikingly different from wild type which depended both on Lut and Zea, in agreement with previous reports[15,35]. In *NoM lut2*, the second actinic illumination was accompanied by an increase in the amplitude of slowly relaxing quenching (qI), the latter being an indicator of photodamage or sustained down-regulation of PSII[4]. The inability of *NoM npq1* plants to undergo qE was maintained even in the second illumination, whereas the increase in max NPQ was mostly due to the higher amplitude of the qI component (Fig. 4d).

From the above results, we conclude that NPQ activity in wild type has three phases: namely, a very fast P1 at the dark-light transition; a second, P2, partially overlapping with P1 due to monomeric LHC proteins, which is absent in *NoM*; and a more slowly activated P3 involving LHCII, retained in *NoM*. The P2 depends on both Lut and Zea, whereas the P3 depends on Zea only. All three components were dependent on PsbS.

Investigations on the mechanism(s) of NPQ. The mechanistic models proposed for excess energy dissipation include (1) the establishment of LHCII aggregates *in vivo*, opening a channel for energy transfer from Chls to the Lut S1 state[19], and (2) the Chl *a* – Zea CT[24], which was proposed to occur within monomeric LHCs[25].

According to the former proposal, the transition into the dissipative state engages a clustering of LHCII proteins into aggregates with low fluorescence yield that can be reproduced *in vitro* by inducing aggregation of purified LHCII antenna proteins in low detergent and low pH[36]. This can be observed *in vivo* by 77 K fluorescence emission spectroscopy of leaves as a decrease of the red emission peak concomitant to an increased far-red emission at 727 nm[37]. In order to determine whether the phases of NPQ described above could be attributed to any of the previously proposed mechanisms, we carried out specific assays: first, we performed 77 K Chl fluorescence quenching experiments on wild-type and *NoM* leaves, either HL-treated using 1,200 μmol photons m^{-2} s^{-1} light, or after recovery of HL-treated leaves in darkness for 10 min[37]. In both wild type and *NoM*, 77 K emission spectra recorded upon HL treatment showed a lower amplitude of the PSII emissions (685 and 695 nm components) with respect to the dark-recovered sample. Instead, the amplitude of the long wavelength component (727 nm) was significantly enhanced (Supplementary Fig. 4). Light minus dark difference spectra clearly showed the HL-induced increase in the 727 nm emission was absent in *npq4* genotypes whereas it was stronger in the case of *NoM* leaves, suggesting the rate of the process undergoing this red-shifted PSII emission, namely the clustering/aggregation of trimeric LHCII[38], was associated with the build-up of NPQ and enhanced in *NoM* with respect to wild type (Fig. 5).

We then proceeded to investigate the relevance of the second quenching mechanism, namely the formation of a CT state between Chl *a* and Zea, which was first observed by ultra-fast pump-probe experiments on isolated thylakoid membranes[24]. In order to verify whether *NoM* was competent in the formation of a Zea^+ radical cation, we measured ultrafast transient absorption (TA) kinetics in isolated thylakoids, before and after inducing qE. The samples were excited at 665 nm and individual TA kinetic traces were measured on spinach, *Arabidopsis* wild-type and *NoM* thylakoids at 1,030 nm, where carotenoid radical cations have substantial absorption[24] (Fig. 6 and Supplementary Fig. 5). In both

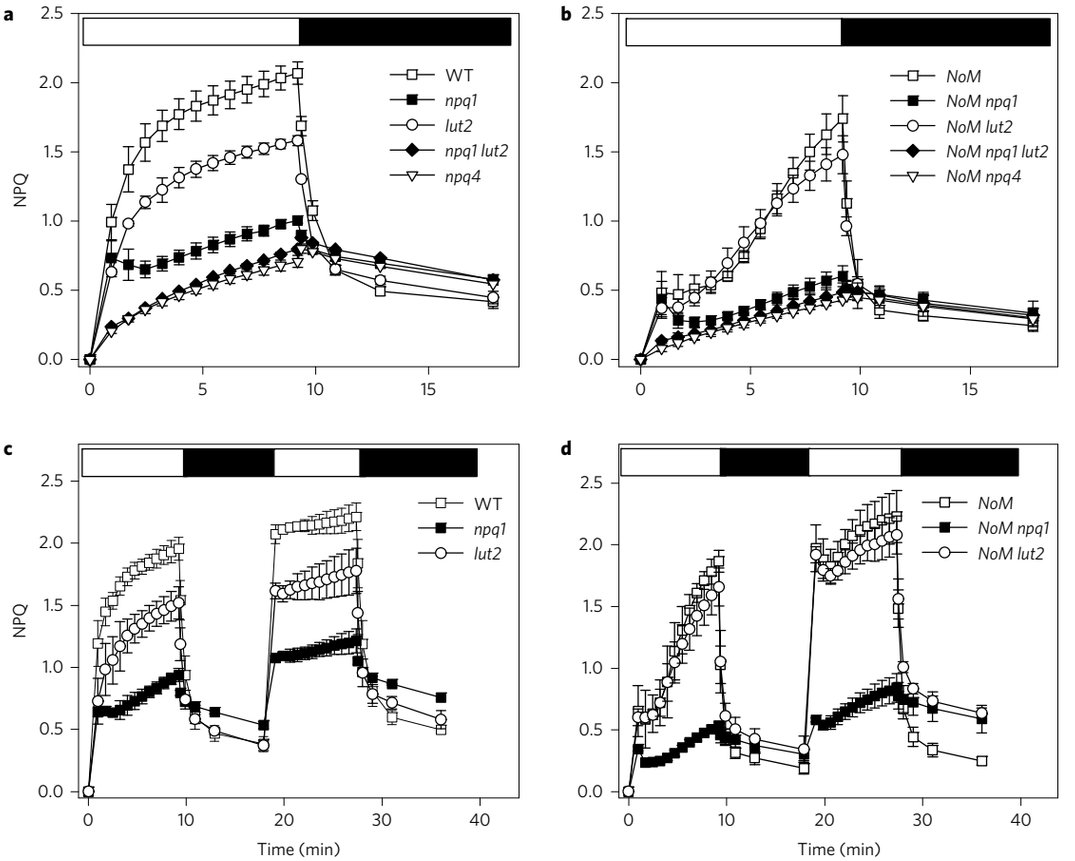

Figure 4 | Kinetics of the formation and relaxation of photoprotective energy dissipation. a,**b**, Measurements of NPQ kinetics on plants either retaining (**a**), or devoid of (**b**), monomeric antennae, and unable to synthesize zeaxanthin (*npq1*), lutein (*lut2*) or PsbS (*npq4*). WT, wild type. **c**,**d**, NPQ kinetics measured on selected genotypes during two consecutive periods of illumination with white light. Leaves were illuminated with 1,200 μmol photons m^{-2} s^{-1}. Symbols and error bars show means ± s.d. ($n > 3$). White and black bars represent light and dark periods.

spinach (Supplementary Fig. 5) and *Arabidopsis* wild-type thylakoids (Fig. 6, upper panel), the differential optical density (ΔOD) traces under actinic light (red lines) revealed additional rise and decay components versus the traces recorded in the absence of qE (black line), thus showing the characteristic pattern of a Zea^+ radical cation signal[24]. The amplitude of the signal was slightly higher in spinach chloroplasts owing to their higher NPQ activity. Thylakoids from *NoM* instead, despite showing NPQ activity, although slightly lower than in wild type, displayed the same kinetics at 1,030 nm (Fig. 6, lower panel) within the experimental error. We conclude that near infrared absorption changes, detected in wild-type thylakoids and reflecting a CT event, can be correlated with the NPQ component associated with monomeric LHCs only. Instead, no TA signals that can be associated with CT could be detected in genotypes retaining LHCII as the only antenna, despite the fact that the LHCII content was increased by 60% in the *NoM* versus wild-type thylakoids.

Discussion

All oxygenic photoautotrophs have mechanisms for regulating the efficiency by which the excited states from absorbed light are transferred to RC for photochemical reactions. Eukaryotic algae and land plants evolved feedback-regulated systems in which thylakoid luminal pH signals excess irradiation. Transduction of the low luminal pH into activation of NPQ reactions requires PsbS in land plants[39]. Pigment interactions, either Chl/Chl pairs[21,22] or Chls/carotenoid pairs[19,23,26], have been proposed to be essential elements of quenching reactions for Chl excited states, thus implying that quenching mechanisms, elicited by the pigment-less subunit PsbS, must occur in interacting pigment-binding subunits of the PSII antenna system. Instead, the organization of PSII–LHCII supercomplexes does not appear to be relevant for NPQ activity since PSII RC level can be reduced by pharmacological treatments or low temperature[17,40], leading to the formation of LHCII-only membranes with enhanced NPQ[17]. The difficulty with identification of quenching sites among LHC gene products is redundancy, since members of the PSII antenna system in *Arabidopsis* are encoded by 14 homologous genes. Reverse genetics has contributed to featuring properties of gene products involved, by showing that quenching reactions are prevented by lack of both Lut and Zea[15] or their ligand LHC proteins[41]. In Lhcb subgroups, down-regulation of Lhcb1[42] and monomeric LHCs[29,30], but not of Lhcb2[43] or Lhcb3[44], affected quenching, thus inciting a lively debate on the mechanisms and localization of quenching reactions in either the monomeric or the trimeric antenna proteins.

Results obtained in the present study from the functional characterization of the *NoM* mutant and by further introducing mutations in this background suggest a series of conclusions.

LHC monomers modulate the middle P2 phase of energy dissipation, namely in the first minutes of transition from darkness to strong illumination (Fig. 3a,b). Slower onset of quenching was previously reported in single KO genotypes[29,30], although the effect was weaker. This evidence indicates that monomeric LHCs collectively contribute to the early phase of the quenching response.

LHCII trimers also participate in quenching but their response rate is slower. Indeed, illumination in the *NoM* genotype leads to

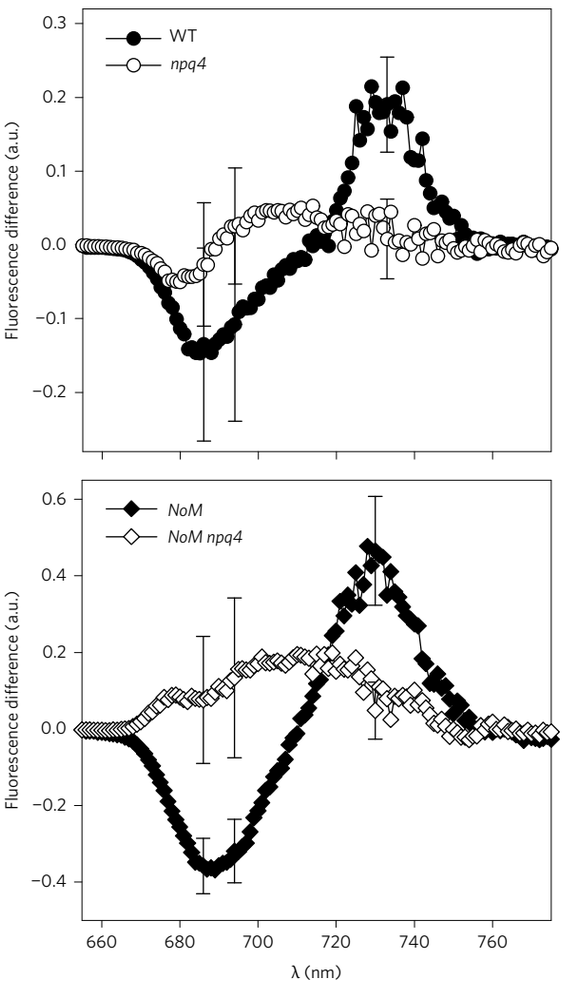

Figure 5 | Spectral changes associated with the formation of NPQ in wild-type, *npq4* and *NoM* genotypes. The 77 K fluorescence emission spectra were recorded from *Arabidopsis* wild-type (WT), *npq4*, *NoM* and *NoM npq4* leaves, either illuminated for 12 min with white actinic light (1,200 μmol photons m^{-2} s^{-1}, RT) or kept for 10 min in darkness upon illumination, to promote NPQ relaxation. Figure displays comparison of light-minus-redark fluorescence difference spectra for *Arabidopsis* wild type versus *npq4* (upper panel) and *NoM* versus *NoM npq4* (lower panel) plants. Error bars represent the s.d. values at 686, 694 and 727 nm, corresponding to eight leaves measured individually for each genotype (for details see ref. 37 and Supplementary Fig. 4).

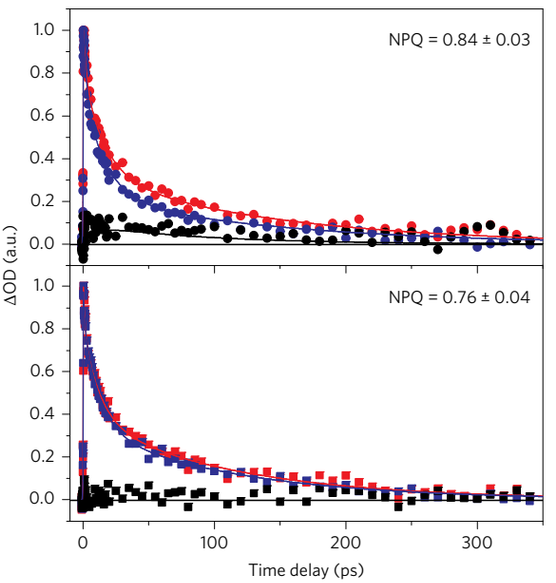

Figure 6 | TA spectroscopy on wild-type and *NoM* thylakoids. TA kinetics have been probed at 1,030 nm on thylakoids of *Arabidopsis* wild type (WT, higher panel) or *NoM* (lower panel) with qE (red line) or without qE (blue line). Difference kinetic traces are reported in black. Symbols show experimental data and solid lines multi-exponential fits.

the same quenching amplitude as wild type only after ~10 min of light. This implies that trimeric and monomeric LHCs synergistically contribute to energy dissipation under the fast-changing conditions caused by variable shading under canopies. When considering the relative abundance of trimeric LHCII versus monomeric complexes in wild type[13] and the further 60% increase in trimeric LHCII observed in *NoM* (Fig. 2d), the specific quenching activity of monomeric LHCs appears far higher than that of trimeric LHCII. The lack of monomeric LHCs leads to dissociation of PSII supercomplexes, confirming that LHCII trimers could be the site of the quenching irrespective of their involvement in PSII supercomplexes[17].

The nature of the quenching reactions is different in monomers versus trimers: the faster-activated P2 in monomers requires both Lut and Zea, whereas the slower-activated P3 in LHCII is dependent on Zea only (Fig. 4b,d), as shown by the phenotype of the *NoM npq1* mutant, hardly distinguishable from the null activity of *NoM npq4* and *NoM npq1 lut2* (Fig. 4b). This indicates that Lut bound to the LHC monomers is responsible for the changes in NPQ observed in the *NoM* mutant, so that deletion of Lut gave rise to no further changes. This is further supported by the results of TA measurements of carotenoid radical cation in thylakoids of wild type versus *NoM*, showing that appearance of the radical cation is associated with the monomeric LHCs (Fig. 6). These findings are fully consistent with previous data on purified LHC proteins showing generation of carotenoid radical cation in LHC monomers and not in LHCII trimers[25]. Moreover, our results show Vio and Lut can substitute for each other in the same quenching site(s) within LHCII, whereas Vio in monomers functions as an inhibitor for quenching. This notion is consistent with evidence that a higher amount of Lut in monomeric LHCs enhances both carotenoid radical cation formation and amplitude of qE[45].

Although the appearance of carotenoid radical cation in wild-type thylakoids under quenching conditions suggests that this mechanism is responsible for quenching in LHC monomers, it can be asked which kind of quenching reaction occurs in trimeric LHCII, leading to sustained fluorescence quenching *in vivo* (Fig. 4b). Previous work suggested LHCII undergoes quenching by clustering in the thylakoid membrane[14], leading to red-shifted 400 ps emission[38] which enhances the amplitude of the 727-nm peak in 77 K emission spectra[37]. In Fig. 5, wild type and *NoM* show an HL-induced 727 nm emission change ($\Delta F_{727\ nm}$). This is PsbS-dependent since it is greatly reduced in *npq4* and *NoM npq4*. The signal is enhanced in *NoM* leaves, in which LHCII content is 60% higher with respect to wild type, implying the $\Delta F_{727\ nm}$ is related to the abundance of trimeric LHCII. These data are consistent with this type of LHCII-dependent quenching being active in both wild type and *NoM*, being the only one in the latter genotype. However, we show that quenching in *NoM* is fully dependent on Zea (Fig. 4) at variance with previous reports[46,47]. Also, NPQ in *NoM* is not affected by the *lut2* mutation, suggesting the processes underlying quenching by LHCII *in vivo* differ in some respect to those induced by aggregation *in vitro*, where Lut was shown to act as a quencher[19]. Our results are consistent with the proposal[48] that quenching sites

might be formed by the interaction of PsbS with the major LHCII complex, with the involvement of a Zea molecule. However, the molecular details of PsbS-mediated LHCII quenching have yet to be determined in future work. Genetic dissection of the interactions between components contributing to LHCII quenching (Fig. 4) allows for at least two hypotheses. First, (1) PsbS and Zea binding to LHCII induce a conformational change in the latter which opens a channel for energy transfer from Chl to the S1 state of a xanthophyll in site L1[19], where Vio or Lut shows the same efficiency (Fig. 4b). Alternatively, (2) it can be proposed that a Chl-Car heterodimer forms between a Zea molecule and a peripheral Chl of LHCII[49,50], leading to a quenching interaction. Although our results point to monomeric LHCs as modulators of the quenching response, it might be asked whether this is consistent with localization of LHC monomers in-between the PSII core complex and trimeric LHCII. Indeed, topological analysis of changes induced in PSII antenna organization upon activation of NPQ has shown that protonated PsbS causes dissociation of CP24 and the LHCII-M trimer from the C2S2M2 supercomplex, thus making CP29 accessible to possible interactors activated by lumen acidification[14], including PsbS itself. The two moieties of the PSII antenna system produced by the dissociation event are, thus, proposed to become the sites for the fast-activated and slow-activated components of NPQ identified by the *NoM* mutant in the present report.

Illumination of dark-adapted *NoM* leaves with saturating light resulted in the fast development of a quenching during the first minute (P1), which transiently reversed in the following 3–4 min (P2); then, quenching resumed and rose to the same amplitude of wild type (P3). P1 is partially affected by either Zea or Lut depletion, and it disappears completely in plants devoid of PsbS (Fig. 4). The fluorescence dynamic of *NoM* leaves is consistent with generation of transient RC quenching, documented both *in vitro*[51] and *in vivo*[34] within the first 1–2 min of illumination. It was detected in wild-type leaves at subsaturating irradiance, whereas it was rapidly converted into a large, antenna-type quenching process at saturating light[34]. In *NoM* genetic background, the RC quenching becomes evident even upon sustained illumination, due to the slower activation of qE. Clearly, PsbS is involved in generation of RC quenching, possibly through direct association to the PSII core complex[52].

We propose that PsbS, upon protonation, increases its affinity for CP29 (and possibly CP26) leading to the disruption of the C2S2M2 supercomplex into a C2S2 moiety and a CP24-LHCII moiety[14], both of which interact with PsbS, although by different modes (Supplementary Fig. 6). Interaction with CP29/CP26 leads to a conformational change, which is favoured by the high rate of Vio/Zea exchange[53], by the presence of proton-binding sites in these two complexes[54] and by the formation of tight interactions between two Chl *a* ligands and either Zea or Lut bound to site L2[25,26,45]. PsbS also interacts with LHCII as shown by the presence of NPQ in the *NoM* mutant, and this interaction requires Zea, but not Lut, for triggering of the quenching. Whether Zea is located in-between PsbS and its LHCII interactor[48] or binds to the V1 site[49,50] is not clear at present and requires further analysis.

Methods

Plant material and growth conditions. Wild-type plants of *Arabidopsis thaliana* (Col-0) and mutants *koLhcb4.1*, *koLhcb4.2*, *koLhcb5* and *koLhcb6* were obtained as previously described[29,30]. Multiple mutant *koLhcb4.1 koLhcb4.2 koLhcb5* (*NoM*) was isolated as previously described[31]. Multiple mutants *NoM npq1*, *NoM npq4*, *NoM lut2* and *NoM npq1 lut2* were obtained by crossing single mutants and selecting progeny by either immunoblotting or HPLC. Plants were grown in a phytotron for 6 weeks at 150 µmol photons m^{-2} s^{-1}, 23 °C, 70% humidity, 8/16 h of day/night.

Membrane isolation. Chloroplasts and stacked thylakoid membranes were isolated as previously described[55].

Pigment analysis. To measure zeaxanthin accumulation, detached leaves floating on water were exposed to 1,200 µmol photons m^{-2} s^{-1} at room temperature (RT, 22 °C). Pigments were extracted from leaf discs with 85% acetone buffered with Na_2CO_3, separated and quantified by HPLC[56].

Spectroscopy. Absorption measurements were performed at RT using an SLM Aminco DW-2000 spectrophotometer. P700 absorption changes of leaves were sampled by weak monochromatic flashes (10-nm bandwidth, 705 nm) provided by light-emitting diodes (JTS10; Biologic Science Instruments).

Gel electrophoresis and immunoblotting. SDS–PAGE analysis was performed using the Tris-Tricine buffer system[57]. Non-denaturing Deriphat-PAGE was performed as described in[58]. For immunotitration, thylakoid samples were loaded for each sample and electroblotted on nitrocellulose membranes, then proteins were detected with alkaline phosphatase-conjugated antibody.

Analysis of Chl fluorescence. PSII function during photosynthesis was measured through Chl fluorescence on whole leaves at RT with a PAM 101 fluorimeter (Heinz–Walz). Chl fluorescence parameters were calculated according to[32]. Colour video images of F_0 (minimal fluorescence from dark-adapted leaves) were obtained with a FluorCam FC 800-C (PSI, Brno, Czech Republic).

Measurement of ΔpH. The kinetics of ΔpH formation across the thylakoid membrane were measured in chloroplast suspension using the method of 9-aminoacridine fluorescence quenching, as previously described[33].

77K fluorescence measurements. The 77 K Chl fluorescence quenching experiments were done according to[37] with minor modifications. Dark-adapted leaves were either illuminated with 1,200 µmol photons m^{-2} s^{-1} of white light at RT for 12 min, or redarkened for 10 min and then immediately frozen in liquid nitrogen. Fluorescence spectra were recorded using a Jobin-Yvon Fluoromax-3 spectrofluorimeter equipped with an optical fibre.

Near infrared TA spectroscopy. Time-resolved experiments to detect the generation of the Car radical cation were performed in a standard pump-probe setup. A KGW amplified laser system (Pharos, Light Conversion) provided the probe wavelength at 1,030 nm and pumped a lab-built non-colinear optical parametric amplifier. The latter provided pump pulses at 665 nm, which were focused to a 220 µm spot at the sample, whereas the probe spot was kept twice smaller. Measured cross-correlation between pump and probe pulses was ~200 fs. A 20 nJ per pulse excitation energy and 200 kHz repetition rate were used for the spinach experiments, whereas 40 nJ per pulse and 20 kHz were used for the *Arabidopsis* experiments. Double-frequency lock-in detection was used to reject high scattering from the sample. Optical choppers operating at 179 and 399 Hz were placed in the pump and probe beams, and TA signal was measured at the sum and difference frequencies[59]. Thylakoid samples with optical density of 0.6–0.8 at the excitation wavelength were kept in the 1 mm path length fused silica optical cell, which was constantly moved in the raster pattern during the experiments. Freshly prepared and activated samples were never measured for longer than 1 h to prevent accumulation of the inactive thylakoids. Dark-adapted kinetics were measured first, followed by HL-induced measurements. HL conditions were induced with 10 min illumination by the 760 µmol photons m^{-2} s^{-1} of white actinic light. A 770-nm pass filter was placed before the detector and a 315–710 nm bandpass filter was placed after the actinic lamp.

Data availability. Sequence data from this article can be found in the *Arabidopsis* Genome Initiative or GenBank/EMBL databases under accession numbers At5g01530 (Lhcb4.1), At3g08940 (Lhcb4.2), At4g10340 (Lhcb5), At1g15820 (Lhcb6), At1g08550 (violaxanthin de-epoxidase), At1g44575 (PsbS) and At5g57030 (lycopene-ε-cyclase). The knock-out lines mentioned in the article were obtained from the NASC under the stock numbers N376476 (*koLhcb4.1*), N877954 (*koLhcb4.2*), N514869 (*koLhcb5*), N577953 (*koLhcb6*) and N505018 (*lut2*).

Received 15 September 2016; accepted 14 February 2017; published 10 April 2017

References

1. Vass, I. *et al.* Reversible and irreversible intermediates during photoinhibition of photosystem II: stable reduced QA species promote chlorophyll triplet formation. *Proc. Natl Acad. Sci. USA* **89,** 1408–1412 (1992).
2. Niyogi, K. K. & Truong, T. B. Evolution of flexible non-photochemical quenching mechanisms that regulate light harvesting in oxygenic photosynthesis. *Curr. Opin. Plant Biol.* **16,** 307–314 (2013).
3. de Bianchi, S., Ballottari, M., Dall'Osto, L. & Bassi, R. Regulation of plant light harvesting by thermal dissipation of excess energy. *Biochem. Soc. Trans.* **38,** 651–660 (2010).
4. Horton, P., Ruban, A. V. & Walters, R. G. Regulation of light harvesting in green plants. *Annu. Rev. Plant Physiol. Plant Mol. Biol.* **47,** 655–684 (1996).
5. Cazzaniga, S., Dall'Osto, L., Kong, S. G., Wada, M. & Bassi, R. Interaction between avoidance of photon absorption, excess energy dissipation and zeaxanthin synthesis against photoxidative stress in *Arabidopsis*. *Plant J.* **76,** 568–579 (2013).

6. Nilkens, M. *et al.* Identification of a slowly inducible zeaxanthin-dependent component of non-photochemical quenching of chlorophyll fluorescence generated under steady-state conditions in *Arabidopsis*. *Biochim. Biophys. Acta.* **1797,** 466–475 (2010).
7. Li, X. P. *et al.* Regulation of photosynthetic light harvesting involves intrathylakoid lumen pH sensing by the PsbS protein. *J. Biol. Chem.* **279,** 22866–22874 (2004).
8. Dominici, P. *et al.* Biochemical properties of the PsbS subunit of photosystem II either purified from chloroplast or recombinant. *J. Biol. Chem.* **277,** 22750–22758 (2002).
9. Fan, M. *et al.* Crystal structures of the PsbS protein essential for photoprotection in plants. *Nat. Struct. Mol. Biol.* **22,** 729–735 (2015).
10. Suga, M. *et al.* Native structure of photosystem II at 1.95 Å resolution viewed by femtosecond X-ray pulses. *Nature* **517,** 99–103 (2015).
11. Jansson, S. A guide to the *Lhc* genes and their relatives in *Arabidopsis*. *Trends Plant Sci.* **4,** 236–240 (1999).
12. Wei, X. *et al.* Structure of spinach photosystem II-LHCII supercomplex at 3.2 Å resolution. *Nature* **534,** 69–74 (2016).
13. Kouril, R., Wientjes, E., Bultema, J. B., Croce, R. & Boekema, E. J. High-light vs. low-light: effect of light acclimation on photosystem II composition and organization in *Arabidopsis thaliana*. *BBA-Bioenergetics* **1827,** 411–419 (2013).
14. Betterle, N. *et al.* Light-induced dissociation of an antenna hetero-oligomer is needed for non-photochemical quenching induction. *J. Biol. Chem.* **284,** 15255–15266 (2009).
15. Niyogi, K. K. *et al.* Photoprotection in a zeaxanthin- and lutein-deficient double mutant of *Arabidopsis*. *Photosynth. Res.* **67,** 139–145 (2001).
16. Havaux, M., Dall'Osto, L. & Bassi, R. Zeaxanthin has enhanced antioxidant capacity with respect to all other xanthophylls in *Arabidopsis* leaves and functions independent of binding to PSII antennae. *Plant Physiol.* **145,** 1506–1520 (2007).
17. Belgio, E., Johnson, M. P., Juric, S. & Ruban, A. V. Higher plant photosystem II light-harvesting antenna, not the reaction center, determines the excited-state lifetime-both the maximum and the nonphotochemically quenched. *Biophys J.* **102,** 2761–2771 (2012).
18. Ruban, A. V., Walters, R. G. & Horton, P. The molecular mechanism of the control of excitation energy dissipation in chloroplast membranes—inhibition of deltapH- dependent quenching of chlorophyll fluorescence by dicyclohexylcarbodiimide. *FEBS Lett.* **309,** 175–179 (1992).
19. Ruban, A. V. *et al.* Identification of a mechanism of photoprotective energy dissipation in higher plants. *Nature* **450,** 575–578 (2007).
20. Niyogi, K. K., Grossman, A. R. & Björkman, O. *Arabidopsis* mutants define a central role for the xanthophyll cycle in the regulation of photosynthetic energy conversion. *Plant Cell* **10,** 1121–1134 (1998).
21. Muller, M. G. *et al.* Singlet energy dissipation in the photosystem II light-harvesting complex does not involve energy transfer to carotenoids. *ChemPhysChem* **11,** 1289–1296 (2010).
22. Wahadoszamen, M., Berera, R., Ara, A. M., Romero, E. & van Grondelle, R. Identification of two emitting sites in the dissipative state of the major light harvesting antenna. *Phys. Chem. Chem. Phys.* **14,** 759–766 (2012).
23. Bode, S. *et al.* On the regulation of photosynthesis by excitonic interactions between carotenoids and chlorophylls. *Proc. Natl Acad. Sci. USA* **106,** 12311–12316 (2009).
24. Holt, N. E. *et al.* Carotenoid cation formation and the regulation of photosynthetic light harvesting. *Science* **307,** 433–436 (2005).
25. Avenson, T. J. *et al.* Zeaxanthin radical cation formation in minor light-harvesting complexes of higher plant antenna. *J. Biol. Chem.* **283,** 3550–3558 (2008).
26. Ahn, T. K. *et al.* Architecture of a charge-transfer state regulating light harvesting in a plant antenna protein. *Science* **320,** 794–797 (2008).
27. Barros, T., Royant, A., Standfuss, J., Dreuw, A. & Kuhlbrandt, W. Crystal structure of plant light-harvesting complex shows the active, energy-transmitting state. *EMBO J.* **28,** 298–306 (2009).
28. Avenson, T. J. *et al.* Lutein can act as a switchable charge transfer quencher in the CP26 light-harvesting complex. *J. Biol. Chem.* **284,** 2830–2835 (2009).
29. de Bianchi, S., Dall'Osto, L., Tognon, G., Morosinotto, T. & Bassi, R. Minor antenna proteins CP24 and CP26 affect the interactions between photosystem II subunits and the electron transport rate in grana membranes of *Arabidopsis*. *Plant Cell* **20,** 1012–1028 (2008).
30. de Bianchi, S. *et al. Arabidopsis* mutants deleted in the light-harvesting protein Lhcb4 have a disrupted photosystem II macrostructure and are defective in photoprotection. *Plant Cell* **23,** 2659–2679 (2011).
31. Dall'Osto, L., Unlu, C., Cazzaniga, S. & van Amerongen, H. Disturbed excitation energy transfer in *Arabidopsis thaliana* mutants lacking minor antenna complexes of photosystem II. *Biochim. Biophys. Acta* **1837,** 1981–1988 (2014).
32. Baker, N. R. Chlorophyll fluorescence: a probe of photosynthesis *in vivo*. *Annu. Rev. Plant Biol.* **59,** 89–113 (2008).
33. Johnson, G. N., Young, A. J. & Horton, P. Activation of non-photochemical quenching in thylakoids and leaves. *Planta* **194,** 550–556 (1994).
34. Finazzi, G. *et al.* A zeaxanthin-independent nonphotochemical quenching mechanism localized in the photosystem II core complex. *Proc. Natl Acad. Sci. USA* **101,** 12375–12380 (2004).
35. Pogson, B. J., Niyogi, K. K., Bjorkman, O. & DellaPenna, D. Altered xanthophyll compositions adversely affect chlorophyll accumulation and nonphotochemical quenching in *Arabidopsis* mutants. *Proc. Natl Acad. Sci. USA* **95,** 13324–13329 (1998).
36. Horton, P. *et al.* Control of the light-harvesting function of chloroplast membranes by aggregation of the LHCII chlorophyll-protein complex. *FEBS Lett.* **292,** 1–4 (1991).
37. Lambrev, P. H., Nilkens, M., Miloslavina, Y., Jahns, P. & Holzwarth, A. R. Kinetic and spectral resolution of multiple nonphotochemical quenching components in *Arabidopsis* leaves. *Plant Physiol.* **152,** 1611–1624 (2010).
38. Holzwarth, A. R., Miloslavina, Y., Nilkens, M. & Jahns, P. Identification of two quenching sites active in the regulation of photosynthetic light-harvesting studied by time-resolved fluorescence. *Chem. Phys. Lett.* **483,** 262–267 (2009).
39. Li, X. P. *et al.* A pigment-binding protein essential for regulation of photosynthetic light harvesting. *Nature* **403,** 391–395 (2000).
40. Caffarri, S., Frigerio, S., Olivieri, E., Righetti, P. G. & Bassi, R. Differential accumulation of *Lhcb* gene products in thylakoid membranes of *Zea mays* plants grown under contrasting light and temperature conditions. *Proteomics* **5,** 758–768 (2005).
41. Briantais, J.-M., Hodges, M. & Moya, I. in *Progress in Photosynthesis Research II* (ed. J. Biggins) 705–708 (Nijhoff Publishers, 1987).
42. Pietrzykowska, M. *et al.* The light-harvesting chlorophyll a/b binding proteins Lhcb1 and Lhcb2 play complementary roles during state transitions in *Arabidopsis*. *Plant Cell* **26,** 3646–3660 (2014).
43. Leoni, C. *et al.* Very rapid phosphorylation kinetics suggest a unique role for Lhcb2 during state transitions in *Arabidopsis*. *Plant J.* **76,** 236–246 (2013).
44. Damkjaer, J. *et al.* The photosystem II light-harvesting protein Lhcb3 affects the macrostructure of photosystem II and the rate of state transitions in *Arabidopsis*. *Plant Cell* **21,** 3245–3256 (2009).
45. Li, Z. *et al.* Lutein accumulation in the absence of zeaxanthin restores nonphotochemical quenching in the *Arabidopsis thaliana npq1* mutant. *Plant Cell* **21,** 1798–1812 (2009).
46. Lambrev, P. H. *et al.* Functional domain size in aggregates of light-harvesting complex II and thylakoid membranes. *BBA-Bioenergetics* **1807,** 1022–1031 (2011).
47. Miloslavina, Y. *et al.* Far-red fluorescence: a direct spectroscopic marker for LHCII oligomer formation in non-photochemical quenching. *FEBS Lett.* **582,** 3625–3631 (2008).
48. Wilk, L., Grunwald, M., Liao, P. N., Walla, P. J. & Kuhlbrandt, W. Direct interaction of the major light-harvesting complex II and PsbS in nonphotochemical quenching. *Proc. Natl Acad. Sci. USA* **110,** 5452–5456 (2013).
49. Liu, Z. *et al.* Crystal structure of spinach major light-harvesting complex at 2.72 Å resolution. *Nature* **428,** 287–292 (2004).
50. Caffarri, S., Croce, R., Breton, J. & Bassi, R. The major antenna complex of photosystem II has a xanthophyll binding site not involved in light harvesting. *J. Biol. Chem.* **276,** 35924–35933 (2001).
51. Weis, E. & Berry, J. A. Quantum efficiency of photosystem II in relation to energy dependent quenching of chlorophyll fluorescence. *Biochim. Biophys. Acta* **894,** 198–208 (1987).
52. Haniewicz, P. *et al.* Isolation of monomeric photosystem II that retains the subunit PsbS. *Photosynth. Res.* **118,** 199–207 (2013).
53. Morosinotto, T., Baronio, R. & Bassi, R. Dynamics of chromophore binding to Lhc proteins *in vivo* and *in vitro* during operation of the xanthophyll cycle. *J. Biol. Chem.* **277,** 36913–36920 (2002).
54. Walters, R. G., Ruban, A. V. & Horton, P. Identification of proton-active residues in a higher plant light-harvesting complex. *Proc. Natl Acad. Sci. USA* **93,** 14204–14209 (1996).
55. Casazza, A. P., Tarantino, D. & Soave, C. Preparation and functional characterization of thylakoids from *Arabidopsis thaliana*. *Photosynth. Res.* **68,** 175–180 (2001).
56. Gilmore, A. M. & Yamamoto, H. Y. Zeaxanthin formation and energy-dependent fluorescence quenching in pea chloroplasts under artificially mediated linear and cyclic electron transport. *Plant Physiol.* **96,** 635–643 (1991).
57. Schägger, H. & von Jagow, G. Tricine-sodium dodecyl sulfate-polyacrylamide gel electrophoresis for the separation of proteins in the range from 1 to 100 kDa. *Anal. Biochem.* **166,** 368–379 (1987).
58. Havaux, M., Dall'Osto, L., Cuine, S., Giuliano, G. & Bassi, R. The effect of zeaxanthin as the only xanthophyll on the structure and function of the photosynthetic apparatus in *Arabidopsis thaliana*. *J. Biol. Chem.* **279,** 13878–13888 (2004).
59. Augulis, R. & Zigmantas, D. Two-dimensional electronic spectroscopy with double modulation lock-in detection: enhancement of sensitivity and noise resistance. *Opt. Express.* **19,** 13126–13133 (2011).

Acknowledgements

This work was supported by the EEC projects ACCLIPHOT (PITN-GA-2012-316427) and SE2B (675006–SE2B) to R.B. Work in Lund was supported by LaserLab Europe, the Swedish Research Council and the Knut and Alice Wallenberg Foundation. The work of K.K.N. and G.R.F. was supported by the Director, Office of Science, Office of Basic Energy Sciences, of the US Department of Energy under Contract No. DEAC02-05CH11231 and the Chemical Sciences, Geosciences and Biosciences Division, Office of Basic Energy Sciences under field work proposal 449B. L.D.'s work was supported by international mobility programme CooperInt 2011/2014, University of Verona.

Author contributions

R.B., K.K.N. and G.R.F. conceived the work and designed the experiments. L.D., S.C. and M.B. performed all the experiments for the isolation of mutants, and their physiological and biochemical characterization. D.Z. coordinated and performed the transient absorption spectroscopy experiments. D.P. and K.Z. contributed to the time resolved analysis experiments. All of the authors contributed to writing the manuscript. All of the authors discussed the results and commented on the manuscript.

Additional information

Supplementary information is available for this paper.

Reprints and permissions information is available at www.nature.com/reprints.

Correspondence and requests for materials should be addressed to R.B.

How to cite this article: Dall'Osto, L. *et al.* Two mechanisms for dissipation of excess light in monomeric and trimeric light-harvesting complexes. *Nat. Plants* **3,** 17033 (2017).

Publisher's note: Springer Nature remains neutral with regard to jurisdictional claims in published maps and institutional affiliations.

Competing interests

The authors declare no competing financial interests.

Supplementary Figure 1. Development kinetics during vegetative growth of wild type and mutant plants. **a**, Changes over time in leaf number for *Arabidopsis thaliana* wild type and *NoM*, grown in soil at 150 µmol photons m^{-2} s^{-1}, 23°C, 8/16 hours light/dark. Each experimental point corresponds to the leaf number in a distinct rosette; these data are representative of two independent experiments. Experimental points were modeled with a linear regression, whose slope (corresponding to mean number of leaves developed per week of growth) is reported. **b**, Kinetics of rise and relaxation of photoprotective energy dissipation, measured at different pre-flowering growth stages. NPQ was induced with 1200 µmol photons m^{-2} s^{-1}, in wild-type and *NoM* plants. For each genotype, curves were gathered into distinct groups, based on the number of leaves per rosette, and averaged. All data are expressed as mean ± SD (n > 4). White and black bars represent light and dark periods.

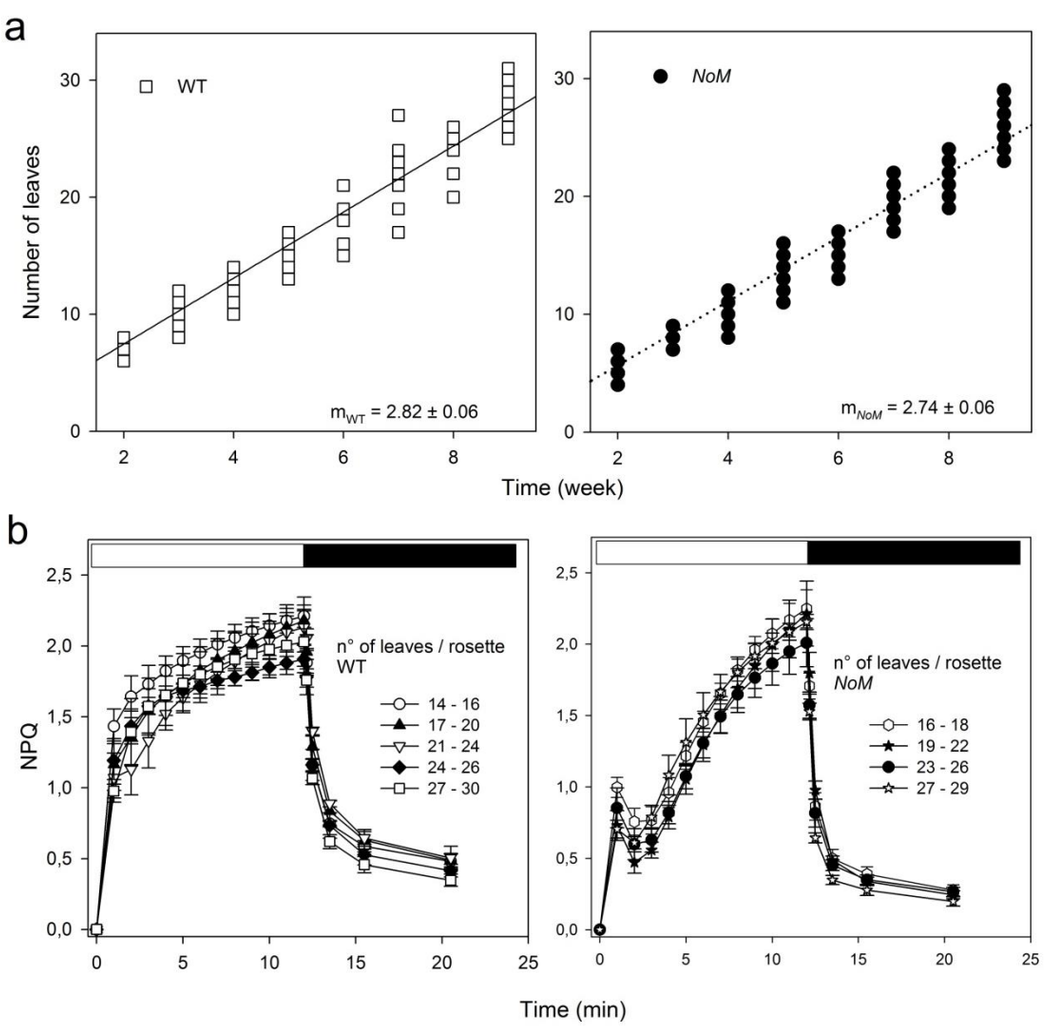

NATURE PLANTS | DOI: 10.1038/nplants.2017.33 | www.nature.com/natureplants

Supplementary Figure 2. Analysis of the main factors controlling NPQ amplitude and kinetic. (A) **a**, Immunotitration of thylakoid membranes with anti-PsbS antibody. **b**,Light-dependent quenching of 9-AA fluorescence in intact chloroplasts, quantified as a measure for trans-thylakoid ΔpH. **c**,Time course of Vio de-epoxidation in wild type and mutant plants. Leaf discs from dark-adapted leaves were illuminated at 1200 µmol photons m^{-2} s^{-1} (white actinic light). At different times, leaf discs were frozen in liquid nitrogen and total pigments extracted before HPLC analysis. **d**, Amplitude of violaxanthin de-epoxidation was measured on leaf discs from the wild type and *NoM* after illumination (15 min) at different light intensities. All data are expressed as mean ± SD (n = 5). White and black bars represent light and dark periods.

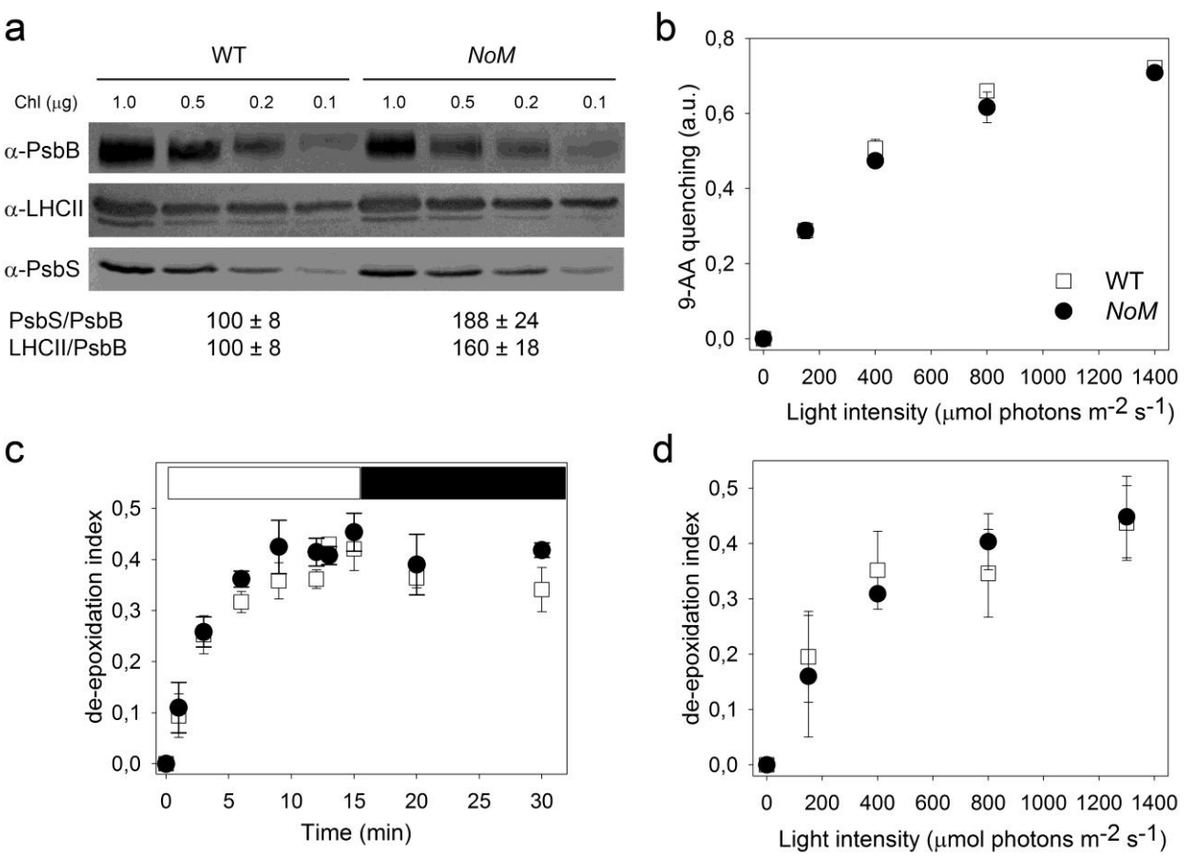

NATURE PLANTS | DOI: 10.1038/nplants.2017.33 | www.nature.com/natureplants

Supplementary Figure 3. Kinetics of rise and relaxation of photoprotective energy dissipation. a,Kinetics of NPQ were measured on leaves from wild-type, *NoM* and double mutants *koLhcb4* and *koLhcb5 Lhcb6*, upon illumination with 1200 µmol photons m^{-2} s^{-1}. Symbols and error bars show means ± SD (n = 4). White and black bars represent light and dark periods.

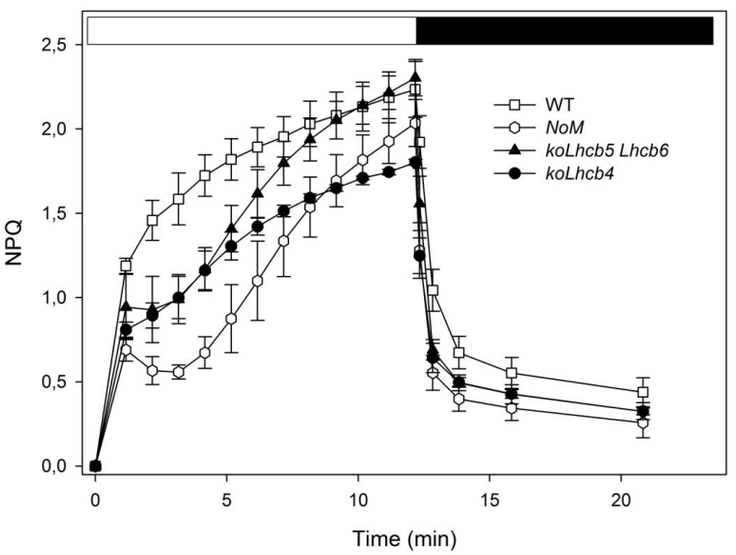

NATURE PLANTS | DOI: 10.1038/nplants.2017.33 | www.nature.com/natureplants

Supplementary Figure 4. Spectral changes associated with the formation of NPQ in wild type, *npq4* and *NoM* genotypes. 77K fluorescence emission spectra were recorded from *Arabidopsis* wild type (**a**), *npq4* (**b**), *NoM* (**c**) and *NoM npq4* (**d**) leaves, either illuminated for 12 min (closed symbols) with white actinic light (1200 µmol photons m^{-2} s^{-1}, RT) or kept for 10 minutes in darkness upon illumination to promote relaxation of NPQ (open symbols). Spectra were normalized to the average amplitude between 755 and 760 nm. The curves represents averages of eight measurements on different leaves, SD is shown for selected λ.

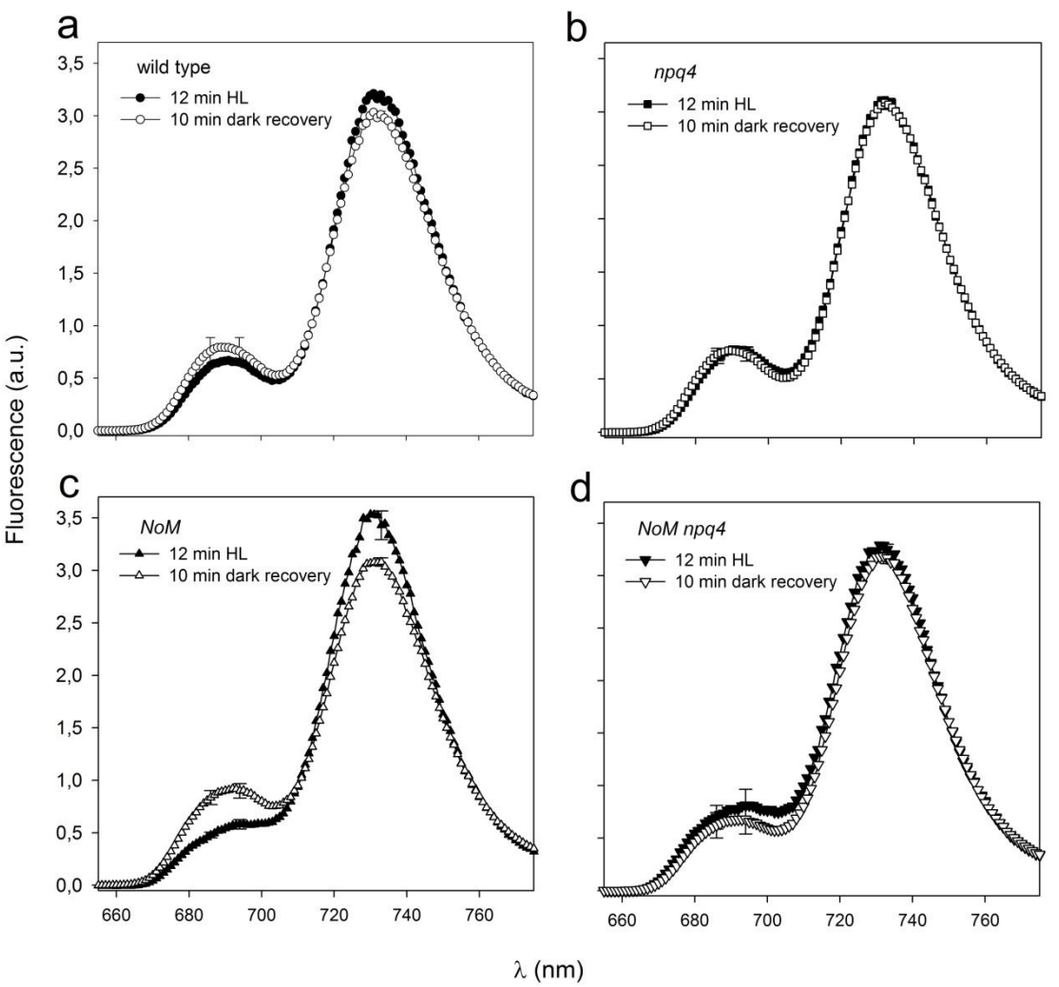

NATURE PLANTS | DOI: 10.1038/nplants.2017.33 | www.nature.com/natureplants

Supplementary Figure 5. TA spectroscopy on spinach thylakoids. TA kinetics have been probed at 1030 nm on thylakoids from spinach with qE (red line) or without qE (blue line). Difference kinetic traces are reported in black. Symbols show experimental data and solid lines multiexponential fits.

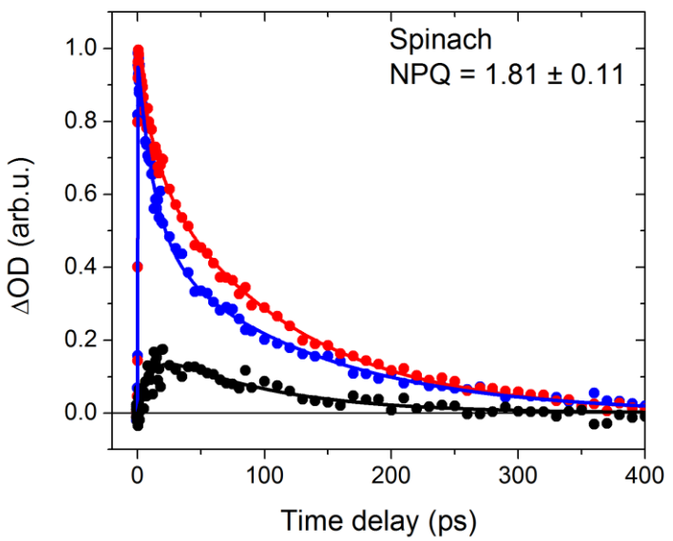

NATURE PLANTS | DOI: 10.1038/nplants.2017.33 | www.nature.com/natureplants

Supplementary Figure 6. Model of the PSII supercomplex reorganization during NPQ activation. Excess light (EL) induces activation of rapid excitation energy quenching response triggered by low lumenal pH, and requires both Zea and Lut [1] and the pH sensor PSBS [2]. Lumen acidification is the signal for xanthophyll cycle activation [3], monomerization of PSBS [4] and dissociation of the CP29-CP24-LHCII supercomplex [5]. Rapid dissipative response is catalyzed by two independent mechanisms in monomeric and trimeric LHCs of PSII: the component catalyzed by monomers requires both Lut and Zea and involves a carotenoid radical cation accumulation; the quenching component by LHCII depends on Zea only. dPSBS and mPSBS denote dimeric and monomeric form of PSBS, respectively. The organization of the antennae in dark-adapted (left hand side) and HL conditions (right hand side) is based on data from [5-8].

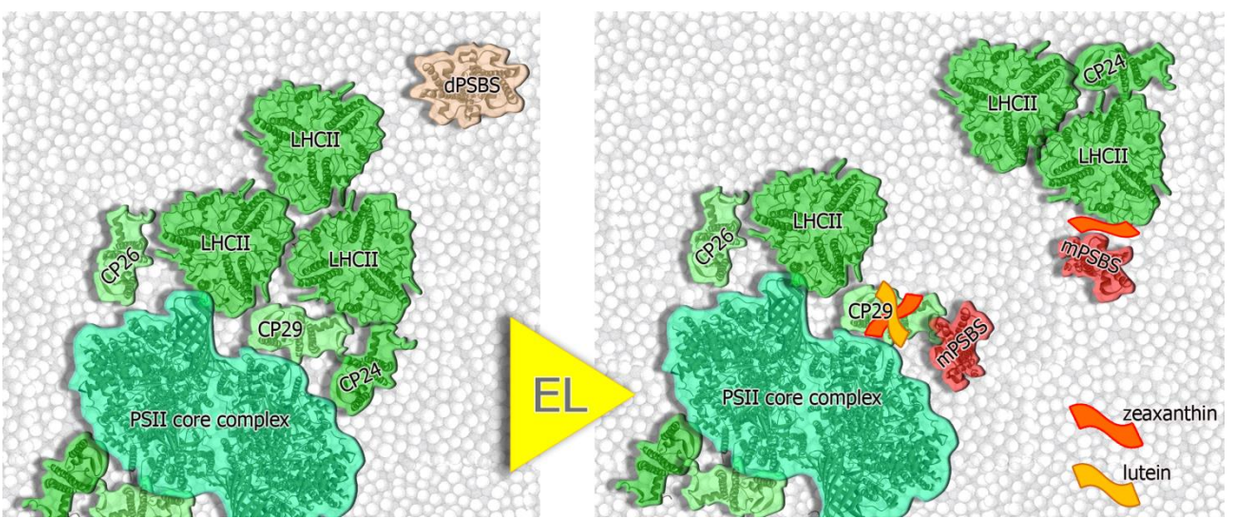

NATURE PLANTS | DOI: 10.1038/nplants.2017.33 | www.nature.com/natureplants

Supplementary Table 1. **Pigment composition of leaves from wild type and *NoM* mutants**. Pigments were extracted from leaves either dark adapted or exposed to high light (1200 µmol photons m^{-2} s^{-1}, 20 min). The data are normalized to 100 Chl *a* + *b* molecules. Symbols and error bars show means ± SD (n = 3). Significantly different values (ANOVA, P < 0.05), within a column and a light regime, are marked with different letters.

		mol pigments / 100 mol Chls							
		Chl *a/b*	**Chl / Car**	**Neo**	**Vio**	**Anthera**	**Lut**	**Zea**	**β-Car**
Dark-adapted	**WT**	3.0 ± 0.1^{a}	4,0 ± 0,1^{a}	3,6 ± 0,2^{a}	2,3 ± 0,1^{a}	-	11,9 ± 0,3^{a}	-	7,5 ± 0,9^{a}
	NoM	2.4 ± 0.1^{b}	3,4 ± 0,2^{b}	4,7 ± 0,3^{b}	3,1 ± 0,3^{b}	-	14,7 ± 0,7^{b}	-	6,9 ± 0,8^{a}
	npq1	2.9 ± 0.1^{a}	3,6 ± 0,2^{a,b}	3,9 ± 0,1^{a}	3,1 ± 0,4^{b}	-	13,0 ± 0,6^{a}	-	8,2 ± 0,7^{a}
	NoM npq1	2.4 ± 0.1^{b}	3,5 ± 0,1^{b}	4,5 ± 0,2^{b}	3,4 ± 0,4^{b}	-	14,2 ± 0,5^{b}	-	6,8 ± 0,6^{a}
	lut2	3.0 ± 0.1^{a}	4,3 ± 0,2^{a}	3,4 ± 0,4^{a}	7,9 ± 1,2^{c}	2,7 ± 0,3^{a}	-	1,1 ± 0,3^{a}	8,0 ± 1,4^{a}
	NoM lut2	2.6 ± 0.1^{b}	3,5 ± 0,2^{b}	4,4 ± 0,4^{b}	9,7 ± 0,5^{c}	4,0 ± 0,4^{b}	-	1,7 ± 0,5^{a}	8,6 ± 1,1^{a}
	npq4	2.9 ± 0.1^{a}	3,7 ± 0,2^{a,b}	3,9 ± 0,4^{a,b}	2,5 ± 0,1^{a}	-	12,7 ± 1,0^{a}	-	8,0 ± 0,1^{a}
	NoM npq4	2.4 ± 0.1^{b}	3,5 ± 0,1^{b}	4,8 ± 0,2^{b}	2,6 ± 0,3^{a,b}	-	15,1 ± 0,8^{b}	-	6,6 ± 1,1^{a}
	npq1 lut2	3.0 ± 0.1^{a}	4,1 ± 0,1^{a}	3,3 ± 0,2^{a}	9,7 ± 0,7^{c}	1,4 ± 0,1^{c}	-	0,4 ± 0,1^{b}	9,9 ± 0,2^{b}
	NoM npq1 lut2	2.7 ± 0.1^{a,b}	3,5 ± 0,3^{b}	4,2 ± 0,6^{a,b}	14,1 ± 1,9^{d}	0,9 ± 0,1^{d}	-	0,4 ± 0,1^{b}	9,1 ± 0,7^{a,b}
High-light	**WT**	3,0 ± 0,1^{a}	3,7 ± 0,1^{a,b}	3,6 ± 0,2^{a}	1,2 ± 0,1^{a}	0,3 ± 0,1^{a}	11,8 ± 0,8^{a}	1,4 ± 0,4^{a}	8,6 ± 0,9^{a,b}
	NoM	2,4 ± 0,1^{b}	3,5 ± 0,1^{b}	4,5 ± 0,2^{b}	1,5 ± 0,2^{a}	0,6 ± 0,1^{a}	14,5 ± 0,5^{b}	1,4 ± 0,3^{a}	6,6 ± 0,6^{a}
	npq1	2,9 ± 0,1^{a}	3,5 ± 0,1^{b}	3,9 ± 0,1^{a}	2,8 ± 0,4^{b}	-	13,3 ± 0,6^{a}	-	8,2 ± 0,5^{a,b}
	NoM npq1	2,4 ± 0,1^{b}	3,4 ± 0,2^{b}	4,7 ± 0,2^{b}	3,5 ± 0,4^{b}	-	14,4 ± 0,7^{b}	-	6,8 ± 1,1^{a}
	lut2	3,0 ± 0,1^{a}	4,1 ± 0,3^{a}	3,2 ± 0,2^{a}	5,6 ± 0,5^{c}	2,6 ± 0,3^{b}	-	3,3 ± 0,4^{b}	9,9 ± 1,1^{b}
	NoM lut2	2,6 ± 0,1^{b}	3,4 ± 0,2^{b}	4,3 ± 0,2^{b}	8,3 ± 1,3^{d}	4,3 ± 0,1^{c}	-	3,1 ± 0,9^{b}	9,3 ± 0,9^{b}
	npq4	2,9 ± 0,1^{a}	3,8 ± 0,1^{a}	3,8 ± 0,2^{a}	1,3 ± 0,1^{a}	0,4 ± 0,1^{a}	12,5 ± 0,5^{a}	1,2 ± 0,1^{a}	7,4 ± 1,1^{a,b}
	NoM npq4	2,4 ± 0,1^{b}	3,4 ± 0,1^{b}	4,7 ± 0,2^{b}	1,4 ± 0,5^{a}	0,5 ± 0,1^{a}	15,3 ± 0,8^{b}	1,2 ± 0,2^{a}	6,4 ± 0,8^{a}
	npq1 lut2	3,1 ± 0,1^{a}	4,1 ± 0,2^{a}	3,0 ± 0,4^{a}	10,0 ± 0,6^{d}	1,3 ± 0,3^{d}	-	0,4 ± 0,1^{c}	9,9 ± 1,0^{b}
	NoM npq1 lut2	2,7 ± 0,1^{a,b}	3,6 ± 0,3^{a,b}	4,0 ± 0,2^{a,b}	13,5 ± 1,0^{e}	1,0 ± 0,1^{d}	-	0,4 ± 0,1^{c}	9,1 ± 1,6^{b}

NATURE PLANTS | DOI: 10.1038/nplants.2017.33 | www.nature.com/natureplants

References

1 Niyogi, K. K. *et al.* Photoprotection in a zeaxanthin- and lutein-deficient double mutant of Arabidopsis. *Photosynth.Res.* **67**, 139-145 (2001).

2 Li, X. P. *et al.* A pigment-binding protein essential for regulation of photosynthetic light harvesting. *Nature* **403**, 391-395 (2000).

3 Demmig-Adams, B. & Adams, W. W. Photoprotection and other responses of plants to high light stress. *Ann.Rev.Plant Physiol.Plant Mol.Biol.* **43**, 599-626 (1992).

4 Bergantino, E. *et al.* Light- and pH-dependent structural changes in the PsbS subunit of photosystem II. *Proc.Natl.Acad.Sci.U.S.A* **100**, 15265-15270 (2003).

5 Betterle, N. *et al.* Light-induced dissociation of an antenna hetero-oligomer is needed for non-photochemical quenching induction. *Journal of Biological Chemistry* **284**, 15255-15266 (2009).

6 Caffarri, S., Kouril, R., Kereiche, S., Boekema, E. J. & Croce, R. Functional architecture of higher plant photosystem II supercomplexes. *EMBO J.* **28**, 3052-3063 (2009).

7 Johnson, M. P. *et al.* Photoprotective energy dissipation involves the reorganization of Photosystem II light-harvesting complexes in the grana membranes of spinach chloroplasts. *Plant Cell* **23**, 1468-1479 (2011).

8 Miloslavina, Y., de Bianchi, S., Dall'Osto, L., Bassi, R. & Holzwarth, A. R. Quenching in Arabidopsis thaliana mutants lacking monomeric antenna proteins of photosystem II. *J.Biol.Chem.* **286**, 36830-36840 (2011).

Chapter 3

Differential Roles of Carotenes and Xanthophylls in Photosystem I Photoprotection

This chapter was published in

Biochemistry, vol 55, 3636−3649 (2016)

BIOCHEMISTRY
including biophysical chemistry & molecular biology

Article

pubs.acs.org/biochemistry

Differential Roles of Carotenes and Xanthophylls in Photosystem I Photoprotection

Stefano Cazzaniga,[†] Mauro Bressan,[†] Donatella Carbonera,[‡] Alessandro Agostini,[‡] and Luca Dall'Osto*[,†]

[†]Dipartimento di Biotecnologie, Università di Verona, Strada Le Grazie 15, 37134 Verona, Italy

[‡]Dipartimento di Scienze Chimiche, Università di Padova, via Marzolo 1, 35100 Padova, Italy

Supporting Information

ABSTRACT: Carotenes and their oxygenated derivatives, xanthophylls, are structural elements of the photosynthetic apparatus and contribute to increasing both the light-harvesting and photoprotective capacity of the photosystems. *β*-Carotene is present in both the core complexes and light-harvesting system (LHCI) of Photosystem (PS) I, while xanthophylls lutein and violaxanthin bind exclusively to its antenna moiety; another xanthophyll, zeaxanthin, which protects chloroplasts against photooxidative damage, binds to the LHCI complexes under conditions of excess light. We functionally dissected various components of the xanthophyll- and carotene-dependent photoprotection mechanism of PSI by analyzing two *Arabidopsis* mutants: *szl1* plants, with a carotene content lower than that of the wild type, and *npq1*, with suppressed zeaxanthin formation. When exposed to excess light, the *szl1* genotype displayed PSI photoinhibition stronger than that of wild-type plants, while removing zeaxanthin had no such effect. The PSI−LHCI complex purified from *szl1* was more photosensitive than the corresponding wild-type and *npq1* complexes, as is evident from its faster photobleaching and increased rate of singlet oxygen release, suggesting that *β*-carotene is crucial in controlling chlorophyll triplet formation. Accordingly, fluorescence-detected magnetic resonance analysis showed an increase in the amplitude of signals assigned to chlorophyll triplets in *β*-carotene-depleted complexes. When PSI was fractioned into its functional moieties, it was revealed that the boost in the rate of singlet oxygen release caused by *β*-carotene depletion was greater in LHCI than in the core complex. We conclude that PSI−LHCI complex-bound *β*-carotene elicits a protective response, consisting of a reduction in the yield of harmful triplet excited states, while accumulation of zeaxanthin plays a minor role in restoring phototolerance.

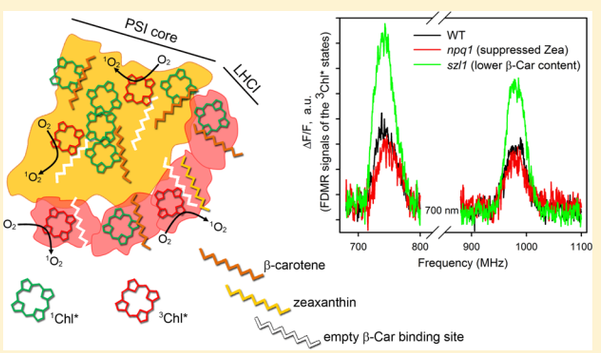

Multimeric pigment−protein complexes present on the thylakoid membrane catalyze light-driven electron transport from water to $NADP^+$, fuel ATP production, and lead to the assimilation of CO_2 into organic matter. Major components of the photosynthetic electron transport chain include Photosystems (PS) II and I, functionally connected by plastoquinone, the cytochrome b_6f complex, and plastocyanin.[1] In each PS, the first stage of solar energy conversion consists of photon absorption by an array of chlorophylls (Chl), which funnel excitation energy to the reaction center where charge separation occurs.[2,3]

Plants are highly effective at photosynthesis, and under steady-state conditions, the singlet excited states of the primary pigment chlorophyll (^{1}Chl*) are efficiently quenched by the photochemical reaction centers.[4] However, the photosynthetic apparatus can easily experience photooxidative damage: excess light (EL) shifts the balance of the captured to utilized energy ratio, increasing the probability of the intersystem crossing to the Chl triplet state (^{3}Chl*) and releasing the highly reactive oxygen species (ROS) singlet oxygen ($^1O_2$).[5,6] This ROS damages its local environment by destroying lipids and proteins, until a depression of the photosynthetic efficiency called photoinhibition occurs.[7] Within the photosynthetic apparatus, the PSII reaction center and its peripheral antenna system were observed to be the major sites of $^1O_2$ release and the main targets of photooxidative damage.[8]

Besides Chls, the major class of pigments present in the photosynthetic apparatus is carotenoids (Car).[9] These are either carotenes, bound to the core complex of both PSs and the light-harvesting complexes (LHC) of PSI,[10−12] or their oxygenated derivatives, xanthophylls (Xan), which are structural elements of the LHC subunits.[10,12,13] Cars are involved in a number of photoprotection mechanisms and are active in (i) preventing overexcitation of the reaction center by de-exciting ^{1}Chl* states,[14,15] (ii) quenching ^{3}Chl* through carotenoid triplet (^{3}Car*) formation,[16] and (iii) acting as antioxidants, thus preventing lipid peroxidation.[17]

Of particular interest for chloroplast photoprotection is xanthophyll zeaxanthin (Zea): absent under low-light conditions, it accumulates in EL only upon the reversible de-

Received: May 2, 2016
Revised: June 6, 2016
Published: June 13, 2016

epoxidation of violaxanthin (Vio).[18,19] Once synthesized, Zea can either be freed into the thylakoids or bound to LHC; the latter process is termed xanthophyll exchange.[20−22] The role of the free Zea pool was investigated in *Arabidopsis thaliana*, where it was observed to possess a capacity to scavenge ROS greater than those of all other xanthophyll species.[23] Furthermore, the photoprotective effect of Zea is greatly enhanced by its binding to LHC subunits,[24,25] where it has been observed to increase the level of PSII photoprotection by (i) enhancing thermal dissipation of ^{1}Chl*[26,27] and (ii) downregulating the ^{3}Chl* yield, thus preventing the release of $^1O_2$.[28]

The role of carotenes in photoprotection has been mainly investigated in the PSII core complex, where most of the β-carotene (β-Car) molecules are in close contact with Chl headgroups, to facilitate ^{3}Chl* quenching. Only the two β-Car ligands in the PSII reaction center are distant from the special pair of Chls[29] and are likely to act as quenchers of $^1O_2$ produced during charge recombination.[30]

Unlike PSII, PSI has been considered to be less sensitive to photooxidative stress: its photoprotection mechanism is believed to rely mainly on ROS scavenging at its acceptor side,[31] because its photosensitivity *in vivo* increases under chilling conditions, which inhibit superoxide scavenging.[32] However, PSI can also be targeted by photoinhibition under conditions unbalancing linear versus cyclic electron transport,[33] or in mutants with a lower β-Car content.[34] Thus, the specific interaction between Chls and Cars in the LHCI antenna system of PSI might play a more relevant role in PSI photoprotection than is generally believed. Supporting this view is the fact that Cars bound to the LHCI system are effective in quenching ^{3}Chl*, thus suggesting that pigments bound to these complexes are well-protected from EL damage.[35,36] Only recently has the presence of a specific binding site for β-Car in LHCI subunits been confirmed,[12,37] whereas differences in the de-epoxidation of Vio in the LHCI subunits suggest different accessibility to the respective Car-binding sites.[38] Despite these observations, the Car-dependent contribution to PSI photoresistance is still rather unclear, and more detailed analyses are needed to understand it.

With this work, we addressed the question of what role both carotene and xanthophyll ligands of PSI play in the photoprotection of this complex. To this aim, we compared a panel of *Arabidopsis* mutants whose biosynthesis of either xanthophylls or carotenes was impaired and analyzed the effect of these depletions on photosensitivity both *in vivo* and *in vitro*. In particular, the *szl1* mutant has both a lower carotene content and an altered xanthophyll composition, whereas Zea does not accumulate in *npq1*. We observed that Zea binds to the peripheral antenna system of PSI; however, it neither enhances photoprotection of the supercomplex under EL conditions nor limits the release of $^1O_2$. On the other hand, however, *szl1* and *szl1 npq1* plants displayed a comparable photoinhibition of PSI but stronger than those of both WT and *npq1* plants, thus suggesting that β-Car ligands play a crucial role in the photoprotection of the supercomplex. Indeed, FDMR analyses of PSI−LHCI complexes from *szl1* plants revealed a greater level of ^{3}Chl*, suggesting a β-Car-specific effect in decreasing the yield of dangerous excited states. Fractionation of PSI supercomplexes from EL-treated plants into core and antenna moieties provided new insight into the photoprotective contribution of β-Car in the domains of PSI. We conclude that, in addition to the previously described effects of carotenes in preventing PSII photoinhibition, a crucial mechanism is mediated by β-Car bound to the peripheral antenna system of PSI, which is instrumental in reducing the yield of harmful ^{3}Chl*.

EXPERIMENTAL METHODS

Plant Material and Growth Conditions. Wild-type plants of *A. thaliana* ecotype Columbia and mutants *chy1chy2*, *lut5*, *szl1*, and *szl1 npq1* were obtained as previously reported.[39,40] T-DNA knockout lines are *chy1* (SAIL line 49A07), *chy2* (SAIL line 1242B12), and *lut5* (SALK line 116660).[39] Mutants *szl1* and *szl1 npq1* were kindly provided by K. K. Niyogi.[41] Plants were grown for 5 weeks on Sondermisch potting mix (Gramoflor) under controlled conditions (~100 μmol of photons m^{-2} s^{-1}, 23 °C, 8 h light/16 h dark).

Stress Conditions. For EL treatments, light was provided by 150 W halogen lamps (Focus 3, Prisma). Short-term EL treatment was performed at 1000 μmol of photons m^{-2} s^{-1} and 20 °C for 1 h to measure the maximal accumulation of Zea on detached leaves. Samples for high-performance liquid chromatography (HPLC) analysis were rapidly frozen in liquid nitrogen prior to pigment extraction. Photooxidative stress was induced in either whole plants or detached leaves: plants were exposed to 550 μmol of photons m^{-2} s^{-1} at 8 °C for 2 days (16 light/8 h dark photoperiod); detached leaves were exposed to 800 μmol of photons m^{-2} s^{-1} at 8 °C for 14 h.

Isolation and Sample Preparation for Chloroplasts and Thylakoids. Chloroplasts and stacked thylakoid membranes were isolated from leaves as previously described.[42] To achieve the maximal de-epoxidation state, thylakoids isolated from dark-adapted leaves were incubated in 0.33 M sorbitol, 1 mM EDTA, 30 mM Hepes, 20 mM MES, and 40 mM ascorbate (pH 5.5) at 23 °C for 45 min.[43] Membranes corresponding to 750 μg of Chls were solubilized in 1% β-DM and then fractionated by ultracentrifugation in a 0.1 to 1 M sucrose gradient (40000 rpm, 22 h) to purify the PSI−LHCI complexes.[44] Once PSI−LHCI bands had been harvested, complexes were further purified by dilution in 5 mM Tricine (pH 7.8) and ultracentrifugation (70000 rpm, 3 h). Sodium dodecyl sulfate−polyacrylamide gel electrophoresis (SDS−PAGE) analysis was performed using the Tris-Glycine buffer system.[45] PSI core and LHCI moieties were dissociated through a further solubilization with 1% β-DM and 0.5% zwittergent.[46]

Pigment Analyses. Pigments were extracted from either leaves or complexes with 80% acetone, then separated, and quantified by HPLC.[47]

Spectroscopy. Steady-state spectra were recorded using samples in 10 mM Hepes (pH 7.5), 0.06% $\alpha(\beta)$-DM, and 0.2 M sucrose. Absorption measurements were performed using an SLM-Aminco DW-2000 spectrophotometer at room temperature (RT). Fluorescence emission spectra were recorded at RT using a Jobin-Yvon Fluoromax-3 spectrofluorometer. *In vivo* P700 absorption changes were sampled by weak monochromatic flashes (10 nm bandwidth, 705 nm) provided by LEDs (JTS10, Bio-Logic Science Instruments).

ROS Production. ROS production was measured on purified complexes using the Singlet Oxygen Sensor Green (SOSG), a fluorescent probe highly selective for $^1O_2$ that increases the intensity of its 530 nm emission band in the presence of this ROS.[48,49] Isolated complexes were illuminated with red light (600 nm < λ < 750 nm, 1600 μmol of photons m^{-2} s^{-1}, 10 °C), and the fluorescence yield of SOSG was

determined before and during light treatment, to quantify the $^1O_2$-dependent fluorescence increase.

Photobleaching Assay. The photobleaching kinetics of pigment−protein complexes were measured as described previously,[50] using actinic light intensities of 6500 μmol of photons m^{-2} s^{-1}; samples were cooled at 10 °C. The initial and maximal absorbance were set, so the same absorbance area (corresponding to ∼5 μg of Chls/mL) was used in the wavelength range of actinic light (600 nm < λ < 750 nm).

Determination of the Sensitivity to Photooxidative Stress. The decay kinetics of the maximal photochemical quantum yield of PSII (F_v/F_m)[51] and the maximal content of photooxidizable P700 (ΔA_{max} at 705 nm)[52] were recorded on leaves during EL treatment to assess the inhibition of PSII and PSI, respectively. ΔA_{max} was recorded during far-red light illumination (2500 μmol of photons m^{-2} s^{-1}; λ_{max} = 720 nm). To precisely evaluate the extent of PSI photoinhibition, leaves were vacuum infiltrated with 50 mM dibromothymoquinone and 1 mM methyl viologen upon EL, a treatment that restores the maximal oxidation level of P700.[32]

Measurement of Electron Transport in PSI Using Artificial Donors. Linear electron transport from artificial donor $TMPDH_2$ (*N*,*N*,*N*,*N*-tetramethyl-*p*-phenylenediamine, reduced form, 250 mM) to $NADP^+$ was measured in a dual-wavelength spectrophotometer (Unicam AA, Thermo scientific) under conditions of red light illumination (150 μmol of photons m^{-2} s^{-1}, RT) as described in ref 42. Thylakoids (15 μg of Chl/mL) were continuously stirred during illumination.

Fluorescence-Detected Magnetic Resonance. For all these experiments, the samples were dissolved in a buffer to a final concentration of 100 μg of Chl/mL. Degassed glycerol was added [60% (v/v)] just before the samples were frozen in a precooled cryostat at 40 K. All experiments were performed at 1.8 K. At this temperature, spin−lattice relaxation is inhibited and the FDMR signals reach maximal intensity. FDMR experiments were performed in a specific apparatus, details of which are described in refs 53−55. All spectra are presented as $\Delta F/F$ versus microwave frequency, where ΔF is the fluorescence change induced by the resonant microwave field and F is the steady-state fluorescence detected by the photodiode at the selected wavelength.

RESULTS

***β*-Carotene Depletion Enhances Photosensitivity under EL and Chilling Conditions.** Because of a point mutation in the lycopene *β*-cyclase gene,[40] *szl1* plants have a lower carotene content and altered xanthophyll composition compared to those of WT plants when grown under low-light conditions (100 μmol of photons m^{-2} s^{-1}, 8 h light, 23 °C/16 h dark, 20 °C), while the *npq1* mutation[41] impairs only the plant's capacity to accumulate Zea without further affecting its carotene/xanthophyll ratio (Figure 1 and Table 1).

Pigment composition in plants both dark-adapted (a condition under which Vio accumulates in WT leaves) and transferred for 60 min to EL (1000 μmol of photons m^{-2} s^{-1}, to maximize de-epoxidation of Vio into Zea) was analyzed via HPLC on acetone extracts. Chl *a*/*b* ratios were essentially the same in the WT, *szl1*, *npq1*, and *szl1 npq1* genotypes, whereas the Chl/Car ratios were significantly reduced in *szl1*; because Chl content is not affected by the mutation of lycopene *β*-cyclase,[34] it means that the total Car content is slightly increased (∼10%) in the *szl1* genetic background. The 65% reduction in *β*-Car content in *szl1* and *szl1 npq1* versus WT

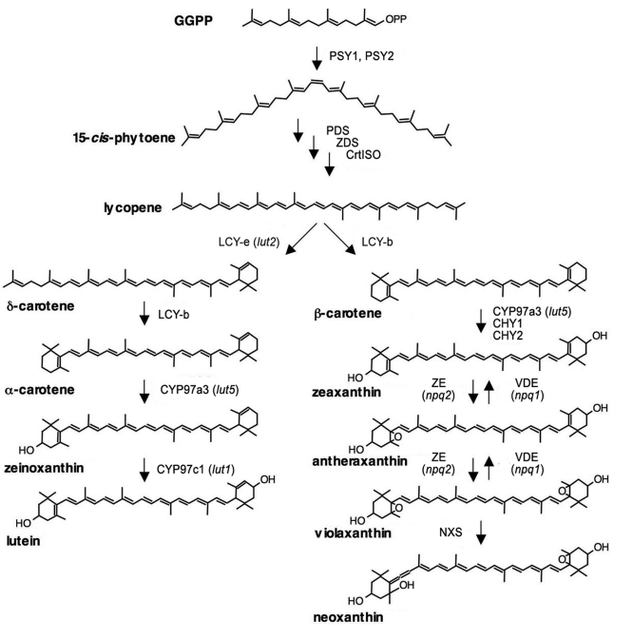

Figure 1. Biosynthetic pathway of carotenoids in *A. thaliana*, showing the enzymes controlling each step: lycopene *β*-cyclase (LCY-b), lycopene *ε*-cyclase (LCY-e), *β*-carotene hydroxylase (CYP97A3), *ε*−*β*-carotene hydroxylase (CYP97C1), *β*-carotene hydroxylase 1 and 2 (CHY1 and CHY2, respectively), Zea epoxidase (ZEP), Vio deepoxidase (VDE), and neoxanthin synthase (NXS). The names of *Arabidopsis* knockout mutants are given in brackets.

leaves (Table 1) was consistent with a previous report.[40] Moreover, both *szl1* genotypes showed an accumulation of the lutein precursor *α*-carotene (10 times that found in WT plants), a smaller amount of *β*,*β*-xanthophylls (Vio, Zea, and neoxanthin), and higher levels of lutein (*ε*,*β*-xanthophyll), and hence a *β*,*β*/*ε*,*β* xanthophyll ratio far lower than that of the WT. When plants were exposed to EL, the level of accumulation of Zea was lower in *szl1* than in the WT [−78% (Table 1)]. The aim of this work was to address the photoprotective function of carotenoid molecules bound to PSI. Previous characterizations of Car biosynthesis mutants[49,56] revealed that changes in the xanthophyll composition of LHC did affect photoprotection. It is worth noting that *szl1* plants, besides having a lower carotene content, also have a *β*,*β*/*ε*,*β* xanthophyll ratio lower than that of the WT, so it is necessary to distinguish the consequences of *β*-Car depletion from those of the increased relative amount of lutein versus *β*,*β*-xanthophylls in the antenna moiety of the PSI. For this reason, we included *chy1 chy2* and *lut5* genotypes in this characterization, which were used as controls: the *chy1 chy2* mutation affects the efficiency of conversion of *β*-Car into Vio, thus yielding the same *β*,*β*/*ε*,*β* xanthophyll ratio seen for *szl1* plants (Figure 1 and Table 1). The *lut5* mutant was included as a control for *α*-carotene accumulation: the latter compound competes for the *β*-Car-binding sites,[49] but because it accumulates in both *szl1* and *lut5* (Table 1), it is possible to trace back their different contributions to photoprotection efficiency. The *chy1 chy2* and *lut5* genotypes had Chl *a*/*b* and Chl/Car ratios similar to those of WT plants, while the xanthophyll versus carotene content was significantly lower in both genotypes than in the WT (Table 1).

Conditions of EL cause photooxidative stress in plants, the severity of which is enhanced by low temperatures, due to a

Table 1. Photosynthetic Pigment Content of Wild-Type and Mutant Plants[a]

				mol of pigment/100 mol of Chl						
	genotype	Chl *a*/*b*	Chl/Car	neoxanthin	violaxanthin	antheraxanthin	zeaxanthin	lutein	α-carotene	β-carotene	$\beta\beta/\varepsilon\beta$ xanthophyll ratio
dark-adapted	WT	3.2 ± 0.1 a	3.7 ± 0.3 a	4.6 ± 0.6 a	2.9 ± 0.3 a	–	–	13.1 ± 0.7 a	0.1 ± 0.1 a	6.6 ± 0.7 a,c	0.6 ± 0.1 a
	npq1	3.2 ± 0.1 a	3.5 ± 0.2 a,b	4.8 ± 0.1 a	3.1 ± 0.2 a	–	–	14.7 ± 1.8 a	0.1 ± 0.1 a	6.2 ± 0.1 a	0.5 ± 0.1 a
	szl1	3.1 ± 0.1 a	3.3 ± 0.1 b	1.6 ± 0.4 b	0.8 ± 0.1 b	–	–	25.0 ± 1.4 b	1.1 ± 0.3 b	2.3 ± 0.1 b	0.1 ± 0.1 b
	szl1 npq1	3.4 ± 0.2 a	3.3 ± 0.3 b	1.8 ± 0.2 b	0.8 ± 0.1 b	–	–	24.4 ± 2.7 b	1.3 ± 0.2 b	2.3 ± 0.5 b	0.1 ± 0.1 b
	chy1 chy2	3.1 ± 0.1 a	3.9 ± 0.3 a	1.4 ± 0.1 b	0.7 ± 0.1 b	–	–	16.1 ± 1.1 a	0.1 ± 0.1 a	7.3 ± 0.6 c	0.1 ± 0.1 b
	lut5	3.1 ± 0.1 a	4.1 ± 0.2 a	3.4 ± 0.6 c	1.5 ± 0.1 c	–	–	11.2 ± 0.5 c	5.4 ± 0.2 c	2.6 ± 0.2 b	0.5 ± 0.1 a
HL	WT	3.1 ± 0.1 a	3.8 ± 0.1 a	4.7 ± 0.1 a	1.3 ± 0.1 a	0.2 ± 0.1 a	1.4 ± 0.1 a	12.3 ± 0.1 a	0.1 ± 0.1 a	6.1 ± 0.1 a	0.6 ± 0.1 a
	npq1	3.1 ± 0.1 a	3.5 ± 0.1 a,b	5.1 ± 0.4 a	2.7 ± 0.1 b	–	–	14.4 ± 0.4 b	0.2 ± 0.1 a	6.0 ± 0.1 a	0.5 ± 0.1 a
	szl1	3.0 ± 0.1 a	3.4 ± 0.1 b	1.7 ± 0.1 b	0.3 ± 0.1 c	0.1 ± 0.1 a	0.3 ± 0.1 b	22.7 ± 0.3 c	1.1 ± 0.1 b	3.1 ± 0.4 b	0.1 ± 0.1 b
	szl1 npq1	3.0 ± 0.1 a	3.4 ± 0.1 b	1.6 ± 0.1 b	0.7 ± 0.1 d	–	–	21.7 ± 0.3 c	1.2 ± 0.1 b	3.1 ± 0.1 b	0.1 ± 0.1 b
	chy1 chy2	3.0 ± 0.1 a	3.9 ± 0.1 a	1.5 ± 0.1 b	0.5 ± 0.1 c,d	0.1 ± 0.1 a	0.4 ± 0.1 b	15.8 ± 0.1 b	0.3 ± 0.1 a	7.3 ± 0.1 c	0.2 ± 0.1 b
	lut5	3.2 ± 0.1 a	3.9 ± 0.1 a	3.4 ± 0.6 c	1.0 ± 0.1 a	0.1 ± 0.1 a	0.6 ± 0.1 b	11.3 ± 0.3 c	6.2 ± 1.1 c	3.2 ± 0.1 b	0.5 ± 0.1 a

[a]Pigment content was determined before (dark-adapted) and after (HL) the leaves were exposed to 1000 μmol of photons m^{-2} s^{-1} for 30 min. Data are normalized to 100 Chl *a* + *b* molecules and are expressed as means ± SD (n = 3). Values within a given column and in a certain light regime that are marked with the same letters do not differ significantly (Student's t test; $P < 0.05$).

greater level of release of $^1O_2$ and the inhibition of scavenging enzymes.[32,57] To analyze the effect of missing Cars on the sensitivity to EL and to determine the primary target of photooxidation, the kinetics of both PSII and PSI photoinhibition were determined (Figure 2). WT and mutant plants were transferred from the control growth conditions to EL with cold stress (550 μmol og photons m^{-2} s^{-1}, 8 °C), and the maximal photochemical yield of PSII (F_v/F_m) was monitored for 30 h. F_v/F_m in WT plants gradually decreased from 0.8 to 0.4 during this interval (half-time for PSII photoinhibition of ∼30 h). The *szl1* plants were more photosensitive than the WT, because their F_v/F_m decreased to 0.16 at the end of the treatment, corresponding to a half-time for PSII photoinhibition of approximately 8 h (Figure 2A). F_v/F_m decay was the same in *chy1chy2* and *lut5* plants and followed a pattern that was roughly between those of WT and *szl1* plants (Figure 2B). Interestingly, the half-time of PSII photoinhibition was significantly shorter for *npq1* versus WT and for *szl1 npq1* versus *szl1* (Figure 2A), thus confirming a role for Zea in PSII photoprotection.[18]

The kinetics of PSI photoinhibition were assessed by quantifying the maximal content of photooxidizable P700 upon exposure of the plants to EL at chilling temperature. These stressing conditions had a much more dramatic effect on the photoinhibition of PSI than on that of PSII, with the photooxidizable P700 of the WT *Arabidopsis* plants gradually decreasing to 50% of its initial value in approximately 4.5 h (Figure 2C). The half-time for photoinhibition was the same as that of WT in *npq1* and *chy1 chy2*, shorter for *lut5* [being 50% inhibited in ∼2 h (Figure 2D)], and far shorter in *szl1* plants (approximately 0.8 h), thus confirming the great increase in photosensitivity caused by β-Car depletion.[34] To investigate the function of Zea in PSI photoprotection, we analyzed mutants lacking the ability to synthesize Zea (*npq1*) in a WT or *szl1* genetic background. The *npq1* mutation did not appear to affect in a significant manner PSI photoinhibition in either *npq1* or *szl1 npq1* (Figure 2C). These findings imply that, although Zea depletion impairs PSII photoprotection (Figure 2A), its role in limiting PSI photoinhibition is less important under the tested conditions.

Photobleaching Rate and $^1O_2$ Production in Purified PSI–LHCI Complexes. The results described above suggest a key role for β-Car in protecting the PSI–LHCI complex by photoinactivation, whereas a lack of Zea has a greater impact on the photoinhibition rate of PSII than on that of PSI.

Previous investigations show that under EL conditions, xanthophyll exchange occurs in the inner L2 site of LHCI,[38] and recent crystallographic data reveal that each LHCI subunit binds one β-Car molecule.[37] To shed more light on the functional role of these ligands, we measured the photosensitivity of isolated PSI–LHCI complexes. To prevent any damage to the complexes by the EL treatment targeted at Zea accumulation, thylakoids isolated from dark-adapted leaves were de-epoxidated in the dark by incubating them at pH 5.2, a treatment that pushes the de-epoxidation index over 50%. Subsequently, PSI–LHCI complexes were purified by sucrose gradient ultracentrifugation (Figure S1) and further characterized (Figure S2): photooxidizable P700 content (Figure S2A) and $NADP^+$ photoreduction rate (Figure S2B) were the same in all samples; SDS–PAGE analysis revealed no major difference in polypeptide composition between mutant and WT complexes (Figure S2C), and moreover, spectral deconvolution analysis of the Q_y absorption band into spectral forms of Chl

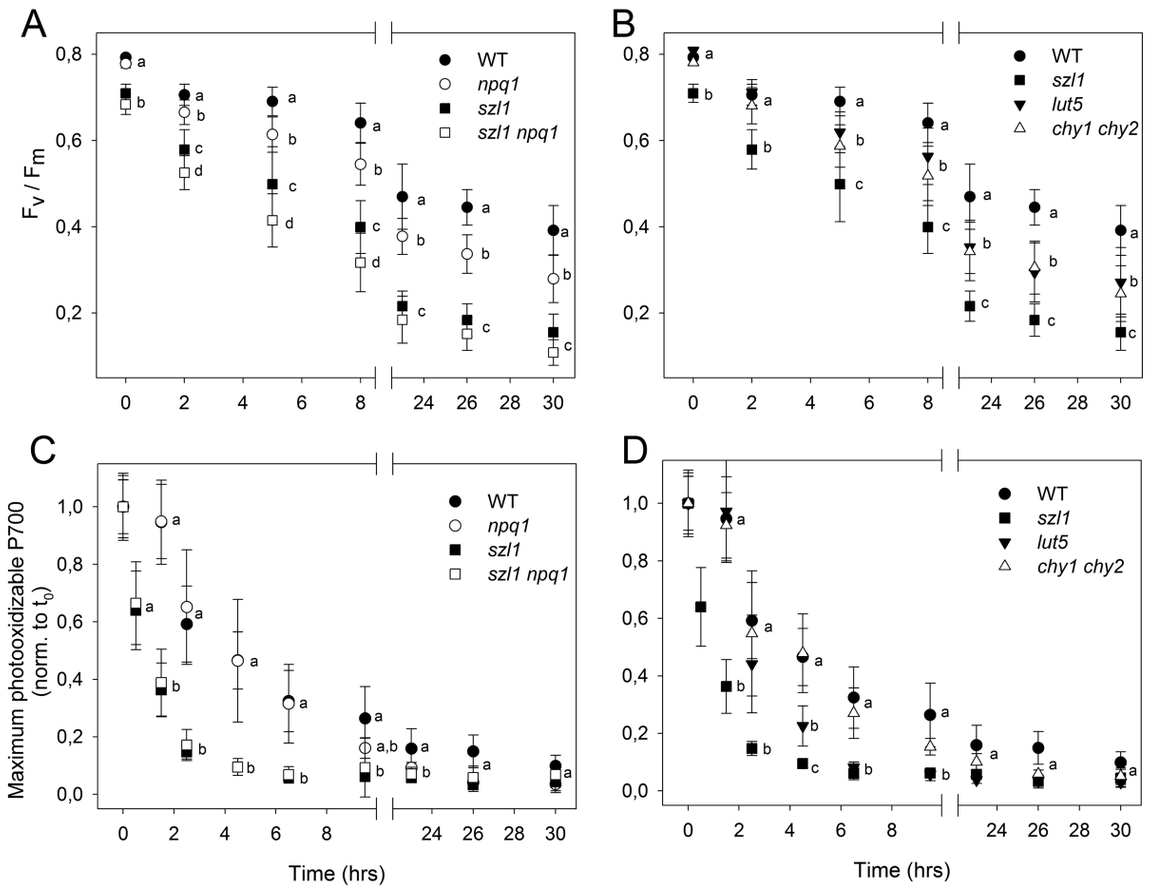

Figure 2. Photooxidation in wild-type and mutant *Arabidopsis* exposed to high light intensity at chilling temperatures. (A and B) F_v/F_m decay kinetics (PSII photoinhibition) was monitored in WT and mutant plants, exposed to 550 μmol of photons m^{-2} s^{-1} at 8 °C for 30 h with a 6 h period of dark between the 12 h of EL stress. (C and D) Decay kinetics of maximal photooxidizable P700 (PSI photoinhibition) were measured on leaves exposed to 500 μmol of photons m^{-2} s^{-1} at 8 °C for 30 h. Data are expressed as means ± SD ($n > 6$). t_0 indicates time zero. Values marked with the same letters are not significantly different from each other at the given time point (Student's t test; $P < 0.05$).

did not show any changes in the pigment organization (Figure S2D). Overall, these data confirm that the introduced mutation did not cause any structural or functional destabilization of the PSI–LHCI complexes in plants grown in low light.

The pigment composition of the complexes was determined by HPLC (Table 2). The Chl/Car ratio was essentially the same in WT, *npq1*, *chy1chy2*, and *lut5* genotypes but higher in *szl1* and *szl1 npq1* because of their lower carotene content (−23%). The relative abundance of *ε,β*- and *β,β*-xanthophylls was similar in the PSI–LHCI complexes from WT, *npq1*, and *lut5* plants, whereas complexes isolated from *szl1*, *szl1 npq1*, and *chy1 chy2* plants had much lower levels of *β,β*-xanthophylls and displayed a compensatory increase in the level of Lut. Only the complexes from WT and *lut5* plants showed signs of Vio–Zea exchange, while PSI–LHCI complexes from *chy1 chy2* and *szl1* plants did not bind any detectable level of Zea.

The hypothesis that the lack of either *β*-Car or Zea might prevent the activation of photoprotective mechanisms localized within the PSI–LHCI complex, thus enhancing ROS production, was further investigated by measuring photobleaching rates on purified complexes. Strong illumination of Chl proteins induces the formation of ^{3}Chl*, which in turn leads to $^1O_2$ release and Chl bleaching with kinetics that are inversely dependent on the efficiency of ^{3}Chl* quenching by bound Car. The results are illustrated in Figure 3. The greatest levels of resistance were found in WT complexes binding Zea and a full complement of *β*-Car molecules, while the PSI–LHCI complex from *npq1* plants was slightly more prone to photobleaching (Figure 3A). Mutations *lut5* and *chy1 chy2* did not affect the photosensitivity of complexes (Figure 3B). On the other hand, the *szl1* complex was far more sensitive to photobleaching than that from the WT, thus suggesting a major role for *β*-Car in photoprotecting PSI, presumably by limiting $^1O_2$ release.

We further compared the photoprotection capacity of the PSI–LHCI complexes by analyzing the amount of $^1O_2$ released. The $^1O_2$ yield was measured upon illumination of the complexes in the presence of fluorescent dye SOSG (see Materials and Methods for details), and the results are shown in Figure 4. *β*-Car depletion in *szl1* complexes significantly increases the amount of $^1O_2$ produced under EL conditions (Figure 4A). On the other hand, a lack of Zea (*npq1*), an altered xanthophyll/carotene ratio (*chy1 chy2*), or larger amounts of *α*-carotene (*lut5*) did not significantly enhance the yield of $^1O_2$ from the PSI–LHCI complexes (Figure 4B). These results suggest that the PSI–LHCI complexes binding a full complement of *β*-Car have a far stronger capacity for photoprotection than those lacking carotenes. No similar effect was observed in Zea-binding complexes; i.e., there was no

Table 2. Pigment Composition of PSI–LHCI Complexes Purified from the Various Genotypes[a]

			mol of pigment/155 mol of Chl[37]						
genotype	Chl *a*/*b*	Chl/Car	neoxanthin	violaxanthin	antheraxanthin	zeaxanthin	lutein	α-carotene	β-carotene	ββ/εβ xanthophyll ratio
WT	12.1 ± 0.2 a	4.6 ± 0.2 a	–	2.7 ± 0.1 a	–	1.7 ± 0.1 a	6.8 ± 0.1 a	–	22.6 ± 0.2 a	0.7 ± 0.1 a
npq1	11.7 ± 0.3 a	4.6 ± 0.1 a	–	4.5 ± 0.1 b	–	–	7.0 ± 0.1 a	–	22.2 ± 0.6 a	0.7 ± 0.1 a
szl1	12.2 ± 0.5 a	5.3 ± 0.2 b	–	0.7 ± 0.1 c,d	–	–	10.9 ± 0.4 b	2.4 ± 0.1 a	15.0 ± 0.6 b	0.1 ± 0.1 b
szl1 npq1	11.8 ± 0.3 a	5.3 ± 0.1 b	–	0.9 ± 0.1 c	–	–	10.7 ± 0.3 b	2.5 ± 0.1 a	15.2 ± 0.5 b	0.1 ± 0.1 b
chy1 chy2	7.6 ± 0.1 b	4.8 ± 0.1 a	–	0.6 ± 0.1 d	–	–	8.7 ± 0.1 c	–	23.2 ± 0.2 c	0.1 ± 0.1 b
lut5	8.9 ± 0.1 c	5.0 ± 0.2 a	–	1.9 ± 0.1 e	–	1.1 ± 0.1 b	6.1 ± 0.1 d	11.6 ± 0.1 b	10.3 ± 0.1 d	0.5 ± 0.1 a

[a]To maximize the accumulation of Zea, these complexes were purified from thylakoids that were de-epoxidized *in vitro*. See Materials and Methods for purification details. Data are normalized to 155 Chl *a* + *b* molecules (Chls bound to one PSI–LHCI complex) and are expressed as means ± SD (n = 3). Values within a given column that are marked with the same letter do not differ significantly (Student's t test; $P < 0.05$).

significant difference in the $^1O_2$ yield based on the Vio versus Zea content of PSI (Figure 4A).

Investigations of Chlorophyll to Carotenoid Triplet Transfer. The reason behind the greater rate of release of $^1O_2$ caused by β-Car depletion could be the lower efficiency of ^{3}Chl* quenching by the remaining Cars. To investigate this hypothesis, we assessed the ^{3}Chl* yield in plants lacking either β-Car or Zea by using FDMR. This is a double-resonance technique by which a triplet population is generated under conditions of steady-state illumination, and then a resonant electromagnetic field applied between a couple of spin sublevels of the triplet state induces a change in the steady-state triplet population itself, caused by anisotropy decay and population rates of the three spin sublevels. This event is detected as a corresponding change in the fluorescence emission of the system.[58,59] The samples were directly frozen by being placed in a precooled sample chamber; hence, the spectra obtained are representative of the conformational distribution present at RT. Moreover, thylakoids isolated from WT and mutant dark-adapted leaves were de-epoxidated in the dark by incubation at pH 5.2 to maximize Zea accumulation while avoiding any damage to the complexes by EL, which could affect the triplet population.

The low-temperature emission spectrum of PSI–LHCI complexes purified from WT and mutant *Arabidopsis* plants displayed the typical Chl *a* fluorescence bands peaking at 735 nm due to the antenna pools of PSI (not shown). The FDMR signals of PSI–LHCI complexes from WT plants, detected at wavelengths ranging between 700 and 740 nm, hence in the microwave frequency range expected for ^{3}Chl*,[54,55] are shown in Figure S3A. These signals suggest a dependence on wavelength detection, revealing the presence of at least four different triplet populations. Two ^{3}Chl* components peak at short wavelengths (700 nm) and may be assigned to a Chl belonging to antenna proteins, while the other two, previously assigned to ^{3}P700,[60] peak at 720–740 nm. Figure S4 shows the reconstructed spectra, while the fitting parameters are reported in Table 1S.

The three FDMR transitions recorded at setup settings selective for ^{3}Car* are shown in Figure S3B. Not surprisingly, the 2|E| transitions are the most intense, as often observed for ^{3}Car*.[60] The |D| + |E| transition, which is usually ∼3 times the |D| − |E| for ^{3}Car*, is here underestimated because of the reduced microwave power used in this region. The linearity of FDMR transitions indicates the presence of different components contributing to the signals, as previously observed in thylakoid FDMR spectra detected at long emission wavelengths where the PSI contribution predominates.[60]

The FDMR spectra of the PSI–LHCI complexes isolated from *npq1* leaves were identical to those of samples from de-epoxidated WT over the entire detection range explored, indicating that the ^{3}Chl* population does not change (Figure 5A). When FDMR measurements were performed on PSI–LHCI complexes isolated from de-epoxidated *szl1* leaves, a significant increase (2 times) in the intensity of the FDMR components assigned to the ^{3}Chl* states was observed (Figure 5B and Figures S4 and S5 and Table 2S for details). Interestingly, a decrease in the intensity of the FDMR signals of the ^{3}Car* states was also observed in the PSI–LHCI complex from *szl1* plants (Figure 5C,D). These findings are consistent with the greater photosensitivity displayed by the mutant *in vivo* (Figure 2C).

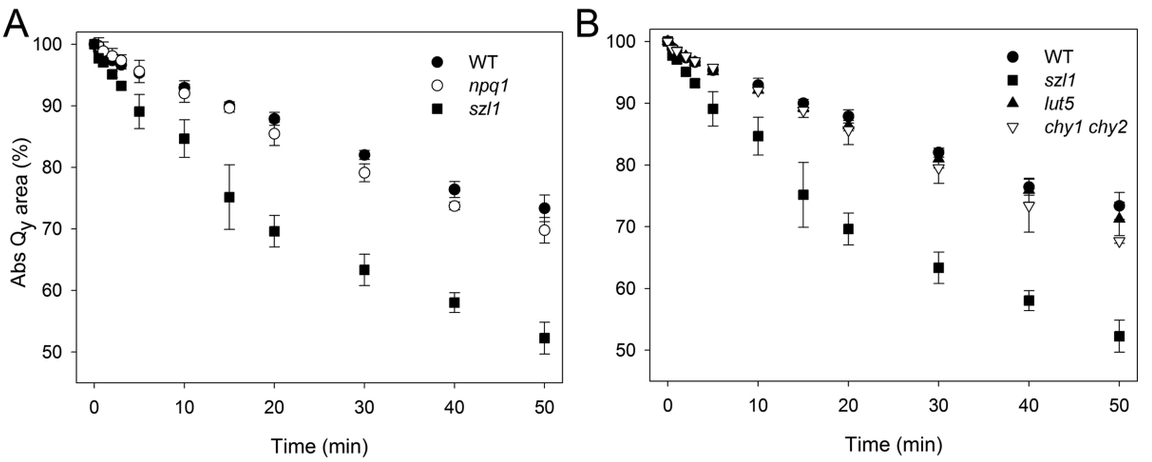

Figure 3. Photobleaching behavior of isolated PSI–LHCI complexes. (A) PSI–LHCI complexes isolated from de-epoxidized thylakoids of WT, *npq1*, and *szl1* plants were analyzed by monitoring the Q_y transition absorbance decay during a period of strong illumination, as described in Materials and Methods. Chl concentrations of complexes were set to 8 μg/mL. Samples were cooled to 10 °C during measurements. (B) Photobleaching kinetics of PSI–LHCI complexes from *lut5* and *chy1 chy2* thylakoids were compared with those of genotypes WT and *szl1*. Data are expressed as means ± SD (n = 3). At all time points, the complexes isolated from *szl1* were significantly more sensitive to photooxidation (Student's t test; $P < 0.05$) than the others.

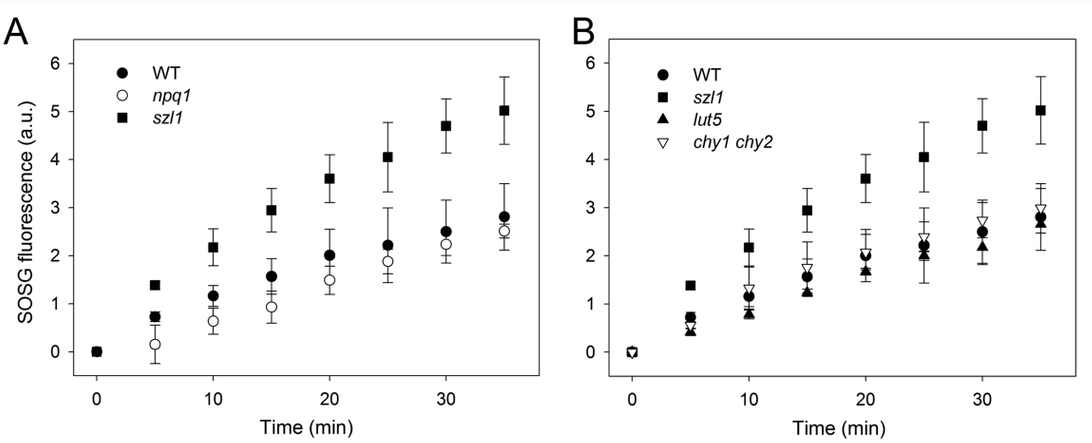

Figure 4. Production of singlet oxygen by PSI–LHCI complexes. (A) Kinetics of $^1O_2$ release was measured in PSI–LHCI complexes purified from de-epoxidated thylakoids of WT, *npq1*, and *szl1* plants. (B) Release of $^1O_2$ from *lut5* and *chy1 chy2* PSI–LHCI complexes was compared with that from the same complexes purified from WT and *szl1*. SOSG was used as an $^1O_2$-specific fluorogenic probe, because its fluorescence emission increases upon reaction with $^1O_2$ in solution. Symbols and error bars indicate means ± SD (n = 3). At all time points, the complexes isolated from *szl1* released significantly more $^1O_2$ (Student's t test; $P < 0.05$) than the others did.

$^1O_2$ Production in LHCI and PSI Core Complexes. The data presented so far indicate that β-Car makes a relevant contribution to protecting the PSI–LHCI complex from radiation damage *in vivo*. However, β-Car molecules are not uniformly distributed within the PSI–LHCI complex, because 85% of the total Car is bound to the core complex and only 15% to the antenna moiety.[37] To test the role of these subpopulations in photoprotection, we purified LHCI and PSI core particles from whole PSI–LHCI complexes of WT, *npq1*, and *szl1* plants (Figure S6) and analyzed the effect of either β-Car or Zea depletion on the $^1O_2$ yield under EL conditions.

Pigment composition analysis of these complexes (Table 3) revealed that the Chl/Car ratio was essentially the same in the LHCI from WT and *npq1*; it was however greater in *szl1* because of a lower carotene content (−20%, corresponding to ∼0.8 molecule of carotene per unit of LHCI); moreover, LHCI from *szl1* had Vio levels lower than and Lut levels higher than those of the *npq1* (−2.6 mol of Vio and +2.4 mol of Lut per unit of LHCI, respectively). These findings suggest that sites N1 (binding β-Car) are partially empty due to β-Car depletion, and that part of the missing Vio in sites L2 is replaced by Lut.[37] Only antenna complexes from WT bound a significant amount of Zea (de-epoxidation index of 24%, corresponding to ∼1 molecule of Zea per unit of LHCI). PSI core complexes from WT and *npq1* plants had the same pigment composition, whereas the corresponding *szl1* complex had a lower carotene content per unit of Chls (−18%, corresponding to ∼4 molecules of carotene per unit of PSI core).

The release of $^1O_2$ was monitored upon illumination of the complexes in the presence of the dye SOSG (Figure 6). β-Car depletion in the *szl1* PSI core significantly enhanced the amount of $^1O_2$ produced [+53% vs that of the WT complex (Figure 6A)], and the effect was even greater in LHCI from *szl1* [+65% (Figure 6B)]. Lack of Zea (*npq1*), on the other hand, did not significantly affect the $^1O_2$ yield of antenna complexes (Figure 6B).

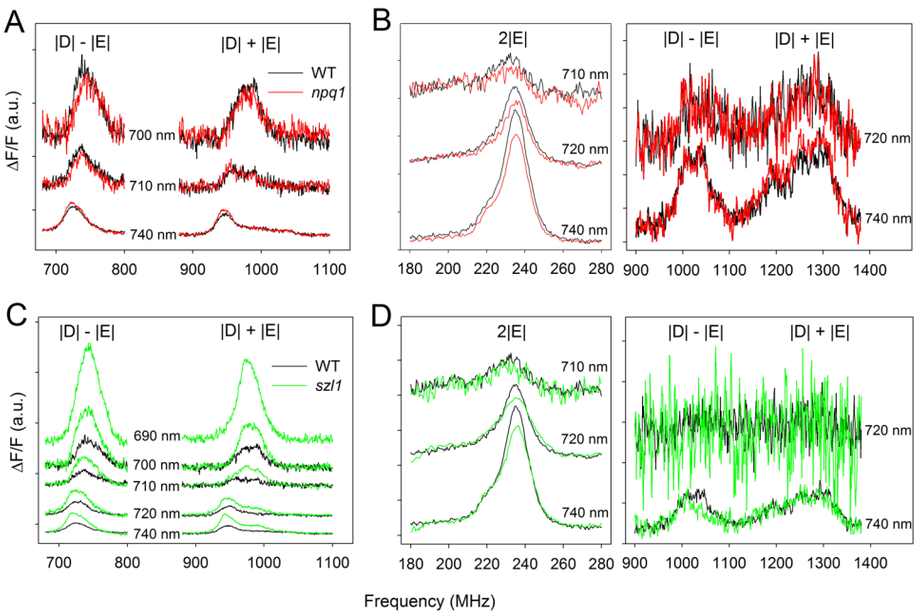

Figure 5. Fluorescence-detected magnetic resonance of the Chl and Car triplet states in purified PSI–LHCI complexes. FDMR signals of the ^{3}Chl* states (|*D*| − |*E*| and |*D*| + |*E*| transitions; panels A and B) and the ^{3}Car* states (2|*E*|, |*D*| − |*E*|, and |*D*| + |*E*| transitions; panels C and D) observed in the PSI–LHCI complex purified from high-light-treated leaves of WT (black), *npq1* (red), and *szl1* (green) plants. FDMR signals were detected at the various wavelengths indicated in each panel. Spectra were vertically shifted to simplify comparison. Amplitude modulation frequency of 33 Hz (^{3}Chl* states) or 325 Hz (^{3}Car* states), time constant of 600 ms, 20 scans, microwave power of 500 mW, temperature of 1.8 K.

Table 3. Pigment Composition of Lhca and PSI Core Complexes Purified from Thylakoids of WT, *npq1*, and *szl1*[a]

				mol of pigment/98 mol of Chl[37]					
sample	genotype	Chl *a*/*b*	Chl/Car	violaxanthin	zeaxanthin	lutein	*α*-carotene	*β*-carotene	*β*,*β*/*ε*,*β* xanthophyll ratio
PSI core	WT	–	5.5 ± 0.1 a	–	–	–	–	18.0 ± 0.4 a	–
	npq1	–	5.5 ± 0.1 a	–	–	–	–	17.9 ± 0.2 a	–
	szl1	–	6.7 ± 0.1 b	–	–	–	1.7 ± 0.1 a	13.0 ± 0.1 b	–
				mol of pigment/57 mol of Chl[37]					
sample	genotype	Chl *a*/*b*	Chl/Car	violaxanthin	zeaxanthin	lutein	*α*-carotene	*β*-carotene	*β*,*β*/*ε*,*β* xanthophyll ratio
Lhca	WT	3.8 ± 0.1 a	4.4 ± 0.1 a	2.5 ± 0.1 a	0.8 ± 0.1 a	5.6 ± 0.1 a	–	4.0 ± 0.1 a	0.6 ± 0.1 a
	npq1	3.9 ± 0.2 a	4.4 ± 0.1 a	3.2 ± 0.2 b	–	5.8 ± 0.2 a	–	4.0 ± 0.1 a	0.6 ± 0.1 a
	szl1	3.9 ± 0.1 a	4.8 ± 0.2 b	0.6 ± 0.1 c	–	8.2 ± 0.1 b	1.1 ± 0.1 a	2.1 ± 0.1 b	0.1 ± 0.1 b

[a]The complexes were purified from thylakoids de-epoxidized *in vitro*, to maximize the accumulation of Zea. See Materials and Methods for details of purification. Data are normalized to either 98 or 57 Chl molecules (Chls bound to one PSI core or LHCII, respectively) and are expressed as means ± SD (n = 3). Values within a given column that are marked with the same letter do not differ significantly (Student's t test; $P < 0.05$).

DISCUSSION

Binding of Zea to Lhcb proteins was observed to play a major role in enhancing photoprotection of PSII *in vivo* by modulating the yield of both the ^{1}Chl*[61,62] and ^{3}Chl* states.[28] The mechanism of Vio de-epoxidation has been described in LHCI,[38] but its importance in the photoprotection of PSI is not clear.[63] Moreover, recent results suggest that the xanthophyll and carotene composition are crucial for PSI stability.[64,65] The focus of this investigation was the relative contribution of carotene versus xanthophyll ligands of Photosystem I to its photoprotection. To this aim, mutants of *Arabidopsis* with altered carotenoid biosynthesis pathways were compared: *szl1*, containing fewer carotenes because of its reduced *β*-cyclase activity,[40] *npq1*, incapable of Zea accumulation,[41] and the double mutant *szl1 npq1*. Because carotenes are intermediate products of carotenoid biosynthesis (Figure 1), variations in carotene levels inevitably affect those of xanthophylls, which are downstream from this metabolic pathway. Moreover, the decrease in *β*-cyclase activity yields a larger amount of *α*-carotene, usually barely detectable in *A. thaliana*. Hence, genotypes *lut5* and *chy1 chy2* were included in the study and used as controls: a comparison with their photosynthetic phenotype helped determine whether photosensitivity could be ascribed to either changes in the xanthophyll/carotene ratio, which is very similar in *szl1* and *chy1 chy2*, or the presence of *α*-carotene, observed in both *szl1* and *lut5*.

Changes in Xanthophyll and Carotene Composition Have a Different Effect on the Photoprotection Capacity of PSII and PSI. Carotenoids mediate photoprotection through a number of mechanisms, which include quenching of ^{3}Chl*,[66,67] scavenging of ROS,[18,68] and quenching of ^{1}Chl*, which prevents ROS release.[69] The photosensitive phenotypes of *Arabidopsis* mutants with an altered xanthophyll composition[49,56,69] suggest that the relative abundance of these pigments is crucial for chloroplast photoprotection.

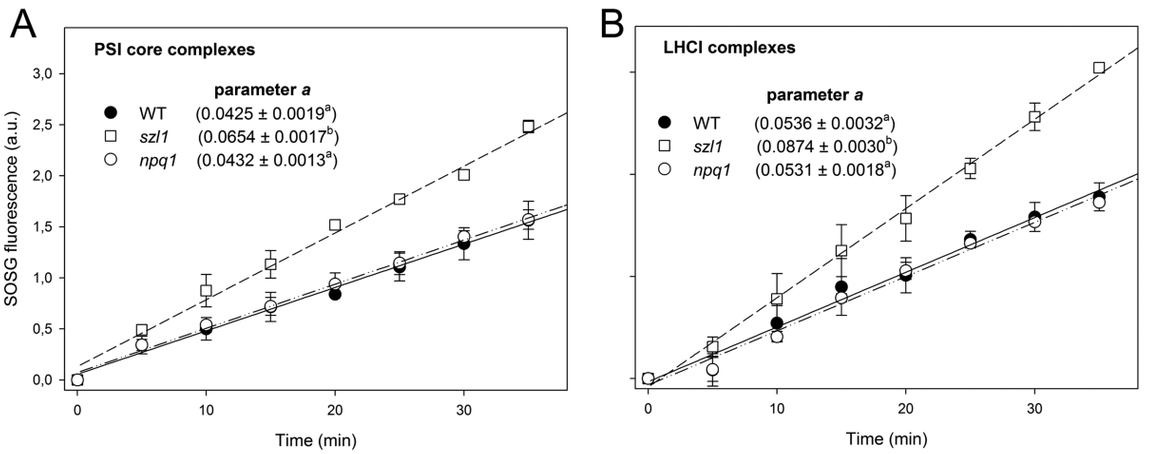

Figure 6. Production of singlet oxygen from the PSI core and LHCI complexes. Kinetics of $^1O_2$ release was measured on (B) PSI core and (C) LHCI complexes, purified from de-epoxidated PSI–LHCI complexes of WT, *npq1*, and *szl1* plants. SOSG was used as an $^1O_2$-specific fluorogenic probe. Symbols and error bars indicate means ± SD (n = 3). Each data set was fitted with a linear function $y = y_0 + ax$, and the kinetics of $^1O_2$ release was assessed in the various samples by comparing their parameter a, which describes the slope of the linear function. Values marked with the same letter are not significantly different (Student's t test).

The *npq1* mutant displayed a PSII photoinhibition rate significantly greater than that of WT plants (Figure 2A), which is consistent with the photoprotective role of Zea versus Vio in PSII.[18] *chy1 chy2* plants, whose $\beta,\beta/\varepsilon,\beta$ xanthophyll ratio is 6-fold lower than that of WT (Table 1) plants, are more prone to PSII photoinhibition (Figure 2B). Even *lut5* plants, containing smaller amounts of xanthophyll versus Chl than WT plants, possessed a greater PSII photosensitivity. This result is consistent with previous investigations, which reveal that optimal photoprotection of the PSII antennas occurs with balanced ^{3}Chl* quenching by Lut and ROS scavenging by β,β-xanthophylls.[49,70] *szl1* plants had the same $\beta,\beta/\varepsilon,\beta$ xanthophyll ratio as *chy1 chy2* plants and are able to synthesize Zea, even if to a lower extent than WT due to a limited Vio pool (Table 1); however, the F_v/F_m decrease was far greater than in *npq1* and *chy1 chy2* plants. These data indicate that (i) β-Car plays a role in PSII photoprotection, promoting the scavenging of $^1O_2$ produced by the PSII core,[30] and (ii) β-Car abundance had an additive effect on PSII photostability with respect to Zea accumulation and β,β-xanthophyll composition.

Interestingly, these changes in carotenoid composition affect PSI differently. HPLC analysis of the PSI–LHCI complex purified from either *chy1 chy2* or *szl1* revealed a similar xanthophyll composition, with a Vio decrease and an equivalent Lut increase (Table 2). Lut and Vio bind to sites L1 and L2, respectively, of each Lhca protein;[37] therefore, in *chy1 chy2* and *szl1*, a lack of Vio in site L2 is most likely compensated by the binding of additional Lut. Conversely, the binding of a xanthophyll in site N1, which is highly selective for β-Car, appears unlikely.

The P700 photoinhibition rate was essentially the same in WT, *npq1*, and *chy1 chy2* plants, whereas the *szl1* genotype revealed a greater degree of photodamage, losing all PSI activity in ∼4 h. Besides carotene depletion, a further feature of *szl1* plants is the presence of α-carotene in both PSI core and LHCI complexes, partially replacing β-Car (Table 3) and potentially being a cause of photosensitivity. However, *lut5* has an α/β-carotene ratio far greater than that of *szl1* (Tables 1 and 2), yet both the photobleaching kinetics and $^1O_2$ production in the PSI complexes isolated from this genotype did not differ significantly from those of WT plants (Figures 3 and 4), suggesting that α-carotene is not the main cause of photosensitivity.

These differences in photosensitivity did not arise from structural changes in the PSI–LHCI complex upon β-Car depletion. Both the maximal P700 and the PSI electron transport rate were identical to those in WT plants (Figure S3), indicating that the PSI of *szl1* plants is fully functional under the control lighting conditions. SDS–PAGE analysis revealed no major changes in either polypeptide composition or relative abundance of subunits in any complex (Figure S3), including the four Lhcas. Deconvolution analysis yielded a description of absorption spectra of all PSI–LHCI complexes with spectral forms very similar in terms of amplitude and λ_{max}. Overall, these data indicate that the greater photosensitivity of *szl1* is not a consequence of a pleiotropic, structural/functional destabilization of PSI–LHCI complexes.

Two conclusions can be drawn. The first is that the replacement of the majority of Vio with Lut within the LHCI system does not significantly affect PSI photosensitivity (Figures 2–4). Hence, PSI behaves differently compared to PSII: in the latter system, the binding of Lut as the only xanthophyll present renders LHCs unable to sustain $^1O_2$ scavenging and causes an extreme photosensitivity and rapid photobleaching of the LHC complexes.[49] The second observation is that while in PSII Lut content, Vio–Zea exchange and β-Car abundance have an additive effect on photoprotection, β-Car depletion is the main factor responsible for PSI phototolerance as shown by the extreme photosensitivity of P700 in *szl1* (Figure 2).

Zeaxanthin and PSI Photoprotection. Previous results indicated that Zea synthesis has multiple effects, such as enhancing energy dissipation[71,72] or scavenging ROS released by pigment-binding complexes.[23] Genetic dissection showed that the photoprotective effect of Zea depends on its binding to LHC proteins, which causes a downregulation of ^{3}Chl* yield in PSII.[28] Upon Vio–Zea exchange, a number of LHC undergo changes in their conformation,[73] which affect Chl–Chl/Chl–protein interactions and downregulate the probability of $^1O_2$ release. Although the molecular mechanism involved is still

unknown, the physiological effect on LHC is remarkable, resulting in an effective photoprotection of PSII.[28]

Xanthophyll exchange takes place in the L2 site of LHC, whose occupancy depends on the type of protein: Lut in trimeric LHCII and Vio in both monomeric Lhcb and LHCI.[37,74,75] With regard to the PSI–LHCI complex, *in vivo* studies reveal a stable binding of Zea upon EL treatment.[38] Previous results showed that, even in the absence of the xanthophyll cycle, PSI was resistant to chilling-induced photoinhibition,[63] while more recently, a Zea-dependent quenching action by ^{1}Chl* has been suggested to occur in LHCI.[76]

Our results indicate that, despite the high de-epoxidation level achieved in *Arabidopsis* thylakoids (Table 1), a small amount of Zea molecules (~1 per unit of PSI–LHCI complex) was stably bound to the antenna moiety of the WT PSI–LHCI complex. This Zea pool was retained even after several purification steps and correlated to a corresponding decrease in the Vio content of the supercomplex (Table 3), thus supporting the idea of xanthophyll exchange rather than nonspecific binding.

In WT thylakoids, however, the binding of Zea to LHCI proteins is insufficient to alter the triplet-state properties of the complex (Figure 5A). This is unlike what was observed in PSII antennas, whose ^{3}Chl* yield is downregulated by Vio–Zea exchange[28] and correlates with a lower rate of $^1O_2$ evolution under EL conditions. Current FDMR data are consistent with the plants' photoprotection capacity *in vivo*: when plants were challenged with EL and cold stress, the level of P700 photoinhibition was no greater in *npq1* than in WT (Figure 2C), which suggests that Zea may not be crucial for PSI photoprotection, or at least not under the conditions tested. The same conclusion could be drawn from analyzing the purified PSI–LHCI complex (Figure 4) and LHCI (Figure 6), which gave the same $^1O_2$ yield, irrespective of the presence (WT sample) or absence (*npq1* sample) of bound Zea. The data also agree with the FDMR results, which show comparable triplet yields in de-epoxidated WT and *npq1* samples (Figure 5A).

We cannot exclude the possibility that the binding of Zea to the PSI–LHCI complex could be more pronounced in other plant species, under different stress conditions, or upon prolonged exposure to EL, thus becoming more important in PSI photoprotection. Alternatively, Zea bound to LHCI might be involved in the downregulation of ^{1}Chl*, as recently suggested by fluorescence decay kinetics of the PSI–LHCI supercomplex.[76]

No Zea was detected in the PSI–LHCI complex purified from *szl1* de-epoxidated thylakoids (Table 2), presumably because of the smaller xanthophyll cycle pigment pool size of the mutant, which limits the amount of Zea to $^1/_5$ of that present in WT plants (Table 1). *szl1* plants have a photosensitivity much greater than those of the WT and *npq1* genotypes both at whole plant (Figure 2) and isolated PSI–LHCI complex (Figures 3 and 4) levels. However, the effect of the *npq1* mutation in limiting PSI photoinhibition was not significant in the *szl1* genetic background (Figure 2C), suggesting that the lack of Zea is not the major cause of its strong photosensitivity.

β-Carotene and PSI Photoprotection. The PSI–LHCI complex of *szl1* plants has a carotene content lower than that of the corresponding WT complex: HPLC analyses (Table 3) reveal that approximately 20% of β-Car-binding sites in both the core complex and N1 sites are devoid of carotenes.[37] This greatly impairs the plant's photoprotection capacity, with PSI being far more affected than PSII.

In the PSII core complex, most β-Car molecules are in close contact with Chl, so that they can effectively quench ^{3}Chl*.[77] The exception is represented by the two β-Car ligands in the PSII reaction center, whose distance from the P680 special pair is too great to allow ^{3}P680* quenching.[29,30] PSII has been reported to be the primary target of EL stress,[5,78] because the D1 subunit is easily photo-oxidized and rapidly turned over. $P700^+$, on the other hand, has been observed to be an efficient quencher of excitation energy and, by removing excess reducing power, can protect PSI from photodamage.[32] However, charge recombination can give rise to ^{3}P700*, and its yield is increased under conditions of acceptor limitation.[79] Furthermore, PSI exposed to intense light generates ^{3}Car* mainly associated with LHCI,[60] and a selective bleaching of Lut bound to the peripheral antenna;[80] hence, the question of the role of carotene ligands arises.

While an efficient PSII repair machinery has been described,[5] no similar mechanism has been identified for PSI: after photooxidative damage, it takes several days to recover its functionality[32,81] because this process entails the degradation and resynthesis of the entire complex. Because its consequences are essentially irreversible, all efforts must be made to avoid PSI photoinhibition. There are a number of mechanisms ensuring effective photoprotection, which include activation of the stromal scavenging enzymes[31] and PGR5-dependent regulation of electron transfer.[33] In several plant species, including *Arabidopsis*, PSI photosensitivity is exacerbated at low temperatures, presumably because they slow these protective mechanisms and decrease the size of sink of reductants.[32] Under these conditions, hyper-reduction of the electron chain occurs, and the yield of both ^{3}P700* and $^1O_2$ increases; the iron–sulfur centers are the primary targets for PSI photooxidation by ROS.[82,83]

The results in Figure 2 show that our stressing conditions damaged PSI in the WT genotype, and the effect is even greater in *szl1* plants, as shown by its 4-fold faster PSI photoinhibition rate (Figure 2C). A plausible hypothesis regarding the molecular mechanism(s) behind the photosensitivity of PSI in *szl1* is that its carotene composition affects its photoprotection capacity. Unlike WT plants, *szl1* plants contain α-carotene in both PSI core and LHCI moieties of the mutant, partially replacing β-Car (Table 3). However, although the PSI–LHCI complex from the *lut5* genotype has an α-carotene content greater than that of the *szl1* genotype (Table 2), similar photobleaching rates (Figure 4B) and $^1O_2$ release (Figure 5B) were observed in PSI–LHCI complexes isolated from *lut5* and WT plants. These findings rule out the possibility that the main reason for PSI photosensitivity in *szl1* plants is the α-carotene present either in its core complex or in its LHCI.

Alternatively, PSI stability might be affected by the amount of carotene molecules available. Most β-Car molecules are coordinated by either different subunits or distant regions within PSI,[84] suggesting that these pigments may have a crucial role in preserving the structural integrity of PSI. In *szl1* plants, a weakened PSI–LHCI structure would make the complex more susceptible to ROS damage. However, electron transfer efficiency and Chl organization are comparable to those of the WT (Figure S2); moreover, harsh solubilization of whole complexes, aimed at promoting antenna detachment, gave the same migration rate of the different moieties on a sucrose

gradient, and similar LHCI detachment efficiency (Figure S6), thus suggesting that the PSI−LHCI complex from *szl1* plants is quite stable. The increased photosensitivity of the PSI core complex from *szl1* (Figure 6A) can therefore be ascribed to a lower carotene content, which leaves a portion of ^{3}Chl* unquenched.

Interestingly, LHCI complexes purified from *szl1* released amounts of $^1O_2$ greater than that released by the PSI core (Figure 6) despite a far lower β-Car depletion in LHCI versus the PSI core [9 and 22% increase in Chl/Car ratio, respectively (Table 3)], thus suggesting that binding of β-Car to PSI antennas is a key factor for PSI photoresistance. Recent investigations of the crystal structure of the PSI−LHCI complex confirm that each Lhca binds one β-Car at its N1 site.[37] Another report[85] reveals that preferential degradation of LHCI upon strong light treatment is effective in preserving P700 activity in isolated PSI−LHCI complexes. Because recovery from photoinhibition entails the degradation and resynthesis of the entire PSI complex, sacrificing the antennae might be a strategy for restricting photooxidative damage in the LHCI moiety, thus protecting Fe−S clusters. The role of LHCI as a safety fuse for PSI might be linked to the presence of red-absorbing forms of LHCI.[35,85,86] Given their low energy level, these "red Chls" concentrate the excitation energy before transferring it to the RC;[87] therefore, the probability of generating ^{3}Chl* is greater here than anywhere else within the PSI−LHCI complex. These triplet excited states are probably quenched by nearby Car, because the efficiency of the mechanism is impaired in LHCI isoforms devoid of red Chl.[35] However, it is unlikely that β-Car is involved in this process, because the cluster that includes red Chls is located too far from β-Car in site N1 for an efficient triplet transfer.[37] On the other hand, xanthophyll in site L2, located close to the Chls absorbing low-energy forms, presumably contributes to a much greater extent to the ^{3}Chl* quenching mechanism. At any rate, LHCI lacking fewer than one β-Car in sites N1 displays a ^{3}Chl* yield and an $^1O_2$ release greater than those of the corresponding WT complex. Moreover, FDMR analyses reveal that the ^{3}Chl* populations assigned to the antenna components are larger in the *szl1* PSI−LHCI complex than in WT ones. A comparison with the FDMR signals of isolated Lhca4 found in the literature[35] suggests that the increase we observed in the PSI−LHCI complex affects at least in part the ^{3}Chl* population of LHCI (Figure S5B). These findings highlight another striking difference between the LHCI and LHCII complexes: β-Car molecules in the N1 site of LHCI actively participate in ^{3}Chl* quenching, unlike the xanthophyll in site N1 of LHCII, which does not directly contribute to this process; the latter compound, however, has been reported to act as a barrier, limiting the access of O_2 to the inner domain of the LHCII and thereby contributing to its photostability.[67]

At the same time, the decrease in the carotenoid triplet states detected would also appear to be linked to certain ^{3}Car* components (Figure S5A) previously found in Lhca4.[35]

CONCLUSIONS

szl1 plants have a less active β-cyclase,[40] and consequently, their PSI−LHCI complex has a carotene content lower than that of the corresponding WT complex and their LHCI moiety an altered xanthophyll composition. In *npq1* plants, which have no functional Vio de-epoxidase, Zea formation is impaired. When challenged with EL and cold stress, the *szl1* genotype displayed PSI photoinhibition more severe than that of the WT plants, and a comparative analysis with the *chy1 chy2* and *lut5* mutants identified carotene depletion in both the PSI core and LHCI complexes as the major source of photodamage. On the other hand, the binding of Zea to the LHCI was far less important. The high levels of $^1O_2$ release in the LHCI complexes from *szl1* (Figure 6) and the presence of larger amounts of ^{3}Chl*, detected by FDMR (Figure 5), suggest that PSI antennas too, like LHCII, constitutively experience ^{3}Chl* formation and that carotenoid species bound to LHCI play a key role in ^{3}Chl* quenching. Consequently, it appears that regulation of the PSI Chl excited states under EL conditions is crucial for the effective protection of the photosynthetic apparatus.

ASSOCIATED CONTENT

Supporting Information

The Supporting Information is available free of charge on the ACS Publications website at DOI: 10.1021/acs.biochem.6b00425.

Purification of PSI−LHCI complexes (Figure S1), characterization of PSI−LHCI complexes purified from WT and mutant genotypes (Figure S2), fluorescence-detected magnetic resonance of the chlorophyll and carotenoid triplet states on PSI−LHCI complexes isolated from dark-adapted, WT plants (Figure S3), reconstruction of the FDMR spectra of the ^{3}Chl* states on purified PSI−LHCI complexes, with Gaussian components (Figure S4), fluorescence-detected magnetic resonance of ^{3}Car* and ^{3}Chl* on purified PSI−LHCI complexes (Figure S5), purification of PSI core and LHCI complexes (Figure S6), parameters of the Global Gaussian Deconvolution of ^{3}Chl* states on purified PSI−LHCI complexes, with Gaussians components (Table 1S), and amplitude of the Gaussian components of ^{3}Chl* states used in the reconstruction of the FDMR spectra on purified PSI−LHCI complexes at different wavelengths (Table 2S) (PDF)

AUTHOR INFORMATION

Corresponding Author

*Dipartimento di Biotecnologie, Università di Verona, Strada Le Grazie 15, 37134 Verona, Italy. E-mail: luca.dallosto@univr.it. Phone: +39 045 8027806. Fax: +39 045 8027929.

Author Contributions

S.C. and M.B. contributed equally to this work. S.C. and M.B. were involved in the photooxidative treatments of plants, measurements of stress-related factors, the purification of pigment−protein complexes, measurements of ROS production and photobleaching kinetics, and data analysis. A.A. and D.C. conducted FDMR analysis. L.D. conceived the study, took part in its design and coordination, and drafted the manuscript.

Funding

This work was supported by MIUR (PRIN2010−2011 prot. 2010FM38P_004).

Notes

The authors declare no competing financial interest.

ACKNOWLEDGMENTS

L.D. is grateful to Prof. K. K. Niyogi for his kind gift of the *szl1* and *szl1 npq1* genotypes.

■ ABBREVIATIONS

Chl, chlorophylls; Car, carotenoids; Crt, carotenes; EL, excess light; FDMR, fluorescence-detected magnetic resonance; LHCI and LHCII, Photosystem I and II light-harvesting systems, respectively; Lhca and Lhcb, Photosystem I and II light-harvesting complexes, respectively; LL, low light; PS, Photosystem; P680 and P700, PSII and PSI reaction centers, respectively; ROS, reactive oxygen species; RT, room temperature; SD, standard deviation; SOSG, singlet oxygen sensor green; Vio, violaxanthin; Xan, xanthophylls; WT, wild type; Zea, zeaxanthin; β-Car, β-carotene; ^{1}Chl* and ^{3}Chl*, singlet and triplet excited states of chlorophyll, respectively; $^1O_2$, singlet oxygen.

■ REFERENCES

(1) Nelson, N., and Ben Shem, A. (2004) The complex architecture of oxygenic photosynthesis. *Nat. Rev. Mol. Cell Biol. 5*, 1−12.

(2) Croce, R., and Van Amerongen, H. (2013) Light-harvesting in photosystem I. *Photosynth. Res. 116*, 153−166.

(3) Van Amerongen, H., and Croce, R. (2013) Light-harvesting in photosystem II. *Photosynth. Res. 116*, 251−263.

(4) Nelson, N., and Junge, W. (2015) Structure and Energy Transfer in Photosystems of Oxygenic Photosynthesis. *Annu. Rev. Biochem. 84*, 659−683.

(5) Aro, E.-M., Virgin, I., and Andersson, B. (1993) Photoinhibition of Photosystem II - inactivation, protein damage and turnover. *Biochim. Biophys. Acta, Bioenerg. 1143*, 113−134.

(6) Long, S. P., Humphries, S., and Falkowski, P. G. (1994) Photoinhibition of photosynthesis in nature. *Annu. Rev. Plant Physiol. Plant Mol. Biol. 45*, 633−662.

(7) Krieger-Liszkay, A. (2004) Singlet oxygen production in photosynthesis. *J. Exp. Bot. 56*, 337−346.

(8) Anderson, J. M., Park, Y. I., and Chow, W. S. (1997) Photoinactivation and photoprotection of photosystem II in nature. *Physiol. Plant. 100*, 214−223.

(9) Frank, H. A., and Cogdell, R. J. (1996) Carotenoids in photosynthesis. *Photochem. Photobiol. 63*, 257−264.

(10) Amunts, A., Toporik, H., Borovikova, A., and Nelson, N. (2010) Structure Determination and Improved Model of Plant Photosystem I. *J. Biol. Chem. 285*, 3478−3486.

(11) Umena, Y., Kawakami, K., Shen, J. R., and Kamiya, N. (2011) Crystal structure of oxygen-evolving photosystem II at a resolution of 1.9 A. *Nature 473*, 55−60.

(12) Mazor, Y., Borovikova, A., and Nelson, N. (2015) The structure of plant photosystem I super-complex at 2.8 Å resolution. *eLife 4*, e07433.

(13) Pan, X., Liu, Z., Li, M., and Chang, W. (2013) Architecture and function of plant light-harvesting complexes II. *Curr. Opin. Struct. Biol. 23*, 515−525.

(14) Ruban, A. V., Johnson, M. P., and Duffy, C. D. (2012) The photoprotective molecular switch in the photosystem II antenna. *Biochim. Biophys. Acta, Bioenerg. 1817*, 167−181.

(15) de Bianchi, S., Ballottari, M., Dall'Osto, L., and Bassi, R. (2010) Regulation of plant light harvesting by thermal dissipation of excess energy. *Biochem. Soc. Trans. 38*, 651−660.

(16) Mathis, P., Butler, W. L., and Satoh, K. (1979) Carotenoid triplet state and chlorophyll fluorescence quenching in chloroplasts and sub chloroplasts particles. *Photochem. Photobiol. 30*, 603−614.

(17) El Agamey, A., Lowe, G. M., McGarvey, D. J., Mortensen, A., Phillip, D. M., Truscott, T. G., and Young, A. J. (2004) Carotenoid radical chemistry and antioxidant/pro-oxidant properties. *Arch. Biochem. Biophys. 430*, 37−48.

(18) Havaux, M., and Niyogi, K. K. (1999) The violaxanthin cycle protects plants from photooxidative damage by more than one mechanism. *Proc. Natl. Acad. Sci. U. S. A. 96*, 8762−8767.

(19) Demmig-Adams, B. (1990) Carotenoids and photoprotection in plants: A role for the xanthophyll zeaxanthin. *Biochim. Biophys. Acta, Bioenerg. 1020*, 1−24.

(20) Jahns, P., Latowski, D., and Strzalka, K. (2009) Mechanism and regulation of the violaxanthin cycle: the role of antenna proteins and membrane lipids. *Biochim. Biophys. Acta, Bioenerg. 1787*, 3−14.

(21) Pinnola, A., Dall'Osto, L., Gerotto, C., Morosinotto, T., Bassi, R., and Alboresi, A. (2013) Zeaxanthin binds to light-harvesting complex stress-related protein to enhance nonphotochemical quenching in Physcomitrella patens. *Plant Cell 25*, 3519−3534.

(22) Betterle, N., Ballottari, M., Hienerwadel, R., Dall'Osto, L., and Bassi, R. (2010) Dynamics of zeaxanthin binding to the photosystem II monomeric antenna protein Lhcb6 (CP24) and modulation of its photoprotection properties. *Arch. Biochem. Biophys. 504*, 67−77.

(23) Havaux, M., Dall'Osto, L., and Bassi, R. (2007) Zeaxanthin has enhanced antioxidant capacity with respect to all other xanthophylls in Arabidopsis leaves and functions independent of binding to PSII antennae. *Plant Physiol. 145*, 1506−1520.

(24) Dall'Osto, L., Cazzaniga, S., Havaux, M., and Bassi, R. (2010) Enhanced photoprotection by protein-bound vs free xanthophyll pools: a comparative analysis of chlorophyll b and xanthophyll biosynthesis mutants. *Mol. Plant 3*, 576−593.

(25) Hartel, H., Lokstein, H., Grimm, B., and Rank, B. (1996) Kinetic studies on the xanthophyll cycle in barley leaves (influence of antenna size and relations to Nonphotochemical chlorophyll fluorescence quenching). *Plant Physiol 110*, 471−482.

(26) Ahn, T. K., Avenson, T. J., Ballottari, M., Cheng, Y. C., Niyogi, K. K., Bassi, R., and Fleming, G. R. (2008) Architecture of a charge-transfer state regulating light harvesting in a plant antenna protein. *Science 320*, 794−797.

(27) Polivka, T., Zigmantas, D., Sundström, V., Formaggio, E., Cinque, G., and Bassi, R. (2002) Carotenoid S-1 state in a recombinant light-harvesting complex of photosystem II. *Biochemistry 41*, 439−450.

(28) Dall'Osto, L., Holt, N. E., Kaligotla, S., Fuciman, M., Cazzaniga, S., Carbonera, D., Frank, H. A., Alric, J., and Bassi, R. (2012) Zeaxanthin protects plant photosynthesis by modulating chlorophyll triplet yield in specific light-harvesting antenna subunits. *J. Biol. Chem. 287*, 41820−41834.

(29) Telfer, A., De Las Rivas, J., and Barber, J. (1991) Beta-Carotene within the isolated photosystem II reaction centre: Photooxidation and irreversible bleaching of this chromophore by oxidised P680. *Biochim. Biophys. Acta, Bioenerg. 1060*, 106−114.

(30) Telfer, A., Dhami, S., Bishop, S. M., Phillips, D., and Barber, J. (1994) β-carotene quenches singlet oxygen formed by isolated photosystem II reaction centers. *Biochemistry 33*, 14469−14474.

(31) Asada, K. (1999) The water-water cycle in chloroplasts: scavenging of active oxygens and dissipation of excess photons. *Annu. Rev. Plant Physiol. Plant Mol. Biol. 50*, 601−639.

(32) Sonoike, K. (2011) Photoinhibition of Photosystem I. *Physiol. Plant. 142*, 56−64.

(33) Suorsa, M., Jarvi, S., Grieco, M., Nurmi, M., Pietrzykowska, M., Rantala, M., Kangasjarvi, S., Paakkarinen, V., Tikkanen, M., Jansson, S., and Aro, E. M. (2012) Proton Gradient Regulation5 Is Essential for Proper Acclimation of Arabidopsis Photosystem I to Naturally and Artificially Fluctuating Light Conditions. *Plant Cell 24*, 2934−2948.

(34) Cazzaniga, S., Li, Z., Niyogi, K. K., Bassi, R., and Dall'Osto, L. (2012) The Arabidopsis szl1 mutant reveals a critical role of β-carotene in photosystem I photoprotection. *Plant Physiol. 159*, 1745−1758.

(35) Carbonera, D., Agostini, G., Morosinotto, T., and Bassi, R. (2005) Quenching of chlorophyll triplet states by carotenoids in reconstituted Lhca4 subunit of peripheral light-harvesting complex of photosystem I. *Biochemistry 44*, 8337−8346.

(36) Croce, R., Mozzo, M., Morosinotto, T., Romeo, A., Hienerwadel, R., and Bassi, R. (2007) Singlet and triplet state transitions of carotenoids in the antenna complexes of higher-plant Photosystem I. *Biochemistry 46*, 3846−3855.

(37) Qin, X., Suga, M., Kuang, T., and Shen, J.-R. (2015) Structural basis for energy transfer pathways in the plant PSI-LHCI supercomplex. *Science 348*, 989−995.
(38) Wehner, A., Storf, S., Jahns, P., and Schmid, V. H. (2004) Deepoxidation of violaxanthin in light-harvesting complex I proteins. *J. Biol. Chem. 279*, 26823−26829.
(39) Fiore, A., Dall'Osto, L., Fraser, P. D., Bassi, R., and Giuliano, G. (2006) Elucidation of the beta-carotene hydroxylation pathway in Arabidopsis thaliana. *FEBS Lett. 580*, 4718−4722.
(40) Li, Z., Ahn, T. K., Avenson, T. J., Ballottari, M., Cruz, J. A., Kramer, D. M., Bassi, R., Fleming, G. R., Keasling, J. D., and Niyogi, K. K. (2009) Lutein accumulation in the absence of zeaxanthin restores nonphotochemical quenching in the Arabidopsis thaliana npq1 mutant. *Plant Cell 21*, 1798−1812.
(41) Niyogi, K. K., Grossman, A. R., and Björkman, O. (1998) Arabidopsis mutants define a central role for the xanthophyll cycle in the regulation of photosynthetic energy conversion. *Plant Cell 10*, 1121−1134.
(42) Casazza, A. P., Tarantino, D., and Soave, C. (2001) Preparation and functional characterization of thylakoids from Arabidopsis thaliana. *Photosynth. Res. 68*, 175−180.
(43) Ruban, A. V., Lee, P. J., Wentworth, M., Young, A. J., and Horton, P. (1999) Determination of the stoichiometry and strength of binding of xanthophylls to the photosystem II light harvesting complexes. *J. Biol. Chem. 274*, 10458−10465.
(44) Croce, R., and Bassi, R. (1998) in *Photosynthesis: Mechanisms and Effects* (Garab, G., Ed.) pp 421−424, Kluwer Academic Publisher, Dordrecht, The Netherlands.
(45) Laemmli, U. K. (1970) Cleavage of structural proteins during the assembly of the head of bacteriophage T4. *Nature 227*, 680−685.
(46) Croce, R., Zucchelli, G., Garlaschi, F. M., and Jennings, R. C. (1998) A thermal broadening study of the antenna chlorophylls in PSI- 200, LHCI, and PSI core. *Biochemistry 37*, 17355−17360.
(47) Lagarde, D., Beuf, L., and Vermaas, M. (2000) Increased production of zeaxanthin and other pigments by application of genetic engineering techniques to Synechocystis sp strain PCC 6803. *Appl. Environ. Microbiol. 66*, 64−72.
(48) Flors, C., Fryer, M. J., Waring, J., Reeder, B., Bechtold, U., Mullineaux, P. M., Nonell, S., Wilson, M. T., and Baker, N. R. (2006) Imaging the production of singlet oxygen in vivo using a new fluorescent sensor, Singlet Oxygen Sensor Green. *J. Exp. Bot. 57*, 1725−1734.
(49) Dall'Osto, L., Fiore, A., Cazzaniga, S., Giuliano, G., and Bassi, R. (2007) Different roles of α- and β-branch xanthophylls in photosystem assembly and photoprotection. *J. Biol. Chem. 282*, 35056−35068.
(50) Croce, R., Weiss, S., and Bassi, R. (1999) Carotenoid-binding sites of the major light-harvesting complex II of higher plants. *J. Biol. Chem. 274*, 29613−29623.
(51) Havaux, M., Dall'Osto, L., Cuine, S., Giuliano, G., and Bassi, R. (2004) The effect of zeaxanthin as the only xanthophyll on the structure and function of the photosynthetic apparatus in Arabidopsis thaliana. *J. Biol. Chem. 279*, 13878−13888.
(52) Yang, J.-S., Wang, R., Meng, J.-J., Bi, Y.-P., Xu, P.-L., Guo, F., Wan, S.-B., He, Q.-W., and Li, X. G. (2010) Overexpressionof Arabidopsis CBF1 gene in transgenic tobacco alleviates photoinhibition of PSII and PSI during chilling stress under low irradiance. *J. Plant Physiol. 167*, 534−539.
(53) Carbonera, D., Giacometti, G., and Agostini, G. (1992) FDMR of carotenoid and chlorophyll triplets in Light-harvesting complex LHCII of spinach. *Appl. Magn. Reson. 3*, 859−872.
(54) Santabarbara, S., Bordignon, E., Jennings, R. C., and Carbonera, D. (2002) Chlorophyll triplet states associated with photosystem II of thylakoids. *Biochemistry 41*, 8184−8194.
(55) Santabarbara, S., Agostini, G., Heathcote, P., and Carbonera, D. (2005) A fluorescence detected magnetic resonance investigation of the carotenoid triplet states associated with photosystem II of isolated spinach thylakoid membranes. *Photosynth. Res. 86*, 283−296.
(56) Kim, J., Smith, J. J., Tian, L., and DellaPenna, D. (2009) The evolution and function of carotenoid hydroxylases in Arabidopsis. *Plant Cell Physiol. 50*, 463−479.
(57) Zhang, S., and Scheller, H. V. (2004) Photoinhibition of Photosystem I at chilling temperature and subsequernt recovery in Arabidopsis thaliana. *Plant Cell Physiol. 45*, 1595−1602.
(58) Clarke, R. H. (1982) *Triplet State ODMR Spectroscopy. Techniques and Applications to Biophysical Systems*, New York.
(59) Hoff, A. J. (1989) *Optically detected magnetic resonance (ODMR) of triplet states in vivo*, Elsevier, Amsterdam.
(60) Santabarbara, S., and Carbonera, D. (2005) Carotenoid triplet states associated with the long-wavelength-emitting chlorophyll forms of Photosystem I in isolated thylakoid membranes. *J. Phys. Chem. B 109*, 986−991.
(61) Horton, P., Ruban, A., and Wentworth, M. (2000) Allosteric regulation of the light-harvesting system of photosystem II. *Philos. Trans. R. Soc., B 355*, 1361−1370.
(62) Avenson, T. J., Ahn, T. K., Zigmantas, D., Niyogi, K. K., Li, Z., Ballottari, M., Bassi, R., and Fleming, G. R. (2008) Zeaxanthin radical cation formation in minor light-harvesting complexes of higher plant antenna. *J. Biol. Chem. 283*, 3550−3558.
(63) Havaux, M., and Kloppstech, K. (2001) The protective functions of carotenoid and flavonoid pigments against excess visible radiations at chilling temperature investigated in Arabidopsis npq and tt mutants. *Planta 213*, 953−966.
(64) Dall'Osto, L., Piques, M., Ronzani, M., Molesini, B., Alboresi, A., Cazzaniga, S., and Bassi, R. (2013) The Arabidopsis nox mutant lacking carotene hydroxylase activity reveals a critical role for xanthophylls in photosystem I biogenesis. *Plant Cell 25*, 591−608.
(65) Toth, T. N., Chukhutsina, V., Domonkos, I., Knoppova, J., Komenda, J., Kis, M., Lenart, Z., Garab, G., Kovacs, L., Gombos, Z., and Van Amerongen, H. (2015) Carotenoids are essential for the assembly of cyanobacterial photosynthetic complexes. *Biochim. Biophys. Acta, Bioenerg. 1847*, 1153−1165.
(66) Peterman, E. J., Dukker, F. M., van Grondelle, R., and Van Amerongen, H. (1995) Chlorophyll a and carotenoid triplet states in light-harvesting complex II of higher plants. *Biophys. J. 69*, 2670−2678.
(67) Mozzo, M., Dall'Osto, L., Hienerwadel, R., Bassi, R., and Croce, R. (2008) Photoprotection in the antenna complexes of photosystem II: role of individual xanthophylls in chlorophyll triplet quenching. *J. Biol. Chem. 283*, 6184−6192.
(68) Trevithick-Sutton, C. C., Foote, C. S., Collins, M., and Trevithick, J. R. (2006) The retinal carotenoids zeaxanthin and lutein scavenge superoxide and hydroxyl radicals: a chemiluminescence and ESR study. *Mol. Vis. 12*, 1127−1135.
(69) Niyogi, K. K., Shih, C., Soon Chow, W., Pogson, B. J., DellaPenna, D., and Björkman, O. (2001) Photoprotection in a zeaxanthin- and lutein-deficient double mutant of Arabidopsis. *Photosynth. Res. 67*, 139−145.
(70) Dall'Osto, L., Lico, C., Alric, J., Giuliano, G., Havaux, M., and Bassi, R. (2006) Lutein is needed for efficient chlorophyll triplet quenching in the major LHCII antenna complex of higher plants and effective photoprotection in vivo under strong light. *BMC Plant Biol. 6*, 32.
(71) Demmig-Adams, B., Winter, K., Kruger, A., and Czygan, F.-C. (1989) in *Photosynthesis. Plant Biology Vol. 8* (Briggs, W. R., Ed.) pp 375−391, Alan R. Liss, New York.
(72) Nilkens, M., Kress, E., Lambrev, P., Miloslavina, Y., Muller, M., Holzwarth, A. R., and Jahns, P. (2010) Identification of a slowly inducible zeaxanthin-dependent component of non-photochemical quenching of chlorophyll fluorescence generated under steady-state conditions in Arabidopsis. *Biochim. Biophys. Acta, Bioenerg. 1797*, 466−475.
(73) Moya, I., Silvestri, M., Vallon, O., Cinque, G., and Bassi, R. (2001) Time-resolved fluorescence analysis of the Photosystem II antenna proteins in detergent micelles and liposomes. *Biochemistry 40*, 12552−12561.

(74) Liu, Z., Yan, H., Wang, K., Kuang, T., Zhang, J., Gui, L., An, X., and Chang, W. (2004) Crystal structure of spinach major light-harvesting complex at 2.72 A resolution. *Nature 428*, 287−292.
(75) Pan, X., Li, M., Wan, T., Wang, L., Jia, C., Hou, Z., Zhao, X., Zhang, J., and Chang, W. (2011) Structural insights into energy regulation of light-harvesting complex CP29 from spinach. *Nat. Struct. Mol. Biol. 18*, 309−315.
(76) Ballottari, M., Alcocer, M. J. P., D'Andrea, C., Viola, D., Ahn, T. K., Petrozza, A., Polli, D., Fleming, G. R., Cerullo, G., and Bassi, R. (2014) Regulation of photosystem I light harvesting by zeaxanthin. *Proc. Natl. Acad. Sci. U. S. A. 111*, E2431−E2438.
(77) Ferreira, K. N., Iverson, T. M., Maghlaoui, K., Barber, J., and Iwata, S. (2004) Architecture of the photosynthetic oxygen-evolving center. *Science 303*, 1831−1838.
(78) Andersson, B., Salter, A. H., Virgin, I., Vass, I., and Styring, S. (1992) Photodamage to Photosystem-II - Primary and Secondary Events. *J. Photochem. Photobiol., B 15*, 15−31.
(79) Rutherford, A. W., Osyczka, A., and Rappaport, F. (2012) Back-reactions, short-circuits, leaks and other energy wasteful reactions in biological electron transfer: redox tuning to survive life in O(2). *FEBS Lett. 586*, 603−616.
(80) Andreeva, A., Abarova, S., Stoitchkova, K., Picorel, R., and Velitchkova, M. (2007) Selective photobleaching of chlorophylls and carotenoids in Photosystem I particles under high-light treatment. *Photochem. Photobiol. 83*, 1301−1307.
(81) Sonoike, K., and Terashima, I. (1994) Mechanism of Photosystem-I Photoinhibition in Leaves of Cucumis-Sativus l. *Planta 194*, 287−293.
(82) Inoue, K., Sakurai, M., and Hiyama, T. (1986) Photoinactivation sites of photosystem I in isolated chloroplasts. *Plant Cell Physiol. 27*, 961−968.
(83) Tjus, S. E., and Andersson, B. (1993) Loss of the trans-thylakoid proton gradient is an early event during photoinhibitory illumination of chloroplast preparations. *Biochim. Biophys. Acta, Bioenerg. 1183*, 315−322.
(84) Amunts, A., Toporik, H., Borovikova, A., and Nelson, N. (2010) Structure determination and improved model of plant Photosystem I. *J. Biol. Chem. 285*, 3478−3486.
(85) Alboresi, A., Ballottari, M., Hienerwadel, R., Giacometti, G. M., and Morosinotto, T. (2009) Antenna complexes protect Photosystem I from photoinhibition. *BMC Plant Biol. 9*, 71.
(86) Morosinotto, T., Breton, J., Bassi, R., and Croce, R. (2003) The nature of a chlorophyll ligand in Lhca proteins determines the far red fluorescence emission typical of photosystem I. *J. Biol. Chem. 278*, 49223−49229.
(87) Croce, R., Zucchelli, G., Garlaschi, F. M., Bassi, R., and Jennings, R. C. (1996) Excited state equilibration in the photosystem I -light - harvesting I complex: P700 is almost isoenergetic with its antenna. *Biochemistry 35*, 8572−8579.

Supporting information

Figure S1. Purification of PSI-LHCI complexes. **S**ucrose gradient fractionation of thylakoid membranes, upon *in vitro* de-epoxidation of chloroplasts. Solubilization of membranes was performed with 0.8% β-DM. For each gradient, fractions harvested are indicated.

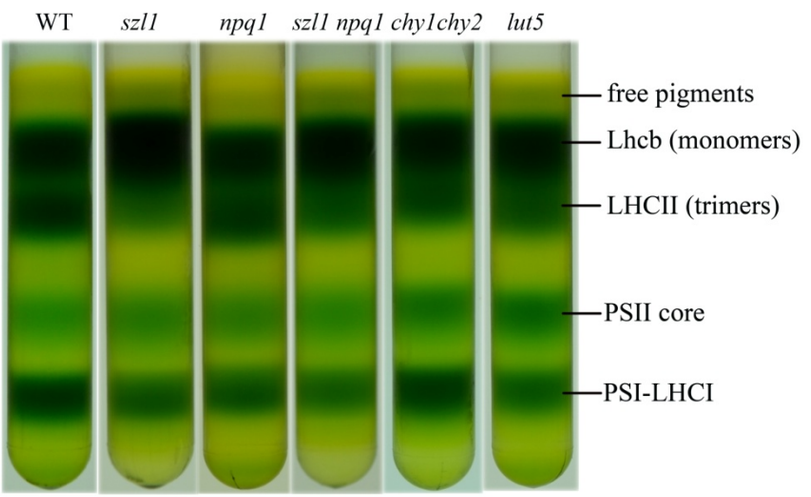

Figure S2. Characterization of PSI-LHCI complexes purified from WT and mutant genotypes. (A) Maximum photoxidizable P700 was measured at room temperature (RT) on PSI-LHCI complexes purified by sucrose gradient ultracentrifugation. $\Delta Abs_{705\ nm}$ has been expressed as percentage of the corresponding WT value. Chl concentration: 40 µg/ml. Data are expressed as mean ± SD, n = 7 (B) Electron transport from plastocyanin to $NADP^+$ was measured on thylakoids, continuously stirred and subjected to illumination (150 µmol photons m^{-2} s^{-1}, 600 nm < λ < 750 nm, RT). Chl concentration: 15 µg/ml. Electron transport rates were assayed by following $NADP^+$ reduction spectrophotometrically, as previously described (Casazza et al., 2001). Data are expressed as mean ± SD, n = 4. (C) SDS-PAGE of PSI-LHCI complexes. Main protein components are indicated. (D) Spectral deconvolution analysis of WT and mutant PSI-LHCI supercomplexes. (*upper panels*) Fitting of the red region absorption spectrum at RT of PSI-LHCI, with the spectra of individual Chl in a protein environment. (*lower panel*) Histogram of areas for the different sub-bands as obtained from deconvolution of the red region (645-735 nm) of the absorption spectra of complexes. Eight forms of Chl *a* and 2 of Chl *b* were the minimum number of forms in order to closely describe all the spectra. In our description of samples, the two Chl *b* forms peak at 640.5 and 652.5 nm, while the Chl *a* forms absorb at 663, 670, 677, 682.5, 689, 698, 708 and 716 nm. Amplitude of the different absorption forms were essentially the same in all complexes, indicating Chl organization in PSI-LHCI was unaffected by either *lut5*, *chy1 chy2* or *szl1* mutations.

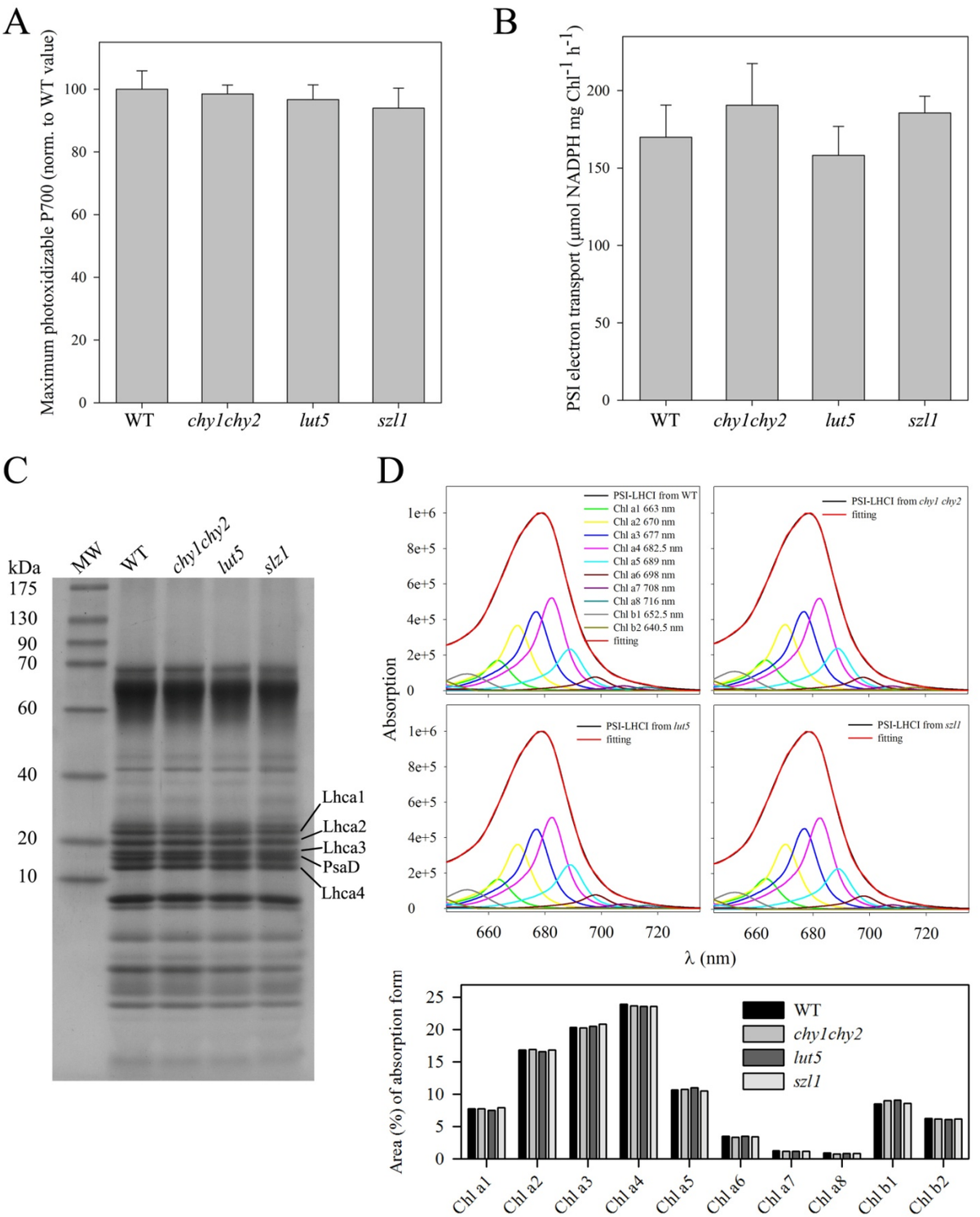
A
Maximum photoxidizable P700 (norm. to WT value)
0
20
40
60
80
100
WT
chy1chy2
lut5
szl1
B
PSI electron transport (μmol NADPH mg Chl-1 h-1)
0
50
100
150
200
WT
chy1chy2
lut5
szl1
C
kDa
MW
WT
chy1chy2
lut5
slz1
175
130
90
70
60
40
20
10
Lhca1
Lhca2
Lhca3
PsaD
Lhca4
D
Absorption
PSI-LHCI from WT
Chl a1 663 nm
Chl a2 670 nm
Chl a3 677 nm
Chl a4 682.5 nm
Chl a5 689 nm
Chl a6 698 nm
Chl a7 708 nm
Chl a8 716 nm
Chl b1 652.5 nm
Chl b2 640.5 nm
fitting
PSI-LHCI from chy1 chy2
fitting
PSI-LHCI from lut5
fitting
PSI-LHCI from szl1
fitting
1e+6
8e+5
6e+5
4e+5
2e+5
0
660
680
700
720
λ (nm)
Area (%) of absorption form
WT
chy1chy2
lut5
szl1
0
5
10
15
20
25
Chl a1
Chl a2
Chl a3
Chl a4
Chl a5
Chl a6
Chl a7
Chl a8
Chl b1
Chl b2

Figure S3. **Fluorescence detected magnetic resonance of the Chl and Car triplet states on isolated PSI-LHCI from dark adapted, WT plants.** FDMR signals of the ^{3}Chl* states (|D|-|E| and |D|+|E| transitions, panel A) and the ^{3}Car* states (2|E|, |D|-|E| and |D|+|E| transitions, panel B), observed in the PSI-LHCI complex purified from dark-adapted WT leaves, were detected at different wavelengths. Spectra have been vertically shifted for better comparison. Amplitude modulation frequency: 33 Hz (^{3}Chl* states) and 325 Hz (^{3}Car* states), tc 600 ms, number of scans 20, mw power 500 milliwatt, temperature 1.8 K.

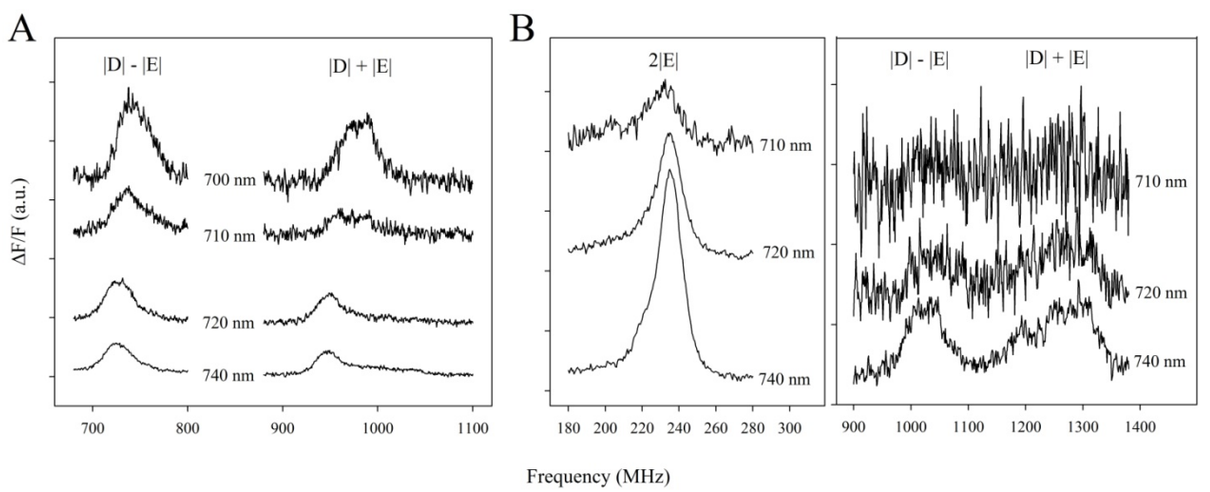

Figure S4. Reconstruction of the FDMR spectra of the ^{3}Chl* states on purified PSI-LHCI complexes, with Gaussians components. WT: left panels; *szl1:* right panels. *Upper panels*: FDMR spectra of the ^{3}Chl* states (|D|-|E| and |D|+|E| transitions, detected at different wavelengths - black traces). Spectra have been vertically shifted for better comparison. Fitting of the spectra are reported in green; single components are also shown in different colors. The constrains introduced for the fitting are the same used before for the same kind of spectral deconvolution (Santabarbara et al., 2002; Santabarbara et al., 2005a; Santabarbara et al., 2005b). Parameters used in the best fitting are reported in Table 1S. The fifth component (magenta) is observed only in the |D|+|E| transition and is assigned to a small contribution deriving from the |D|+|E| transition of the carotenoids. *Bottom panels*: amplitude of the main four gaussian components *vs.* detection wavelength (see Table 2S).

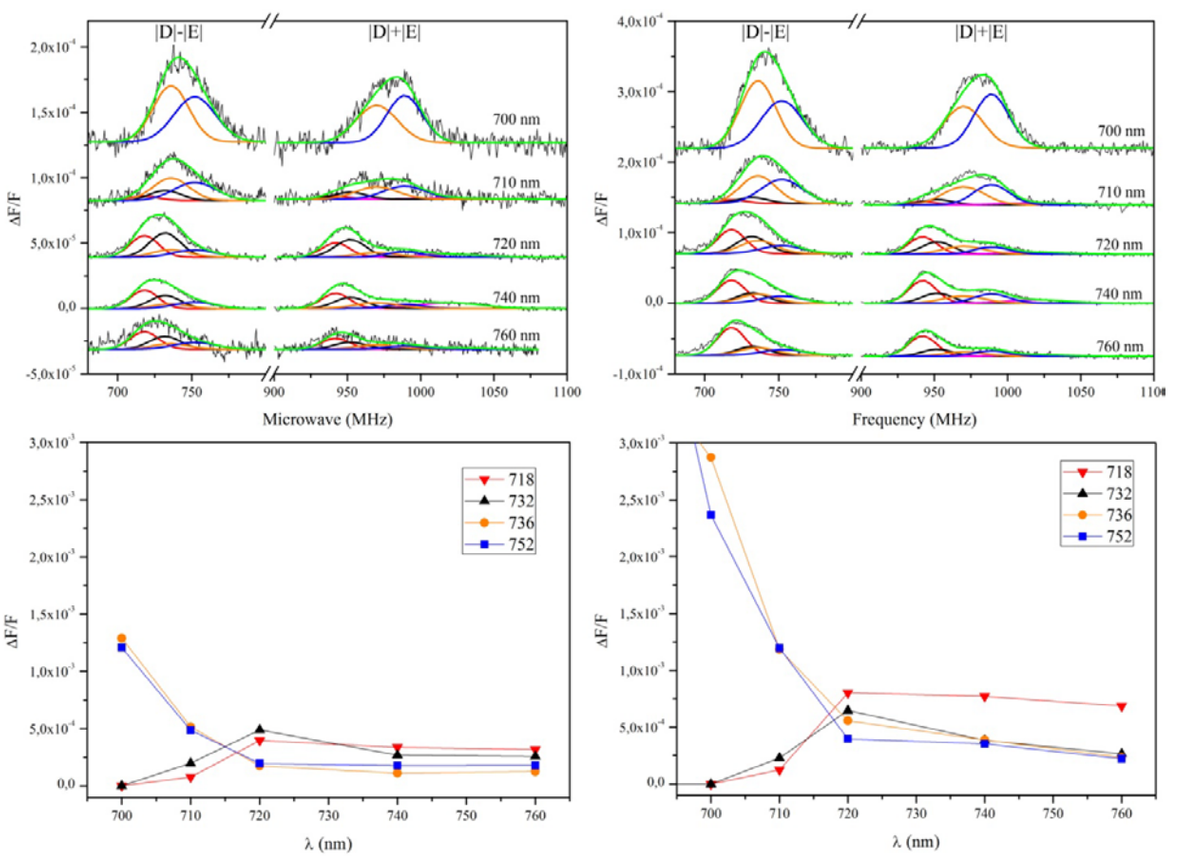

Figure S5. Fluorescence detected magnetic resonance of the ^{3}Car* and ^{3}Chl* on purified PSI-LHCI complexes. Comparison with Lhca4. FDMR signals of the ^{3}Car* states (2|E|, |D|-|E| and |D|+|E| transitions, panel A) and ^{3}Chl* states (|D|-|E| and |D|+|E| transitions, panel B) in the PSI-LHCI complex from WT (black lines) and *szl1* (green lines) in comparison with purified Lhca4 (red lines; modified from previously published data (Carbonera et al., 2005)). FDMR signals were detected at the wavelengths indicated in each panel.

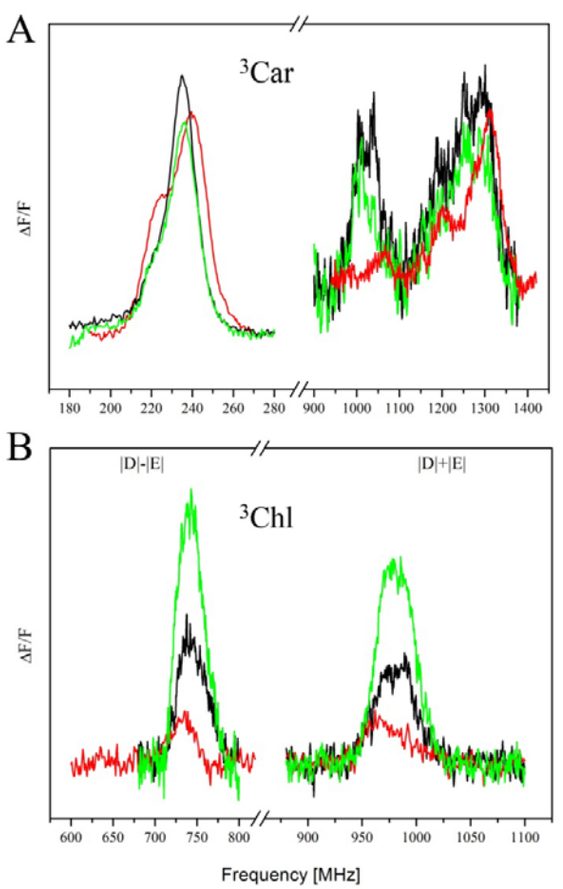

Figure S6. Purification of PSI core and LHCI complexes. Sucrose gradient fractionation of PSI core and LHCI complexes, upon solubilization of PSI-LHCI from WT, *npq1* and *szl1* with β-DM and Zwittergent (see Methods for details). For each gradient, fractions harvested are indicated.

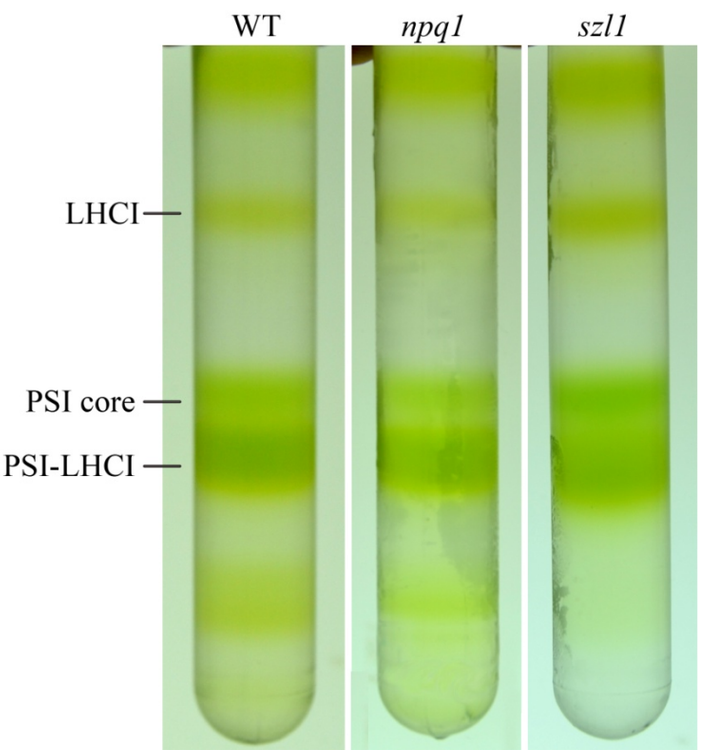

Table 1S. Parameters of the Global Gaussian Deconvolution of ^{3}Chl* states on purified PSI-LHCI complexes, with Gaussians components.

	|D|-|E|		**|D|+|E|**		**ZFS**	
	Center (MHz)	FWHM (MHz)	Center (MHz)	FWHM (MHz)	|D| (cm^{-1})	|E| (cm^{-1})
T_1	718	19	942	19	0.0277	0.0037
T_2	732	21	952	21	0.0281	0.0037
T_3	736	24	970	28	0.0284	0.0039
T_4	752	28	986	24	0.0290	0.0039
T_5	-	-	1020	42	-	-

Table 2S. Amplitude of the Gaussian components of ^{3}Chl* states used in the reconstruction of the FDMR spectra on purified PSI-LHCI complexes at different wavelengths.

|D|-|E|

WT	Center (MHz)	700 nm	710 nm	720 nm	740 nm	760 nm
T_1	718	-	$0.76*10^{-4}$	$3.96*10^{-4}$	$3.36*10^{-4}$	$3.17*10^{-4}$
T_2	732	-	$1.98*10^{-4}$	$4.88*10^{-4}$	$2.69*10^{-4}$	$2.57*10^{-4}$
T_3	736	$12.9*10^{-4}$	$5.15*10^{-4}$	$1.74*10^{-4}$	$1.11*10^{-4}$	$1.25*10^{-4}$
T_4	752	$12.1*10^{-4}$	$4.86*10^{-4}$	$1.95*10^{-4}$	$1.77*10^{-4}$	$1.78*10^{-4}$

szl1	Center (MHz)	700 nm	710 nm	720 nm	740 nm	760 nm
T_1	718	-	$1.25*10^{-4}$	$8.02*10^{-4}$	$7.71*10^{-4}$	$6.85*10^{-4}$
T_2	732	-	$2.28*10^{-4}$	$6.46*10^{-4}$	$3.84*10^{-4}$	$2.65*10^{-4}$
T_3	736	$28.7*10^{-4}$	$11.8*10^{-4}$	$5.57*10^{-4}$	$3.89*10^{-4}$	$2.34*10^{-4}$
T_4	752	$23.7*10^{-4}$	$12.0*10^{-4}$	$3.97*10^{-4}$	$3.54*10^{-4}$	$2.21*10^{-4}$

|D|+|E|

WT	Center (MHz)	700 nm	710 nm	720 nm	740 nm	760 nm
T_1	942	-	$0.52*10^{-4}$	$2.65*10^{-4}$	$2.76*10^{-4}$	$1.96*10^{-4}$
T_2	952	-	$1.34*10^{-4}$	$3.58*10^{-4}$	$2.30*10^{-4}$	$1.38*10^{-4}$
T_3	970	$10.8*10^{-4}$	$3.51*10^{-4}$	$1.22*10^{-4}$	$0.95*10^{-4}$	$0.73*10^{-4}$
T_4	989	$10.0*10^{-4}$	$3.31*10^{-4}$	$1.27*10^{-4}$	$1.54*10^{-4}$	$1.11*10^{-4}$
T_5	1020	-	$0.44*10^{-4}$	$1.36*10^{-4}$	$2.30*10^{-4}$	$0.54*10^{-4}$

szl1	Center (MHz)	700 nm	710 nm	720 nm	740 nm	760 nm
T_1	942	-	$1.10*10^{-4}$	$5.99*10^{-4}$	$7.62*10^{-4}$	$6.95*10^{-4}$
T_2	952	-	$2.00*10^{-4}$	$4.68*10^{-4}$	$3.62*10^{-4}$	$2.49*10^{-4}$
T_3	970	$20.1*10^{-4}$	$8.71*10^{-4}$	$3.13*10^{-4}$	$3.89*10^{-4}$	$2.24*10^{-4}$
T_4	989	$22.9*10^{-4}$	$9.03*10^{-4}$	$4.02*10^{-4}$	$3.98*10^{-4}$	$2.43*10^{-4}$
T_5	1020	-	$4.86*10^{-4}$	$1.95*10^{-4}$	$1.77*10^{-4}$	$1.78*10^{-4}$

References

Carbonera, D., Agostini, G., Morosinotto, T., and Bassi, R. (2005). Quenching of chlorophyll triplet states by carotenoids in reconstituted Lhca4 subunit of peripheral light-harvesting complex of photosystem I. Biochemistry **44**:8337-8346.

Casazza, A.P., Tarantino, D., and Soave, C. (2001). Preparation and functional characterization of thylakoids from Arabidopsis thaliana. Photosynth.Res. **68**:175-180.

Santabarbara, S., Agostini, G., Heathcote, P., and Carbonera, D. (2005a). A fluorescence detected magnetic resonance investigation of the carotenoid triplet states associated with photosystem II of isolated spinach thylakoid membranes. Photosynt.Res. **86**:283-296.

Santabarbara, S., Bordignon, E., Jennings, R.C., and Carbonera, D. (2002). Chlorophyll triplet states associated with photosystem II of thylakoids. Biochemistry **41**:8184-8194.

Santabarbara, S. and Carbonera, D. (2005b). Carotenoid triplet states associated with the long-wavelength-emitting chlorophyll forms of Photosystem I in isolated thylakoid membranes. J.Phys.Chem.B **109**:986-991.

Chapter 4

LHCII can substitute for LHCI as an antenna for Photosystem I but with reduced light harvesting capacity.

This chapter was published in

Nature Plants, Article number: 16131 (2016)

nature plants

ARTICLES

PUBLISHED: 26 AUGUST 2016 | ARTICLE NUMBER: 16131 | DOI: 10.1038/NPLANTS.2016.131

LHCII can substitute for LHCI as an antenna for photosystem I but with reduced light-harvesting capacity

Mauro Bressan[1], Luca Dall'Osto[1], Ilaria Bargigia[2], Marcelo J. P. Alcocer[2,3], Daniele Viola[3], Giulio Cerullo[3], Cosimo D'Andrea[2,3], Roberto Bassi[1]* and Matteo Ballottari[1]

Light-harvesting complexes (LHCs) are major constituents of the antenna systems in higher plant photosystems. Four Lhca subunits are tightly bound to the photosystem I (PSI) core complex, forming its outer antenna moiety called LHCI. The *Arabidopsis thaliana* mutant *ΔLhca* lacks all Lhca1–4 subunits and compensates for its decreased antenna size by binding LHCII trimers, the main constituent of the photosystem II antenna system, to PSI. In this work we have investigated the effect of LHCI/LHCII substitution by comparing the light harvesting and excitation energy transfer efficiency properties of PSI complexes isolated from *ΔLhca* mutants and from the wild type, as well as the consequences for plant growth. We show that the excitation energy transfer efficiency was not compromised by the substitution of LHCI with LHCII but a significant reduction in the absorption cross-section was observed. The absence of LHCI subunits in PSI thus significantly limits light harvesting, even on LHCII binding, inducing, as a consequence, a strong reduction in growth.

The conversion of light into chemical energy occurs in pigment–protein complexes, the photosystems. In eukaryotic photosynthetic organisms, two photosystems, namely PSI) and PSII, undergo light-driven charge separation. PSI and PSII bind chlorophyll (Chl) and carotenoid (Car) chromophores, whose spectroscopic properties are tuned by the protein environment. The initial reactions within PSI and PSII are catalysed by Chl *a* dimers, which absorb at 700 and 680 nm respectively. These dimers are served by a closely interacting array of Chl *a* and β-carotene pigments which are bound to plastid-encoded proteins in the so-called core complexes. More specifically, the PSI core (PSIc) complex comprises 95–98 Chls[1,2], but the PSII core complex binds fewer Chls (36). The optical absorption cross-section of both core complexes is enhanced by an outer antenna system composed of nuclear-encoded LHC subunits[3–6]. Higher plants evolved four LHC subunits (Lhca1–4) arranged in a half-moon structure adjacent to the PsaF/PsaJ subunits of the PSI core complex[1,2,7–9]. The PSIc/LHCI stoichiometry has been shown to be maintained at 1:4 irrespective of light growth conditions[10]. In contrast, the dimeric PSII core is encircled by a larger LHC antenna system composed of Lhcb1–6 subunits. These are organized into monomers (Lhcb4–6) and trimers (Lhcb1–3, also known as LHCII complexes), with the monomers located in between the core complex and the more peripheral trimers. Lhcb proteins can, however, migrate from PSII to PSI along the thylakoid membranes, depending on photosystem excitation[11–17]. When PSI is preferentially excited, plastoquinole (PQH_2) is oxidized and LHCII is almost exclusively associated to PSII (state 1). Upon preferential PSII excitation, however, PQH_2 undergoes over-reduction and triggers a threonine kinase activity which targets LHCII, freeing it from PSII grana and allowing diffusion to PSI (state 2)[16,18–21]. This transition balances excitation energy pressure between the photosystems, restoring the plastoquinone/PQH_2 ratio. It is reversed by TAP38/PPH1 phosphatase on PQH_2 re-oxidation[22–24]. The interaction of LHCII with PSI was observed under several growth conditions as a consequence of acclimation to low or moderate light levels[10,20,25], and was observed even in the absence of LHCII phosphorylation[15]. Upon binding to PSI, LHCII trimers have been shown to efficiently transfer excitation energy to the PSI reaction centre[25–27]. PSI supercomplexes binding either LHCI or LHCII, or both, differ as to their spectra and the strength of the PSIc–LHC interactions. In this work we investigated whether LHCI and LHCII are functionally equivalent when bound to PSI. To this extent, we isolated a *ΔLhca* mutant of *A. thaliana* which lacks the Lhca1–4 subunits and accumulates PSI core complexes with LHCII bound, analysing plant growth, light-harvesting and excitation energy transfer properties of its PSI complexes compared to wild type.

Results

ΔLhca is a triple knockout mutant of *Arabidopsis*, lacking all four Lhca subunits of the PSI peripheral antenna system. *ΔLhca* plants were obtained by crossing homozygous T-DNA mutants carrying insertions in genes encoding Lhca2, Lhca3 and Lhca4. We identified single knockout homozygous plants *koLhca2*, *koLhca3* and *koLhca4* in T-DNA F5 seed pools by polymerase chain reaction (PCR) analysis of genomic DNA (see Methods section). The triple knockout mutant, hereafter referred to as *ΔLhca*, was obtained by crossing single mutants and screening of the progeny. RT–PCR showed that mRNAs encoding Lhca2–4 were absent in the triple mutant (Fig. 1a); transcription of *Lhca1*, on the contrary, was similar in wild type and *ΔLhca* within experimental error (Supplementary Fig. 1). PSI antenna protein composition in triple mutant plants was investigated by one- and two-dimensional (2D) SDS–polyacrylamide gel electrophoresis (PAGE). Thylakoids from *ΔLhca* plants lacked Lhca2, Lhca3 and Lhca4 proteins (Fig. 1b); moreover, an additional band with higher molecular mass

[1]Dipartimento di Biotecnologie, Università di Verona, Strada Le Grazie 15, I-37134 Verona, Italy. [2]Centre for Nano Science and Technology @PoliMi, Istituto Italiano di Tecnologia, via Pascoli 70/3, 20133 Milan, Italy. [3]IFN-CNR, Department of Physics, Politecnico di Milano, Piazza Leonardo da Vinci 32, 20133 Milan, Italy. *e-mail: roberto.bassi@univr.it

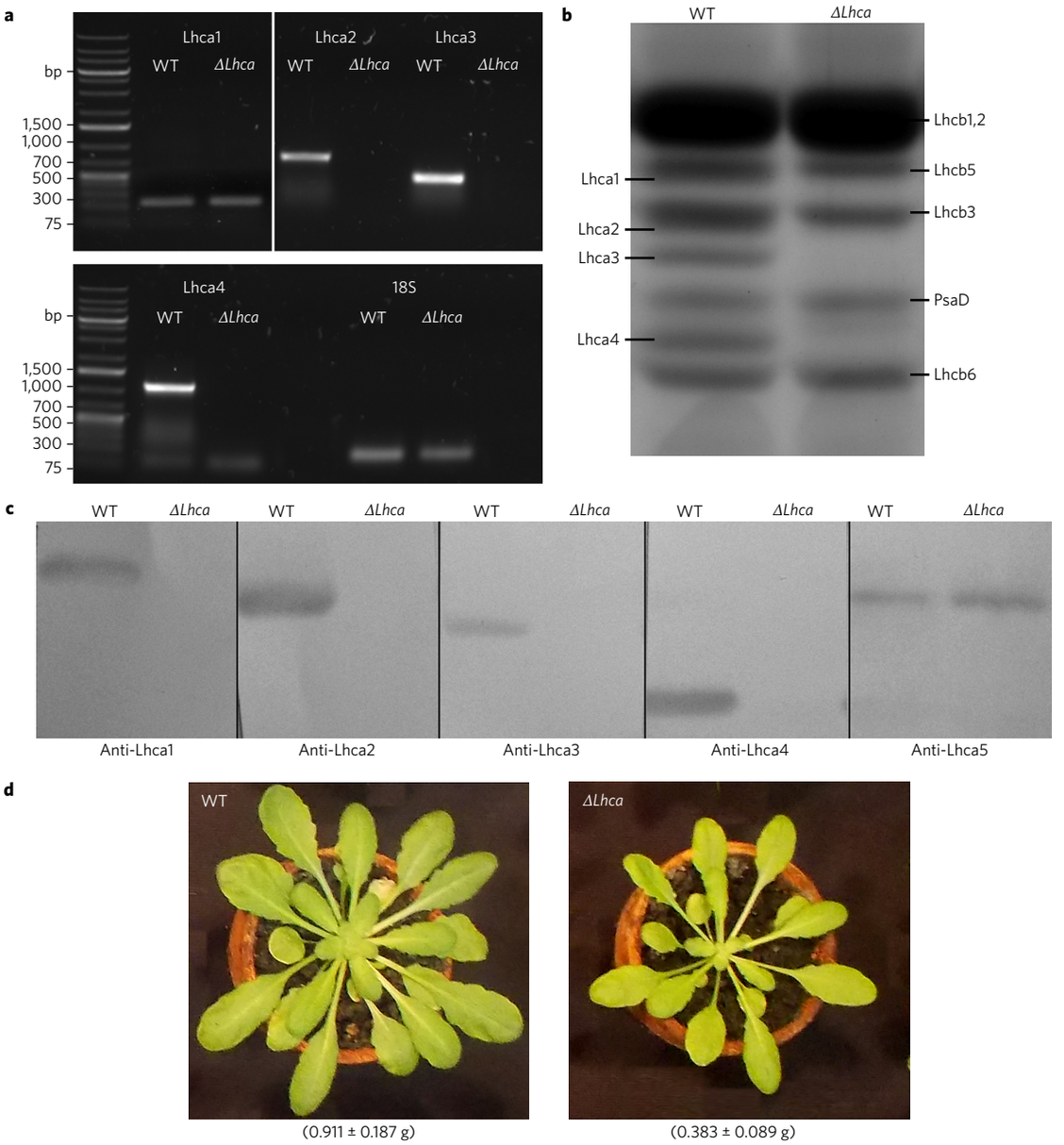

Figure 1 | Genetic and biochemical characterization of the *ΔLhca* mutant. a, RT–PCR verification of gene-specific transcripts. See Methods for sequences of the oligonucleotides used. For each gene, RNA extracted from wild-type (WT) and *ΔLhca* leaves was subjected to reverse transcription (top panel). Amplification of the housekeeping rRNA 18S from the same RNAs was used as loading control (bottom panel). bp, base pairs of molecular weight marker. Expected sizes of the amplicons: Lhca1, 752 bp; Lhca2, 751 bp; Lhca3, 487 bp; Lhca4, 1,049 bp and 18S, 149 bp. **b**, SDS-PAGE analysis of wild-type and *ΔLhca* thylakoid proteins. In each lane 15 μg of Chl was loaded. Selected apoprotein bands are marked. **c**, Immunoblot analysis. Thylakoid samples from the wild type and mutant were probed with antibodies specific for the different Lhca proteins. **d**, Phenotype of wild-type and mutant plants grown on soil for 4 weeks under constant, standard conditions (150 μmol photons m^{-2} s^{-1}, 23 °C, 8 h/16 h day/night). Fresh weight recovery is reported in grams, resulting from the average of five independent biological replicates. Standard deviation is reported.

than Lhca2 was also missing, which corresponded to Lhca1 as revealed by immunoblotting (Fig. 1c), implying that the *ΔLhca* mutant was devoid of all four Lhca subunits. This is consistent with Lhca4 being needed for the stable association of Lhca1 with the core[28,29]. Immunotitration showed that Lhca5 protein was present in higher amounts in *ΔLhca* (+50%) than in the wild type (Fig. 1c), consistent with a previous report on the Lhca4 single mutant[28]. To assess whether in *ΔLhca* Lhca5 was present in stoichiometric amounts with PSI, as in the case of Lhca1–Lhca4 proteins in the wild type, the 20–30 kDa region including LHC proteins was analysed by 2D SDS–PAGE. The separation allowed for identification of individual *Lhc* gene products as distinct spots (Supplementary Fig. 2), showing the complete lack of Lhca1–4 subunits in *ΔLhca*. Western blotting analysis on 2D maps localized Lhca5 in a region devoid of Coomassie-stained protein spots both in the wild type and in *ΔLhca* (Supplementary Fig. 2), implying Lhca5 was accumulated in sub-stoichiometric levels in both genotypes.

When grown in a climate chamber for 4 weeks under controlled conditions (150 μmol photons m^{-2} s^{-1}, 23 °C, 8 h/16 h, day/night), *ΔLhca* plants grew significantly less than wild-type plants with an almost 60% reduction in fresh weight (Fig. 1) indicating a significant reduced plant fitness in the absence of LHCI antenna proteins.

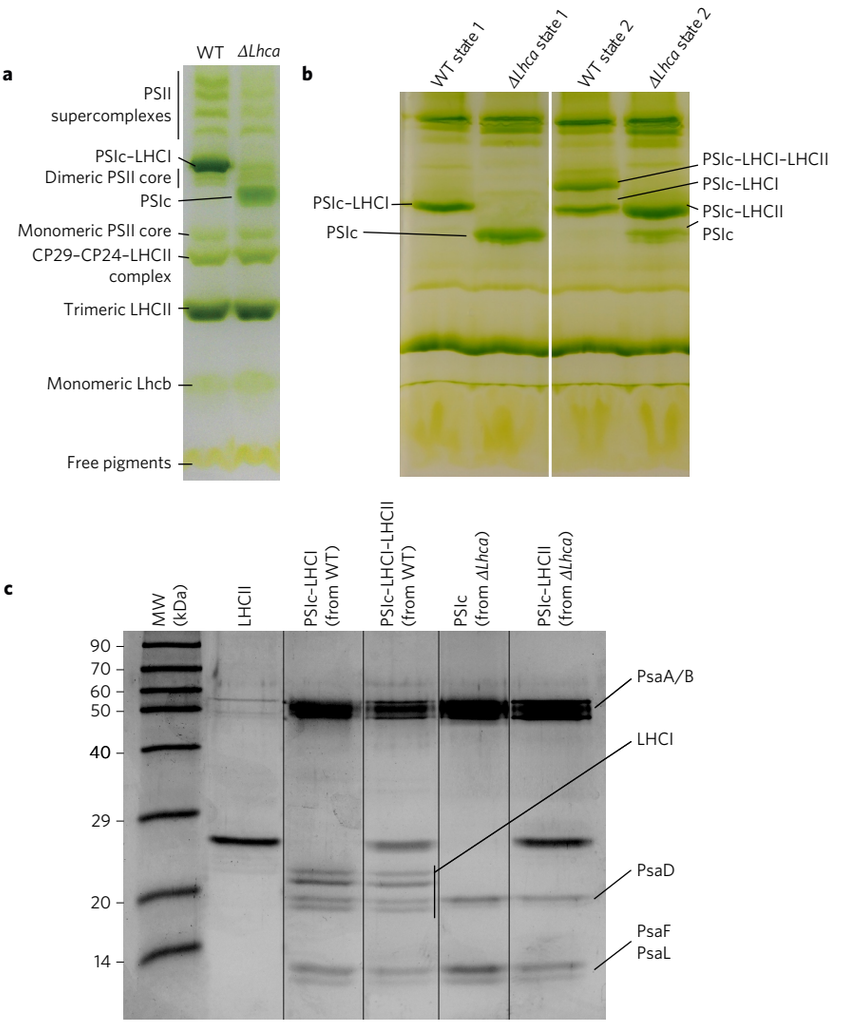

Figure 2 | Biochemical characterization of pigment–protein complexes. a, Thylakoid pigment–protein complexes were separated by non-denaturing Deriphat-PAGE on solubilization with 0.8% α-DM (n-Dodecyl α-D-maltoside). **b**, Native PAGE of thylakoid proteins isolated from wild-type and *ΔLhca* plants acclimated either to PSI or PSII light for 45 min before membrane isolation. A PSIc–LHCI–LHCII supercomplex is visible only in wild-type leaves treated with PSII light (state 2), whereas in the corresponding mutant sample a complex with higher apparent mass than PSI core represents the PSIc–LHCII supercomplex. These complexes are absent in samples from leaves treated with PSI light (state 1). **c**, SDS-PAGE of LHCII, PSIc, PSIc–LHCI, PSIc–LHCII and PSIc–LHCI–LHCII complexes eluted from native PAGE. The main protein components of each fraction and the molecular mass (MW) in kDa are indicated.

Photosynthetic function was investigated in intact leaves by measuring both PSII and PSI activities. Maximal quantum efficiency of PSII (F_v/F_m) was slightly higher in *ΔLhca* vs. wild-type plants (Supplementary Table 1). The time required to reach two-thirds of the maximum Chl fluorescence rise ($t_{2/3}$) in 3-(3,4-dichlorophenyl)-1, 1-dimethylurea (DCMU)-treated leaves, a measure of the functional antenna size of PSII (ref. 30), was slightly but significantly lower in the mutant (Supplementary Table 1). The functional antenna size of PSI was estimated from the ratio of P700 oxidation in limiting vs. high light exposure, obtaining a reduced antenna size in the *ΔLhca* mutant, thus confirming that LHCI depletion did reduce the overall optical cross-section of PSI. *ΔLhca* plants grown under control light did not differ from wild-type plants for Chl content per leaf area. However, a significant increase in both Chl *a*/*b* and Car/Chl ratios was observed (Supplementary Table I).

Isolation of PSI supercomplexes. The organization of pigment-binding complexes was analysed by non-denaturing Clear Native PAGE[31] (Fig. 2), on solubilization of wild type and *ΔLhca* thylakoids with 0.8% dodecyl maltoside. Several green bands were resolved in the wild type: the PSII pigment–proteins migrated as multiple bands with different apparent masses, namely the PSII core and the antenna sub-complexes, including the Lhcb4–Lhcb6–LHCII-M complex, the trimeric LHCII and the monomeric LHCBs. Instead, the PSI supercomplex was found as a single major band in the middle section of the gel. Green bands, with apparent mass higher than PSI–LHCI, contained undissociated PSII supercomplexes with different LHCII complements[29]. Densitometric analysis of the green band profile showed very similar distribution of pigment–protein complexes of PSII, implying that the lack of LHCI polypeptides had no effects on the relative abundance of PSII subunits. The major difference detected was the lack of PSIc–LHCI supercomplex and the appearance of a green band with lower apparent mass containing the PSIc in *ΔLhca*. To fully identify these green complexes, green bands in the region of PSI were excised and further analysed: depletion of Lhca1–4 polypeptides and the presence of PSI subunits PsaA/PsaB and PsaD (Fig. 2) confirmed that *ΔLhca* plants only accumulated the PSI core moiety of the supercomplex. Wild-type and *ΔLhca* plants were then treated with either orange (650 nm) or far red (735 nm) light, thereby preferentially exciting

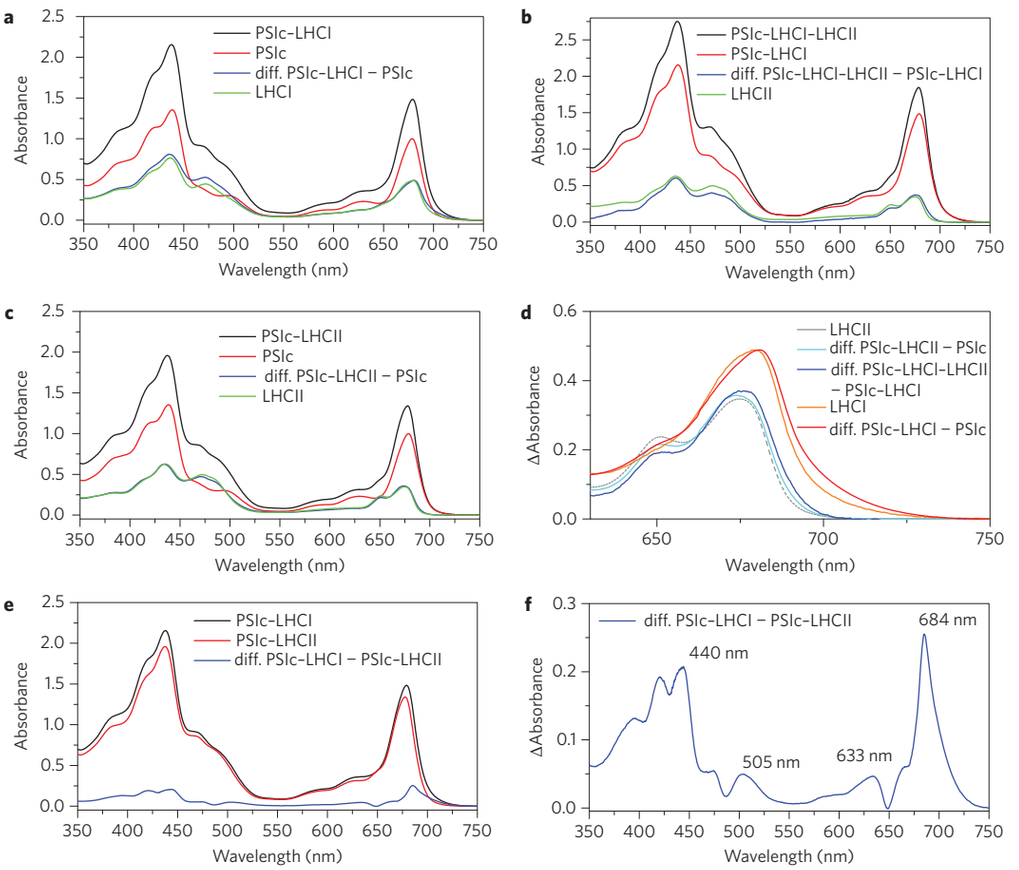

Figure 3 | Absorption spectra of PSI complexes. a–c, Spectra were normalized in order to have the same P700 content, as indicated in the Methods section. The difference (diff.) spectra reported in blue were obtained by subtracting PSIc from PSIc–LHCI (**a**), PSIc from PSIc–LHCII (**c**) or PSIc–LHCI from PSIc–LHCI–LHCII (**b**) and compared with LHCI (**a**) or LHCII (**b**,**c**), in both cases reported in green. **d**, The difference spectra in the Qy spectral region reported in **a**–**c** are compared with the absorption spectra of one LHCII trimer or one LHCI complex (four Lhca proteins). **e**, Comparison of PSIc–LHCI and PSIc–LHCII. The difference spectrum obtained by subtracting PSIc–LHCII from PSIc–LHCI is reported in **e** and in **f** in blue.

PSII or PSI (ref. 20). This results in LHCII phosphorylation and binding to PSI (state 2) or LHCII dephosphorylation and binding to PSII (state 1) respectively[13,20,32]. Purified thylakoid membranes were solubilized[26] and fractionated by Deriphat-PAGE[10], which allowed differential migration based on their apparent molecular size. The PSI supercomplexes of wild-type thylakoids from far-red-light-treated plants (state 1) migrated as a single major green band (Fig. 2)[29]. Fractionation of thylakoids from *ΔLhca* yielded similar results but the mobility of the PSI bands was higher, consistent with the lack of the LHCI moiety. It is important to notice that the abundance of the upper band in *ΔLhca* was strongly increased on treatment with orange light (state 2). PSI supercomplex bands were eluted from the acrylamide matrix and analysed. Western blot analysis (Supplementary Fig. 3) confirmed that the faster band in the wild type contained the PSIc–LHCI supercomplex and the slower band contained the PSIc–LHCI–LHCII supercomplex. The upper and lower bands from the *ΔLhca* sample consisted of PSIc and PSIc–LHCII complexes respectively. Even if Lhca5 was still present in *ΔLhca* thyalkoids, no traces of this subunit could be detected in any PSI complexes (Supplementary Fig. 3). The Chl *a*/*b* ratios of the isolated complexes are reported in Supplementary Table 2. The Chl *b* content per P700 was found to be highest in PSIc–LHCI–LHCII, decreasing in PSIc–LHCII and PSIc–LHCI in that order. This is in good agreement with the higher Chl *b* content in LHCII compared with LHCI (refs 1,2,33,34). As expected, only minor traces of Chl *b* were found in PSIc because of the absence of any LHC subunit in this complex. Interestingly, the Chl *a*/*b* ratios measured for PSIc–LHCII and PSIc–LHCI–LHCII were consistent with the addition of a single LHCII trimer per reaction centre, as previously reported[25,26].

Absorption properties of PSI supercomplexes. Differences in absorption cross-section of PSI on binding of LHCI and/or LHCII to PSIc were investigated by recording the absorption spectra of the PSIc, PSIc–LHCI, PSIc–LHCI–LHCII and PSIc–LHCII supercomplexes in the visible spectral region. The absorption spectra were normalized to be representative of PSI complexes with the same P700 content. This normalization was performed by taking into account the amount of Chl *a* and *b* bound by each complex (Supplementary Table 2), the ratio between the excitation coefficients of Chl *b*/*a* (0.7 as described in ref. 35), the Chls bound by PSIc (95–98 Chl *a*), LHCI (57–61) and LHCII (42), and finally the stoichiometry of PSIc/LHCI (1:4) and PSIc/LHCII (1:1)[1,2,7,8,33,34,36] (Fig. 3). Essentially the same absorption spectra and difference spectra were obtained by using the data reported by Mazor and coworkers[2], or Qin and coworkers[1]. The PSIc–LHCI minus PSIc difference spectrum peaked at 680 nm and had a low Chl *b* contribution (650 nm), closely mirroring the absorption spectrum of LHCI preparations[7] (Fig. 3a). Similarly, the PSIc–LHCI–LHCII minus PSIc–LHCI and PSIc–LHCII minus PSIc difference spectra closely resembled the absorption of trimeric LHCII, including a 676 nm peak and an enhanced 650 nm Chl *b* feature (Fig. 3b–d). It is worth noting that the difference spectra, which we tentatively attribute to PSI-connected

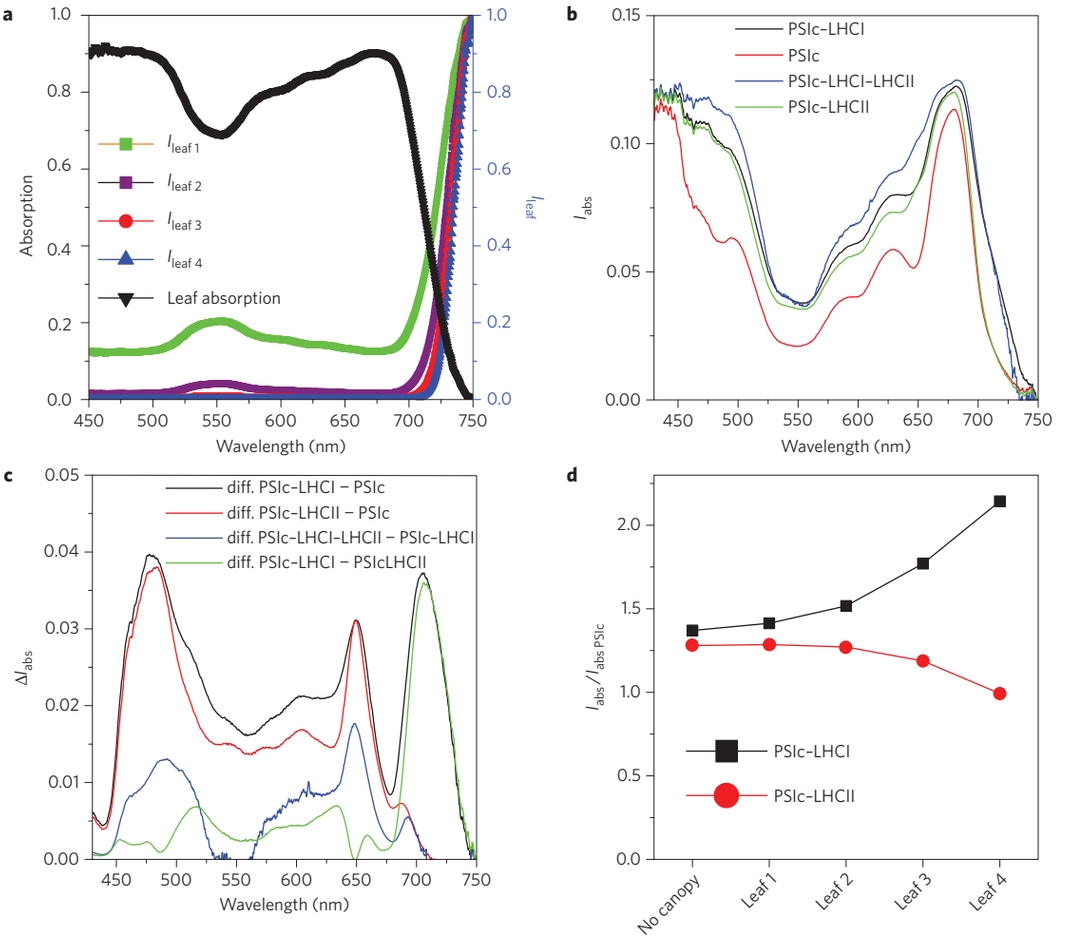

Figure 4 | Role of red-shifted absorption forms under canopy conditions. a, Leaf absorption in the visible region and wavelength dependence of the intensity of the light transmitted by four leaves (I_{leaf}) with each leaf shading the subsequent leaf. **b**, Light intensity absorbed (I_{abs}) by PSI complexes calculated considering the shading effect of one leaf. **c**, Differences in I_{abs} at the difference wavelengths calculated by subtracting the contribution of PSIc from PSIc–LHCI (black), from PSIc–LHCII (red), subtracting PSIc–LHCI from PSIc–LHCI–LHCII (blue) or subtracting PSIc–LHCII from PSIc–LHCI (green). **d**, Contribution of LHCI or LHCII to the capacity of PSIc to absorb light in different canopy conditions with shading of zero to four leaves. $I_{abs}/I_{abs\ PSIc}$ indicates the ratio between the light intensity absorbed by PSI-LHCI or PSI-LHCII and the light intensity absorbed by PSIc alone.

LHCII, closely matched the absorption spectrum of one LHCII trimer in both shape and amplitude based on the total number of Chls bound (24 Chl *a* and 18 Chl *b*) (Fig. 3d). We conclude that a single LHCII trimer was bound to either PSIc–LHCI or PSIc yielding PSIc–LHCI–LHCII and PSIc–LHCII supercomplexes respectively. When subtracting PSIc–LHCII from PSIc–LHCI (Fig. 3e), a positive difference spectrum was obtained throughout the visible range, as expected due to the different chlorophyll content bound by LHCI (57–61) and LHCII (42) (Fig. 3f). In particular, the difference spectrum was characterized by peaks at 420, 440, 633 and 684 nm, which are typical of Chl *a* bound to LHC proteins. Absorption forms above 700 nm were also detected, corresponding to the peculiar 'red forms' of LHCI (ref. 37). In addition, a small peak at 505 nm was evident, which is likely to be related to increased carotenoid content in LHCI compared with LHCII (13 vs. 12)[1,33]. To estimate the absorption cross-section in the different samples, the areas below the absorption spectra were computed and are reported in Supplementary Table 3; the values of each absorption cross-section were normalized to that of PSIc. The addition of LHCI or LHCII to PSIc caused an increase in cross-section of 67% and 51% respectively, and the absorption cross-section was more than doubled compared to PSIc when both LHCI and LHCII were bound to PSIc (PSIc–LHCI–LHCII supercomplex).

LHCI subunits allow PSI complexes to absorb light energy at wavelengths longer than 700 nm whose relative weight is enriched deeper in the canopy[38]. The absorption spectrum of a single leaf[39] was used to calculate the intensity of light transmitted through zero to four leaves (Fig. 4a), thus mimicking the intensity of the light absorbed by PSI complexes at different wavelengths (Fig. 4b) under canopy conditions. The presence of LHCI or LHCII bound to PSIc caused a strong difference in light absorption above 700 nm (Fig. 4c). When considering the cumulative effect of up to four leaves, the presence of LHCI becomes increasingly important, enhancing the amplitude of the absorption contribution by red forms at >700 nm by a factor of two or more compared with PSIc–LHCII (Fig. 4d).

Excitation energy transfer properties of PSI supercomplexes. The excitation energy transfer dynamics of LHCI vs. LHCII bound to PSIc were investigated using time-resolved fluorescence analysis. The kinetics of fluorescence decay on ultrafast femtosecond excitation of the Chls at either 440 or 475 nm were acquired by streak camera detection in the 500–900 nm range, as previously described[25,40–42]. The different excitation wavelengths were chosen to preferentially excite Chl *a* (440 nm) bound to both core complexes and antenna proteins, or Chl *b* (475 nm) bound to LHCI/LHCII only (Supplementary Table 4). The fraction of the

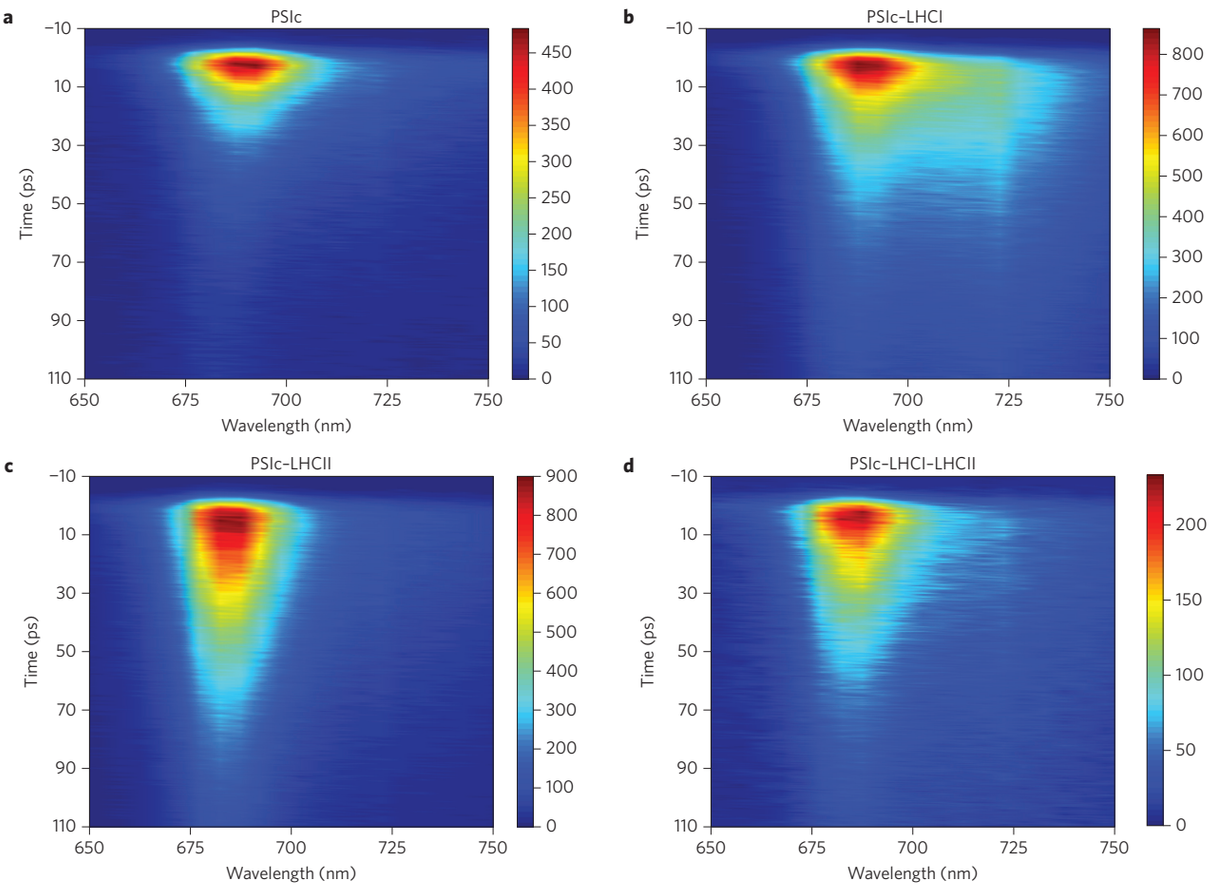

Figure 5 | Time-resolved fluorescence maps of different supercomplexes. a–d, Maps were obtained for the supercomplexes PSIc (**a**), PSIc–LHCI (**b**), PSIc–LHCII (**c**) and PSIc–LHCI–LHCII (**d**). Wavelength (nm) and time (ps) dependence of fluorescence emission are indicated on the *x* and *y* axes, respectively. The colour scale from blue to red represents fluorescence intensity from the lowest (blue) to the highest (red) intensity. The excitation wavelength was 475 nm.

PSI core excited at 440 or 475 nm in PSI–LHCI and PSI–LHCII was similar (65–70% on excitation at 440 nm and 38–39% on excitation at 475 nm), allowing a direct comparison of LHCI or LHCII contributions to the PSI complex excitation energy transfer (Supplementary Table 4). The fluorescence decay maps, as a function of wavelength and time, are reported in Fig. 5 (excitation at 475 nm) and Supplementary Fig. 5 (excitation at 440 nm). The main fluorescence peak was detected at ~688 nm in all the samples. In addition, a second peak was detected at ~725 nm, and can be attributed to the low energy emitting forms of LHCI (red forms) in both PSIc–LHCI and PSIc–LHCI–LHCII supercomplexes. To identify the decay components and their spectra (decay-associated spectra, DAS), the fluorescence decay kinetics in the 650–800 nm region were subjected to global analysis (Fig. 6 and Supplementary Fig. 7). Residues maps are reported for the different samples in Supplementary Figs 8 and 9 for excitation at 440 and 475 nm respectively. Fitting results at specific wavelengths are shown in Supplementary Fig. 10. Briefly, for each sample, the decay traces at the different wavelengths were fitted with multi-exponential functions, with the same decay constants being maintained through the entire spectral range. The amplitudes of the exponential functions, thus, form spectra associated to each decay constant (the DAS), as reported in Fig. 6. A fast DAS component with a lifetime between 3.8 and 8.8 ps was found to be present in all samples with positive/negative features. The presence of negative signal in the shortest DAS component of PSI was previously attributed to the excitation energy equilibration between bulk pigments and the low-energy forms[40–43]. Accordingly, the negative feature of the fastest DAS component was increased on preferential antenna excitation (475 nm) compared with 440 nm excitation, particularly in the presence of the red form containing LHCI. The predominant positive component in the shortest DAS, however, is mainly related to fluorescence decay rather than excitation energy transfer, likely to be from Chls in the core complex. In the case of PSIc, the main DAS obtained had a lifetime of 19 ps with a fluorescence emission peak at 692 nm. This 19–36.3 ps component was present in all complexes, and it has been previously associated with the bulk inner antenna Chls of PSIc (refs 40–43). Interestingly, in all samples with LHCII connected to a PSI core (PSIc–LHCI–LHCII and PSIc–LHCII), this DAS showed a slight blue shift to 687 nm and a significantly higher lifetime of 28–36 ps, independent of excitation wavelength. This suggests that the binding of LHCII to PSIc strongly contributed to the intermediate DAS (refs 25,26), most likely to be due to rapid equilibration of the energy absorbed by LHCII itself, with the strongest effect in the absence of LHCI (PSIc–LHCII complex). On excitation at 475 nm, the complexes containing LHC proteins (PSIc–LHCI, PSIc–LHCII and PSIc–LHCI–LHCII) were characterized by a major component with a relatively long lifetime between 58.3 and 68.2 ps, which was also detected on 440 nm excitation (61.3–72.8 ps), although with reduced amplitude (Supplementary Fig. 7). This long lifetime component has been previously associated with the outer LHCI antenna moiety in PSIc–LHCI as suggested by its dual emissions at 688 and 722 nm. In the case of the PSIc–LHCI–LHCII, the

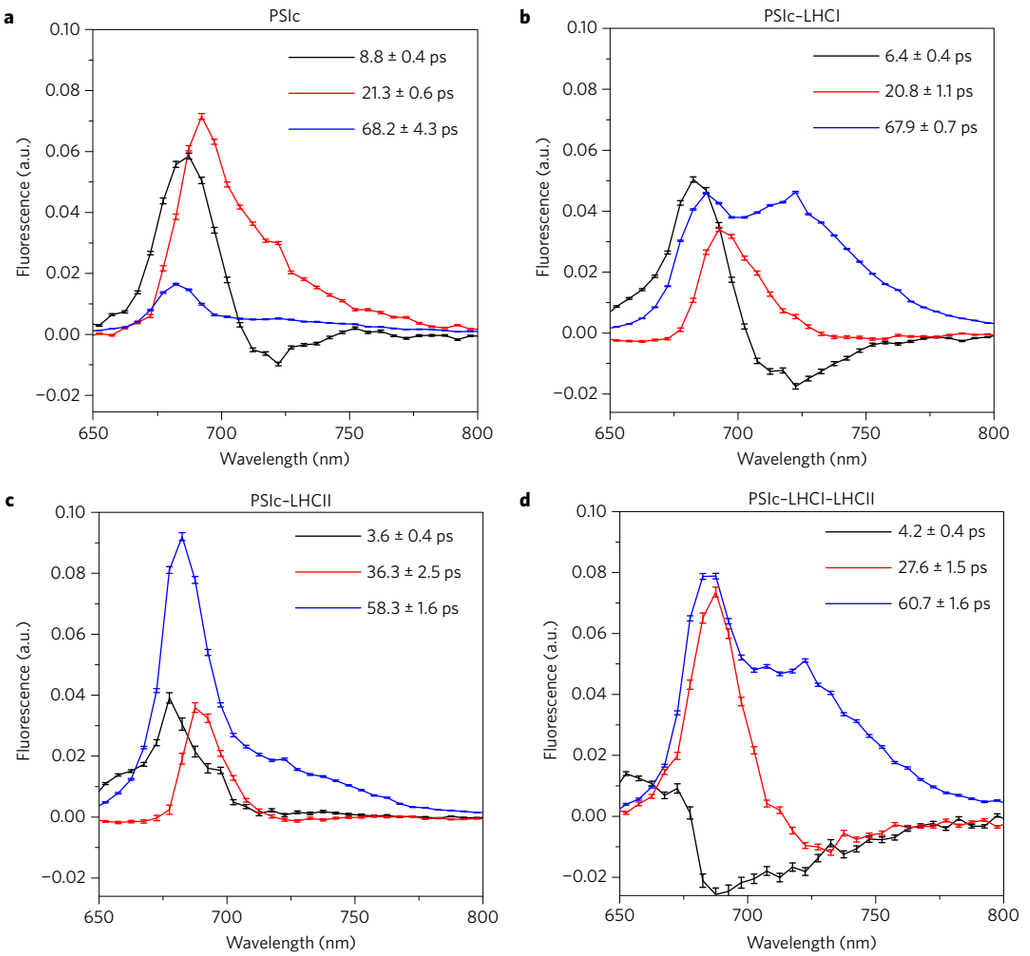

Figure 6 | Decay-associated spectra of PSI supercomplexes. a–d, The DAS were obtained for PSIc (**a**), PSIc–LHCI (**b**), PSIc–LHCII (**c**) and PSIc–LHCI–LHCII (**d**) from global analysis of the maps reported in Fig. 5. The excitation wavelength was 475 nm. The time constant associated with each DAS is indicated for each sample. Errors bars on DAS and time constants indicate the standard deviation.

weight of the 688 nm emission compared with the 722 nm emission was enhanced in the 60.7 ps DAS because of the LHCII contribution. In the case of the PSIc–LHCII, the long-lived DAS (58.3 ps) showed a reduced amplitude around 722 nm because of the lack of LHCI. Observation of this DAS component suggests that fast excitation energy transfer from LHCII to PSIc does occur, even in the absence of LHCI. A small 722 nm emission component with a 67.9 ps lifetime was detected in the PSIc decays, and was attributed to the red-shifted forms localized in the core complexes[40,42]. It is worth noting that this red-shifted component in PSIc can hardly be attributed to contamination from residual LHCI proteins, since this complex was purified from *ΔLhca* plants that lack the necessary encoding genes. To determine the influence of LHCI and LHCII on the excitation energy transfer to the PSI reaction centre, trapping times were estimated from the average fluorescence lifetimes of PSIc, PSIc–LHCI, PSIc–LHCII and PSIc–LHCI–LHCII. The results obtained are reported in Supplementary Table 5. The trapping time of PSIc was similar on 440 or 475 nm excitation, and binding of LHCI and/or LHCII significantly increased, in a similar way, the trapping time as a consequence of energy migration from the outer antenna proteins to the reaction centre. The calculation of the quantum efficiency of the different samples was performed based on previously reported methods[26,40,42] and yielded quantum yields higher than 98% in all samples. The spectral dependence of trapping time and quantum yield of PSI are shown in Fig. 7. An increased trapping time and reduced PSI quantum yield is evident in the 670–690 nm regions in the presence of LHCII or LHCI, and above 700 nm only in presence of LHCI. This result is consistent with the emission of LHCII at 680 nm, and of LHCI at both 680 and > 700 nm. Interestingly, at any emission wavelength, the quantum efficiency of PSI was always higher than 96%, indicating that the photochemical efficiency of PSI was not undermined when LHCI was substituted with LHCII as peripheral antenna moiety. Indeed, the PSIc–LHCII complex showed a reduction in the quantum yield of less than 0.01% in the 670–690 nm region compared with PSIc–LHCI.

Discussion

In this work we obtained a mutant with PSI complexes lacking LHCI complexes but with an increased association of LHCII. We therefore for the first time have been able to investigate the consequences of substituting LHCI by LHCII as an antenna system of PSI. The absence of LHCI subunits in the ΔLhca mutant induces an increase in LHCII binding to PSIc on state 2 induction, as a compensatory mechanism. The isolation of the PSIc–LHCII complex revealed the presence of a single LHCII trimer per PSI core based on carefully performed antenna cross-section measurements. The quantum efficiency of PSI in the presence of any combination of the LHC proteins investigated (LHCI, LHCII or LHCI plus LHCII

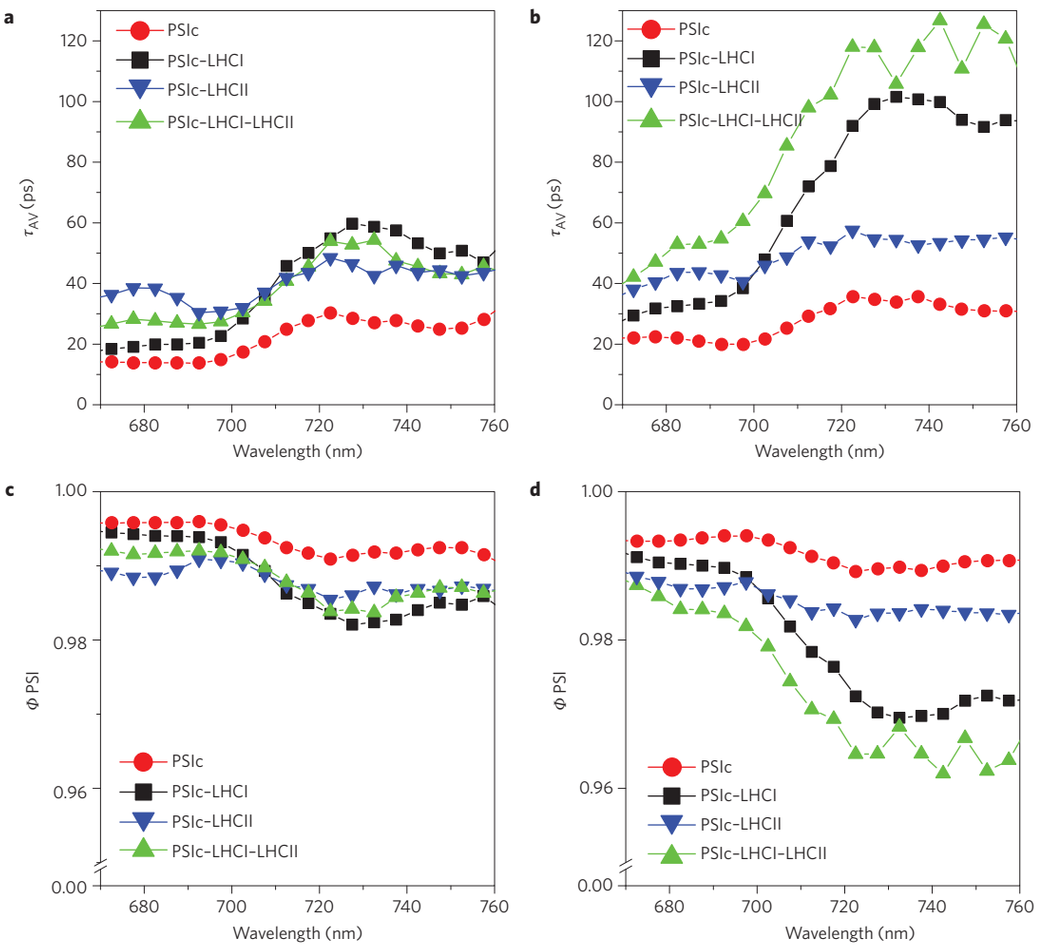

Figure 7 | Trapping time and quantum yield of PSI supercomplexes. a,b, Fluorescence average lifetime (τ_{AV}) was used to calculate the trapping time at the different wavelengths for PSIc, PSIc-LHCI, PSIc-LHCII and PSIc-LHCI-LHCII complexes upon excitation at 440 nm (**a**) and 475 nm (**b**). τ_{AV} was calculated using the time constants reported in Fig. 6 weighted by the amplitudes of the exponentials at each wavelength. **c,d**, Quantum yield (Φ) of PSI supercomplexes at each wavelength of emission, calculated as described in refs 25,26.

bound to the PSI core) was only slightly decreased compared with the bare PSI core and remained extremely high (>98%), in agreement with previous investigations of PSIc–LHCI vs. PSIc–LHCI–LHCII (refs 25,26,44). Here, we show that a PSIc–LHCII complex lacking LHCI is also characterized by very high quantum efficiency (Supplementary Table 5). LHCIs are thus not essential for excitation energy transfer from LHCII to PSIc, as demonstrated by the similar or even faster trapping time of PSIc–LHCII compared with PSIc–LHCI–LHCII (Supplementary Table 5). It is worth noting that a more evident reduction of trapping time would be expected in PSIc–LHCII, considering the reduced Chls content compared with PSIc–LHCI and PSIc–LHCI–LHCII: the discrepancy obtained could be ascribed to the very low amount of disconnected complexes present in PSIc–LHCII (<1%). Supplementary Fig. 6 indicates the presence of some disconnection in the PSIc–LHCII complex: on excitation at 475 nm, a very small population of PSIc and PSIc–LHCII still fluoresces on the nanosecond time scale, after more than 99% of the photoexcited population has already decayed. This small long-lived decay component was not resolved by global analysis because of its very low amplitude (<1%) but it can be ascribed to the presence of disconnected Chls or LHCIIs in PSIc and PSIc–LHCII samples, as revealed by 77 K fluorescence emission spectra (Supplementary Fig. 4). It should be noted that this long-lived component cannot be attributed to LHCI since the PSI samples were purified from *ΔLhca* plants and no traces of Lhca1-6 were detected in PSIc–LHCII (Supplementary Fig. 3). The detailed time-resolved fluorescence emission analysis presented here demonstrates that virtually all LHCII bound to PSI–LHCII in *ΔLhca* plants efficiently transfer energy to P700. It cannot be excluded, however, that the binding or energetic connection of some extra LHCII to PSI is impaired in *ΔLhca* plants; such an extra LHCII pool was indeed recently reported to be bound to PSI–LHCI in *A. thaliana* wild type, but was easily detached by digitonin treatment[45]. Our results clearly demonstrate that when LHCII was bound to PSI through digitonin-insensitive binding, the LHCI proteins were not essential for excitation energy transfer to the PSI reaction centre.

The main functional limitation of substituting LHCI by LHCII as an antenna system of PSI appears to be the reduction of the PSI absorption cross-section by 16% (Fig. 3 and Supplementary Table 3). Considering the 67% increase in PSI absorption cross-section on binding to LHCI, the contribution of each Lhca subunit can be roughly quantified at 16.5%. The substitution of the two Lhca1–4 and Lhca2–3 dimers by an LHCII trimer reduces the number of LHC proteins from four to three, and leads to the 16% reduction in absorption cross-section. The spectral form of the absorption loss upon substitution is evident in Fig. 3f. Reduced PSI excitation arising from the lower absorption cross-section of PSIc and PSIc–LHCII, compared with PSIc–LHCI or PSIc–LHCI–LHCII, has a consequence on the growth and wellness

of the *ΔLhca* mutant, as witnessed by the ~60% reduced growth reported in Fig. 1. Reduced fitness observed in the *ΔLhca* mutant is consistent with previous data reported for a mutant with antisense inhibition of the *Lhca4* gene only, resulting in reduction of LHCI proteins[46]. The reason why only LHCI adds four LHC proteins to PSI and LHCII binds as a trimer can be ascribed to the specific interactions involved in LHCI–PSIc binding, as in particular the Lhca1–PsaG, Lhca2–PsaJ, Lhca3–PsaA and Lhca4–PsaF interactions, which require specific charge pairing that is unlikely to be established by any LHCII monomer[2]. It is important to note that the substitution of LHCI by LHCII reduces the absorption at wavelengths above 700 nm (Fig. 4). When a plant grows under canopy conditions, the incident light is filtered by upper leaves, being enriched in far red light: in this conditions the presence of LHCI with its red forms is important to absorb at wavelengths above 700 nm, with a dramatic reduction of the intensity of the light absorbed by PSIc–LHCII compared with PSIc–LHCI on a filtering effect of only four leaves (Fig. 4). It should be considered that this effect is not only important under shaded canopy conditions but also within multicellular photosynthetic organisms that evolved red-shifted forms in their LHCI antenna moiety to fight competition by PSII antenna systems in the same organism or in others belonging to the same canopy.

Methods

Plant material and growth conditions. *Arabidopsis thaliana* T-DNA insertion mutant lines GT_5_2454 (N101690, insertion into the *Lhca* 2gene), SAIL_749_D03 (N876497, insertion into the *Lhca*3 gene) and SALK_118680C (N679009, insertion into the *Lhca4* gene) were obtained from the NASC collection. Plants were grown in a phytotron for 5 weeks at 150 μmol photons m^{-2} s^{-1} (Epistar 35 mil Chip High Power LED, warm white LEDE-P20B-DW, Wayjun Tech.), 23 °C, 70% humidity, 8 h/16 h of day/night. Homozygous plants were identified by immunoblot for the lack of the corresponding gene product. The *kolhca2 kolhca3 kolhca4* (*ΔLhca*) genotype was obtained by crossing single mutant plants and selecting progeny. For RT–PCR, total RNA was isolated from 4-week-old plants following the Trizol protocol. Reverse transcription was performed using M-MLV reverse transcriptase with the oligo (dT) primer. 18S ribosomal RNA was chosen as an endogenous control. The transcripts were amplified from 25 ng of cDNA as a template and 2.5 units of TaqDNA polymerase using the followings cycles: 94 °C for 30 s, annealing at 55 °C for 30 s, 72 °C for 30 s, followed by a final extension step at 72 °C for 1 min. The primers used were as follows: 5′-TGGGTTAAGGCTCAGGAATG-3′ and 5′-CAATTCCTCGAGCTTCTTGG-3′ for Lhca1 cDNA; 5′-TTCGGATTTGATCCTCTTGG-3′ and 5′-TTTATGCTCCGAATGACAATG-3′ for Lhca2 cDNA; 5′-CAAGGAGCCAACAGACCATT-3′ and 5′-TTCCCATAGATCCTGGGTTG-3′ for Lhca3 cDNA; 5′-CAGCCACAAAACTCGTTTCA-3′ and 5′-CATGGAGCTACAACGGTTCA-3′ for Lhca4 cDNA, and 5′-CAAATTTCTGCCCTATCAACTTTCGATGG-3′ and 5′-AATTTGCGCGCCTGCCTTCCTTT-3′ for 18S cDNA. To highlight the exponential phase, the amplification was stopped after 19, 23 and 27 cycles, and 5 μl for each gene was collected.

For excess light growth experiments, 2-week-old seedlings were transferred to either HL (1,000 μmol photons m^{-2} s^{-1}, 23 °C) or fluctuating light (alternations of 5 min at 150 μmol photons m^{-2} s^{-1} and 1 min at 1,000 μmol photons m^{-2} s^{-1}, 23 °C) during the 8 hour photoperiod. The growth rate was derived from the development of the rosette area by non-invasive image analysis and by measuring the fresh weight. All the growth trials were carried out using an LED light source (Epistar 35 mil Chip High Power LED, warm white LEDE-P20B-DW, Wayjun Tech.).

Isolation of PSI complexes. State 1 and state 2 were induced in the wild-type and mutant plants by exposure for 45 min to far red light (30 W incandescent bulbs filtered through a Lee Filters 027 Medium Red) or orange light (30 W warm white fluorescent lamps filtered through Lee Filters 105 Orange) respectively, as previously reported[20]. Thylakoid membranes were purified from treated leaves as described in previously[10] and solubilized by digitonin and α-dodecylmaltoside as reported[26]. Solubilized thylakoid membranes were loaded on Deriphat-PAGE native gel[31]. The bands corresponding to PSI-CORE (PSIc), PSI–LHCI (from now on named PSIc–LHCI), PSIc–LHCII and PSIc–LHCI–LHCII were eluted from acrylamide matrix using a solution with 10% glycerol, 10 mM HEPES pH 7.5 and 0.03% digitonin, protease inhibitors benzamidine (2 mM), PMSF (0.5 mM), ε-aminocaproic acid (5 mM). The experiments of state 1 and state 2 induction and purification of PSI supercomplexes were performed three times on independent biological material (at least 10 leaves for each genotype) obtaining reproducible results.

Pigment analysis. Pigments bound by the isolated PSI supercomplexes were extracted and analysed by fitting absorption spectra of pigment extracts fitted with chlorophyll and carotenoid absorption forms as previously described[47].

Absorption measurement. Absorption measurements of isolated PSI complexes were performed as described[47]. The spectra obtained were normalized to the same P700 content considering the Chl *a*/*b* ratio measured in the different samples, the different molar extinction coefficients of Chl *b* and Chl *a*, and the Chl/protein stoichiometry for PSIc, PSc–LHCI (refs 1,2) and LHCII (ref. 33). Absorption spectra were recorded for PSI supercomplexes purified in three different independent experiments obtaining reproducible results

Time-resolved fluorescence measurements. Time-resolved fluorescence measurements were performed using a femtosecond laser source and streak camera detection system, as described[40,48]. Briefly, samples were excited by ≅200 fs laser pulses at 440 or 475 nm, obtained from the second harmonic of a Ti:sapphire laser (Coherent Chamaleon Ultra II) and time-resolved fluorescent spectra were measured by a streak camera system (Hamamatsu C5680) with a time resolution of ≈3 ps. The laser power applied was 56 μW with a repetition rate of 80 MHz. Triplet-singlet annihilation could be excluded since no excitation power dependence of the decay kinetics was observed (Supplementary Fig. 11). Measurements were performed in an orthogonal geometry (beam waist in the focus of ~60 μm) and the sample was placed in a cooled cuvette at OD (absorbance) 0.06 cm^{-1}. The experiments for time-resolved fluorescence measurements were repeated three times on independent samples obtaining consistent results.

Global analysis. Global analysis of the time-resolved fluorescence data was performed using custom-coded Matlab software as previously described[49]. A confidence interval of 95% on amplitude and time constants was considered so that error bars could be calculated.

Photosystem II quantum yield and antenna size. The PSII quantum yield was determined as F_v/F_m, where F_m and F_v are respectively the maximum and variable fluorescence ($F_m - F_0$, where F_0 is the basal fluorescence of dark adapted samples) observed on exposure of intact leaf to a saturating pulse (6,000 μmol m^{-2} s^{-1}). Fluorescence measurements were performed with a DUAL PAM 100 (Walz) as previously described[30]. The PSII antenna size was measured following the kinetics of fluorescence emission in the millesecond time range upon illumination of DCMU-treated leaves as described[30].

P700 measurements. P700 measurements were performed using a time-resolved spectrophotometer (JTS-10 from BioLogic) following the decrease of absorption at 705 nm. For P700 measurements leaves were infiltrated with 50 μM DCMU, 50 μM dibromothymoquinone inhibiting linear and cyclic electron transport and 1 mM methyl-viologen to avoid limitation from the PSI electron acceptor. Maximum P700 oxidation per leaf surface was measured by absorption on illumination of leaves with an actinic orange light at 940 μmol m^{-2} s^{-1}). PSI antenna size was estimated from the ratio of P700 oxidation in limiting (12 μmol m^{-2} s^{-1}) vs. high light (940 μmol m^{-2} s^{-1})[50].

Received 29 January 2016; accepted 28 July 2016; published 26 August 2016

References

1. Qin, X., Suga, M., Kuang, T. & Shen, J. R. Photosynthesis. Structural basis for energy transfer pathways in the plant PSI-LHCI supercomplex. *Science* **348,** 989–995 (2015).
2. Mazor, Y., Borovikova, A. & Nelson, N. The structure of plant photosystem I super-complex at 2.8 Å resolution. *Elife* **4,** e07433 (2015).
3. Croce, R. & van Amerongen, H. Light-harvesting in photosystem I. *Photosynth. Res.* **116,** 153–166 (2013).
4. van Amerongen, H. & Croce, R. Light harvesting in photosystem II. *Photosynth. Res.* **116,** 251–263 (2013).
5. Jansson, S. A guide to the Lhc genes and their relatives in *Arabidopsis*. *Trends Plant Sci.* **4,** 236–240 (1999).
6. Ballottari, M., Girardon, J., Dall'Osto, L. & Bassi, R. Evolution and functional properties of Photosystem II light harvesting complexes in eukaryotes. *Biochim. Biophys. Acta* **1817,** 143–157 (2012).
7. Ballottari, M., Govoni, C., Caffarri, S. & Morosinotto, T. Stoichiometry of LHCI antenna polypeptides and characterization of gap and linker pigments in higher plants photosystem I. *Eur. J. Biochem.* **271,** 4659–4665 (2004).
8. Ben-Shem, A., Frolow, F. & Nelson, N. Crystal structure of plant photosystem I. *Nature* **426,** 630–635 (2003).
9. Amunts, A., Toporik, H., Borovikova, A. & Nelson, N. Structure determination and improved model of plant photosystem I. *J. Biol. Chem.* **285,** 3478–3486 (2010).
10. Ballottari, M., Dall'Osto, L., Morosinotto, T. & Bassi, R. Contrasting behavior of higher plant photosystem I and II antenna systems during acclimation. *J. Biol. Chem.* **282,** 8947–8958 (2007).

11. Williams, W. P. & Salamon, Z. Enhancement studies on algae and isolated chloroplasts. Part I.: Variability of photosynthetic enhancement in *Chlorella pyrenoidosa*. *Biochim. Biophys. Acta.* **430,** 282–299 (1976).
12. Hodges, M. & Barber, J. State 1-state 2 transitions in a unicellular green algae: analysis of in vivo chlorophyll fluorescence induction curves in the presence of 3-(3,4-dichlorophenyl)-1, 1-dimethylurea (DCMU). *Plant Physiol.* **72,** 1119–1122 (1983).
13. Wollman, F. A. State transitions reveal the dynamics and flexibility of the photosynthetic apparatus. *EMBO J.* **20,** 3623–3630 (2001).
14. Allen, J. F. Botany. State transitions–a question of balance. *Science* **299,** 1530–1532 (2003).
15. Grieco, M., Suorsa, M., Jajoo, A., Tikkanen, M. & Aro, E. M. Light-harvesting II antenna trimers connect energetically the entire photosynthetic machinery – including both photosystems II and I. *Biochim. Biophys. Acta* **1847,** 607–619 (2015).
16. Goldschmidt-Clermont, M. & Bassi, R. Sharing light between two photosystems: mechanism of state transitions. *Curr. Opin. Plant Biol.* **25,** 71–78 (2015).
17. Wientjes, E., Drop, B., Kouřil, R., Boekema, E. J. & Croce, R. During state 1 to state 2 transition in *Arabidopsis thaliana*, the photosystem II supercomplex gets phosphorylated but does not disassemble. *J. Biol. Chem.* **288,** 32821–6 (2013).
18. Bellafiore, S., Barneche, F., Peltier, G. & Rochaix, J. D. State transitions and light adaptation require chloroplast thylakoid protein kinase STN7. *Nature* **433,** 892–895 (2005).
19. Depège, N., Bellafiore, S. & Rochaix, J. D. Role of chloroplast protein kinase Stt7 in LHCII phosphorylation and state transition in *Chlamydomonas*. *Science* **299,** 1572–1575 (2003).
20. Pesaresi, P. *et al. Arabidopsis* STN7 kinase provides a link between short- and long-term photosynthetic acclimation. *Plant Cell* **21,** 2402–2423 (2009).
21. Pesaresi, P. *et al.* Optimizing photosynthesis under fluctuating light: the role of the *Arabidopsis* STN7 kinase. *Plant Signal. Behav.* **5,** 21–25 (2010).
22. Rochaix, J. D. *et al.* Protein kinases and phosphatases involved in the acclimation of the photosynthetic apparatus to a changing light environment. *Philos. Trans. R. Soc. Lond. B* **367,** 3466–3474 (2012).
23. Pribil, M., Pesaresi, P., Hertle, A., Barbato, R. & Leister, D. Role of plastid protein phosphatase TAP38 in LHCII dephosphorylation and thylakoid electron flow. *PLoS Biol.* **8,** e1000288 (2010).
24. Shapiguzov, A. *et al.* The PPH1 phosphatase is specifically involved in LHCII dephosphorylation and state transitions in *Arabidopsis*. *Proc. Natl Acad. Sci. USA* **107,** 4782–4787 (2010).
25. Wientjes, E., van Amerongen, H. & Croce, R. LHCII is an antenna of both photosystems after long-term acclimation. *Biochim. Biophys. Acta* **1827,** 420–426 (2013).
26. Galka, P. *et al.* Functional analyses of the plant photosystem I-light-harvesting complex II supercomplex reveal that light-harvesting complex II loosely bound to photosystem II is a very efficient antenna for photosystem I in state II. *Plant Cell* **24,** 2963–2978 (2012).
27. Akhtar, P. *et al.* Excitation energy transfer between light-harvesting complex II and photosystem I in reconstituted membranes. *Biochim. Biophys. Acta* **1857,** 462–472 (2016).
28. Wientjes, E., Oostergetel, G. T., Jansson, S., Boekema, E. J. & Croce, R. The role of Lhca complexes in the supramolecular organization of higher plant photosystem I. *J. Biol. Chem.* **284,** 7803–7810 (2009).
29. Morosinotto, T., Ballottari, M., Klimmek, F., Jansson, S. & Bassi, R. The association of the antenna system to photosystem I in higher plants. Cooperative interactions stabilize the supramolecular complex and enhance red-shifted spectral forms. *J. Biol. Chem.* **280,** 31050–31058 (2005).
30. Malkin, S., Armond, P. A., Mooney, H. A. & Fork, D. C. Photosystem II photosynthetic unit sizes from fluorescence induction in leaves: correlation to photosynthetic capacity. *Plant Physiol.* **67,** 570–579 (1981).
31. Järvi, S., Suorsa, M., Paakkarinen, V. & Aro, E. M. Optimized native gel systems for separation of thylakoid protein complexes: novel super- and mega-complexes. *Biochem. J.* **439,** 207–214 (2011).
32. Allen, J. F. Plastoquinone redox control of chloroplast thylakoid protein phosphorylation and distribution of excitation energy between photosystems: discovery, background, implications. *Photosynth. Res.* **73,** 139–148 (2002).
33. Liu, Z. *et al.* Crystal structure of spinach major light-harvesting complex at 2.72 A resolution. *Nature* **428,** 287–292 (2004).
34. Standfuss, J., Terwisscha van Scheltinga, A. C., Lamborghini, M. & Kühlbrandt, W. Mechanisms of photoprotection and nonphotochemical quenching in pea light-harvesting complex at 2.5 A resolution. *EMBO J.* **24,** 919–928 (2005).
35. Bassi, R., Croce, R., Cugini, D. & Sandonà, D. Mutational analysis of a higher plant antenna protein provides identification of chromophores bound into multiple sites. *Proc. Natl Acad. Sci. USA* **96,** 10056–10061 (1999).
36. Kouril, R. *et al.* Structural characterization of a complex of photosystem I and light-harvesting complex II of *Arabidopsis thaliana*. *Biochemistry* **44,** 10935–10940 (2005).
37. Morosinotto, T., Breton, J., Bassi, R. & Croce, R. The nature of a chlorophyll ligand in Lhca proteins determines the far red fluorescence emission typical of photosystem I. *J. Biol. Chem.* **278,** 49223–49229 (2003).
38. Rivadossi, A., Zucchelli, G., Garlaschi, F. M. & Jennings, R. C. The importance of PSI chlorophyll red forms in light-harvesting by leaves. *Photosynt. Res.* **60,** 209–215 (1999).
39. Laisk, A., Oja, V., Eichelmann, H. & Dall'Osto, L. Action spectra of photosystems II and I and quantum yield of photosynthesis in leaves in state 1. *Biochim. Biophys. Acta* **1837,** 315–325 (2014).
40. Ballottari, M. *et al.* Regulation of photosystem I light harvesting by zeaxanthin. *Proc. Natl Acad. Sci. USA* **111,** E2431–E2438 (2014).
41. Gobets, B. *et al.* Time-resolved fluorescence emission measurements of photosystem I particles of various cyanobacteria: a unified compartmental model. *Biophys. J.* **81,** 407–424 (2001).
42. Wientjes, E., van Stokkum, I. H., van Amerongen, H. & Croce, R. The role of the individual Lhcas in photosystem I excitation energy trapping. *Biophys. J.* **101,** 745–754 (2011).
43. Slavov, C., Ballottari, M., Morosinotto, T., Bassi, R. & Holzwarth, A. R. Trap-limited charge separation kinetics in higher plant photosystem I complexes. *Biophys. J.* **94,** 3601–3612 (2008).
44. Jennings, R. C., Zucchelli, G., Croce, R. & Garlaschi, F. M. The photochemical trapping rate from red spectral states in PSI-LHCI is determined by thermal activation of energy transfer to bulk chlorophylls. *Biochim. Biophys. Acta* **1557,** 91–98 (2003).
45. Benson, S. *et al.* An intact light harvesting complex I antenna system is required for complete state transitions in *Arabidopsis*. *Nat. Plants* **1,** 15176 (2015).
46. Ganeteg, U., Külheim, C., Andersson, J. & Jansson, S. Is each light-harvesting complex protein important for plant fitness? *Plant Physiol.* **134,** 502–509 (2004).
47. Ballottari, M., Mozzo, M., Croce, R., Morosinotto, T. & Bassi, R. Occupancy and functional architecture of the pigment binding sites of photosystem II antenna complex Lhcb5. *J. Biol. Chem.* **284,** 8103–8113 (2009).
48. Cesaratto, A. *et al.* Analysis of cadmium-based pigments with time-resolved photoluminescence. *Anal. Methods* **6,** 130–138 (2014).
49. van Stokkum, I. H., Larsen, D. S. & van Grondelle, R. Global and target analysis of time-resolved spectra. *Biochim. Biophys. Acta* **1657,** 82–104 (2004).
50. Bonente, G., Pippa, S., Castellano, S., Bassi, R. & Ballottari, M. Acclimation of *Chlamydomonas reinhardtii* to different growth irradiances. *J. Biol. Chem.* **287,** 5833–5847 (2012).

Acknowledgements

The work was financed by the Italian Ministry of Agriculture, Food and Forestry (MIPAAF) project HYDROBIO and by the Marie Curie Actions Initial Training Networks ACCLIPHOT (PITN-GA-2012-316427) and S2B (675006–SE2B) to R.B. G.C. acknowledges support from the European Research Council Advanced Grant STRATUS (ERC-2011-AdG No. 291198).

Author contributions

M.Ba., L.D. and R.B. conceived the work and designed the experiments. M.Br. and L.D. performed all the experiments for the isolation of the *ΔLhca* mutant, its physiological and biochemical characterization and purification of PSI complexes. M.Ba. performed all the experiments for the spectroscopic characterization of PSI complexes. C.D. and G.C. coordinated the time-resolved fluorescence analysis experiments. I.B., M.J.P.A. and C.D. contributed to the time-resolved fluorescence analysis experiments. I.B., M.J.P.A., D.V., G.C., M.Ba. and C.D. analysed the fluorescence decay results by global analysis. All of the authors contributed to writing the manuscript. All of the authors discussed the results and commented on the manuscript.

Additional information

Supplementary information is available for this paper. Reprints and permissions information is available at www.nature.com/reprints. Correspondence and requests for materials should be addressed to R.B.

Competing interests

The authors declare no competing financial interests.

DOI: 10.1038/NPLANTS.2016.131

Supplementary Table 1. Pigment content and PSII/PSI functionality, measured on wild type and *ΔLhca* leaves. Chl *a*/Chl *b* and carotenoid/chlorophyll ratios in WT and *ΔLhca* leaves are reported in the first two columns. PSII quantum yield is reported as Fv/Fm; the maximum P700 oxidation per leaf surface is reported as maximum of absorption at 705 nm ($P700^{+}_{MAX}$) measured using an actinic light at 940 µmol m^{-2} s^{-1} upon leaves treatment with DCMU, DBMIB and methyl-viologen. PSII antenna size is reported as the reciprocal of the time required to reach the two third of maximum fluorescence emission upon illumination of DCMU treated leaves with limiting light (12 µmol m^{-2} s^{-1}). PSI antenna size was estimated from the ratio of the value of $P700^{+}$ measured upon illumination of DCMU, DBMIB and methyl-viologen treated leaves with either 12 ($P700^{+}_{12}$) or 940 ($P700^{+}_{940}$) µmol m^{-2} s^{-1} . Data are expressed as mean ± SD (n > 5), and significantly different values (Student's *t* test, P < 0.05) with respect to the wild type are marked with an asterisk. a.u., arbitrary units.

	Chl a/b	**Car / Chl**	**F_v / F_m**	**$P700^{+}_{MAX}$ (705 nm, a.u.)**	**PSII antenna size ($\tau_{2/3}^{-1}$) (· 10^3, ms^{-1})**	**$P700^{+}_{12}$ / $P700^{+}_{940}$ (705 nm)**
WT	2.85 ± 0.04	0.27 ± 0.01	0.79 ± 0.01	100 ± 7	3.33 ± 0.22	0.43 ± 0.08
ΔLhca	3.16 ± 0.13 *	0.30 ± 0.01 *	0.82 ± 0.01 *	121 ± 9 *	2.89 ± 0.37 *	0.29 ± 0.05 *

Supplementary Table 2: **Pigment binding properties of PSI complexes.** Chlorophyll a/b ratio (Chl a/b) and the Chlorophyll/Carotenoid ratio (Chl/Car) was determined by fitting the absorption spectra of pigment extracts with chlorophyll and carotenoid absorption forms as described in [1].

	Chl a/b	Chl/Car
PSIc-LHCI	7.06	4.57
PScI-LHCI-LHCII	5.44	3.99
PSIc	28.83	4.75
PSIc-LHCII	5.65	5.01

Supplementary Table 3: **Absorption cross section of PSI complexes**. Absorption (Abs) areas were calculated as indicated in the Methods section and normalized to 100% in the case of PSIc. Changes in absorption area (ΔArea) are reported with standard deviation. PSIc, PSI core complex.

	Area Abs (%)	**stdev**
PSIc	100%	0.50%
PSIc-LHCI	167%	2.71%
PSIc-LHCII	151%	0.31%
PSIc-LHCI-LHCII	207%	3.08%
	ΔArea Abs (%)	**stdev**
LHCI added to PSIc	67%	2.71%
LHCII added to PSIc	51%	0.31%
LHCII added to PSIc-LHCI	41%	0.38%
both LHCI and LHCII added to PSIc	107%	3.08%
LHCI substituted by LHCII	-16%	2.40%

DOI: 10.1038/NPLANTS.2016.131

Supplementary Table 4: Fraction of PSI-core, LHCI and LHCII excited upon excitation at 440 or 475 nm. The fraction of PSI-core, LHCI and LHCII excited during time resolved fluorescence measurement was calculated as reported in [2]. In particular, the PSI core, LHCI and LHCII contributions to 440 nm and 475 nm absorption in PSIc-LHCI, PSIc-LHCII and PSIc-LHCI-LHCII were estimated from the spectra reported in the main text in Figure 3. The fraction of PSI-core, LHCI and LHCII excited at the different wavelength was then estimated correcting the absorption contribution of each complex with the carotenoid to chlorophyll energy transfer efficiency as described in [2]. For this calculation the carotenoid to chlorophyll excitation energy transfer was estimated to be 70%, 67% and 90% as reported in [2-4]

EX 440 nm	**PSIc**	**PSIc-LHCI**	**PSIc-LHCII**	**PSIc-LHCI-LHCII**
PSI-core	100%	65%	70%	51%
LHCI	0%	35%	0%	28%
LHCII	0%	0%	30%	21%
EX 475nm	**PSIc**	**PSIc-LHCI**	**PSIc-LHCII**	**PSIc-LHCI-LHCII**
PSI-core	100%	39%	38%	26%
LHCI	0%	61%	0%	74%
LHCII	0%	0%	62%	0%

Supplementary Table 5: **Average fluorescence lifetimes and photochemical quantum yield of PSI complexes**. The decay kinetics obtained upon excitation (EX) at either 440 or 475 nm were fitted by global analysis with three exponential functions whose time constants (τ_{1-3}) and amplitudes (A_{1-3}) were used to calculate the average lifetime (τ_{AV}) as $\Sigma A_i\tau_i/\Sigma A_i$. The photochemical quantum yield of PSI (Φ PSI) was calculated as reported in [5] and [6]. Errors reported for τ_{AV} were obtained considering a confidence interval of 95% on both amplitude and time constants during fitting procedure.

.

EX 440 nm	**τ_{AV} (ps)**	**Φ PSI**
PSIc	18.0 ± 0.7	99.45% ± 0.02%
PSIc-LHCI	31.1 ± 0.6	99.04% ± 0.02%
PSIc-LHCII	35.7 ± 0.9	98.92% ± 0.03%
PSIc-LHCI-LHCII	33.1 ± 1.8	98.98% ± 0.05%
EX 475 nm	**τ_{AV} (ps)**	**Φ PSI**
PSIc	24.4 ± 0.7	99.27% ± 0.02%
PSIc-LHCI	54.7 ± 0.6	98.36% ± 0.02%
PSIc-LHCII	45.5 ± 1.3	98.63% ± 0.04%
PSIc-LHCI-LHCII	63.9 ± 1.7	98.04% ± 0.05%

DOI: 10.1038/NPLANTS.2016.131

Supplementary Figure 1. Trascription analysis of *Lhca1* gene in wild type and *ΔLhca* by semi-quantitative RT-PCR. The amplification reaction was stopped after 19, 23 and 27 cycles. Retrotranscribed 18S rRNA was used as internal standard for the total RNA amount. Densitometric analysis of amplicons abundance revealed no significant variation of gene expression regulation (Student's *t* test, $P < 0.05$). bp, base pairs.

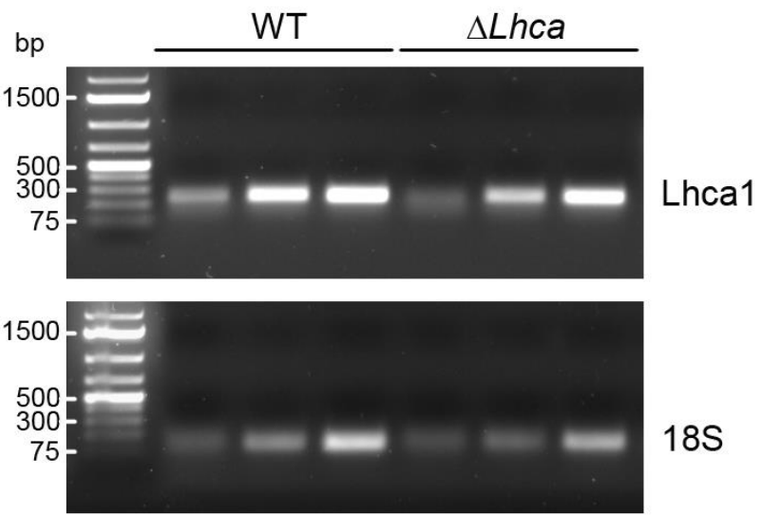

Supplementary Figure 2. 2D SDS–PAGE of thylakoid membrane proteins of wild type and *ΔLhca* mutant. Panel a: 2D SDS–PAGE separation of both purified PSI-LHCI supercomplex and the LHC region of thylakoids allows a better investigation of the protein composition in the membrane, and highlights the depletion of all Lhca subunits in thylakoids from mutant plants**.** Panel b: Immunolocalization of Lhca5 on the 2D PAGE map obtained from WT thylakoids.

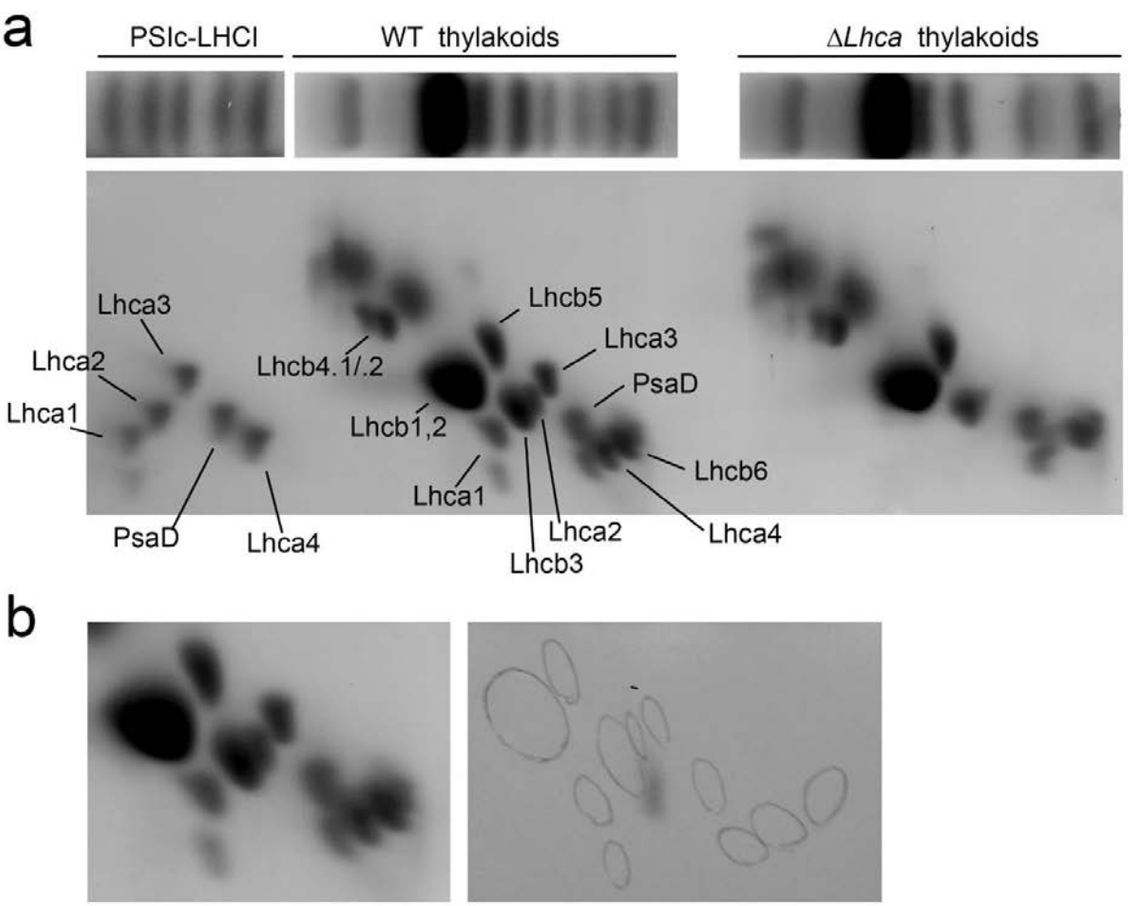

DOI: 10.1038/NPLANTS.2016.131

Supplementary Figure 3. Western blot analysis on purified PSI complexes. (a) Immunoblot reactions were performed on isolated PSI complexes using antibodies against the core subunit PsaA, the antenna proteins Lhca1-4 and the LHCII trimers. (b) Presence of Lhca5 in both isolate PSI complexes and thylakoids was investigated by western blot.

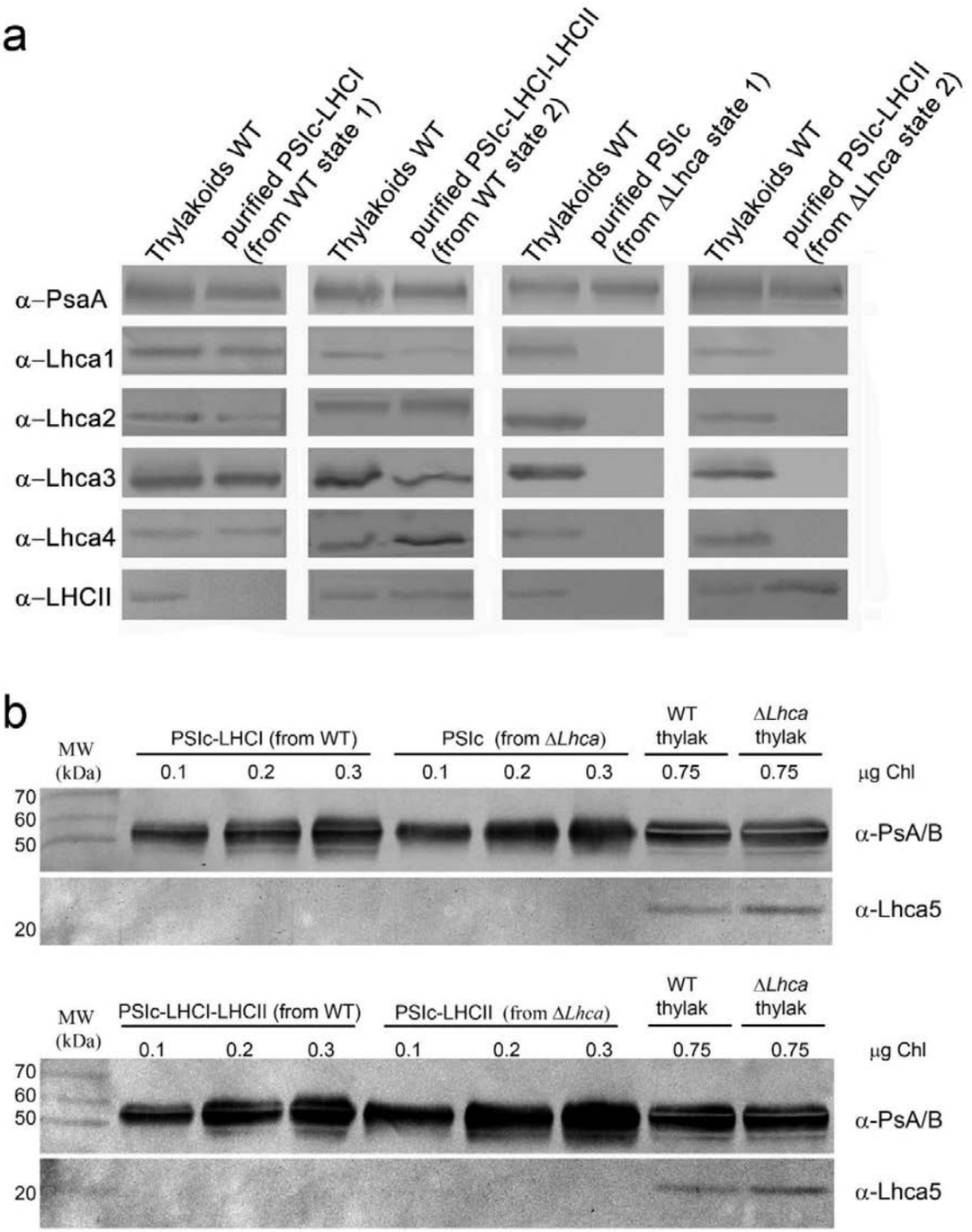

Supplementary Figure 4. Emission spectra of isolated PSI complexes at 77K. Emission spectra of isolated PSI complexes were recorded at 77K, upon excitation at 475 nm.

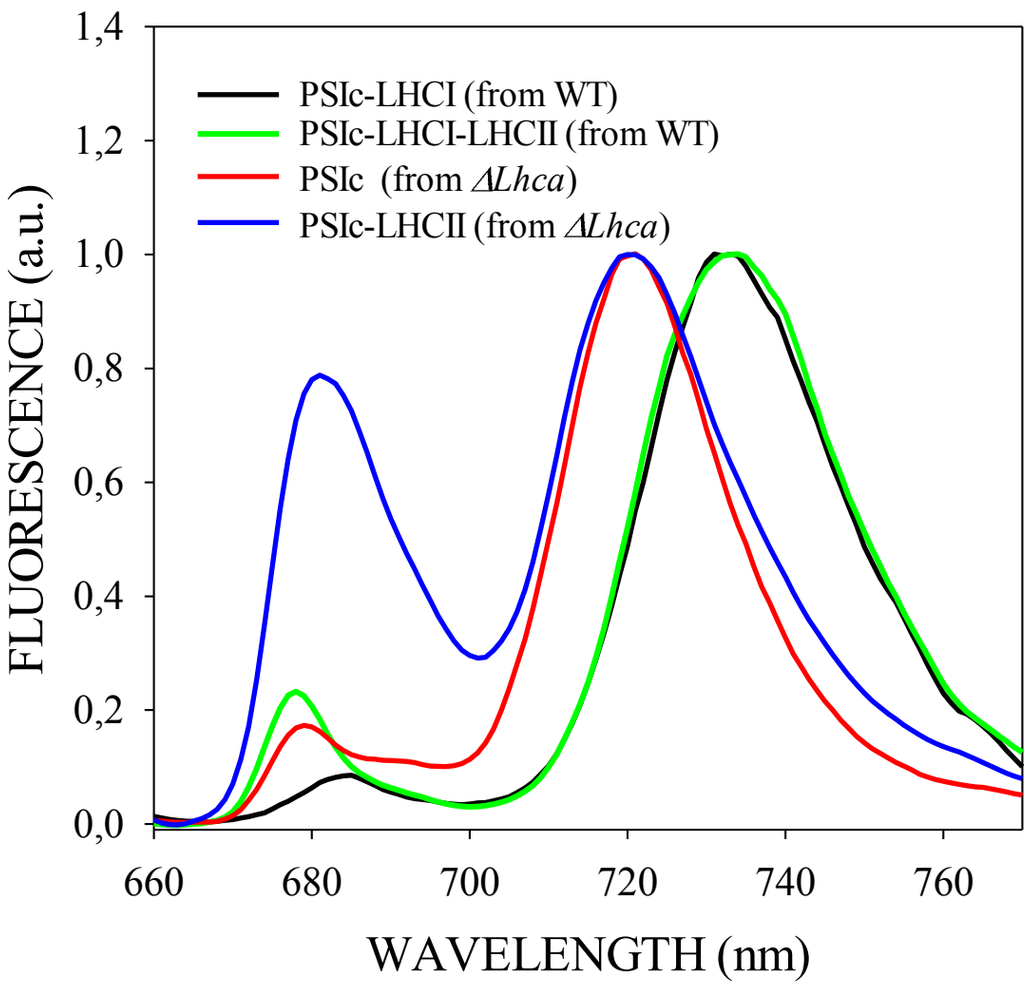

DOI: 10.1038/NPLANTS.2016.131

Supplementary Figure 5. Time resolved fluorescence decay maps obtained from streak camera analysis. Wavelength (nm) and time (ps) dependence of fluorescence emission are indicated on the X and Y axes, respectively. Color scale from blue to red represents fluorescence intensity from the lowest (blue) to the highest (red) intensity. Excitation wavelength: 440 nm.

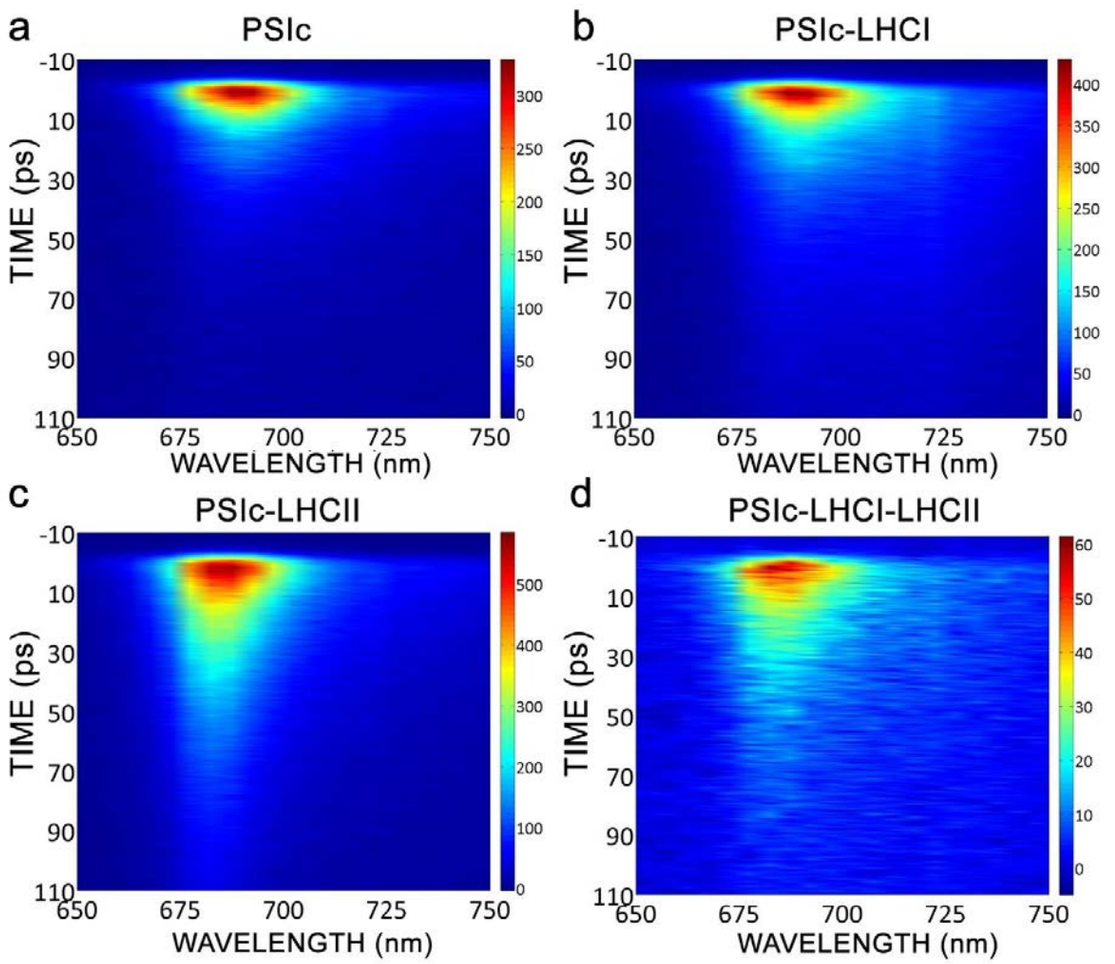

Supplementary Figure 6. Kinetics of fluorescence emission upon excitation at either 440 or 475 nm. Fluorescence emission kinetics were recorded in the 650-800 nm range, upon excitation at either 440 nm (Panel a-b) or 475 nm (Panel c-d). Signal acquisitions were performed with a time window of 2 ns (Panel a, c) and 200 ps (Panel b, d). Panel e: decay kinetics, upon excitation at 475 nm with a time window of 2 ns, were reported in linear scale with an enlargement in the 300-1750 ps region.

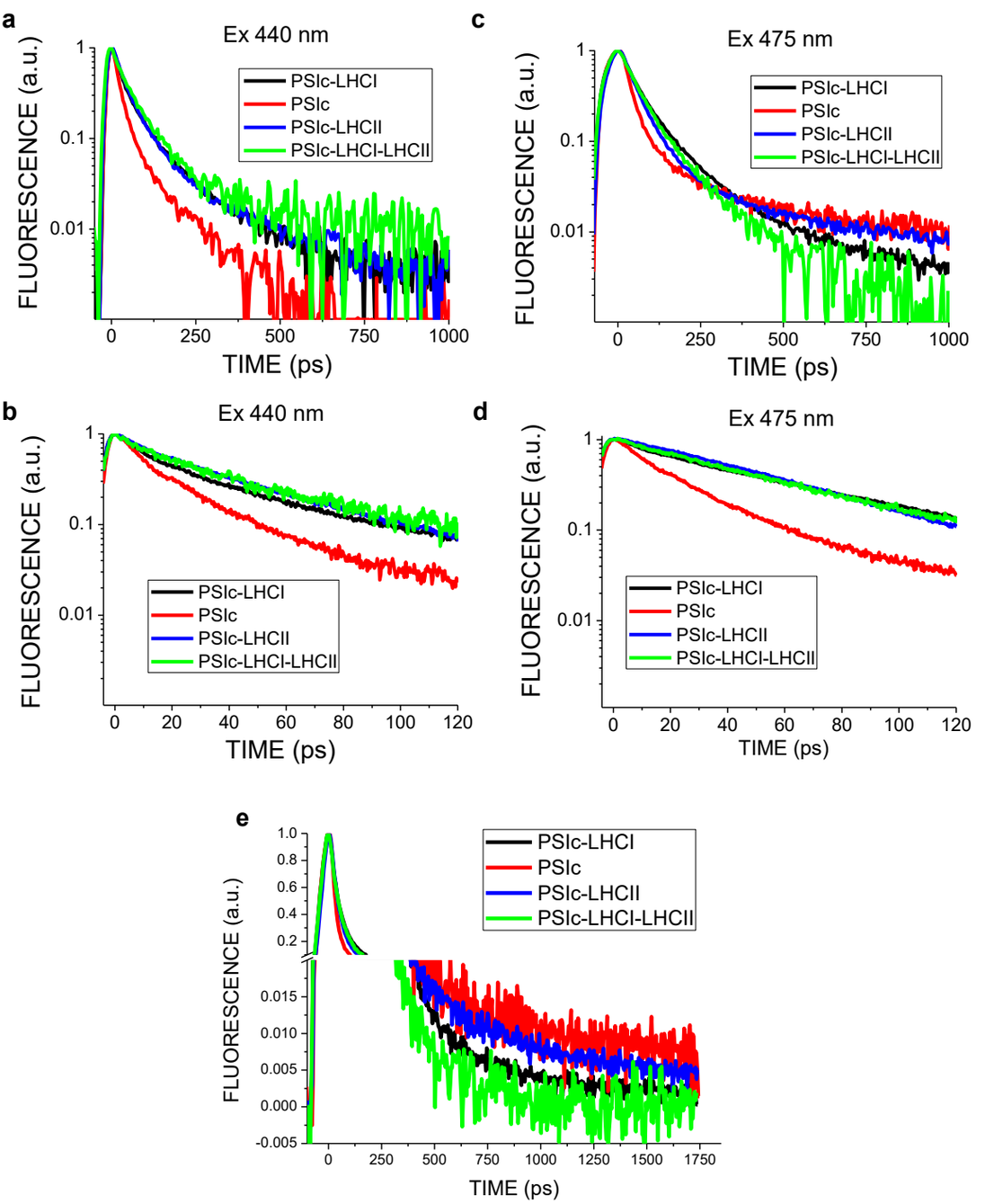

DOI: 10.1038/NPLANTS.2016.131

Supplementary Figure 7. Decay Associated Spectra (DAS) of PSI supercomplexes. The time-resolved fluorescence decay maps reported in Supplementary Figure 5 were analyzed in terms of global fits. The DAS obtained are reported for PSIc (Panel a), PSIc-LHCI (Panel b), PSIc-LHCII (Panel c) and PSIc-LHCI-LHCII (Panel d). Excitation wavelength is 440 nm. The time constant associated with each DAS is indicated for each sample. Errors bars on DAS and time constants indicate standard deviation associated to fitting procedure.

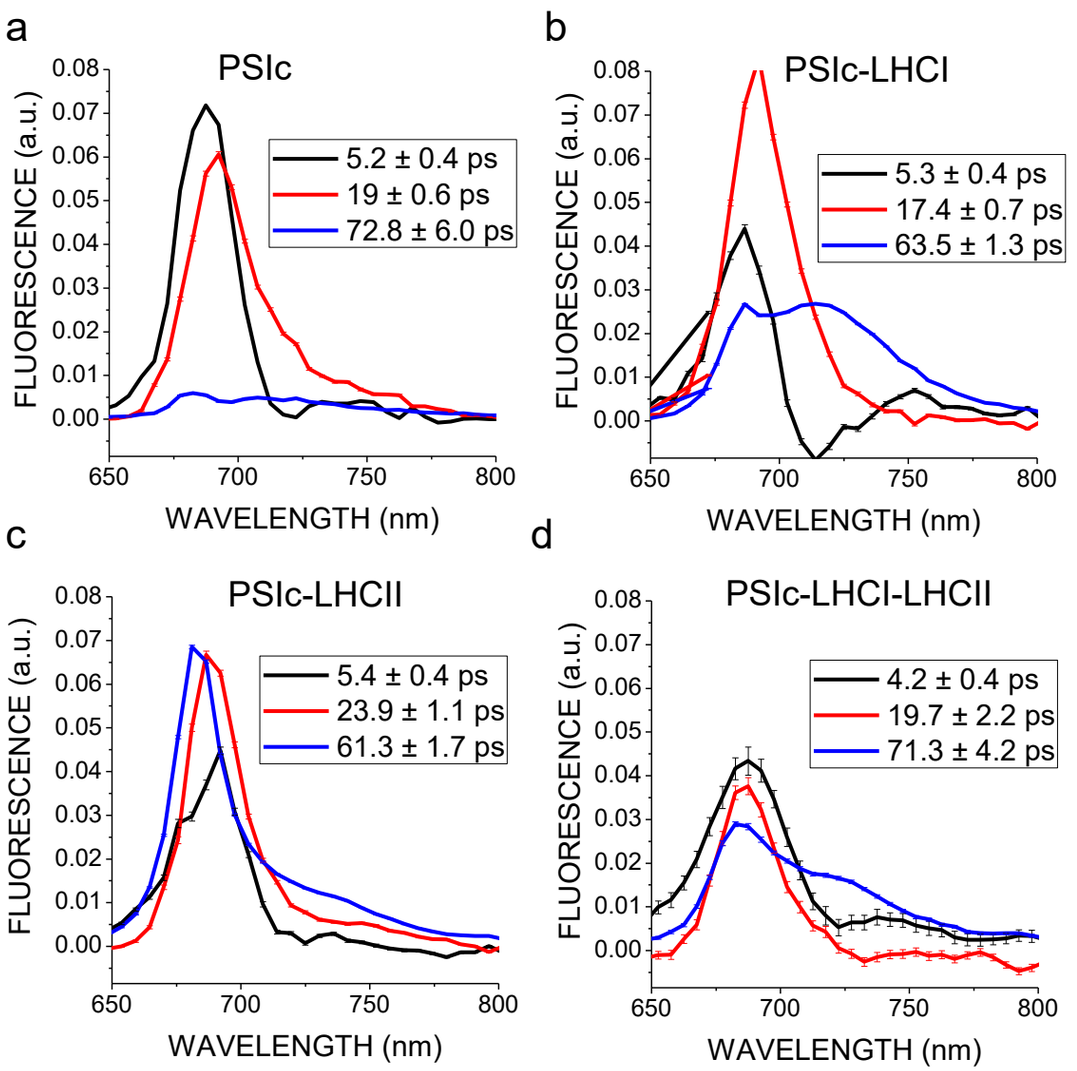

Supplementary Figure 8. Residues maps from global analysis of Streak camera maps upon excitation at 440 nm. The time-resolved fluorescence decay maps reported in Supplementary Figure 5 (excitation at 440 nm) were analyzed in terms of global fits: the residues maps are reported in Panel A-D for PSIc, PSIc-LHCI, PSIc-LHCII and PSIc-LHCI-LHCII, respectively. Residues resulting from global analysis are less than 6.5% of original map.

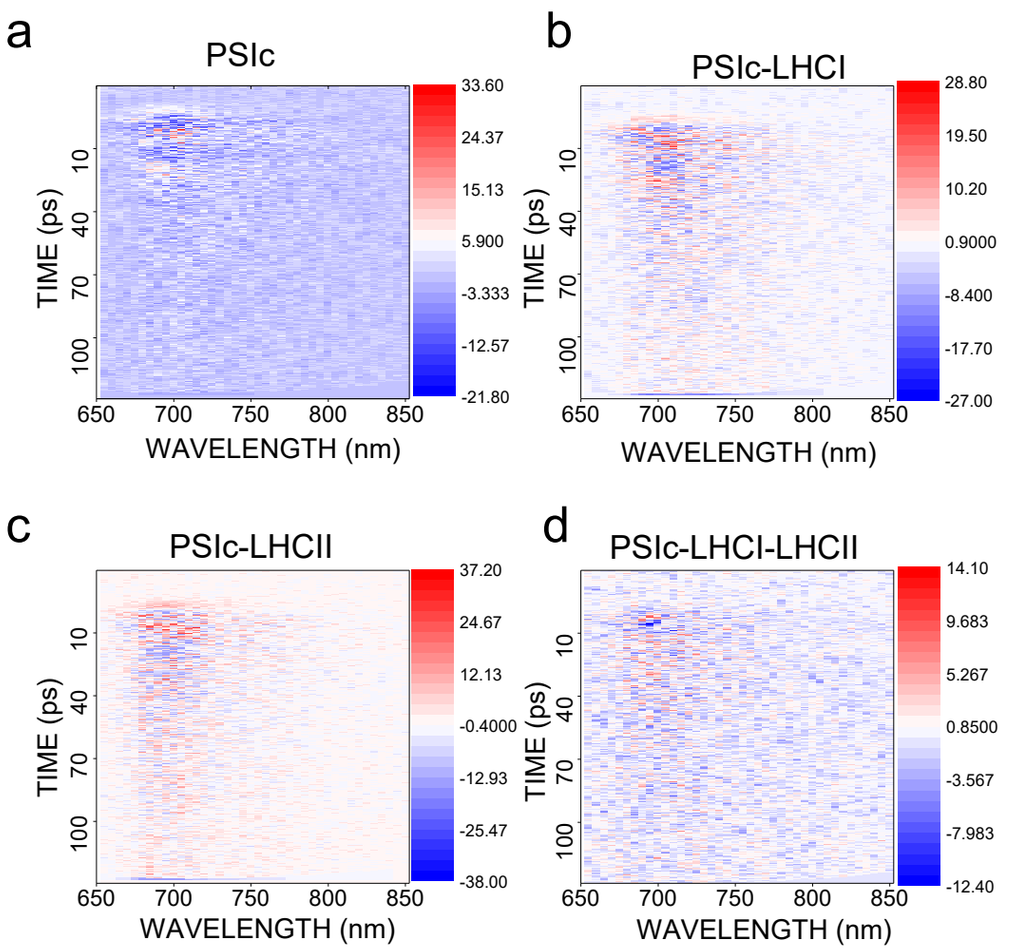

DOI: 10.1038/NPLANTS.2016.131

Supplementary Figure 9. Residues maps from global analysis of Streak camera maps upon excitation at 475 nm. The time-resolved fluorescence decay maps reported in Figure 5 (excitation at 475 nm) were analyzed in terms of global fits: the residues maps are reported in Panel A-D for PSIc, PSIc-LHCI, PSIc-LHCII and PSIc-LHCI-LHCII respectively. Residues resulting from global analysis are less than 11.6% of original map.

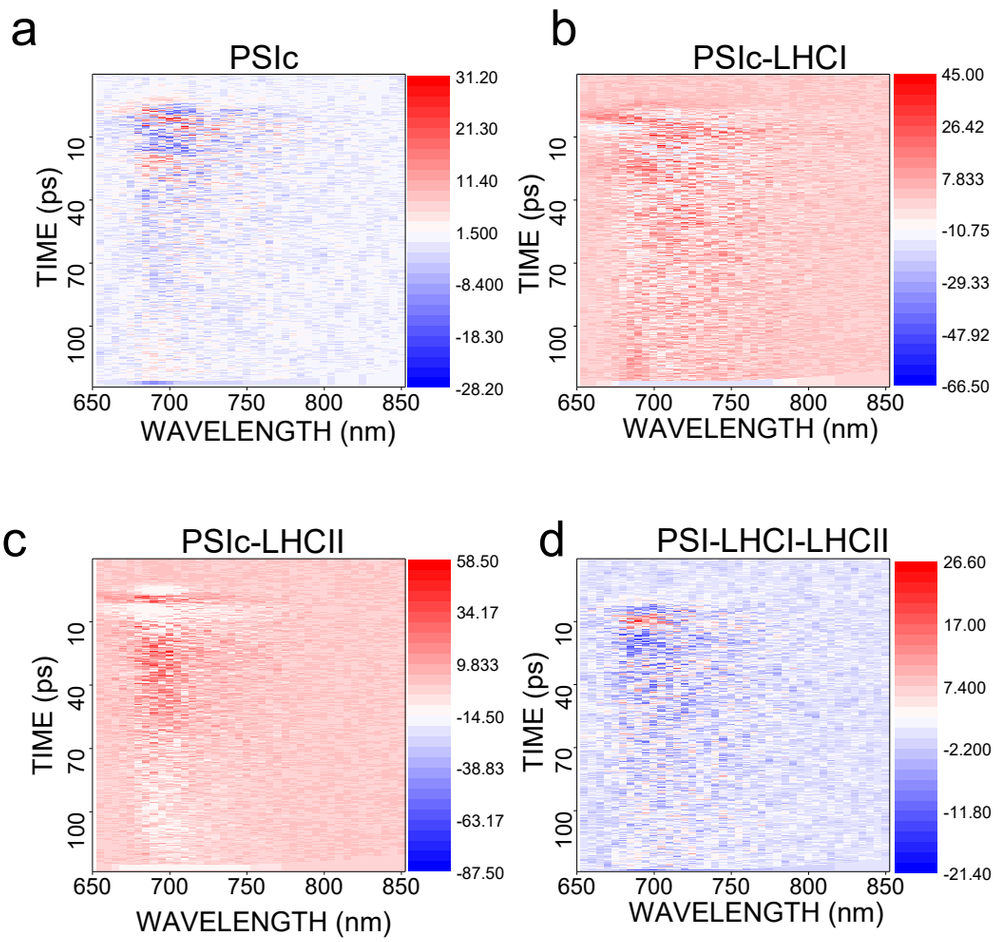

Supplementary Figure 10. Fitting of fluorescence decay traces at specific wavelengths. Fluorescence decay traces at specific wavelengths are reported together with the respective fitting curves form global analysis and residues.

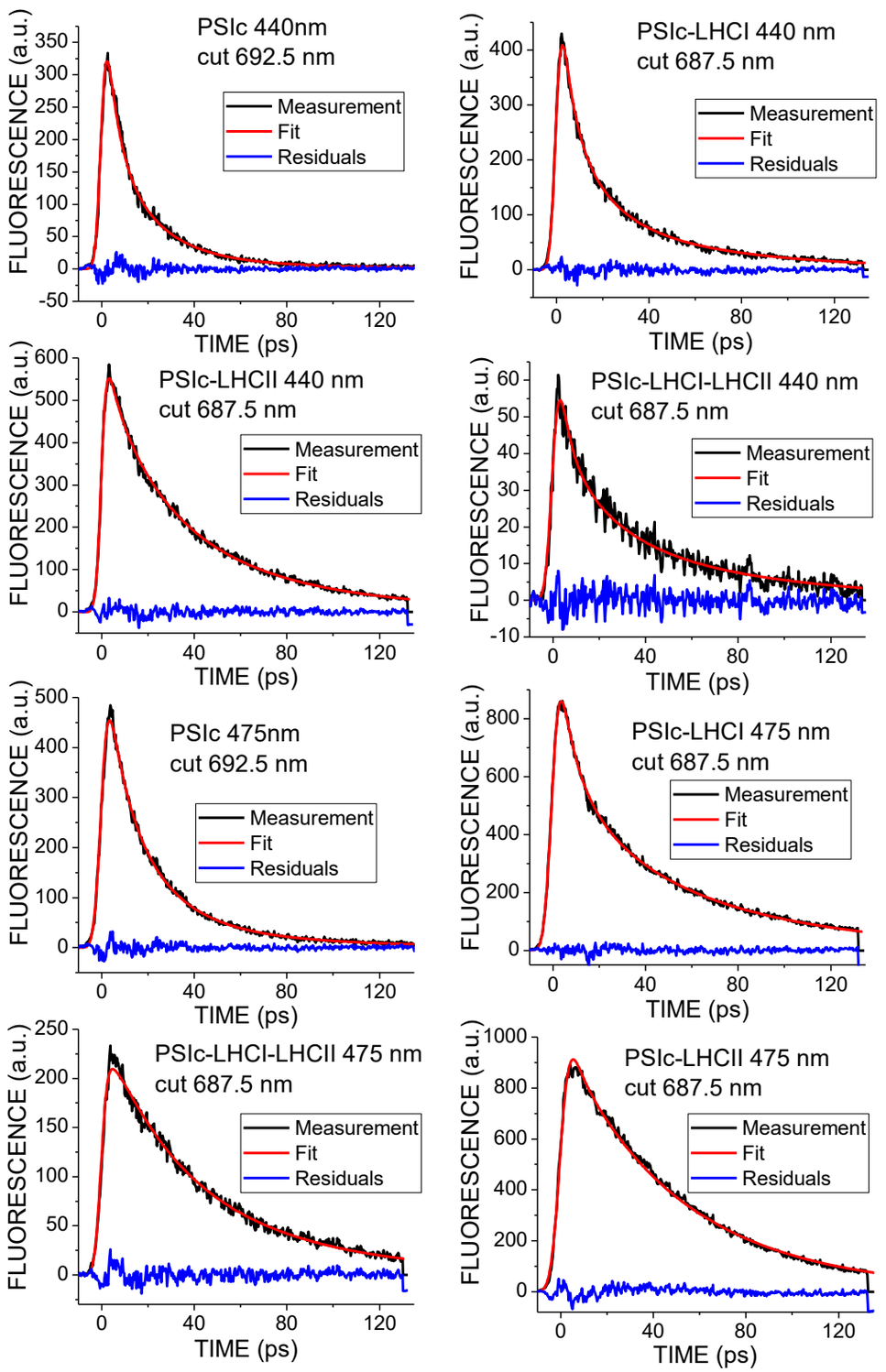

DOI: 10.1038/NPLANTS.2016.131

Supplementary Figure 11. Fluorescence decay kinetics of PSIc-LHCI upon excitation at 475 nm at different powers. Power of laser beam at 475 nm used for sample excitation is reported in the legend.

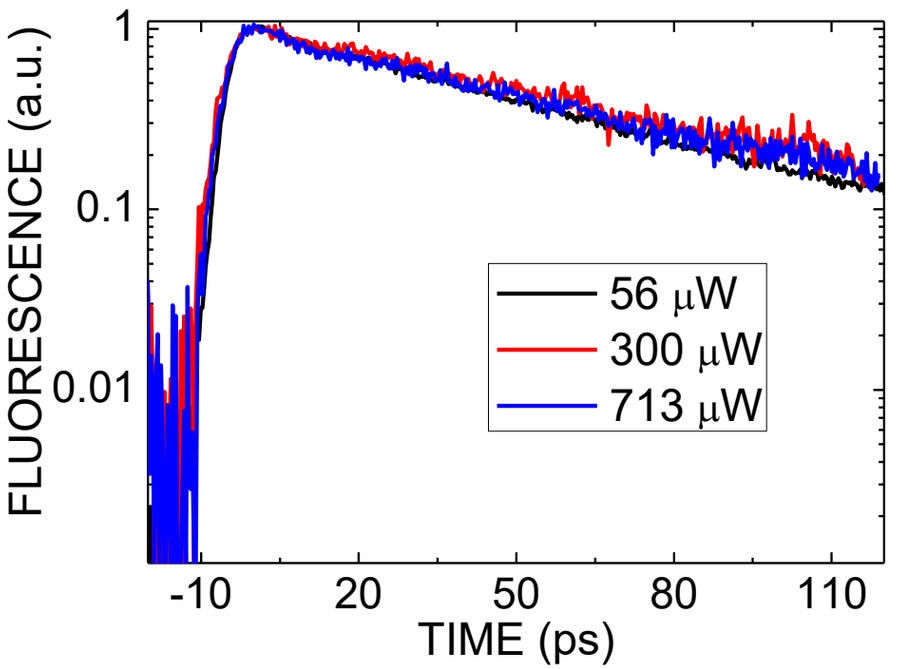

REFERENCES

1. Ballottari, M., Mozzo, M., Croce, R., Morosinotto, T. & Bassi, R. Occupancy and functional architecture of the pigment binding sites of photosystem II antenna complex Lhcb5. *J Biol Chem* **284**, 8103-13 (2009).
2. Wientjes, E., van Stokkum, I.H., van Amerongen, H. & Croce, R. The role of the individual Lhcas in photosystem I excitation energy trapping. *Biophys J* **101**, 745-54 (2011).
3. van Oort, B. *et al.* Picosecond fluorescence of intact and dissolved PSI-LHCI crystals. *Biophys J* **95**, 5851-61 (2008).
4. Formaggio, E., Cinque, G. & Bassi, R. Functional architecture of the major light-harvesting complex from higher plants. *J Mol Biol* **314**, 1157-66 (2001).
5. Galka, P. *et al.* Functional analyses of the plant photosystem I-light-harvesting complex II supercomplex reveal that light-harvesting complex II loosely bound to photosystem II is a very efficient antenna for photosystem I in state II. *Plant Cell* **24**, 2963-78 (2012).
6. Wientjes, E., van Amerongen, H. & Croce, R. LHCII is an antenna of both photosystems after long-term acclimation. *Biochim Biophys Acta* **1827**, 420-6 (2013).

Chapter 5

Light harvesting complex I is essential for Photosystem II photoprotection under variable light conditions

This chapter was submitted to

Photosynthesis research

Light harvesting complex I is essential for Photosystem II photoprotection under variable light conditions in *Arabidopsis thaliana*

Mauro Bressan[a], Roberto Bassi[a,§], Luca Dall'Osto[a]

[a]*Dipartimento di Biotecnologie, Università di Verona, Strada Le Grazie 15, 37134 Verona, Italy*

Abstract

Higher plant Photosystem I (PSI) includes a peripheral antenna system (LHCI) composed of four light-harvesting proteins (Lhca1-Lhca4). The LHCI system is highly conserved, suggesting that it plays a specific role within the LHC family. In order to elucidate the specific function of LHCI, the phenotype of an *Arabidopsis* mutant devoid of the whole LHCI system was studied over a range of conditions, including rapid changes in irradiation. *ΔLhca* plants displayed stunted growth and reduced thylakoid lumen acidification respect to wild type, suggesting that the lack of LHCI affected electron transport rate. Under rapidly changing light intensity, growth rate of the mutant was further reduced and the redox balance of the photosynthetic electron chain impaired. Instead under constant, excess light regime, the *ΔLhca* plants did not suffer enhanced photooxidation *vs.* wild type, implying LHCI optimizes the flow rate through the electron transport chain by maintaining high PSI activity at all irradiances. We conclude that a complete PSI supercomplex, including LHCI, is crucial for the dynamic regulation of PQ redox state and therefore for PSII photoprotection.

Introduction

In oxygenic photosynthesis, multiple reactions catalyze light-driven electron transport from water to $NADP^+$, fuel ATP production and convert CO_2 into organic compounds. The major components of the photosynthetic machinery include the thylakoid membrane multiprotein complexes Photosystems (PS) II and I, which operate in a concerted way and are functionally connected by plastoquinone (PQ), cytochrome b_6f complex and plastocyanin. The first step in solar energy conversion consists of photon absorption by the chlorophylls (Chl) and carotenoids (Car) bound to each PS in an ordered array, which ensure a rapid transfer of the excitation energy to the reaction centre (RC), where excitonic energy is then converted into chemical form (Nelson *et al*., 2004).

Photosystem I catalyzes the light-driven transmembrane transport of electrons from plastocyanin to ferredoxin. Its core carries 98 Chl *a* and 22 β-carotene chromophores as well as the co-factors for electron transport (Qin *et al*., 2015; Mazor *et al*., 2015). PSI supercomplex also includes a peripheral antenna complex (LHCI, light-harvesting complex of PSI), consisting of 4 nuclear-encoded light-harvesting proteins (Lhca1-Lhca4) which, in *Arabidopsis thaliana* are each encoded by single genes (Jansson 1999) and bind Chl *a*, Chl *b,* β-carotene and xanthophylls (Qin *et al*., 2015; Mazor *et al*., 2015) (Supplemental Figure S1). Two additional close homologues were identified in *Arabidopsis*, namely Lhca5 and Lhca6, whose levels are, however, sub-stoichiometric with respect to PSI (Klimmek *et al*., 2006) and are linked to a minor population of this PS involved in cyclic electron transfer (Peng *et al*., 2011).

Although pigment organization is similar among all the members of the LHC family (Liu *et al*., 2004; Amunts *et al*., 2010; Pan *et al*., 2011; Qin *et al*., 2015), Lhca subunits display unusual spectroscopic properties, including “red spectral forms”, with energies lower than P700 (Lam *et al*., 1984). The biological role of these forms is still a source of controversy: they might provide preferential absorption of photons transmitted under a canopy, and/or catalyze photoprotective reactions such as Chl triplet quenching (Rivadossi *et al*., 1999; Carbonera *et al*., 2005).

The antenna system does modulate the light-harvesting efficiency of PSs in order to avoid the damaging effects of fluctuating and excessive illumination, common in natural environments and potentially dangerous (Horton *et al*., 1996; Dall'Osto *et al*., 2015). Upon saturation of photochemical reactions (acting within ps), concentration of Chl singlet excited states (^{1}Chl*) rises. This increases the probability of generating Chl triplets (^{3}Chl*), which react with O_2, yielding singlet oxygen ($^1O_2$) and ultimately resulting in photo-inhibition (Krieger-Liszkay 2005). PSII has been identified as both the major site of $^1O_2$ release and the main target of photooxidative damage (Barber *et al*., 1992; Telfer *et al*., 1994).

PSI, on the other hand, is considered to be less sensitive to photooxidative stress and its photoprotection was less investigated. It has been suggested that PSI photoprotection mainly relies on detoxification of reactive oxygen species (ROS) generated at the acceptor side (Asada 1999), consistent with PSI photosensitivity being enhanced under chilling conditions (Sonoike 2011). However, more recent investigation indicates that PSI undergoes photoinhibition in mutants with a decreased β-carotene content (Cazzaniga *et al*., 2012; Cazzaniga *et al*., 2016) or under conditions unbalancing linear *vs.* cyclic electron transport (Suorsa *et al*., 2012). PSI and PSII regulate light harvesting differently: sustained over-excitation does not change the PSI-core/LHCI ratio, whereas PSII typically displays a long-term decrease in LHCII content (Anderson 1986; Ballottari *et al*., 2007). The PSII/PSI excitation imbalance is compensated by recruiting LHCII as a supplementary antenna for PSI (Allen 1992; Bellafiore *et al*., 2005; Galka *et al*., 2012).

In higher plants, the high degree of conservation of LHCI subunits and their spectroscopic peculiarities suggest a specific function for this system, which is not fully understood. Previous investigations analyzed individual gene products refolded *in vitro* (Croce *et al*., 2002; Castelletti *et al*., 2003; Morosinotto *et al*., 2005) and characterized *Arabidopsis* mutants which have suppressed levels of Lhca subunits (Klimmek *et al*., 2005). The overall fitness of all these Lhca-deficient plants was reduced under natural conditions, with ΔLhca4 plants showing retarded growth (Ganeteg *et al*., 2004).

The clustering of *Lhca* genes into clades distinct from that of *Lhcbs* suggests the former genes share properties, making plants in which all Lhca subunits have been deleted suitable for elucidating LHCI function. We therefore constructed an *Arabidopsis* knock-out (KO) mutant

devoid of LHCI system, referred to as *ΔLhca* (Bressan *et al*., 2016), and analyzed its photosynthetic phenotype while acclimating to different light regimes. The capacity of building a ΔpH gradient across the thylakoid membrane was reduced in the mutant. The redox state of the plastoquinone pool was more reduced than in wild type and growth was impaired, especially under conditions of rapidly changing light. When exposed to excess light intensity (EL), however, *ΔLhca* plants did not appear to be more sensitive to photooxidative stress than wild type, even under chilling conditions. Rather we found that completeness of PSI supercomplex, including LHCI, is crucial for balancing PSI *vs.* PSII photosynthetic electron transport under different light conditions. The specific properties of LHCI, which likely contributed to land colonization by plants and their adaptation to life under ever-changing light conditions typical of canopies, are discussed.

Material and Methods

Plant material and growth conditions – The *Arabidopsis thaliana ΔLhca* mutant was obtained as reported in (Bressan *et al*., 2016). Moreover, during this research work, three additional lines (RATM13-5011-1_H, N1010069 and N664137) were identified, having a T-DNA insertion mapped onto the *Lhca2, Lhca3* and *Lhca4* genes, respectively. All lacked the corresponding gene product. The phenotype of these lines was very similar to that N101690 (*koLhca2*), N876497 (*koLhca3*) and N679009 (*koLhca4*) lines previously reported and suggest the reduced growth phenotype was only related to lack of LHCI proteins. Plants were grown in a phytotron for 5 weeks at 150 µmol photons m^{-2} s^{-1} (OSRAM halogen HQI-T 250W and/or OSRAM lumilux cool white L58W), 23°C, 70% humidity, and 8/16 h of day/night.

For excess light growth experiments, 2-week-old seedlings were transferred to either EL (1000 µmol photons m^{-2} s^{-1}, 23°C) or fluctuating light (FL, alternations of 5 min at 150 µmol photons m^{-2} s^{-1} and 1 min at 1000 µmol photons m^{-2} s^{-1}, 23°C) during the 8-h photoperiod. The growth rate was determined by both monitoring the rosette area through image analyses and measuring the plants fresh weight. All growth trials were carried out using LED light sources (Epistar 35mil Chip High Power LED, warm white LEDE-P20B-DW, Wayjun Tech., China). Induction of either state I or state II was obtained by illuminating leaves, placed on moist paper, for 45 min with a PSI light (30-W incandescent bulbs filtered through Lee Filters 027 Medium Red) or a PSII light (30-W warm white fluorescent lamps filtered through Lee Filters 105 Orange) respectively, as previously reported (Pesaresi *et al*., 2009).

Membrane isolation – Chloroplasts and stacked thylakoid membranes were isolated as reported in (Casazza *et al*., 2001). For isolation of membranes in state II, 10 mM NaF was added to both GB and RB buffers.

Pigment analysis – Maximum zeaxanthin accumulation was measured in leaves, placed on moist paper and exposed to 1000 µmol photons m^{-2} s^{-1} for 30 min, at room temperature (RT, 23°C). Pigments were extracted from leaf discs with 85% acetone buffered with Na_2CO_3, separated and quantified by HPLC (Gilmore *et al*., 1991).

Spectroscopy - Absorption measurements were performed using a SLM Aminco DW-2000 spectrophotometer at RT either on samples in 10 mM HEPES pH 7.5, 20% (w/v) glycerol, 0.05% α-DM or 0.05% digitonin, or directly on leaves. Fluorescence excitation spectra (350 nm < λ_{exc} < 550 nm, λ_{ems} = 725 nm) were measured at RT using a Jobin-Yvon Fluoromax-3 spectrofluorimeter, in chloroplasts isolated from wild type and *ΔLhca* plants.

Gel electrophoresis, immunoblotting and sample preparation – SDS-PAGE analysis was performed with the Tris-Glycine buffer system (Laemmli 1970) with some modifications (Ballottari *et al*., 2004), and the Tris-Tricine buffer system (Schägger *et al*., 1987). Nondenaturing Deriphat-PAGE and CN-PAGE were performed following the methods described by (Peter *et al*., 1991; Jarvi *et al*., 2011) respectively. For both gel systems, thylakoids brought to 1 mg/mL Chls were solubilized in α/β-DM and digitonin (Galka *et al*., 2012). After electrophoresis, bands corresponding to PSI supercomplexes were excised, grinded in extraction buffer (0.02% digitonin, 30% glycerol, 10 mM Hepes pH 7.5), then further purified by ultracentrifugation (Galka *et al*., 2012). For immunotitration, thylakoid total proteins (0.1, 0.2, 0.4, and 0.8 µg Chl) were separated by SDS-PAGE, electroblotted to a nitrocellulose membrane, then proteins were detected using specific primary antibodies: α-Lhca2/3/4 (AS01 006/007/008), α-PsaA (AS06 172), α-PsbB (AS04 038) from Agrisera; home-made, polyclonal α-LHCII (immunogen: heterotrimeric LHCII from *Arabidopsis*). The alkaline phosphatase-conjugated secondary antibody was purchased from Sigma-Aldrich (A3687).

Analysis of Chl fluorescence - PSII function during photosynthesis was measured through Chl fluorescence on leaves at RT with a PAM 101 fluorimeter (Heinz-Walz, Germany). Minimum fluorescence (F_0) was measured with a 0.15 µmol photons m^{-2} s^{-1} beam, F_M was determined with a 1.5 s light pulse (5000 µmol photons m^{-2} s^{-1}). White continuous light (1200 µmol photons m^{-2} s^{-1}) was supplied by a KL1500 halogen lamp (Schott, Germany). Far-red light (30 µmol photons m^{-2} s^{-1} at 720–730 nm, 3 s) was supplied by a 102-FR LED. Fluorescence was monitored in leaves from plants dark-adapted for 2 hours, leaves were maintained in a chamber (G219 Arabidopsis Leaf Chamber, Qubit, Canada) and were given 23 min of illumination in the presence of saturating CO_2. Parameters Φ_{PSII} (F_q'/F_m') and qL were calculated according to (Baker 2008).

Ferredoxin-dependent plastoquinone reduction activity (CEF, cyclic electron flow) was measured in ruptured chloroplasts as described in (Munekage *et al*., 2002), at RT and under continuous stirring, by adding 5 µM spinach ferredoxin and 0.25 mM NADPH, and following Chl fluorescence changes with the measuring light of the PAM.

Analysis of P700 – In vivo P700 absorption changes were sampled by weak monochromatic flashes (10-nm bandwidth, 705 nm) provided by LEDs (JTS10; Biologic Science Instruments, France) as reported in (Cazzaniga *et al*., 2012).

Gas-exchange measurements - Measurements of O_2 evolution in saturating CO_2 were performed on leaves using a S101 O_2 electrode (Qubit System, Canada). Light response curves were determined using broadband red light (LH36/2R, Hansatech, UK).

Measurement of ΔpH - The kinetics of ΔpH formation across the thylakoid membrane was measured at RT in chloroplasts using the 9-AA fluorescence quenching method, as described in (Johnson *et al*., 1994).

Determination of the sensitivity to photooxidative stress - Photooxidative stress was induced in either whole plants or detached leaves, exposed to EL (600 or 1400 µmol photons m^{-2} s^{-1}) at 8°C for 2 days. Decay kinetics of maximal quantum yield of PSII photochemistry (F_v/F_M; (Havaux *et al*., 2004)) and maximum content of photoxidizable P700 (ΔA_{max} at 705 nm; (Yang *et al*., 2010)) were recorded on detached leaves during illumination to assess inhibition of PSII and PSI, respectively. Content of oxidizable P700 (ΔA_{max}) was recorded during far-red-light illumination (2500 µmol photons m^{-2} s^{-1}, λ_{max} = 720 nm); to have a precise estimation of the PSI photoinhibition, ΔA_{max} has been determined in detached leaves, vacuum infiltrated with 50 µM dibromothymoquinone and 1 mM methyl viologen (Munekage *et al*., 2002; Sonoike 2011). Photooxidation levels were assessed on leaf discs floating on water and exposed to white light (1400 µmol photons m^{-2} s^{-1}, 5°C), by measuring MDA formation as an indirect quantification of lipid hydroperoxides (Havaux *et al*., 2005).

***Accession Numbers*.** Sequence data from this article can be found in the Arabidopsis Genome Initiative or GenBank/EMBL databases under accession numbers At3g61470 (Lhca2), At1g61520

(Lhca3), At3g47470 (Lhca4). The KO lines mentioned in the article can be obtained from the NASC under the stock numbers N101690 (*koLhca2*), N876497 (*koLhca3*), N679009 (*koLhca4*).

Results

Analysis of the photosynthetic function of ΔLhca, a knock-out mutant of Arabidopsis lacking the PSI peripheral antenna system

ΔLhca plants, grown in a climate chamber (150 µmol photons m^{-2} s^{-1}, 23°C, 8/16 day/night) for 5 weeks were significantly smaller than wild type (Supplemental Figure S2A) (Bressan *et al*., 2016). In order to confirm that this phenotype was not due to the presence of unrelated mutation(s), we measured the fresh weight of parental single KO mutants (Supplemental Figure S2B-C). All genotypes were less stunted than *ΔLhca* and more similar to the wild type.

Pigment analysis (Table I) showed that β-carotene levels per unit Chl were slightly higher in dark-adapted *ΔLhca* plants respect to wild type, whereas xanthophyll content per unit Chl was the same in both genotypes.

		mol pigment / 100 mol Chl					
		neoxanthin	**violaxanthin**	**antheraxanthin**	**lutein**	**zeaxanthin**	**β-carotene**
dark-adpated	**Wild type**	4.1 ± 0.1	2.8 ± 0.2	-	13.8 ± 0.6	-	7.8 ± 0.1
	ΔLhca	4.3 ± 0.1	2.5 ± 0.3	-	13.5 ± 0.6	-	8.7 ± 0.6 *
excess-light	**Wild type**	3.9 ± 0.1	1.2 ± 0.1	0.2 ± 0.1	12.4 ± 0.2	1.1 ± 0.1	6.8 ± 0.1
	ΔLhca	4.2 ± 0.1 *	1.0 ± 0.1 *	0.2 ± 0.1	13.0 ± 0.2 *	1.7 ± 0.1 *	7.8 ± 0.3 *

Table I. Photosynthetic pigment composition of wild type and *ΔLhca* leaves. Pigment content was determined by HPLC before and after the leaves were illuminated for 30 min at 1000 µmol photons m^{-2} s^{-1}. Data are normalized to 100 Chl molecules and are expressed as means ± SD (n = 3). Values marked with an asterisk are significantly different from those of the corresponding wild type (Student's *t* test, P < 0.05).

The ability to form zeaxanthin was assayed upon a 30-min exposure to EL: the de-epoxidation state was significantly higher in *ΔLhca* plants (+55%) than in the wild type.

The organization of pigment-binding complexes was analyzed by non-denaturing CN-PAGE (Supplemental Figure S3), after solubilizing wild type and *ΔLhca* thylakoids in 0.1% α-DM and 0.6% digitonin. Several green bands were resolved in the wild type: the PSII pigment–proteins migrated as multiple bands with different apparent masses, i.e. the PSII core complex, the antenna sub-complexes, including the Lhcb4-Lhcb6-LHCII-M complex, the trimeric LHCII and the monomeric Lhcbs. The PSI-LHCI supercomplex was present as a single major band in the middle section of the gel. The most evident difference detected in *ΔLhca vs.* wild type was the lack of PSI-LHCI supercomplex and the presence of a green band with lower apparent mass. Green bands in the region of PSI were excised and further analyzed: the absence of both Chl *b* and red spectral forms (Supplemental Figure S3B) and depletion of Lhca1-4 polypeptides in 2D SDS-/native-PAGE (Supplemental Figure S4) confirmed that *ΔLhca* plants only accumulated the PSI core moiety of the supercomplex. In order to detect possible alterations in the relative amount of protein components in the photosynthetic apparatus, the stoichiometry of pigment-binding polypeptides was determined by immunotitration (Supplemental Figures S3C, S4C): the PSI/PSII (PsaA/CP47) and LHCII/PSII ratios were the same in both genotypes within experimental error.

To investigate whether the lack of LHCI affected photosynthetic electron flow, the activity of the PSs during steady state photosynthesis was analyzed *in vivo*. PSII operating efficiency (Φ_{PSII}, Figure 1A) and O_2 production (Figure 1B) were measured on leaves at increasing light intensities and saturating CO_2. *ΔLhca* revealed a significant reduction in Φ_{PSII} and O_2 yield when light was dim (below 200 µmol photons m^{-2} s^{-1}), while no significant difference with the wild type emerged at higher levels of irradiance. In the former case, the Q_A pool was more reduced in the mutant plants, as indicated by the increase in 1-qL plots (Figure 1C), suggesting an imbalance in the distribution of excitation between the two photosystems. At higher light intensities, however, the Q_A redox state of the two genotypes was the same.

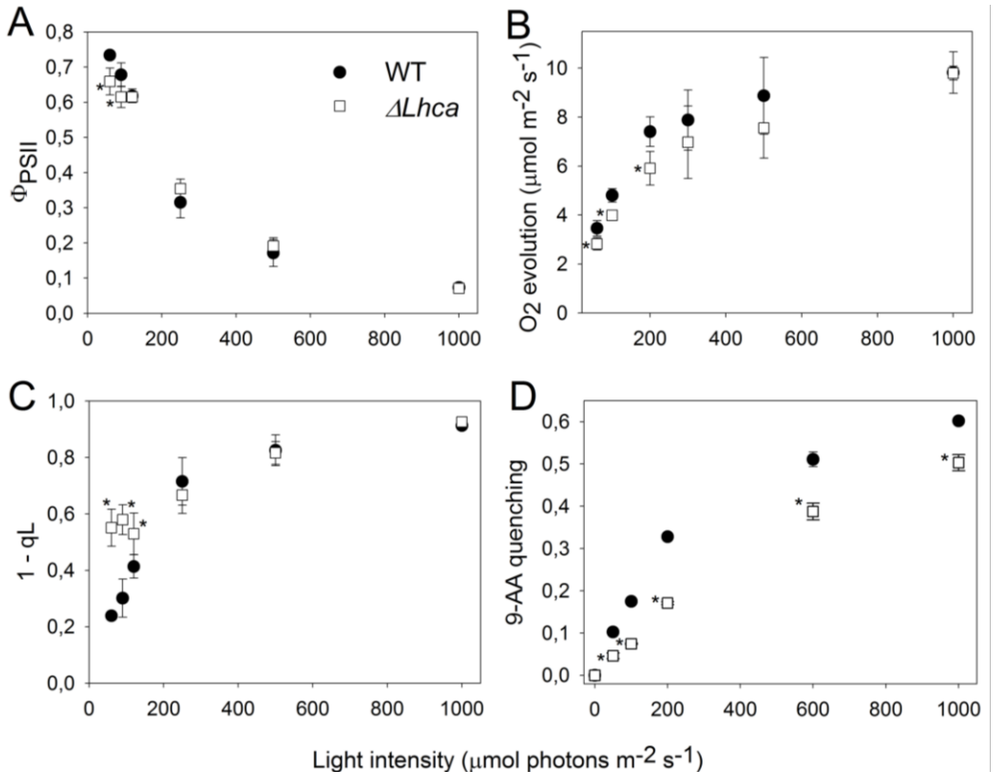

Figure 1. Characterization of the photosynthetic electron flow in wild type and *ΔLhca* leaves. (A) Dependence of the PSII operating efficiency (ΦPSII), and (B) photosynthetic O_2 evolution in saturating CO_2, measured on whole leaves during illumination at various levels of actinic light. (C) Amplitude of 1-qL values measured at different light intensities. 1-qL reflects the redox state of the primary electron acceptor Q_A, hence the portion of open PSII centers. (D) The light-dependent quenching of 9-aminoacridine (9-AA) fluorescence in chloroplasts was quantified as a measure for trans-thylakoid ΔpH. Symbols and error bars show means ± SD (n > 3). Values that are significantly different (P < 0.05) from the wild type are marked with an asterisk (*).

The origin of these differences might be related to altered cyclic electron flow (CEF) around PSI. If indeed ferredoxin (Fd)-dependent CEF is affected in *ΔLhca*, it is expected an effect on the oxidation state of both the PSI reaction center and Q_A.

To investigate this point, electron transfer from Fd to plastoquinone during CEF was monitored in ruptured chloroplasts, as an increase in Chl fluorescence under low measuring light (Munekage *et al*., 2002). In wild type sample, the addition of NADPH and Fd yields into a marked increase in Chl fluorescence that reaches a plateau after 30 s. *ΔLhca* behaved as the wild type, as indicated by identical plateau and rise of Chl fluorescence (Supplemental Figure S5), thus ruling out the hypothesis that LHCI depletion affect CEF efficiency.

The stunted growth of *ΔLhca* plants could therefore be ascribed to an imbalance in the distribution of excitation energy between the two photosystems, which would affect the trans-thylakoid pH gradient. To test this hypothesis, we determined the capacity of intact chloroplasts to acidify lumen pH by monitoring the light-induced quenching of 9-aminoacridine (9-AA) (Johnson *et al*., 1994). Mutant chloroplasts had a lower 9-AA quenching activity than the wild type controls over a wide range of light intensities (Figure 1D).

Photosensitivity at high light intensity and chilling temperatures

Treatment of plants with excess light causes the formation of $^1O_2$ and the onset of photooxidative stress, the severity of which is enhanced by low temperatures (Zhang *et al*., 2004). In order to verify whether LHCI depletion affected the sensitivity to photooxidative stress, wild type and *ΔLhca* plants were transferred to EL + cold (600 µmol photons m^{-2} s^{-1}, 5°C), and we proceeded to monitor the maximal photochemical yield of PSII (F_v/F_m) for 2 days. In both wild type and *ΔLhca* plants, F_v/F_m gradually decreased from 0.8 to 0.2 during the treatment (Figure 2A). Similar results were obtained for the kinetics of PSI photoinhibition measured in both whole plants at 1400 µmol photons m^{-2} s^{-1}, 5° (Figure 2B) and detached leaves at 1800 µmol photons m^{-2} s^{-1}, 24°C (data not shown). The trends were essentially the same in both genotypes. Lipid peroxidation was determined as malondialdehyde (MDA) content (Havaux *et al*., 2005) under stressing conditions (Figure 2C). Wild type plants underwent a significant photooxidative stress in the conditions used in this experiment, and no additive effect of LHCI depletion was observed, thus indicating that LHCI is not needed to ensure an effective photoprotection of P700 under the stress conditions tested.

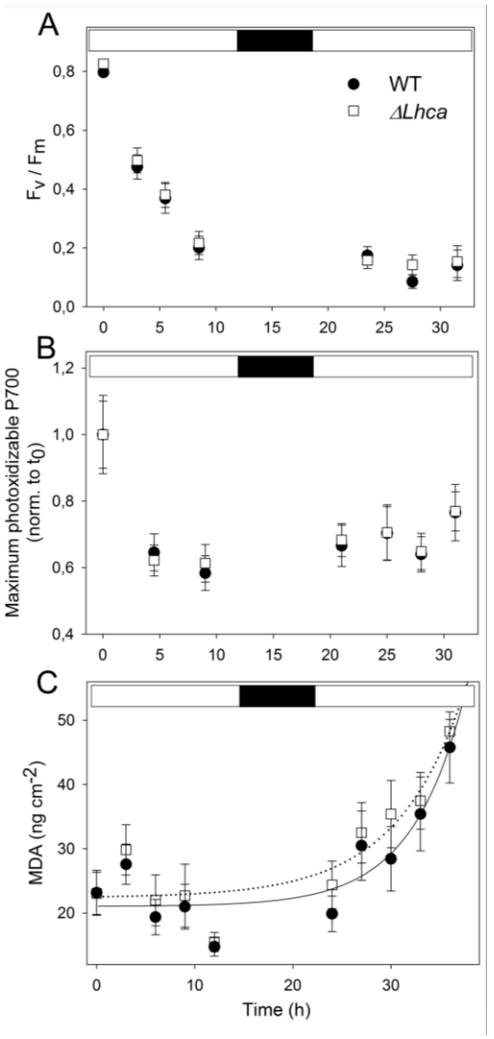

Figure 2. **Photooxidation of *Arabidopsis* wild type and *ΔLhca* plants exposed to excess light intensity and chilling temperatures.** (A) Fv/Fm decay kinetics (PSII photoinhibition) were monitored in wild type and mutant plants, treated at 600 µmol photons m^{-2} s^{-1}, 4°C for 30 h, with a 6-h period of dark between the 12 h of EL stress. (B) Decay kinetics of the maximum photooxidizable P700 (PSI photoinhibition) were measured on whole plants exposed to 1400 µmol photons m^{-2} s^{-1}, 4°C for 30 hours. (C) Detached leaves floating on water were treated at 1400 µmol photons m^{-2} s^{-1}, 4°C, and the kinetics of MDA formation were recorded. Data are expressed as means ± SD (n > 5). t_0, time zero (beginning of the treatment).

Growth under constant vs. fluctuating light conditions

To further investigate acclimation under stressing conditions, wild type and *ΔLhca* plants were grown either at constant moderate light intensity (150 µmol photons m^{-2} s^{-1}, 23°C – Figure 3A,

D), constant strong light (1000 µmol photons m^{-2} s^{-1}, 23°C – Figure 3B, D) or in fluctuating light (FL, 5 min at 150 µmol photons m^{-2} s^{-1}, 1 min at 1000 µmol photons m^{-2} s^{-1}, 23°C – Figure 3C, D), so as to mimic outdoor conditions. The growth of *ΔLhca* was less than that of the wild type under all these conditions, but the mutant's reduction in fresh weight was higher when exposed to continuous low light intensity (-51%) than to continuous strong light (-38%). The greatest impairment in growth, however, was observed under conditions of fluctuating light (-75% of wild type fresh weight, Figure 3C, D).

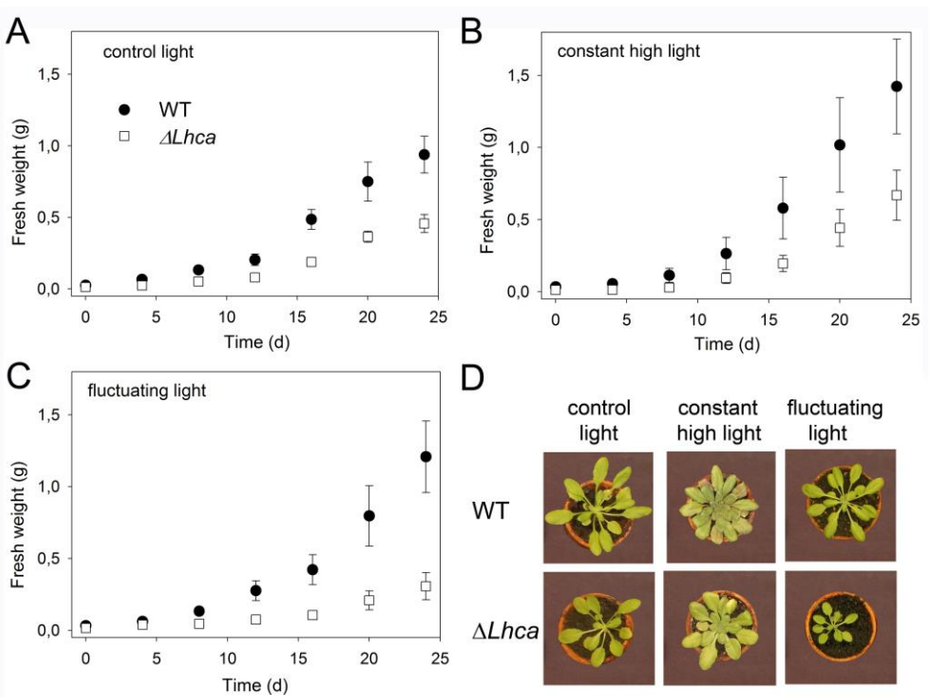

Figure 3. Growth rate of wild type and *ΔLhca* plants in either constant or fluctuating white light. Fresh weight of plants grown for 25 days in dim light (150 µmol photons m^{-2} s^{-1}, panel A), constant high intensity light (1000 µmol photons m^{-2} s^{-1}, panel B) or fluctuating light (5 min at 150 µmol photons m^{-2} s^{-1}, 1 min at 1000 µmol photons m^{-2} s^{-1}, panel C) was determined. Mean values of 15 independent measurements ± SD are shown. Under every condition tested, the growth rate of the mutant plant was significantly lower than that of the corresponding wild type (Student's *t* test, $P<0.0001$), with the greatest difference recorded under conditions of fluctuating light ($P<0.0001$). (D) Phenotype of wild type and mutant plants at the end of the experiment.

The impact of the different growth conditions on photosynthetic reactions was assessed by measuring the PSII yield, the Q_A redox state, the level of photooxidizable P700 and the amplitude of state I – state II transition on plants grown for 3 weeks under the control

conditions and subsequently subjected to FL regimes for 3 days. During the treatment, the PSII quantum yield dropped more in *ΔLhca* than in wild type plants (Figure 4A), a result that is consistent with their increased Q_A reduction level (Figure 4B). Photooxidizable P700, in contrast, was reduced to the same extent in both genotypes (Figure 4C).

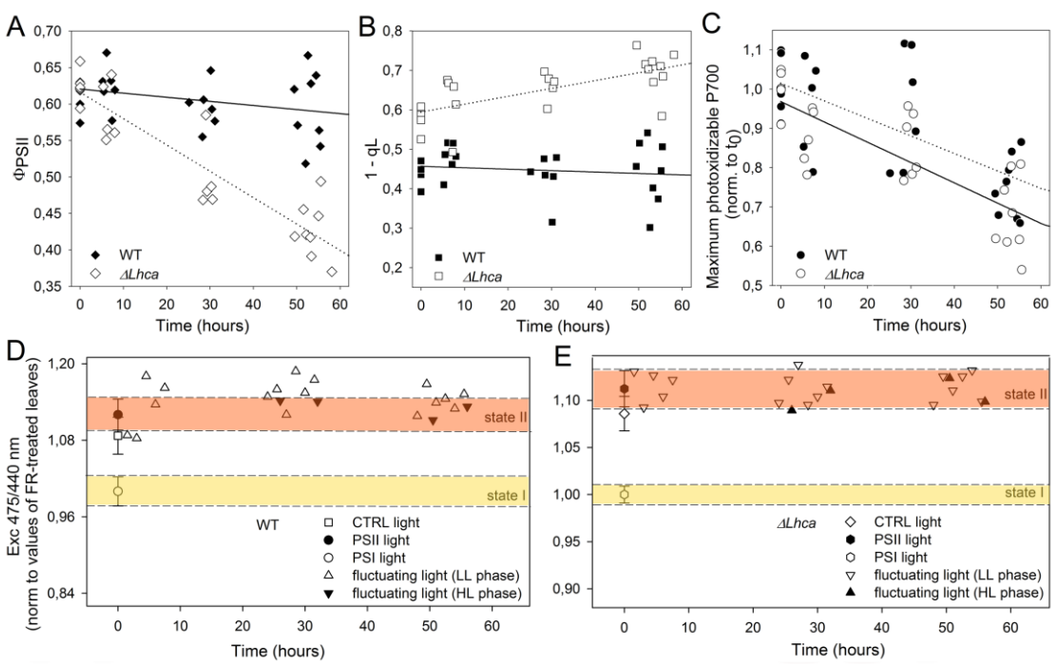

Figure 4. Photosynthetic parameters of wild type and *ΔLhca* plants under conditions of fluctuating light. Plants were grown in constant light (150 µmol photons m^{-2} s^{-1}) for 3 weeks (time point 0) and then transferred to fluctuating light (5 min at 150 µmol photons m^{-2} s^{-1}, 1 min at 1000 µmol photons m^{-2} s^{-1}, panel C) for a further 3 days. The relative changes in the (A) photochemical quantum yield of PSII (Φ_{PSII}), (B) Q_A reduction level (1-qL), and (C) maximum photooxidizable P700 were then measured. Each experimental point corresponds to a different sample; data are representative of two independent experiments. Experimental points were modeled with a linear regression. Statistical analysis (Test F) reveals that *ΔLhca* plants display a significantly lower Φ_{PSII} and more reduced Q_A than the wild type ($p < 0.0001$, panels B and C) at the end of treatment; on the other hand, no significant difference was detected in the kinetics of maximum photooxidizable P700 decay between the two genotypes ($p > 0.1$, panel D). (D, E) Fluorescence excitation spectra (350 nm < λ_{exc} < 550 nm, λ_{ems} = 725 nm) were determined in chloroplasts isolated from wild type (D) and *ΔLhca* plants (E) during treatment with fluctuating light. The relative contribution to PSI emission of λ_{exc} at 475 *vs.* 440 nm was used to estimate the amplitude of state I – state II transition. Chloroplasts from leaves in state I (treated with PSI light) or state II (treated with PSII light) were measured and used as reference.

Taken together, these results suggest that the short-term FL treatment impaired the photosynthetic electron transport of the *ΔLhca* plants by increasing the reduction state of the PQ pool and decreasing PSII yield. This effect was not due to the difficulty or inability to change the PSI/PSII or LHCII/PSII ratios under conditions of fluctuating light, because these responses were similar in wild type and mutant plants (Supplemental Figure S6), thus indicating that both genotypes were capable of reorganizing their pigment-proteins during acclimation to this light regime.

We estimated the efficiency of energy transfer from LHCII to PSI under FL by measuring the relative contribution of Chl *b vs.* Chl *a* to the PSI emission at 725 or 738 nm, depending on the genotype, from 77K fluorescence excitation spectra: the fluorescence excitation ratio at 475 nm *vs.* 440 nm (F_{475}/F_{440}) was calculated and compared to that of chloroplasts isolated from leaves in either state I or II (Figure 4D, E). Wild type plants maintained F_{475}/F_{440} values close to those of leaves treated with PSII light over the entire trial period, which is consistent with previous work (Grieco *et al*., 2012); *ΔLhca* plants displayed a similar behavior, thus indicating that FL conditions forced both genotypes to their maximum towards state II.

Discussion

We analyzed the effect of LHCI depletion on the plant ability to acclimate to different light conditions. In *ΔLhca* plants, lack of LHCI could not be compensated by over-accumulation of other LHC gene products (Bressan *et al*., 2016). This is different from previous reports on PSII antenna mutants, according to which down-regulation of LHCII was compensated by an over-expression of CP26 (Ruban *et al*., 2003), and other investigations on CP24, CP26 and CP29, the loss of which was observed to cause an over-accumulation of LHCII (Dall'Osto *et al*., 2014). These results confirm that PSI-LHCI is a stable system, lacking the dynamic properties of PSII (Klimmek *et al*., 2005; Ballottari *et al*., 2007). In *ΔLhca* plants, the composition of the photosynthetic apparatus appeared to be essentially unaffected, apart from, obviously, the absence of LHCI (Supplemental Figures S3 and S4, (Bressan *et al*., 2016)). Moreover, the mutant

did not suffer photoinhibition in EL at chilling temperatures, as long as the lighting conditions remained constant (Figure 2). However, under rapidly changing light intensity, *ΔLhca* lost its capacity for maintaining redox balance. As a consequence its PSII quantum yield was impaired and growth was more stunted than that of the wild type plants (Figures 3, 4).

Lack of LHCI does not affect short-term photoprotection.

At constant EL and low temperatures, *ΔLhca* displayed no stronger symptoms of photodamage respect to wild type (Figure 2), thus proving that LHCI is not crucial for PSI photoprotection under these stressing conditions. This is a response different from that of PSII, where photoprotection relies on PSII-Lhcb interactions, as revealed by the marked increase in $^1O_2$ production and photoinhibition in the *Arabidopsis ch1* mutant lacking Lhcb proteins (Havaux *et al*., 2007; Dall'Osto *et al*., 2010).

Fitness experiments on LHC KO plants revealed that of all genotypes with differing LHC protein content, *ΔLhca4* displayed the greatest reduction in both growth rate and seed production (Ganeteg *et al*., 2004). EL treatment on isolated PSI-LHCI (Alboresi *et al*., 2009) showed that a preferential degradation of LHCI helped preserve RC activity, thus suggesting a role for LHCI in PSI photoprotection. Moreover, the red absorbing forms, mostly found in Lhca4, were observed to increase the efficiency of ^{3}Chl* quenching by xanthophylls (Carbonera *et al*., 2005). Nevertheless, PSI activity was fully protected in both wild type and *ΔLhca* plants (Figures 2, 4). This is consistent with excitation energy transfer and trapping in the PSI core being extremely fast processes (20–40 ps), so that Chl excited states are rapidly quenched both in the presence and absence of LHCI (Wientjes *et al*., 2011b; Wientjes *et al*., 2011c).

Role of Lhca subunits in maximizing photosynthetic quantum yield at PSI-favoring light regimes

Long-term acclimatory responses allow plants to cope with environmental changes, thus ensuring optimal growth rates and fitness (Pesaresi *et al*., 2011; Tikkanen *et al*., 2012). Moreover, rapid fluctuations in both the spectrum and intensity of incident light need to be

counteracted in order to optimize photosynthetic electron transport. This is done by mechanisms balancing PSI *vs.* PSII functional antenna size (Bellafiore *et al*., 2005; Li *et al*., 2009; Allahverdiyeva *et al*., 2015) and quenching of excess energy (Li *et al*., 2000; Dall'Osto *et al*., 2005; Ahn *et al*., 2008; Cazzaniga *et al*., 2013). The hallmark of plant LHCI is its ability to absorb long wavelength light via the so-called "red forms" present in the Lhca3 and Lhca4 subunits (Morosinotto *et al*., 2003; Wientjes *et al*., 2011a). These forms have been investigated in purified complexes, but little is known about their function *in vivo*. Their effect on the overall trapping rate of PSI is negligible and, indeed, in their absence, trapping efficiency remains greater than 97% (Wientjes *et al*., 2011c). Our data (Figure 2) do not support the hypothesis of a specific function of LHCI in PSI photoprotection (Ihalainen *et al*., 2005; Alboresi *et al*., 2009). Finally, it has been suggested (Rivadossi *et al*., 1999) that LHCI enhances PSI cross section under specific light regimes under canopy, i.e. radiation with $\lambda > 680$ nm. Despite accounting for a small fraction (4–5%) of the light absorbed under normal daylight conditions, red forms are responsible for absorbing up to 40% of the light reflected and scattered by the leaf layers (Rivadossi *et al*., 1999), which seems to indicate that the role of LHCI is to optimize long-term acclimation at light regimes favoring PSI. However, it is known that growth under low light conditions (Q_A largely oxidized) causes an accumulation of LHCII bound to PSI, while the LHCI antenna system remains unchanged (Ballottari *et al*., 2007), and this response proves effective for balancing photon absorption by the two PSs, and maintaining high quantum efficiency for electron transport (Rivadossi *et al*., 1999). A similar mechanism has been observed in *C. reinhardtii* whose PSI-LHCI, though lacking red forms, exhibits a larger LHCI moiety than that of plant supercomplexes but a similar average lifetime (50 ps) (Le Quiniou *et al*., 2015), thus suggesting that a larger antenna size can compensate for the absence of red Chls in algal *vs.* plant PSI-LHCI.

Fluctuating light strongly affects ΔLhca plant growth

Successful acclimation of the photosynthetic apparatus to changing light intensity relies on maintaining the PQ pool oxidized (Bellafiore *et al*., 2005; Joliot *et al*., 2011; Suorsa *et al*., 2012).

ΔLhca plants grown under FL conditions were significantly more stunted than when exposed to constant EL. An alteration in the STN7-dependent retrograde signaling cascade (Pesaresi *et al*., 2009) can be ruled out as a cause, because STN7 is fully active in both genotypes, as proved by the similar modulation patterns of their PSI/PSII and LHCII/PSII ratios under conditions of FL and CL (Supplemental Figure S6).

Recently, fluctuating light conditions were reported to cause stunted growth in the *pgr5* mutant by disrupting the regulation of electron transport to the PSI via the Cyt b_6f complex (Suorsa *et al*., 2012), a result supporting the idea that PGR5 plays an active role in protecting PSI from photodamage to its Fe-S centers when the light intensity shifts from low to high (Tikkanen *et al*., 2012; Allahverdiyeva *et al*., 2015). The phenotype of *ΔLhca* plants is clearly different, in that P700 activity inhibition rates were similar to those of wild type plants (Figure 4C).

Rather, a greater perturbation of redox homeostasis was observed in *ΔLhca vs.* wild type exposed to FL. NPQ buffers the effect of LL to EL transitions by adjusting its PSII to PQ electron transfer rate, yet a balanced excitation of PSs ensured by the reversible migration of LHCII is also required. Under conditions of FL, the redox unbalance displayed by *ΔLhca* plants reveals that the depletion of LHCI cannot be entirely compensated by greatly enhancing the transition to state II (Figure 4D, E). Indeed, reiteration of HL pulses leads to an over-reduction of PQ and a progressive decline in PSII quantum yield, while the decay rate in maximum photooxidizable P700 is the same in both genotypes (Figure 4C). Hence, in the absence of a compensatory increase in PSI core content (Supplemental Figure S6), the reduced cross section of PSI fails to oxidize the electron transport chain during the LL intervals. Indeed, the state of sustained Q_A over-reduction is the most relevant feature of *ΔLhca* plants. We conclude that the stunted growth of this genotype cannot be explained only by the missing Chl complement of LHCI (57 Chl) which to a large extent compensated by a LHCII trimer (42 Chl) (Liu *et al*., 2004; Qin *et al*., 2015) provided by state transitions (Figure 4D-E). The difference in the size of the PSI cross-section observed in mutant plants respect to wild type upon state transitions could be larger than expected on the assumption that a single LHCII trimer can bind to PSI (Galka *et al*., 2012), according to recent findings suggesting that PSI-LHCI-LHCII supercomplexes of the grana margins contain two or even three LHCII (Benson *et al*., 2015) (Bos *et al*., 2017). However, this

possibility does account for the over-reduction of PQ at low light intensity but not at high irradiances. An additional reason for the reduced PQ in low light and for the inability to restore PQ during the low light periods under intermittent illumination could be the narrower range of wavelengths absorbed by the PSI core-bound LHCII of the mutant respect to that provided by LHCI in wild type plants. The abundant PSII-LHCII antenna system competes for the same wavelengths with LHCII bound to PSI. Thus the LHCII antenna of PSI in *ΔLhca* is "over-shaded" while the PSI antenna of wild type extends its absorption to far-red spectral forms transmitted by LHCII (Laisk *et al*., 2014). Figure 5 illustrates the light harvesting differences between wild type and mutant plants. As shown in Panel A, the wild type PSI-LHCI is strongly favored in absorbing wavelengths >685 nm, very abundant under canopies or in multicellular organisms, with respect to PSI-LHCII which, on the other hand, transmits more photons in the 685-750 nm range (Figure 5A,B) thus limiting PSI activity and causing PQ over-reduction (Figure 5C). This suggests LHCI optimizes light-to-biomass conversion efficiency under different light environments. To verify this hypothesis, wild type and *ΔLhca* plants were grown under fluorescent *vs*. halogen lamps, the latter being enriched in far-red wavelengths (Figure 5D). Fresh weights measured at the end of growth period consistently showed the highest biomass production in wild type grown under halogen lamps, while FW of *ΔLhca* plants was (i) significantly lower than wild type, and (ii) unaffected by the presence of light enriched in wavelengths above 680 nm (Figure 5E).

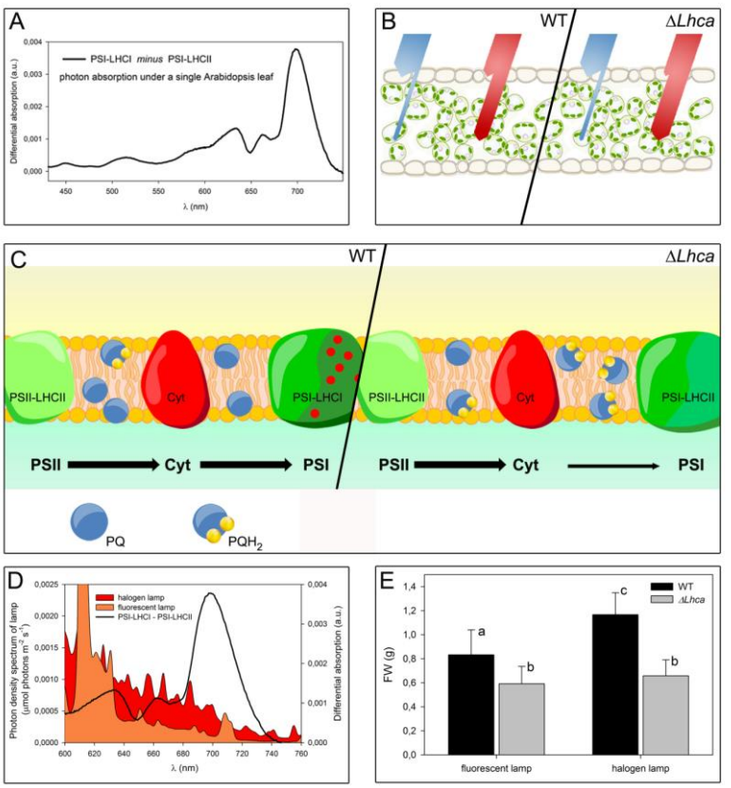

Figure 5. Functional significance of LHCI in optimizing photosynthetic electron flow. (A) Differential absorption of PSI-LHCI (from wild type) *vs.* PSI-LHCII (from *ΔLhca*) complexes. Spectra were normalized to the same molar concentration and corrected for leaf transmittance. Replacing LHCI with LHCII reduces the absorption cross section of the PSI complex, particularly at wavelengths > 690 nm. (B) In a multicellular situation, such as a leaf, and under canopy, the strong absorption of PSII-LHCII endorses the preferential transmittance of far-red wavelengths. In *ΔLhca,* the lack of red forms leads to a lower photon absorption as compared to the wild type. (C) The reduced PSI absorption cross section in mutant leaves is responsible for the decreased excitation of PSI and over-reduction of PQ observed in *ΔLhca*. Abbreviations: PSI/PSII, Photosystem I/II; Cyt, cytochrome b_6f, PQ/PQH_2, plastoquinone/plastoquinol; the thickness of the black arrows is linked to electron flow intensity. (D) The photon density spectrum of direct light was measured for growth chamber set at ~120 µmol photons m^{-2} s^{-1}, and equipped with either halogen lamps OSRAM HQI-T 250W (red area in the graph) or fluorescent lamps OSRAM lumilux coolwhite L58W (orange area). Differential absorption of PSI-LHCI *vs.* PSI-LHCII is reported (black line). The Red/Far Red photon ratio (photons in the 600-680 nm / photons in the 680-760 nm range) of the two light conditions was of 9.24 and 3.15, respectively for the fluorescent light and the halogen light. (E) Fresh weight of plants, grown for 25 days in the two different light regimes, was determined. Values marked with the same letters are not significantly different from each other (Student's *t* test, $P < 0.05$, $n > 7$). Under every condition tested, the growth rate of the mutant plant was significantly lower than that of the corresponding wild type, with the greatest difference recorded under FR-enriched light.

Taken together, our data indicate that a complete PSI-LHCI supercomplex endowed with red-spectral forms plays a crucial role in optimizing the thylakoid electron flow by outcompeting LHCII in harvesting far-red photons and maintaining high PSI activity and PQ oxidation particularly under LL, making the effect of FL conditions especially photoinhibitory for PSII. The evolution of light harvesting systems with distinct spectral properties for PSI *vs.* PSII has been a long process. Early prasinophyceae share the same light-harvesting proteins in PSI and PSII (Durnford *et al*., 1999; Six *et al*., 2005) and the development of red form-enriched LHCI is incomplete in green algae, presumably due to the low availability of red photons in water (Mass *et al*., 2010). In mosses, the first colonizers of land, the red chlorophyll-rich antenna complex Lhca4 is still absent (Alboresi *et al*., 2008), and is partially compensated by accumulation of LHCII in stroma (PSI) membranes. In more recent evolutionary times, thick canopies developed: the light passing through, reflected and scattered by the leaves, altered its wavelength, shifting towards $\lambda > 680$ nm (Ballare *et al*., 1990). The diversity of the PSI and PSII antennas hence contributed to maintaining the PQ redox state and avoiding photoinhibition under these highly variable lighting conditions. We therefore suggest that the function of LHCI is to optimize linear electron flow, particularly in limiting light conditions, rather than enhance PSI photoprotection (Alboresi *et al*., 2009).

References

Ahn TK, Avenson TJ, Ballottari M, Cheng YC, Niyogi KK, Bassi R, Fleming GR. 2008. Architecture of a charge-transfer state regulating light harvesting in a plant antenna protein. Science **320**, 794-797.

Alboresi A, Ballottari M, Hienerwadel R, Giacometti GM, Morosinotto T. 2009. Antenna complexes protect Photosystem I from photoinhibition. BMC.Plant Biol. **9**, 71.

Alboresi A, Caffarri S, Nogue F, Bassi R, Morosinotto T. 2008. In silico and biochemical analysis of Physcomitrella patens photosynthetic antenna: identification of subunits which evolved upon land adaptation. PLoS.One. **3**, e2033.

Allahverdiyeva Y, Suorsa M, Tikkanen M, Aro E-M. 2015. Photoprotection of photosystems in fluctuating light intensities. J.Exp.Bot. **66**, 2427-2436.

Allen JF. 1992. Protein phosphorylation in regulation of photosynthesis. Biochim.Biophys.Acta **1098**, 275-335.

Amunts A, Toporik H, Borovikova A, Nelson N. 2010. Structure determination and improved model of plant Photosystem I. J.Biol Chem. **285**, 3478-3486.

Anderson JM. 1986. Photoregulation of the composition, function and structure of thylakoid membranes. Ann.Rev.Plant Physiol. **37**, 93-136.

Asada K. 1999. The water-water cycle in chloroplasts: scavenging of active oxygens and dissipation of excess photons. Annu.Rev.Plant Physiol Plant Mol.Biol. **50**, 601-639.

Baker NR. 2008. Chlorophyll fluorescence: a probe of photosynthesis in vivo. Annu.Rev.Plant Biol. **59**, 89-113.

Ballare CL, Scopel AL, Sanchez RA. 1990. Far-Red Radiation Reflected from Adjacent Leaves - An Early Signal of Competition in Plant Canopies. Science **247**, 329-332.

Ballottari M, Dall'Osto L, Morosinotto T, Bassi R. 2007. Contrasting behavior of higher plant photosystem I and II antenna systems during acclimation. Journal of Biological Chemistry **282**, 8947-8958.

Ballottari M, Govoni C, Caffarri S, Morosinotto T. 2004. Stoichiometry of LHCI antenna polypeptides and characterisation of gap and linker pigments in higher plants Photosystem I. Eur.J.Biochem. **271**, 4659-4665.

Barber J, Andersson B. 1992. Too Much of a Good Thing - Light Can Be Bad for Photosynthesis. Trends Biochem.Sci. **17**, 61-66.

Bellafiore S, Barneche F, Peltier G, Rochaix JD. 2005. State transitions and light adaptation require chloroplast thylakoid protein kinase STN7. Nature **433**, 892-895.

Benson SL, Maheswaran P, Ware MA, Hunter CN, Horton P, Jansson S, Ruban AV, Johnson MP. 2015. An intact light harvesting complex I antenna system is required for complete state transitions in Arabidopsis. Nature plants **1**, 15176.

Bos I, Bland KM, Tian L, Croce R, Frankel LK, Van Amerongen H, Bricker TM, Wientjes E. 2017. Multiple LHCII antennae can transfer energy efficiently to a single Photosystem I. Biochim.Biophys.Acta **1858**, 371-378.

Bressan M, Dall'Osto L, Bargigia I, Alcocer MJP, Viola D, Cerullo G, D'Andrea C, Bassi R, Ballottari M. 2016. LHCII can substitute for LHCI as an antenna for Photosystem I but with reduced light harvesting capacity. Nature plants **2**, 16131.

Carbonera D, Agostini G, Morosinotto T, Bassi R. 2005. Quenching of chlorophyll triplet states by carotenoids in reconstituted Lhca4 subunit of peripheral light-harvesting complex of photosystem I. Biochemistry **44**, 8337-8346.

Casazza AP, Tarantino D, Soave C. 2001. Preparation and functional characterization of thylakoids from Arabidopsis thaliana. Photosynth.Res. **68**, 175-180.

Castelletti S, Morosinotto T, Robert B, Caffarri S, Bassi R, Croce R. 2003. Recombinant Lhca2 and Lhca3 subunits of the photosystem I antenna system. Biochemistry **42**, 4226-4234.

Cazzaniga S, Bressan M, Carbonera D, Agostini A, Dall'Osto L. 2016. Differential Roles of Carotenes and Xanthophylls in Photosystem I Photoprotection. Biochemistry **55**, 3636-3649.

Cazzaniga S, Dall'Osto L, Kong SG, Wada M, Bassi R. 2013. Interaction between avoidance of photon absorption, excess energy dissipation and zeaxanthin synthesis against photoxidative stress in Arabidopsis. Plant Journal **76**, 568-579.

Cazzaniga S, Li Z, Niyogi KK, Bassi R, Dall'Osto L. 2012. The Arabidopsis szl1 mutant reveals a critical role of b-carotene in photosystem I photoprotection. Plant Physiol. **159**, 1745-1758.

Croce R, Morosinotto T, Castelletti S, Breton J, Bassi R. 2002. The Lhca antenna complexes of higher plants photosystem I. Biochimica et Biophysica Acta-Bioenergetics **1556**, 29-40.

Dall'Osto L, Bressan M, Bassi R. 2015. Biogenesis of light harvesting proteins. Biochimica Biophysica Acta **1847**, 861-871.

Dall'Osto L, Caffarri S, Bassi R. 2005. A mechanism of nonphotochemical energy dissipation, independent from Psbs, revealed by a conformational change in the antenna protein CP26. Plant Cell **17**, 1217-1232.

Dall'Osto L, Cazzaniga S, Havaux M, Bassi R. 2010. Enhanced photoprotection by protein-bound vs free xanthophyll pools: a comparative analysis of chlorophyll b and xanthophyll biosynthesis mutants. Mol.Plant **3**, 576-593.

Dall'Osto L, Unlu C, Cazzaniga S, Van Amerongen H. 2014. Disturbed excitation energy transfer in Arabidopsis thaliana mutants lacking minor antenna complexes of photosystem II. Biochimica Biophysica Acta **1837**, 1981-1988.

Durnford DG, Deane JA, Tan S, McFadden GI, Gantt E, Green BR. 1999. A phylogenetic assessment of the eukaryotic light-harvesting antenna proteins, with implications for plastid evolution. J.Mol.Evolution **48**, 59-68.

Galka P, Santabarbara S, Khuong TTH, Degand H, Morsomme P, Jennings RC, Boekema EJ, Caffarri S. 2012. Functional analyses of the plant Photosystem I–Light-harvesting complex II supercomplex reveal that Light-harvesting complex II loosely bound to Photosystem II is a very efficient antenna for Photosystem I in state II. Plant Cell **24**, 2963-2978.

Ganeteg U, Kulheim C, Andersson J, Jansson S. 2004. Is each light-harvesting complex protein important for plant fitness? Plant Physiol **134**, 502-509.

Gilmore AM, Yamamoto HY. 1991. Zeaxanthin formation and energy-dependent fluorescence quenching in pea chloroplasts under artificially mediated linear and cyclic electron transport. Plant Physiol. **96**, 635-643.

Grieco M, Tikkanen M, Paakkarinen V, Kangasjarvi S, Aro EM. 2012. Steady-State Phosphorylation of Light-Harvesting Complex II Proteins Preserves Photosystem I under Fluctuating White Light. Plant Physiology **160**, 1896-1910.

Havaux M, Dall'Osto L, Bassi R. 2007. Zeaxanthin has enhanced antioxidant capacity with respect to all other xanthophylls in Arabidopsis leaves and functions independent of binding to PSII antennae. Plant Physiol **145**, 1506-1520.

Havaux M, Dall'Osto L, Cuine S, Giuliano G, Bassi R. 2004. The effect of zeaxanthin as the only xanthophyll on the structure and function of the photosynthetic apparatus in Arabidopsis thaliana. J.Biol.Chem. **279**, 13878-13888.

Havaux M, Eymery F, Porfirova S, Rey P, Dormann P. 2005. Vitamin E protects against photoinhibition and photooxidative stress in *Arabidopsis thaliana*. Plant Cell **17**, 3451-3469.

Horton P, Ruban AV, Walters RG. 1996. Regulation of light harvesting in green plants. Annu.Rev.Plant Physiol.Plant Mol.Biol. **47**, 655-684.

Ihalainen JA, Croce R, Morosinotto T, van Stokkum IH, Bassi R, Dekker JP, van Grondelle R. 2005. Excitation decay pathways of Lhca proteins: a time-resolved fluorescence study. Journal of Physical Chemistry B **109**, 21150-21158.

Jansson S. 1999. A guide to the Lhc genes and their relatives in Arabidopsis. Trends Plant Sci. **4**, 236-240.

Jarvi S, Suorsa M, Paakkarinen V, Aro E-M. 2011. Optimized native gel systems for separation of thylakoid protein complexes: novel super- and mega-complexes. Biochem.J. **439**, 207-214.

Johnson GN, Young AJ, Horton P. 1994. Activation of non-photochemical quenching in thylakoids and leaves. Planta **194**, 550-556.

Joliot P, Johnson GN. 2011. Regulation of cyclic and linear electron flow in higher plants. Proc.Natl.Acad.Sci.U.S.A **108**, 13317-13322.

Klimmek F, Ganeteg U, Ihalainen JA, van Roon H, Jensen PE, Scheller HV, Dekker JP, Jansson S. 2005. The structure of higher plant LHCI: in vivo characterisation and structural interdependence of the Lhca proteins. Biochemisty **44**, 3065-3073.

Klimmek F, Sjodin A, Noutsos C, Leister D, Jansson S. 2006. Abundantly and rarely expressed Lhc protein genes exhibit distinct regulation patterns in plants. Plant Physiol **140**, 793-804.

Krieger-Liszkay A. 2005. Singlet oxygen production in photosynthesis. J.Exp.Bot. **56**, 337-346.

Laemmli UK. 1970. Cleavage of structural proteins during the assembly of the head of bacteriophage T4. Nature **227**, 680-685.

Laisk A, Oja V, Eichelmann H, Dall'Osto L. 2014. Action spectra of photosystems II and I and quantum yield of photosynthesis in leaves in State 1. Biochimica et Biophysica Acta **1837**, 315-325.

Lam E, Ortiz W, Malkin R. 1984. Chlorophyll a/b proteins of photosystem I. FEBS Lett. **168**, 10-14.

Le Quiniou C, Tian LJ, Drop B, Wientjes E, van Stokkum IHM, van Oort B, Croce R. 2015. PSI-LHCI of Chlamydomonas reinhardtii: Increasing the absorption cross section without losing efficiency. Biochimica et Biophysica Acta-Bioenergetics **1847**, 458-467.

Li XP, Bjorkman O, Shih C, Grossman AR, Rosenquist M, Jansson S, Niyogi KK. 2000. A pigment-binding protein essential for regulation of photosynthetic light harvesting. Nature **403**, 391-395.

Li ZR, Wakao S, Fischer BB, Niyogi KK. 2009. Sensing and responding to excess Light. Ann.Rev.Plant Biol. **60**, 239-260.

Liu Z, Yan H, Wang K, Kuang T, Zhang J, Gui L, An X, Chang W. 2004. Crystal structure of spinach major light-harvesting complex at 2.72 A resolution. Nature **428**, 287-292.

Mass T, Kline DI, Roopin M, Veal CJ, Cohen S, Iluz D, Levy O. 2010. The spectral quality of light is a key driver of photosynthesis and photoadaptation in Stylophora pistillata colonies from different depths in the Red Sea. Journal of Experimental Biology **213**, 4084-4091.

Mazor Y, Borovikova A, Nelson N. 2015. The structure of plant photosystem I super-complex at 2.8 Å resolution. Elife **4:e07433**.

Morosinotto T, Breton J, Bassi R, Croce R. 2003. The nature of a chlorophyll ligand in Lhca proteins determines the far red fluorescence emission typical of photosystem I. J.Biol.Chem. **278**, 49223-49229.

Morosinotto T, Mozzo M, Bassi R, Croce R. 2005. Pigment-pigment interactions in Lhca4 antenna complex of higher plants photosystem I. Journal of Biological Chemistry **280**, 20612-20619.

Munekage Y, Hojo M, Meurer J, Endo T, Tasaka M, Shikanai T. 2002. PGR5 is involved in cyclic electron flow around photosystem I and is essential for photoprotection in Arabidopsis. Cell **110**, 361-371.

Nelson N, Ben Shem A. 2004. The complex architecture of oxygenic photosynthesis. Nature **5**, 1-12.

Pan X, Li M, Wan T, Wang L, Jia C, Hou Z, Zhao X, Zhang J, Chang W. 2011. Structural insights into energy regulation of light-harvesting complex CP29 from spinach. Nat.Struct.Mol.Biol. **18**, 309-315.

Peng LW, Shikanai T. 2011. Supercomplex Formation with Photosystem I Is Required for the Stabilization of the Chloroplast NADH Dehydrogenase-Like Complex in Arabidopsis. Plant Physiology **155**, 1629-1639.

Pesaresi P, Hertle A, Pribil M, Kleine T, Wagner R, Strissel H, Ihnatowicz A, Bonardi V, Scharfenberg M, Schneider A, Pfannschmidt T, Leister D. 2009. Arabidopsis STN7 Kinase Provides a Link between Short- and Long-Term Photosynthetic Acclimation. Plant Cell **21**, 2402-2423.

Pesaresi P, Pribil M, Wunder T, Leister D. 2011. Dynamics of reversible protein phosphorylation in thylakoids of flowering plants: The roles of STN7, STN8 and TAP38. Biochimica et Biophysica Acta-Bioenergetics **1807**, 887-896.

Peter GF, Takeuchi T, Thornber JP. 1991. Solubilization and two-dimensional electrophoretic procedures for studying the organization and composition of photosynthetic membrane polypeptides. Methods: A Companion to Methods in Enzymology **3**, 115-124.

Qin X, Suga M, Kuang T, Shen J-R. 2015. Structural basis for energy transfer pathways in the plant PSI-LHCI supercomplex. Science **348**, 989-995.

Rivadossi A, Zucchelli G, Garlaschi FM, Jennings RC. 1999. The importance of PSI chlorophyll red forms in light-harvesting by leaves. Photosynt.Res. **60**, 209-215.

Ruban AV, Wentworth M, Yakushevska AE, Andersson J, Lee PJ, Keegstra W, Dekker JP, Boekema EJ, Jansson S, Horton P. 2003. Plants lacking the main light-harvesting complex retain photosystem II macro-organization. Nature **421**, 648-652.

Schägger H, von Jagow G. 1987. Tricine-sodium dodecyl sulfate-polyacrylamide gel electrophoresis for the separation of proteins in the range from 1 to 100 kDa. Anal.Biochem. **166**, 368-379.

Six C, Worden AZ, Rodriguez F, Moreau H, Partensky F. 2005. New insights into the nature and phylogeny of prasinophyte antenna proteins: Ostreococcus tauri, a case study. Molecular Biology and Evolution **22**, 2217-2230.

Sonoike K. 2011. Photoinhibition of Photosystem I. Physiol Plant **142**, 56-64.

Suorsa M, Jarvi S, Grieco M, Nurmi M, Pietrzykowska M, Rantala M, Kangasjarvi S, Paakkarinen V, Tikkanen M, Jansson S, Aro EM. 2012. Proton Gradient Regulation5 Is Essential for Proper Acclimation of Arabidopsis Photosystem I to Naturally and Artificially Fluctuating Light Conditions. Plant Cell **24**, 2934-2948.

Telfer A, Dhami S, Bishop SM, Phillips D, Barber J. 1994. b-carotene quenches singlet oxygen formed by isolated photosystem II reaction centers. Biochemistry **33**, 14469-14474.

Tikkanen M, Grieco M, Nurmi M, Rantala M, Suorsa M, Aro EM. 2012. Regulation of the photosynthetic apparatus under fluctuating growth light. Philosophical Transactions of the Royal Society B-Biological Sciences **367**, 3486-3493.

Wientjes E, Croce R. 2011a. The light-harvesting complexes of higher-plant Photosystem I: Lhca1/4 and Lhca2/3 form two red-emitting heterodimers. Biochemical Journal **433**, 477-485.

Wientjes E, van Stokkum IHM, Van Amerongen H, Croce R. 2011b. Excitation-Energy Transfer Dynamics of Higher Plant Photosystem I Light-Harvesting Complexes. Biophysical Journal **100**, 1372-1380.

Wientjes E, van Stokkum IHM, Van Amerongen H, Croce R. 2011c. The Role of the Individual Lhcas in Photosystem I Excitation Energy Trapping. Biophysical Journal **101**, 745-754.

Yang J-S, Wang R, Meng J-J, Bi Y-P, Xu P-L, Guo F, Wan S-B, He Q-W, Li XG. 2010. Overexpressionof Arabidopsis CBF1 gene in transgenic tobacco alleviates photoinhibition of PSII and PSI during chilling stress under low irradiance. J.Plant Physiol. **167**, 534-539.

Zhang S, Scheller HV. 2004. Photoinhibition of Photosystem I at chilling temperature and subsequernt recovery in Arabidopsis thaliana. Plant and Cell Physiology **45**, 1595-1602.

Supplemental Data

Supplemental Figure S1. Structural model of the PSI-LHCI-LHCII supercomplex. The model has been assembled based on the high-resolution structures of PSI-LHCI ((Qin et al. 2015), PDB ID: 3LW5) and LHCII ((Liu et al. 2004), PDB ID: 1RWT) and on the electron microscopy map from (Galka et al. 2012).

Figure S2. Phenotype of wild type and mutant plants. (A) Wild type and *ΔLhca* plants were grown in soil for 5 weeks under controlled conditions (150 µmol photons m^{-2} s^{-1}, 23°C, 8/16 hours day/night regime). Fresh weights (mg): wild type, 911 ± 185; *ΔLhca*, 383 ± 89. (B) Fresh weight of wild type and single *koLhca* rosettes. Plants were grown as in (A). Values marked with the same letters are not significantly different from each other (Student's *t* test, $P < 0.05$, $n = 7$). (C) Western-blot analysis of leaf extracts, with antibodies specific for the proteins indicated in each filter. MW, pre-stained molecular weight marker.

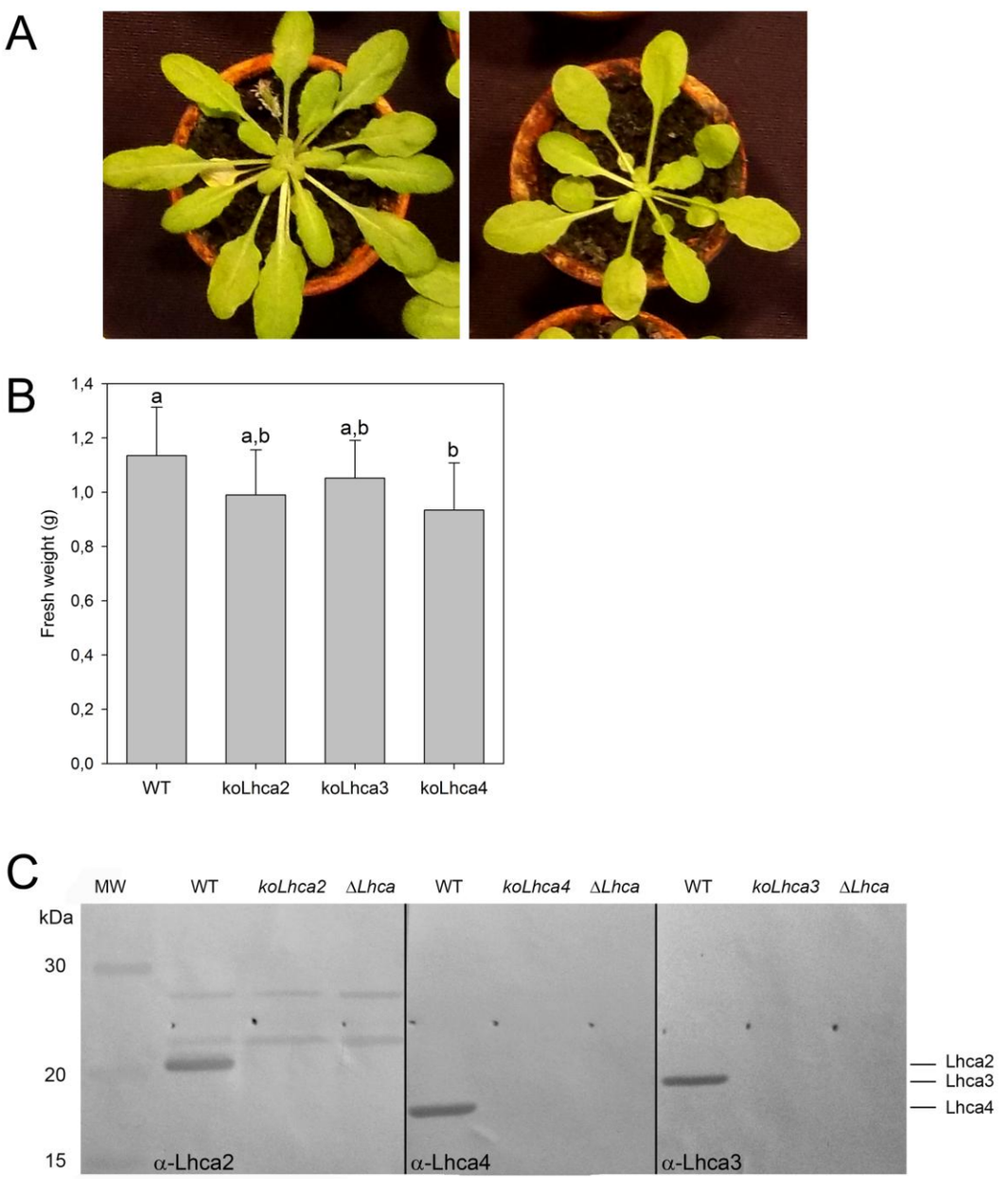

Figure S3. Composition of thylakoid pigment-binding complexes from wild type and *ΔLhca* plants. (A) Thylakoid pigment-protein complexes were separated by nondenaturing CN-PAGE after solubilization with 0.1% α-DM and 0.6% digitonin. Thylakoids corresponding to 25 µg of Chls were loaded onto each lane. (B) The RT absorption spectra of PSI-LHCI (from wild type, black line) and the PSI core complex (from *ΔLhca*, red line) purified by CN-PAGE were determined. These spectra were normalized to the maximum in the red region. Inset: detail of abs spectra at λ > 680 nm, together with the difference spectra (dotted) multiplied by 10. (C) PSI/PSII and LHCII/PSII were measured by immunotitration in wild type and *ΔLhca* thylakoids. Ratios were expressed as a percentage of the corresponding wild type value. PSIIc/PSIc, PSII/PSI core complex.

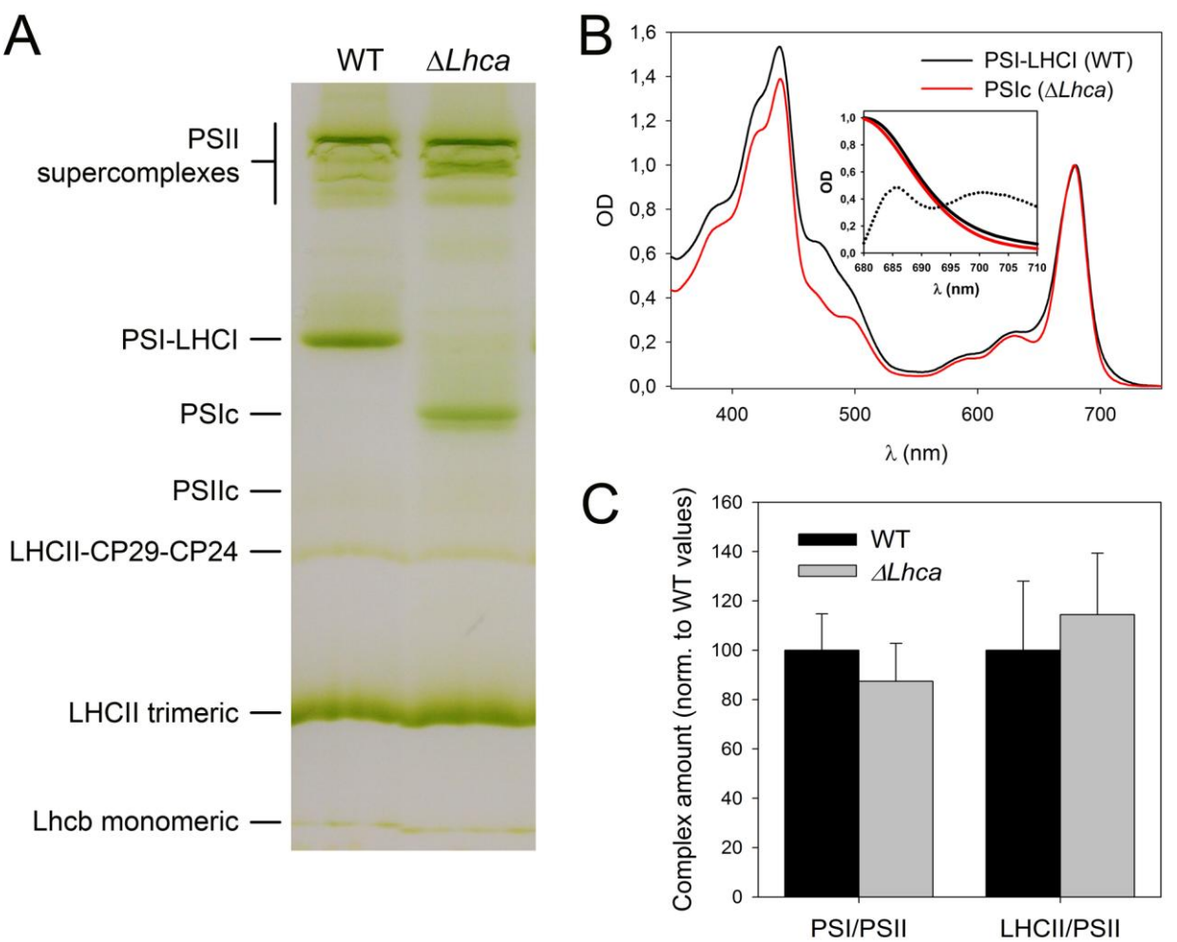

Supplemental Figure S4. Biochemical characterization of pigment-protein complexes. (A) Thylakoid pigment-protein complexes were separated by nondenaturing Deriphat-PAGE upon solubilization with 0.6% digitonin. Thylakoids corresponding to 25 µg of Chls were loaded in each lane. (B) Two-dimensional PAGE analysis of wild type and *ΔLhca* thylakoids membrane proteins. Native PAGE (panel A) was followed by separation of proteins in the second dimension by SDS-PAGE, and Coomassie staining. Bands of PSI-LHCI and monomeric PSII core were included in the 2D-PAGE as reference. Few distinctive proteins useful to identify the different complexes are indicated, according to molecular weight and previous analyses (Ballottari et al. 2004;Caffarri et al. 2009;Jarvi et al. 2011). (C) Western-blot used for immunotitration of photosynthetic subunits in the wild type and *ΔLhca* thylakoids (see histogram, Figure S3C). Analysis was performed with antibodies directed against the PSI core subunit PsaA, the PSII core subunit PsbB (CP47), the major light-harvesting complex LHCII.

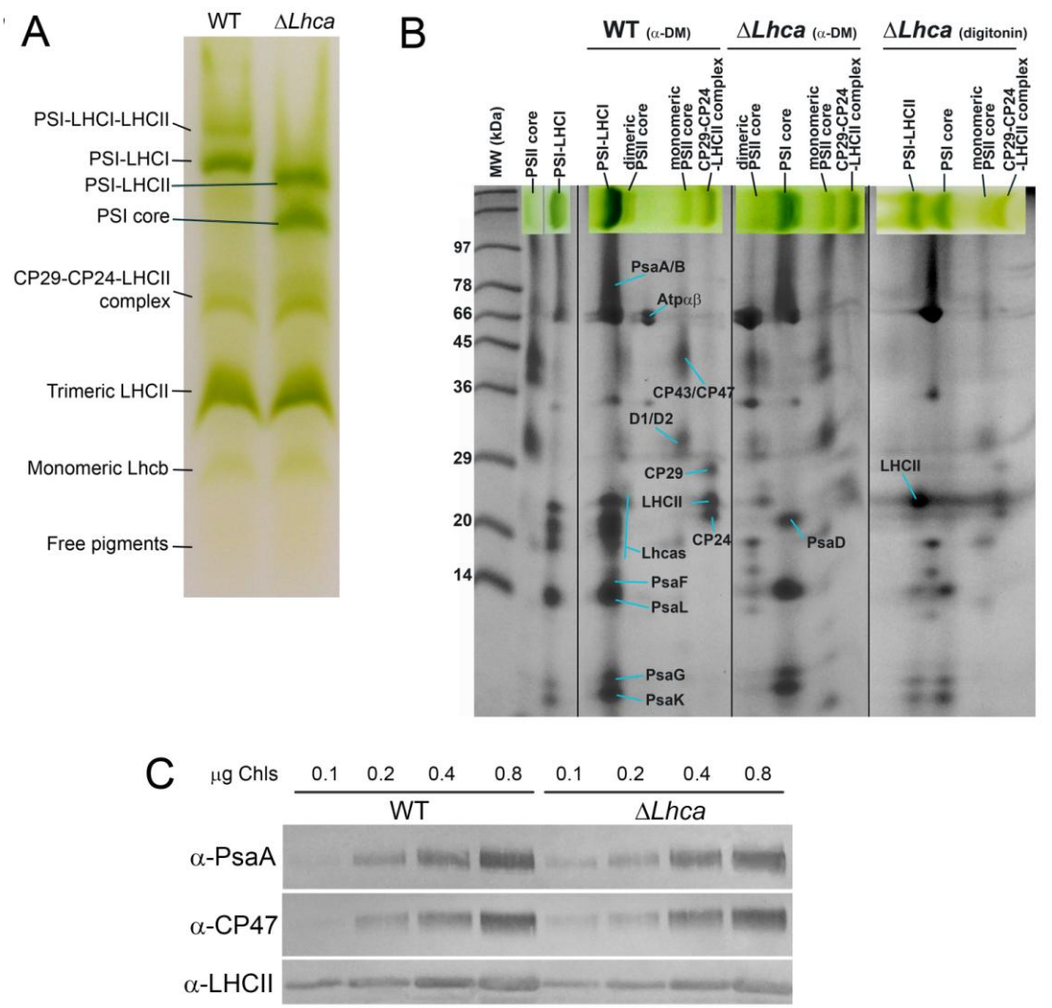

Supplemental Figure S5. Cyclic electron flow (CEF) in wild type and *ΔLhca*. CEF was quantified by measuring the increases in Chl fluorescence in thylakoids, under low measuring light at the PAM, after the addition of NADPH and ferredoxin (Fd) (see Methods for details).

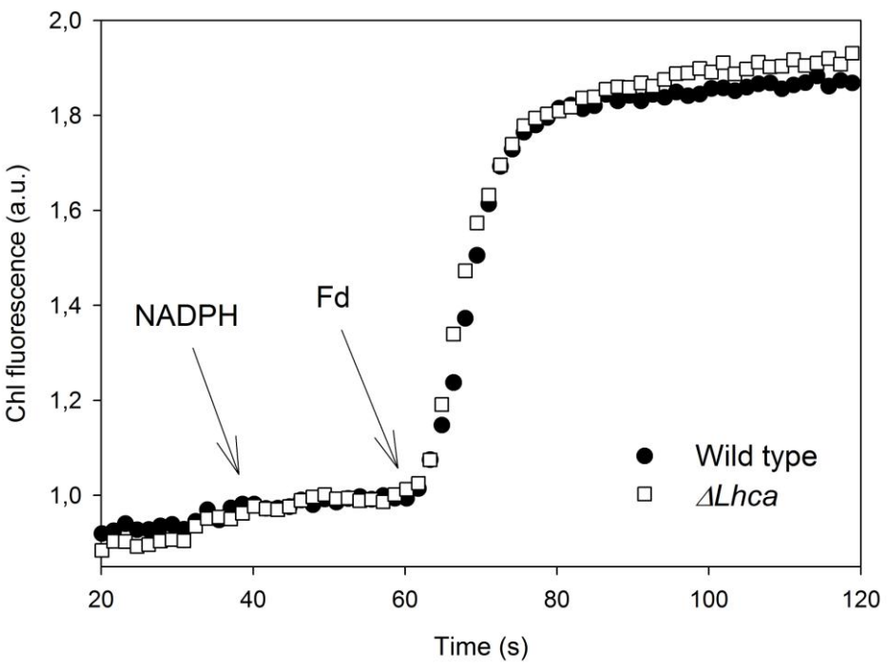

Supplemental Figure S6. Regulation of pigment-protein composition upon acclimation to fluctuating light. Changes of the PSI/PSII and Lhcb/PSII ratios following acclimation to fluctuating light conditions is reported. Lhcb, PSI and PSII core content were evaluated from non-denaturing gels. Data are expressed as mean ± SD, n = 3.

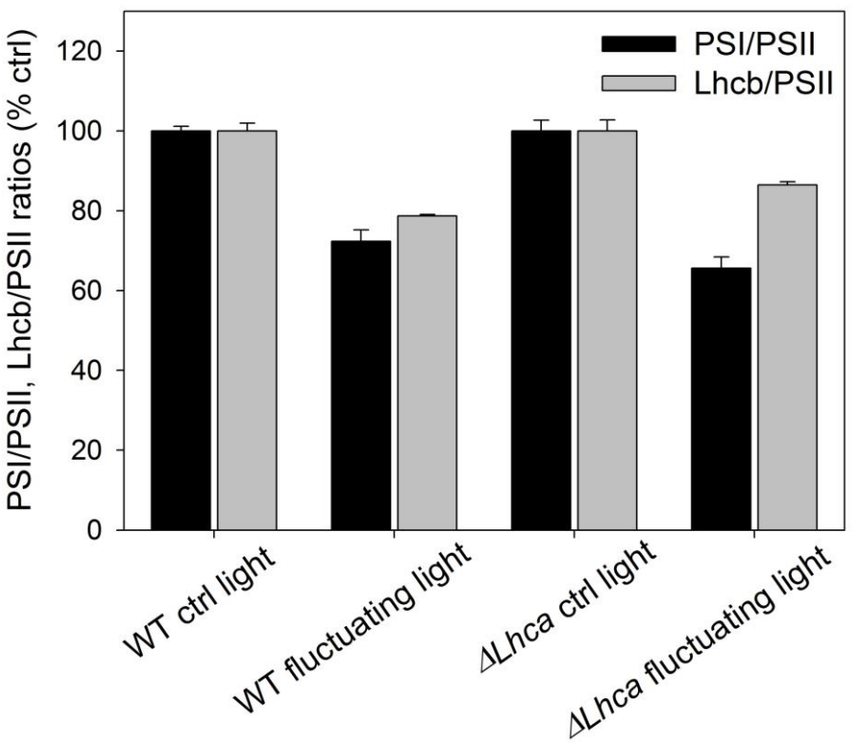

Reference List

1. Ballottari M. et al. (2004) Stoichiometry of LHCI antenna polypeptides and characterisation of gap and linker pigments in higher plants Photosystem I. *Eur.J.Biochem.* **271**, 4659-4665.

2. Caffarri S. et al. (2009) Functional architecture of higher plant photosystem II supercomplexes. *EMBO J.* **28**, 3052-3063.

3. Galka P. et al. (2012) Functional analyses of the plant Photosystem I–Light-harvesting complex II supercomplex reveal that Light-harvesting complex II loosely bound to Photosystem II is a very efficient antenna for Photosystem I in state II. *Plant Cell* **24**, 2963-2978.

4. Jarvi S. et al. (2011) Optimized native gel systems for separation of thylakoid protein complexes: novel super- and mega-complexes. *Biochem.J.* **439**, 207-214.

5. Liu Z. et al. (2004) Crystal structure of spinach major light-harvesting complex at 2.72 A resolution. *Nature* **428**, 287-292.

6. Qin X. et al. (2015) Structural basis for energy transfer pathways in the plant PSI-LHCI supercomplex. *Science* **348**, 989-995.

Chapter 6

Loss of LHCI system impairs the dynamics of LHCII re-distribution between thylakoid domains

This chapter was submitted to

Journal of Environment and Experimental Botany

Loss of LHCI system impairs the dynamics of LHCII re-distribution between thylakoid domains

Mauro Bressan, Roberto Bassi*, Luca Dall'Osto.

Dipartimento di Biotecnologie, Università di Verona, Strada Le Grazie 15, 37134 Verona, Italy

Abstract

LHCI, the peripheral antenna system of Photosystem I, includes four light-harvesting proteins (Lhca1-Lhca4) in higher plants, all of which are devoid in the *Arabidopsis thaliana* knock-out mutant *ΔLhca*. PSI absorption cross-section was reduced in the mutant, thus affecting the redox balance of the photosynthetic electron chain and yielding into a more reduced PQ respect to the wild type. *ΔLhca* plants developed compensatory response by enhancing LHCII binding to PSI. However, the state transition phenotype, as measured by changes of chlorophyll fluorescence *in vivo,* did not match the high level of PSI-LHCII supercomplex measured biochemically. In order to elucidate the reasons for discrepancy, we further analyzed state transition in *ΔLhca* plants. The STN7 kinase was fully active in the mutant as judged from up-regulation of LHCII phosphorylation in state II. Instead, the lateral heterogeneity of thylakoids was affected by lack of LHCI, yielding into higher LHCII content in stromal membranes respect to the wild type. This redistribution of the highly fluorescent complex affected the overall fluorescence yield of thylakoids already in state I and minimized changes in RT fluorescence yield when LHCII did connect to PSI reaction center. We conclude that interpretation of chlorophyll fluorescence analysis of state transitions becomes problematic when applied to mutants whose thylakoid architecture is significantly modified respect to wild type.

Introduction

In plants and algae, multiple reactions catalyze light-driven electron transport from water to $NADP^+$, sustain ATP production and lead to CO_2 fixation into organic compounds. The photosynthetic machinery includes the thylakoid membrane supercomplexes Photosystems (PS) II and I, which are functionally connected by the electron carrier plastoquinone (PQ), cytochrome b_6f complex and plastocyanin. Chlorophylls (Chl) and carotenoids (Car), chromophores binding to each PS, ensure photon absorption and rapid transfer of the excitation energy to the reaction centre (RC), to fuel charge separation (Nelson and Ben Shem 2004).

Photosystem I catalyzes electron transport from plastocyanin to ferredoxin. PSI core binds Chl *a*, β-carotene and all the co-factors required for electron transport (Qin et al., 2015;Mazor et al., 2015). Also, a peripheral antenna complex (LHCI, light-harvesting complex of PSI) enlarges the PSI absorption cross-section. LHCI, in *Arabidopsis thaliana,* consists of 4 light-harvesting proteins (Lhca1-Lhca4), encoded by single genes (Jansson 1999), that bind Chl *a*, Chl *b,* xanthophylls and β-carotenes (Qin et al., 2015;Mazor et al., 2015). Despite Lhcas share similarities in structure and pigment organization with members of the LHC family (Liu et al., 2004;Amunts et al., 2010;Pan et al., 2011;Qin et al., 2015), these antennae display peculiar spectroscopic properties, including “red spectral forms”, which originates from Chl with energies lower than P700 RC (Lam et al., 1984).

However, the high conservation of LHCI subunits suggests a specific function for LHCI in the acclimation to environmental cues. Indeed, characterization of *Arabidopsis* mutants with decreased levels of Lhca subunits (Klimmek et al., 2005) showed a reduced fitness under natural conditions (Ganeteg et al., 2004).

A peculiar property of the peripheral antenna system is its ability to modulate the light-harvesting capacity of PSs and optimize electron transport in response to the light environment (Horton et al., 1996;Dall'Osto et al., 2015), namely the fluctuations in both intensity and spectrum, which easily yield into unbalanced excitation of PSs and decrease the photosynthetic efficiency (Pesaresi et al., 2010). PSII and PSI regulate light harvesting differently: PSII typically displays (i) a short-term feed-back control of excess excitation energy (Ruban et al., 2012) and (ii) long-term decrease in LHCII content under excess light. Instead, the light-harvesting efficiency of LHCI nor the PSI-core/LHCI ratio were affected by sustained over-excitation (Anderson 1986;Ballottari et al., 2007;Cazzaniga et al., 2016).

Rather, the PSII/PSI excitation imbalance is compensated by recruiting LHCII as a supplementary antenna for PSI by the mechanism of state transitions (ST) (Allen 1992;Galka et al., 2012). ST reorganize the PSs antenna system on a timescale of minutes, and involve the lateral movement of a mobile LHCII pool , which reversibly associates with either PSI or PSII. PSII over-excitation reduces PQ to PQH_2 which activates thylakoid protein kinase STN7 and, in turn, phosphorylates LHCII (Bellafiore et al., 2005). These reactions ultimately yields into the so-called state II, with enhanced PSI antenna size and electron transport activity. Conversely, over-excitation of PSI results into oxidation of the PQ pool, inactivation of the LHCII kinase and dephosphorylation of P-LHCII by TAP38 phosphatase (Pribil et al., 2010). De-phosphorylated LHCII detaches from PSI and return to PSII (state I).

While ST involve LHCII, recent results (Benson et al., 2015) showed that absence of specific Lhca subunits reduces amplitude of ST in Arabidopsis, with *ΔLhca4* plants showing the most severe phenotype. On the other hand, (Bressan et al., 2016) reported that energy transfer efficiency from LHCII to PSI was, if any, slightly increased in the absence of LHCI, meaning that LHCII is a very good antenna for PSI, with or without its LHCI moiety. Here, we analyze in details the mechanism of ST in absence of LHCI system. To this aim we used the Arabidopsis *ΔLhca* mutant, devoid of all Lhca1-4 subunits (Bressan et al., 2016), and studied its response to changes in light quality. Due to a smaller PSI antenna size, even under conditions promoting the formation of PSI-LHCII supercomplexes (Bressan et al., 2016), PQ pool of *ΔLhca* plants was more reduced than in the wild type and, consistently, LHCII binding to PSI was greatly increased. Instead, decrease of Fm, commonly observed upon state I-state II transition was strongly reduced in the mutant, suggesting LHCII fluorescence quenching by PSI was impaired. We observed that lateral heterogeneity of thylakoids membranes, and distribution of LHCII between grana, margins and stromal lamellae were affected in the mutant respect to the wild type, which might explains the decreased amplitude of fluorescence changes upon ST.

Material and Methods

Plant material and growth conditions – The *Arabidopsis thaliana ΔLhca* mutant was obtained as reported in (Bressan et al., 2016). Plants were maintained in a growth chamber for 5 weeks at 150 µmol photons m^{-2} s^{-1} (OSRAM halogen HQI-T 250W and/or OSRAM lumilux cool white L58W), 23°C, 70% humidity, and 8/16 h of day/night. Induction of either state I or state II was obtained by illuminating plants for 45 min with a PSI light (30-W incandescent bulbs filtered through Lee Filters 027 Medium Red) or a PSII light (30-W warm white fluorescent lamps filtered through Lee Filters 105 Orange) respectively, according to (Pesaresi et al., 2009).

Membrane isolation – Stacked thylakoid membranes were isolated as in (Casazza et al., 2001). Grana-, margin-, and stroma-enriched fractions were isolated as in (Barbato et al., 2000).

Pigment analysis – Pigments were extracted from leaf discs with 85% acetone buffered with Na_2CO_3, separated and quantified by HPLC (Gilmore and Yamamoto 1991).

Spectroscopy - Absorption measurements were performed using a SLM Aminco DW-2000 spectrophotometer at RT either on samples in 10 mM HEPES pH 7.5, 20% (w/v) glycerol, 0.05% α-DM or 0.05% digitonin, or directly on leaves. Fluorescence emission spectra were measured at RT using a Jobin-Yvon Fluoromax-3 spectrofluorimeter.

Gel electrophoresis, immunoblotting and sample preparation – SDS-PAGE analysis was performed with the Tris-Glycine buffer system (Laemmli 1970) with some modifications (Ballottari et al., 2004), and the Tris-Tricine buffer system (Schägger and von Jagow 1987). Nondenaturing Deriphat-PAGE and CN-PAGE were performed following the methods described by (Peter et al., 1991;Jarvi et al., 2011). Thylakoids brought to 1 mg/mL Chls were solubilized in α-DM and digitonin (Galka et al., 2012). After electrophoresis, bands corresponding to PSI supercomplexes were excised, grinded in extraction buffer (0.02% digitonin, 30% glycerol, 10 mM Hepes pH 7.5), then further purified by ultracentrifugation (Galka et al., 2012). For immunotitration, thylakoid samples were loaded onto SDS-PAGE and then electroblotted on nitrocellulose membranes, then proteins were detected using an alkaline phosphatase-conjugated antibody. Primary antibodies: α-Lhca2/3/4 (AS01 006/007/008), α-PsaA (AS06 172), α-PsbB (AS04 038), α-Lhcb1-P/2-P (AS13 2704/705)and α-PsaK (AS04 049) from Agrisera; home-made, polyclonal α-LHCII (immunogen: heterotrimeric LHCII from Arabidopsis).

Cross-linking was carried out as described in (Jansson et al., 1996): purified PSI-LHCI-LHCII and PSI-LHCII complexes (0.05 nmol complex/µl in 10 mM Hepes pH 7.5, 0.1% digitonin) were cross-linked with DTSP (final concentration 0.015%) at RT for 30 min. Samples were solubilized in a non-reducing sample buffer and electrophoresed on 10-20% polyacrylamide gels (Tris-Glycine buffer system). The lanes were then cut out and incubated for 30 min in a sample buffer containing 50 mM DTT + 5% β-mercaptoethanol to cleave the cross-links. The gel slice was placed on top of a second 8-25% polyacrylamide gel and re-electrophoresed. Both α-P-Lhcb2- and α-PsaH-conjugates were detected.

Analysis of Chl fluorescence - State transitions were measured through Chl fluorescence on leaves at RT with a PAM 101 fluorimeter (Heinz-Walz) according to (Jensen et al., 2000). Preferential PSII excitation was provided by illumination with white light filtered through Lee Filters 105 Orange (Pesaresi et al., 2009). F_m levels in state I (F_m') and state II (F_m'') were determined at the end of each cycle by applying a saturating light pulse. The parameter qT (PSII cross-section changes) was calculated as $(F_m' - F_m'')/F_m'$.

Electron microscopy – Intact leaf fragments from wild type and mutant 5-week-old plants, grown under controlled conditions, were fixed, embedded and observed in thin section (de Bianchi et al., 2008).

Results

ΔLhca is a knock-out mutant of Arabidopsis, devoid of the PSI peripheral antenna system

ΔLhca plants (Bressan et al., 2016), grown in a climate chamber (150 µmol photons m^{-2} s^{-1}, 23°C, 8/16 day/night) for 5 weeks, were significantly smaller than wild type (Figure 1A). The organization of pigment-binding supercomplexes was analyzed by non-denaturing Deriphat-PAGE, after solubilizing wild type and *ΔLhca* thylakoids in 0.6% α-DM (Figure 1B).

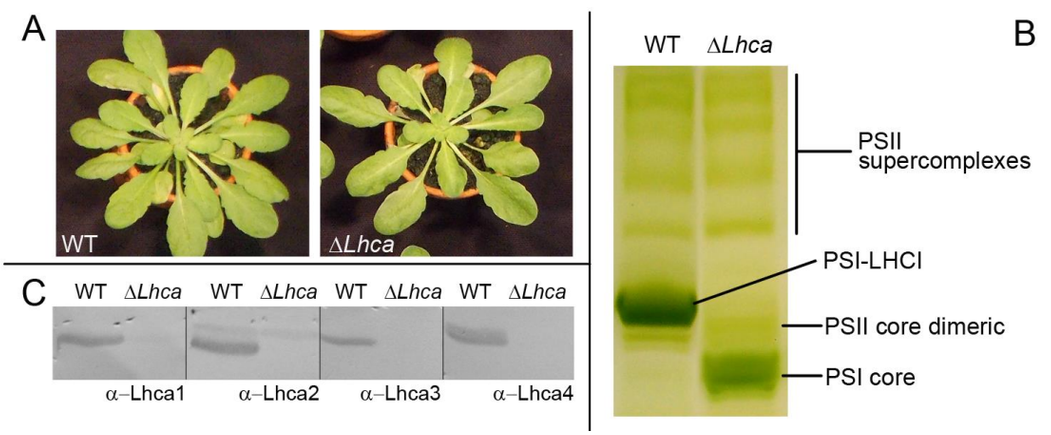

Figure 1. **Characterization of *koLhca* mutant line.** (A) Phenotype of wild type and mutant plants, grown in soil for 5 weeks under controlled conditions (150 µmol photons m^{-2} s^{-1}, 23°C, 8/16 hours day/night regime). (B) Thylakoid pigment-protein complexes were separated by nondenaturing Deriphat-PAGE upon solubilization with 0.6% α-DM. Thylakoids corresponding to 25 µg of Chls were loaded in each lane. The major pigment-protein complexes are indicated. (C) Western-blot analysis of leaf extracts, with antibodies specific for the proteins indicated in each filter.

Several green bands were resolved: in both wild type and mutant, the PSII pigment–proteins migrated as multiple bands with different apparent masses, i.e. the PSII dimeric core and the PSII supercomplexes of different LHCII composition. No significant differences were observed in both mobility and relative abundance of PSII bands in thylakoids from wild type and *ΔLhca*. The PSI-LHCI supercomplex was present as a single major band in the wild type, co-migrating with PSII dimeric core. The most evident difference detected in *ΔLhca vs.* wild type was the lack of PSI-LHCI supercomplex and the presence of a green band with lower apparent mass, corresponding to the core

moiety of PSI (Bressan et al., 2016). As revealed by immunoblotting (Figure 1C), the *ΔLhca* mutant was devoid of all four Lhca subunits.

Regulation of PSI antenna size upon state I – state II transitions

The stunted growth of *ΔLhca* plants (Figure 1A) could be ascribed to an imbalance in the distribution of excitation energy between the two photosystems, as consequence of LHCI depletion and reduced optical cross-section of PSI. Optimization of linear electron transport is normally ensured by rapid relocation of LHCII between PSs through the process of state I – state II transitions, providing a balanced absorption cross section of the two PSs (Bellafiore et al., 2005): over-reduction of the PQ pool promotes LHCII phosphorylation, which causes the displacement of LHCII from PSII to PSI (state II); in contrast, an enhanced excitation of PSI oxidizes the PQ pool and reverses the process to state I.

To investigate whether the lack of LHCI affected photosynthetic electron flow under different light quality, the ST activity was measured on leaves as changes in Chl fluorescence upon PQ reduction (Jensen et al., 2000) (Figure 2A). The fluorescence pattern of *ΔLhca* differed in many respects from that of the wild type and, in particular, the fluorescence level induced (F_s) was far higher in *ΔLhca* during illumination with orange light. Upon addition of 725 nm far-red (FR) light, a marked decrease in fluorescence was observed in both genotypes, consistent with the oxidation of the PQ pool. When the FR light was switched off, both genotypes displayed a similar increase in fluorescence, brought about by the reduction of the PQ pool, followed by a decay whose amplitude was far smaller in *ΔLhca* than the wild type, leading to a greatly reduced qT value (see methods) in *ΔLhca* (1.9 ± 0.5%) respect to wild type (7.9 ± 0.1%). Thus, despite F_s/F_o being higher, consistent with a chronically higher reduction level of PQ, the apparent amplitude of ST was lower in *ΔLhca* than in wild type plants.

We checked the phosphorylation state of both Lhcb1 and Lhcb2 by immunoblotting with specific antibodies after a 45-min exposure of the plants to either PSI or PSII light (Supplemental Figure S1). In state I, no LHCII phosphorylation was detected in either the wild type or *ΔLhca*. In state II, P-LHCII was detected in both and yet, while the level of P-Lhcb1 was similar in both genotypes, P-Lhcb2 was far more abundant (+75%) in the *ΔLhca* mutant, thus implying the decreased amplitude of ST in *ΔLhca* was not due to altered activity of the kinase STN7 nor to a reduced level of the mobile LHCII subpopulation (Leoni et al., 2013). We investigated the ability of *ΔLhca* to form PSI-LHCII

supercomplexes by non-denaturing CN-PAGE of thylakoid samples, adapted to either state I or state II and solubilized by digitonin (Figure 2B). Exposure to PSII light led to the formation of new PSI-containing green bands with higher MW in both the wild type and *ΔLhca,* which were absent in samples harvested from state I-adapted leaves. These high MW bands, which appeared in state II, were consistent with formation of LHCII-binding PSI supercomplexes. In *ΔLhca*, the PSI-LHCII band was three times more abundant than the corresponding PSI-LHCI-LHCII band found in the wild type sample under the same conditions (Figure 2B). These pigment-protein bands were eluted from the gel matrix and characterized.

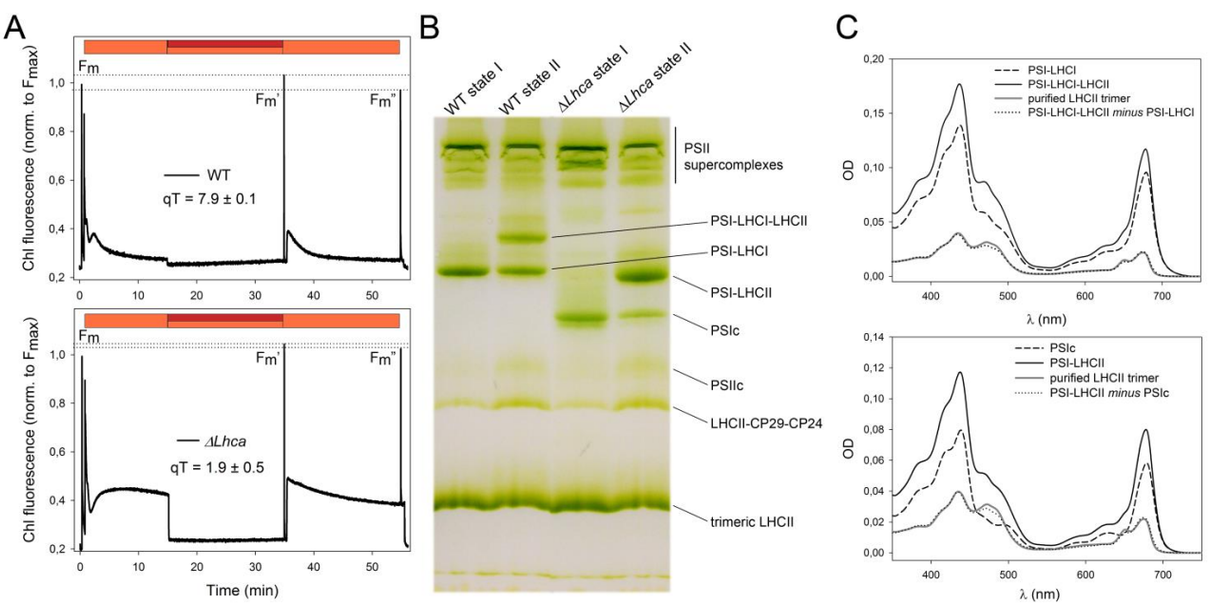

Figure 2. Measurement of state I - state II transitions and identification of the PSI-LHCI-LHCII complex. (A) Dark-adapted wild type (upper panel) and mutant (lower panel) leaves were illuminated with orange light (50 µmol photons m^{-2} s^{-1}, Lee Filters 105 Orange, see methods) for 15 min to reach state II, then a far-red light (PAM lamp FR-105) was superimposed on the orange one to induce a transition to state I. Values of Fm, Fm' and Fm" were determined using light saturation pulses. Amplitudes of state transitions (parameter qT) were determined as reported in Methods. (B) CN-PAGE of thylakoid proteins isolated from wild type and *ΔLhca* plants acclimated either to PSI or PSII light for 45 min before membrane isolation. A PSI-LHCI-LHCII supercomplex is only visible in wild type leaves treated with PSII light, whereas in the corresponding mutant sample a complex with higher apparent mass than that of the PSI core represents the PSI-LHCII supercomplex. These complexes are absent in the leaves treated with PSI light. (C) Absorption spectra of PSI-LHCI and PSI-LHCI-LHCII purified from wild type plants (upper panel), and of the PSI core and PSI-LHCII purified from *ΔLhca* ones (lower panel), normalized to the same molar concentration. For each genotype, the difference spectrum is compared with the spectrum of a purified trimeric LHCII. PSIc/PSIIc, PSI/PSII core complex.

Absorption spectra (Figure 2C) were normalized based on their molar concentration and Chl to protein stoichiometry (Liu et al., 2004;Qin et al., 2015) and the difference spectra were calculated, namely (PSI-LHCI-LHCII *minus* PSI-LHCI) from wild type samples and (PSI-LHCII *minus* PSI core) from *ΔLhca.* In both cases a typical trimeric LHCII spectrum was obtained while the amplitude was consistent with a single LHCII trimer per PSI. To determine whether the interaction mode between PSI and LHCII was the same in the presence or absence of LHCI, the LHCII-containing complexes were subjected to chemical cross-linking with DTSP and analyzed by diagonal electrophoresis (see methods). The final 2D map was probed with anti-PsaH, a subunit involved in the association of the mobile pool of LHCII to PSI (Zhang and Scheller 2004;Crepin and Caffarri S 2015) and with anti-P-Lhcb2 (phosphorylated-Lhcb2). The pattern of cross-linked products was essentially the same for both samples (Supplemental Figure S2), suggesting the site of LHCII interaction with PSI was the same in both supercomplexes.

Distribution of LHCII among thylakoid domains upon state I – state II transitions

Both biochemical and functional analysis indicated a stronger increase in PSI antenna size in *ΔLhca vs.* wild type , inconsistent with the RT Chl fluorescence analysis (Figure 2A). In order to elucidate the origin of this discrepancy, we proceeded to the characterization of thylakoid lateral heterogeneity in the two genotypes. EM analysis showed wild type thylakoids had the typical organization with grana stacks interconnected by stroma membranes, while the mutant plants had fewer granal partitions but with larger diameter, as determined by the number of thylakoids per granum, the distribution of partition sections and the length of stromatic lamellae (Figure 3, Table I).

	WT	***ΔLhca***
Grana per chloroplast[a]	31.3 ± 1.4	38.4 ± 6.1*
Stacks per granum[b]	6.9 ± 2.4	4.9 ± 1.9*
Diameter of grana (μm)[b]	0.50 ± 0.08	0.76 ± 0.20*
Length of stromatic lamellae (μm)[b]	0.35 ± 0.12	0.69 ± 0.22*

Table I. Statistical analysis of differences in chloroplast ultrastructure in wild type and mutant. Data are expressed as means ± SD ([a]n = 10 or [b]n > 40). Values that are significantly different (Student's *t* test, P < 0.05) from the wild type are marked with an asterisk (*).

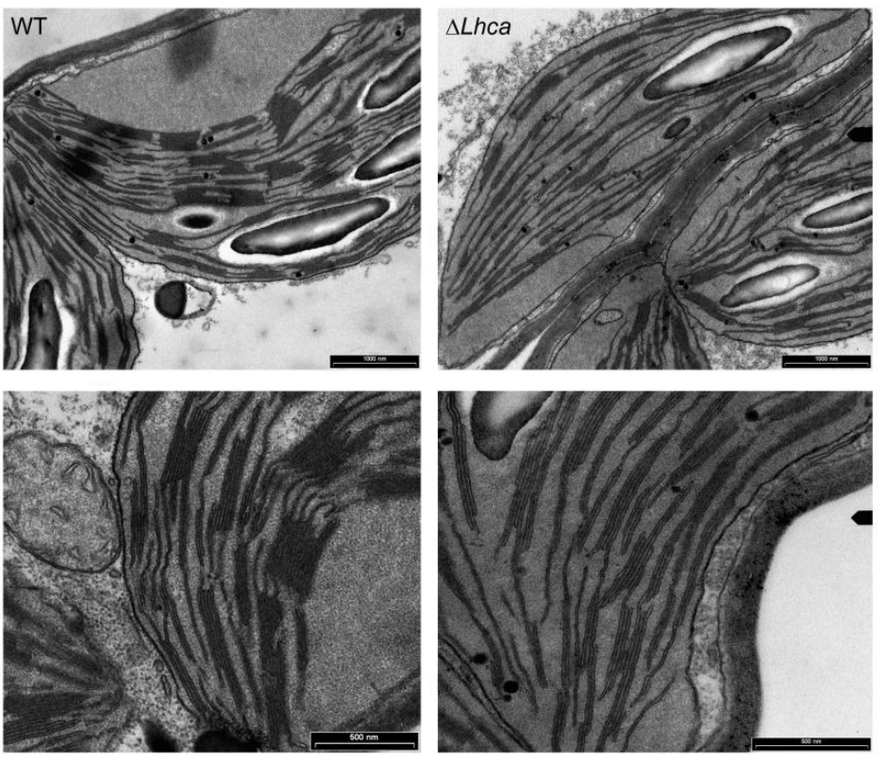

Figure 3. Transmission electron micrographs of plastids from mesophyll cells of the wild type and *ΔLhca*. Plants grown in short-day conditions were dark-adapted for 6 hours before harvesting leaf samples.

Fractionation of the membranes in grana, margin and stroma preparations by treatment with digitonin (Barbato et al., 2000), and quantification of Chl distribution between the different domains, led to results consistent with EM analysis: yield of grana-enriched membrane was significantly lower in mutant plants (-20%), while yield of stromatic fractions was 31% higher in *ΔLhca vs.* wild type (Table II).

	Mol Chl (%)		
	grana	margins	stromal fractions
WT	47 ± 4	24 ± 3	29 ± 4
ΔLhca	38 ± 3	24 ± 2	38 ± 3

Table II. Chl distribution between different thylakoid domains in wild type and *ΔLhca*. Upon treatment with digitonin and differential centrifugation, we quantified the distribution of Chl into different domains as a measure of the yield. Values are reported as mean of 2 independent preparations. Values that are significantly different (Student's *t* test, $P < 0.05$, $n = 4$) from that of the corresponding wild type samples, are marked with an asterisk (*).

To gain additional insights on the effect of ST on the quenching capacity of LHCII by PSI, we then proceeded to evaluate changes in fluorescence separately from the different domains, measured at RT (Figure 4, upper panels). In both wild type and *ΔLhca*, grana showed the highest fluorescence yield, followed by margins and, much lower, by stroma lamellae.

This suggests that the contribution of stroma membranes to the overall fluorescence yield of thylakoids is indeed limited, consistent with PSII in grana fractions being the major source of fluorescence at RT. Transition to state II decreased fluorescence yield of both grana and margins in wild type, consistent with the loss of LHCII caused by migration of LHCII towards the stromal regions in state II and efficient quenching in these domains; while, emission of stroma membranes was less affected by ST (Figure 4A). In contrast, fluorescence yield of all thylakoid domains from *ΔLhca* was far less affected by state II induction (Figure 4B).

Re-distribution of LHCII in the different domains is likely the major determinant in such fluorescence changes; thus we quantified the lateral distribution of the major antenna upon ST, by SDS-PAGE (Supplemental Figure S3). In wild type, as a consequence of state II induction, a decrease in the LHCII was observed in grana membranes (-25.1% of total LHCII), while a fraction of LHCII migrated to margin (11.2%) and stroma-exposed regions (13.9%) (Figure 4C).

Such a migration of LHCII is consistent with the observed decrease in fluorescence yield of grana domain and with an effective quenching of LHCII fluorescence in both margin and stroma-exposed domains (Figure 4A).

LHCII was more abundant in the stroma membranes of the mutant (14.8% of total LHCII) *vs*. wild type (8.6%) already in state I, and further increased upon ST (Figure 4D).

However, such an increase was smaller than in wild type membranes: a lower fraction of LHCII (12.2% of total LHCII in *ΔLhca vs*.14.0% in wild type) migrated to stroma domains from grana partitions, while LHCII content of margins was unaffected.

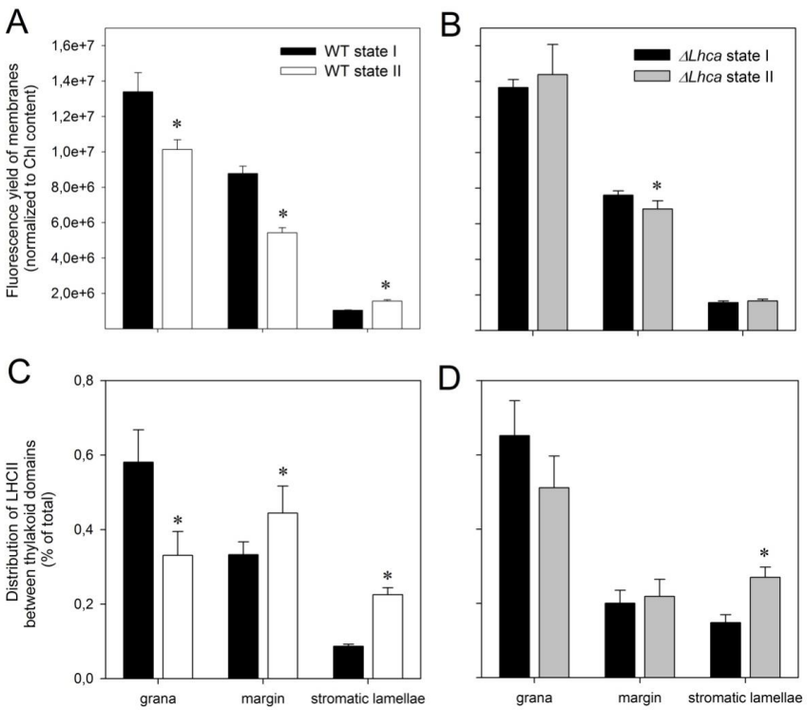

Figure 4. Effect of altered lateral heterogeneity on RT fluorescence analysis of state transitions. Grana, margins and stromatic lamellae were isolated with digitonin solubilization of thylakoids either in state I or state II, analyzed by SDS-PAGE (see Supplemental figure S3), then their fluorescence emission yield determined (*upper panels*). Spectra were recorded at RT, λexc = 475 nm, λems = 680 nm. Samples were diluted to the same Chl concentration (0.2 µg/ml). GFP (1 µM) was added to the membranes suspension as an internal standard. Each measure is the average of 4 records. Quantitative analysis of LHCII distribution between thylakoid fractions were carried out by SDS-PAGE and comassie staining analysis (*lower panels*). Results are representative of two independent procedures of thylakoids isolation and solubilization. Significantly different values, within the same domain, are marked with an asterisk (Student's *t* test, $P < 0.05$).

It is worth noting that the increase in LHCII content in stromal lamellae affected only slightly the fluorescence yield of this fraction in both genotypes (Figure 4A, B), thus implying a quenching of LHCII by PSI. This was verified by measuring the increase in fluorescence yield of purified stroma membranes upon addition of the mild detergent α-DM at 0.05% (Supplemental Figure S4). The fluorescence yield of PSI-LHCII complexes was low, owing to quenching by P700, while α-DM yielded into dissociation of LHCII from PSI and enhanced fluorescence level (Bassi et al., 1988;Galka et al., 2012). Once normalized to the respective emission upon DM solubilization, the unsolubilized stroma membranes from either wild type or *ΔLhca* were less fluorescent in state II *vs.* state I, suggesting phosphorylation was necessary for fully efficient LHCII quenching by PSI

Discussion

In *ΔLhca* plants, the knocking out of three of the four *Lhca* genes, encoding LHCI subunits, caused the deletion of the entire PSI peripheral antenna system. Lack of LHCI could not be compensated by binding other LHC gene products within Lhca binding sites (Bressan et al., 2016). These results confirm that PSI-LHCI is a stable system (Klimmek et al., 2005;Ballottari et al., 2007), lacking the plasticity in the composition of outer antenna typical of PSII (Ruban et al., 2003). We thus analyzed the effect of LHCI depletion on the plant ability to respond to light conditions which preferentially stimulate one or the other of the PSs. In *ΔLhca* plants, the reduced absorption cross-section of PSI affected its capacity for maintaining redox balance. A compensatory mechanism increases the levels of PSI-LHCII$_{n=1}$ supercomplexes (digitonin-insensitive) with respect to the wild type (Figures 2). Nevertheless, a single LHCII trimer (42 Chls) cannot fully compensate for the missing LHCI (57 Chls) (Liu et al., 2004;Qin et al., 2015;Bressan et al., 2016). Therefore, despite greatly enhancing the formation of PSI-LHCII supercomplexes, the mutant cannot entirely restore a normal growth rate in limiting light.

Contrasting biochemical vs. fluorescence ST phenotype

The *ΔLhca* mutant exhibited an intriguing ST phenotype. Its PQ pool was more reduced than in the wild type and the capacity for ST in terms of formation of PSI-LHCII$_{n=1}$ supercomplexes was strongly enhanced, as consistently shown by biochemical measurements (Figures 2, 3). However, F_m changes upon switching off far red light (Figure 2A) suggest a reduced capacity for LHCII fluorescence quenching by PSI in the mutant. Since a recent report (Bressan et al., 2016) showed that excitation transfer efficiency to PSI from LHCII in the absence of LHCI was slightly increased, rather than impaired, implying LHCII is a good antenna for the PSI complex irrespective of being endowed with LHCI or not, the biochemical phenotype appeared to be in contrast with the RT fluorescence phenotype. To understand the reasons for discrepancy, we considered the possibility that the lack of LHCI could affect the lateral heterogeneity of thylakoids membranes. Indeed an altered distribution of LHCII, namely the thylakoid pigment-protein complex with the highest fluorescence yield (Engelmann et al., 2005), between grana and stromal lamellae respect to the wild type, could well affect the

overall fluorescence yield of thylakoids. The mutant had (i) a higher ratio of stroma membranes to grana stacks, and (ii) grana membranes with fewer partitions than the wild type (Figure 4, Table I). Upon fractionation of thylakoids into grana, margins and stromal lamellae, we found that transition to state II in wild type led to a significant decrease in fluorescence yield of both grana and margins per unit of Chl, while stromal lamellae maintained a low fluorescence yield which, moreover, was only slightly affected by ST (Figure 4A). Decreased fluorescence yield correlated with a migration of P-LHCII towards margins and stromal lamellae (Figure 4C), where it was efficiently quenched by PSI (Supplemental Figure S4)(Galka et al., 2012). This evidence suggests that the reduced ST phenotype in wild type (Figure 2A) was not due to events occurring in stroma membranes but rather in grana and margin domains. It is relevant to discuss for both genotypes the relation between LHCII content and fluorescence yield in thylakoid domains, whose composition and the changes induced by state I – state II transition can be measured by SDS-PAGE analysis (Liu et al., 2004;Qin et al., 2015) and quantification of Chl distribution between thylakoid domains (Supplemental Figure S3, Table II). In wild type stroma membranes, the stoichiometry of trimeric LHCII per PSI core increased from 0.81 ± 0.07 in state I to 1.85 ± 0.15 in state II. In the mutant, stromal lamellae contained more LHCII already in state I (1.65 ± 0.08 trimers/PSI), raising to 3.22 ± 0.45 in state II. This LHCII pool was efficiently quenched by PSI (Supplemental Figure S4). Clearly, phosphorylation was needed for optimal quenching of LHCII fluorescence by PSI since the stroma lamellae from *ΔLhca* in state I and state II exhibited similar fluorescence yield despite the lower LHCII content in the former case (Supplemental Figure S4, Figure 4B). LHCII content of margins in state I was higher in wild type (35% of total LHCII localizes in this domain) respect to the mutant (20% of total LHCII in margins); moreover, LHCII content of margins (i) increased upon ST, and (ii) was efficiently quenched as showed by the lower fluorescence yield of margins in state II respect to state I. This results is consistent with previous reports (Tikkanen et al., 2008;Benson et al., 2015) showing that PSI cross section upon ST increases preferentially in margins. In *ΔLhca*, instead, ST did not affect neither LHCII content nor fluorescence yield of margins, suggesting an impairment in both LHCII migration out of grana partitions and LHCII quenching mechanisms active in the margins of wild type plants.

It can thus be concluded that the overall decrease in F_m exhibited by wild type upon ST correlates with an increased LHCII content in margin and stromal domains, and decreased LHCII/PSII ratio in grana. This is due to the shorter lifetime of PSII core respect to LHCII (Engelmann et al., 2005). LHCII

migration out of grana partitions did occur to a reduced extent in the case of *ΔLhca,* despite the increase in LHCB2 phosphorylation (Supplemental Figure S1), thus minimizing the F_m decrease upon transition to state II (Figure 2A).

LHCII migration between thylakoid domains is impaired in ΔLhca

It is relevant to discuss the reason for the decreased efficiency of LHCII migration out of grana partitions in *ΔLhca*. One possibility is that the increased grana size and the larger surface of stroma lamellae in mutant *vs.* wild type (Figure 3) might limit the interface between these domains. Also, the higher reduction state of PQ might cause an enrichment of Lhcb2 in stoma membranes and deprivation from grana domains. During state II-inducing treatment, Lhcb2 would be more exposed to STN7 activity, also located in stroma (Pesaresi et al., 2011;Betterle et al., 2015) yielding into high phosphorylation but reduced migration. In addition, the LHCII population of stroma membranes of the mutant (Figure 4), might have a lower fluorescence yield due to its aggregation state (Dall'Osto et al., 2014;Unlu et al., 2014;Tian et al., 2015) thus undergoing a reduced level of quenching when binding to PSI.

Alternatively, lack of LHCI could impair LHCII association to PSI. A number of studies indicate that multiple LHCIIs can bind to PSI in plants (Benson et al., 2015;Bell et al., 2015;Yadav et al., 2017), and (Bos et al., 2017) recently demonstrated these LHCIIs increased the absorption cross section of PSI in spinach. A fraction of the LHCIIs in state II stroma membranes dissociates in the presence of digitonin, while all of the LHCIIs are detached by α-DM. The digitonin-insensitive fraction of trimers bound to PSI is attached near the PsaH subunit (Lunde et al., 2000;Galka et al., 2012). Instead, the fraction which dissociates in the presence of digitonin likely represent the LHCIIs that are coupled to the LHCI side of the PSI-$LHCII_{n>1}$ complex. This is consistent with report by (Benson et al., 2015), showing that a subpopulation of PSI and LHCII energetically interacts through LHCI in margins, and with identification by EM of PSI-$LHCII_2$ particles, with one LHCII at the PsaH side and a second one close to Lhca2 (Yadav et al., 2017).

Moreover, based on antenna size measurements (Benson et al., 2015), it has been proposed that all PSI in the margins are associated with at least one LHCII trimer in wild type state II thylakoids, while deeper in the stromatic domains only a fraction of PSI coordinates LHCII complexes.

In *ΔLhca* plants, the reduced absorption cross-section of PSI might be exacerbated by the impaired formation of PSI-LHCII$_{n>1}$ supercomplexes, thus up-regulating a compensatory mechanism which increases the levels of PSI-LHCII$_{n=1}$ supercomplexes (digitonin-insensitive) in stromatic lamellae with respect to the wild type (Figure 2).

In *A. thaliana,* both LHCII-S and LHCII-M trimers are thought not to be involved in ST (Galka et al., 2012;Bos et al., 2017) while the mobile antenna involves the so-called "extra LHCIIs". The model of state transitions predicts that LHCII phosphorylation triggers its dissociation from PSII and its migration to PSI. However, in mutants devoid of either PSI (Delosme et al., 1996) or PsaH-binding site for LHCII (Lunde et al., 2000), docking is impaired and P-LHCII is retained in the grana, thus suggesting a "molecular recognition" mechanism is active in determining LHCII re-distribution upon ST (Allen and Forsberg 2001;Wientjes et al., 2013). Thus, the decreased efficiency of LHCII migration out of grana partitions in *ΔLhca* might be explained by the lack of LHCI, namely lack of digitonin-sensitive binding site for LHCII to PSI. In wild type, existence of these sites yields into effective quenching of extra LHCII in both margins and stroma lamellae, while only LHCII bound to the PsaH side is efficiently quenched in the mutant. Even though mutant up-regulates formation of PSI-LHCII$_{n=1}$ supercomplexes, this effect is insufficient to match the level of F_m" quenching obtained with wild type plants.

Overall, these results suggest that existence of LHCI binding site is instrumental in promoting P-LHCII migration to PSI. Moreover, it comes that caution should be applied to RT Chl fluorescence analysis of ST (Jensen et al., 2000) when thylakoid architecture is significantly modified by mutation or when comparing species with different distribution of LHCII between thylakoid domains (Pinnola et al., 2015).

Literature cited

Allen JF (1992) Protein phosphorylation in regulation of photosynthesis. Biochim Biophys Acta **1098**: 275-335

Allen JF, Forsberg J (2001) Molecular recognition in thylakoid structure and function. Trends Plant Sci **6**: 317-326

Amunts A, Toporik H, Borovikova A, Nelson N (2010) Structure determination and improved model of plant Photosystem I. J Biol Chem **285**: 3478-3486

Anderson JM (1986) Photoregulation of the composition, function and structure of thylakoid membranes. Ann Rev Plant Physiol **37**: 93-136

Ballottari M, Dall'Osto L, Morosinotto T, Bassi R (2007) Contrasting behavior of higher plant photosystem I and II antenna systems during acclimation. Journal of Biological Chemistry **282**: 8947-8958

Ballottari M, Govoni C, Caffarri S, Morosinotto T (2004) Stoichiometry of LHCI antenna polypeptides and characterisation of gap and linker pigments in higher plants Photosystem I. Eur J Biochem **271**: 4659-4665

Barbato R, Bergo E, Szabo I, Dalla Vecchia F, Giacometti GM (2000) Ultraviolet B exposure of whole leaves of barley affects structure and functional organization of photosystem II. J Biol Chem **275**: 10976-10982

Bassi R, Rigoni F, Barbato R, Giacometti GM (1988) Light-harvesting chlorophyll a/b proteins (LHCII) populations in phosphorylated membranes. Biochim Biophys Acta **936**: 29-38

Bell AJ, Frankel LK, Bricker TM (2015) High yield non-detergent isolation of Photosystem I-Light harvesting chlorophyll II membranes from spinach thylakoids. Implications for the organization of the PS I antennae in higher plants. J Biol Chem **290**: 18429-18437

Bellafiore S, Barneche F, Peltier G, Rochaix JD (2005) State transitions and light adaptation require chloroplast thylakoid protein kinase STN7. Nature **433**: 892-895

Benson SL, Maheswaran P, Ware MA, Hunter CN, Horton P, Jansson S, Ruban AV, Johnson MP (2015) An intact light harvesting complex I antenna system is required for complete state transitions in Arabidopsis. Nature plants **1**: 15176

Betterle N, Ballottari M., Baginsky S, Bassi R (2015) High light-dependent phosphorylation of photosystem II inner antenna CP29 in monocots is STN7 independent and enhances nonphotochemical quenching. Plant Physiol **167**: 457-471

Bos I, Bland KM, Tian L, Croce R, Frankel LK, Van Amerongen H, Bricker TM, Wientjes E (2017) Multiple LHCII antennae can transfer energy efficiently to a single Photosystem I. Biochim Biophys Acta **2017 Feb 22**:

Bressan M, Dall'Osto L, Bargigia I, Alcocer MJP, Viola D, Cerullo G, D'Andrea C, Bassi R, Ballottari M. (2016) LHCII can substitute for LHCI as an antenna for Photosystem I but with reduced light harvesting capacity. Nature plants **2**: 16131

Casazza AP, Tarantino D, Soave C (2001) Preparation and functional characterization of thylakoids from Arabidopsis thaliana. Photosynth Res **68**: 175-180

Cazzaniga S, Bressan M, Carbonera D, Agostini A, Dall'Osto L (2016) Differential Roles of Carotenes and Xanthophylls in Photosystem I Photoprotection. Biochemistry **55**: 3636-3649

Crepin A, Caffarri S (2015) The specific localizations of phosphorylated Lhcb1 and Lhcb2 isoforms reveal the role of Lhcb2 in the formation of the PSI-LHCII supercomplex in Arabidopsis during state transitions. Biochimica et Biophysica Acta **1847**: 1539-1548

Dall'Osto L, Bressan M, Bassi R (2015) Biogenesis of light harvesting proteins. Biochimica Biophysica Acta **1847**: 861-871

Dall'Osto L, Unlu C, Cazzaniga S, Van Amerongen H (2014) Disturbed excitation energy transfer in Arabidopsis thaliana mutants lacking minor antenna complexes of photosystem II. Biochimica Biophysica Acta **1837**: 1981-1988

de Bianchi S, Dall'Osto L, Tognon G, Morosinotto T, Bassi R (2008) Minor antenna proteins CP24 and CP26 affect the interactions between photosystem II subunits and the electron transport rate in grana membranes of Arabidopsis. Plant Cell **20**: 1012-1028

Delosme R, Olive J, Wollman F-A (1996) Changes in light energy distribution upon state transitions: An *in vivo* photoacoustic study of the wild type and photosynthesis mutants from *Chlamydomonas reinhardtii*. Biochim Biophys Acta **1273**: 150-158

Engelmann E, Zucchelli G, Garlaschi FM, Casazza AP, Jennings RC (2005) The effect of outer antenna complexes on the photochemical trapping rate in barley thylakoid Photosystem II. Biochimica Biophysica Acta **1706**: 276-286

Galka P, Santabarbara S, Khuong TTH, Degand H, Morsomme P, Jennings RC, Boekema EJ, Caffarri S (2012) Functional analyses of the plant Photosystem I–Light-harvesting complex II supercomplex reveal that Light-harvesting complex II loosely bound to Photosystem II is a very efficient antenna for Photosystem I in state II. Plant Cell **24**: 2963-2978

Ganeteg U, Kulheim C, Andersson J, Jansson S (2004) Is each light-harvesting complex protein important for plant fitness? Plant Physiol **134**: 502-509

Gilmore AM, Yamamoto HY (1991) Zeaxanthin formation and energy-dependent fluorescence quenching in pea chloroplasts under artificially mediated linear and cyclic electron transport. Plant Physiol **96**: 635-643

Horton P, Ruban AV, Walters RG (1996) Regulation of light harvesting in green plants. Annu Rev Plant Physiol Plant Mol Biol **47**: 655-684

Jansson S (1999) A guide to the Lhc genes and their relatives in Arabidopsis. Trends Plant Sci **4**: 236-240

Jansson S, Andersen B, Scheller HV (1996) Nearest-neighbor analysis of higher-plant photosystem I holocomplex. Plant Physiol **112**: 409-420

Jarvi S, Suorsa M, Paakkarinen V, Aro E-M (2011) Optimized native gel systems for separation of thylakoid protein complexes: novel super- and mega-complexes. Biochem J **439**: 207-214

Jensen PE, Gilpin M, Knoetzel J, Scheller HV (2000) The PSI-K subunit of photosystem I is involved in the interaction between light-harvesting complex I and the photosystem I reaction center core. J Biol Chem **275**: 24701-24708

Klimmek F, Ganeteg U, Ihalainen JA, van Roon H, Jensen PE, Scheller HV, Dekker JP, Jansson S (2005) The structure of higher plant LHCI: in vivo characterisation and structural interdependence of the Lhca proteins. Biochemisty **44**: 3065-3073

Laemmli UK (1970) Cleavage of structural proteins during the assembly of the head of bacteriophage T4. Nature **227**: 680-685

Lam E, Ortiz W, Malkin R (1984) Chlorophyll a/b proteins of photosystem I. FEBS Lett **168**: 10-14

Leoni C, Pietrzykowska M, kiss az, Suorsa M, Ceci LR, Aro E-M, Jansson S (2013) Very rapid phosphorylation kinetics suggest a unique role for Lhcb2 during state transitions in Arabidopsis. Plant Journal **76**: 236-246

Liu Z, Yan H, Wang K, Kuang T, Zhang J, Gui L, An X, Chang W (2004) Crystal structure of spinach major light-harvesting complex at 2.72 A resolution. Nature **428**: 287-292

Lunde C, Jensen PE, Haldrup A, Knoetzel J, Scheller HV (2000) The PSI-H subunit of photosystem I is essential for state transitions in plant photosynthesis. Nature **408**: 613-615

Mazor Y, Borovikova A, Nelson N (2015) The structure of plant photosystem I super-complex at 2.8 Å resolution. Elife **4:e07433**:

Nelson N, Ben Shem A (2004) The complex architecture of oxygenic photosynthesis. Nature **5**: 1-12

Pan X, Li M, Wan T, Wang L, Jia C, Hou Z, Zhao X, Zhang J, Chang W (2011) Structural insights into energy regulation of light-harvesting complex CP29 from spinach. Nat Struct Mol Biol **18**: 309-315

Pesaresi P, Hertle A, Pribil M, Kleine T, Wagner R, Strissel H, Ihnatowicz A, Bonardi V, Scharfenberg M, Schneider A, Pfannschmidt T, Leister D (2009) Arabidopsis STN7 Kinase Provides a Link between Short- and Long-Term Photosynthetic Acclimation. Plant Cell **21**: 2402-2423

Pesaresi P, Hertle A, Pribil M, Schneider A, Kleine T, Leister D (2010) Optimizing photosynthesis under fluctuating light. Plant Signaling & Behavior **5**: 21-25

Pesaresi P, Pribil M, Wunder T, Leister D (2011) Dynamics of reversible protein phosphorylation in thylakoids of flowering plants: The roles of STN7, STN8 and TAP38. Biochimica et Biophysica Acta-Bioenergetics **1807**: 887-896

Peter GF, Takeuchi T, Thornber JP (1991) Solubilization and two-dimensional electrophoretic procedures for studying the organization and composition of photosynthetic membrane polypeptides. Methods: A Companion to Methods in Enzymology **3**: 115-124

Pinnola A, Cazzaniga S, Alboresi A, Nevo R, Levin-Zaidman S, Reich Z, Bassi R (2015) Light-Harvesting Complex Stress-Related Proteins Catalyze Excess Energy Dissipation in Both Photosystems of Physcomitrella patens. Plant Cell **27**: 3213-3227

Pribil M, Pesaresi P, Hertle A, Barbato R, Leister D (2010) Role of plastid protein phosphatase TAP38 in LHCII dephosphorylation and thylakoid electron flow. Plos Biology **8**: 1-12

Qin X, Suga M, Kuang T, Shen J-R (2015) Structural basis for energy transfer pathways in the plant PSI-LHCI supercomplex. Science **348**: 989-995

Ruban AV, Johnson MP, Duffy CD (2012) The photoprotective molecular switch in the photosystem II antenna. Biochim Biophys Acta **1817**: 167-181

Ruban AV, Wentworth M, Yakushevska AE, Andersson J, Lee PJ, Keegstra W, Dekker JP, Boekema EJ, Jansson S, Horton P (2003) Plants lacking the main light-harvesting complex retain photosystem II macro-organization. Nature **421**: 648-652

Schägger H, von Jagow G (1987) Tricine-sodium dodecyl sulfate-polyacrylamide gel electrophoresis for the separation of proteins in the range from 1 to 100 kDa. Anal Biochem **166**: 368-379

Tian L, Dinc E, Croce R (2015) LHCII Populations in Different Quenching States Are Present in the Thylakoid Membranes in a Ratio that Depends on the Light Conditions. J Phys Chem Lett **6**: 2339-2344

Tikkanen M, Nurmi M, Suorsa M, Danielsson R, Mamedov F, Styring S, Aro E-M (2008) Phosphorylation-dependent regulation of excitation energy distribution between the two photosystems in higher plants. Biochim Biophys Acta **1777**: 425-432

Unlu C, Drop B, Croce R, Van Amerongen H (2014) State transitions in Chlamydomonas reinhardtii strongly modulate the functional size of photosystem II but not of photosystem I. Proceedings of the National Academy of Sciences of the United States of America **111**: 3460-3465

Wientjes E, Drop B, Kouril R, Boekem EJ, Croce R (2013) During state 1 to state 2 transition in *Arabidopsis thaliana*, the Photosystem II supercomplex gets phosphorylated but does not disassemble. J Biol Chem **288**: 32821-32826

Yadav KN, Semchonok DA, Nosek L, Kouril R, Fucile G, Boekema EJ, Eichacker L (2017) Supercomplexes of plant Photosystem I with cytochrome b6f, Light-harvesting complex II and NDH. Biochim Biophys Acta **1858**: 12-20

Zhang S, Scheller HV (2004) Light-harvesting complex II binds to several small subunits of Photosystem I. Journal of Biological Chemistry **279**: 3180-3187

Supplemental Data

Supplemental Figure S1. LHCII phosphorylation in wild type and *ΔLhca* plants. (A) Immunodetection of Lhcb1 and Lhcb2 phosphorylation. Lanes contain the wild type or the *ΔLhca* leaf extracts isolated from plants illuminated for 45' with either PSII light or PSI light, to induce transition to state II or I, respectively. 1.5, 3 and 4.5 µg Chl were loaded per lane. (B) The abundance of P-Lhcb1/P-Lhcb2 subunits in *ΔLhca* was normalized to α-PsaA signal, and expressed as a percentage of the corresponding content in the wild type. Error bars show mean ± SD, n = 3. Values that are significantly different (Student's *t* test, P < 0.05) from the wild type are marked with an asterisk (*). St I/II, state I/II.

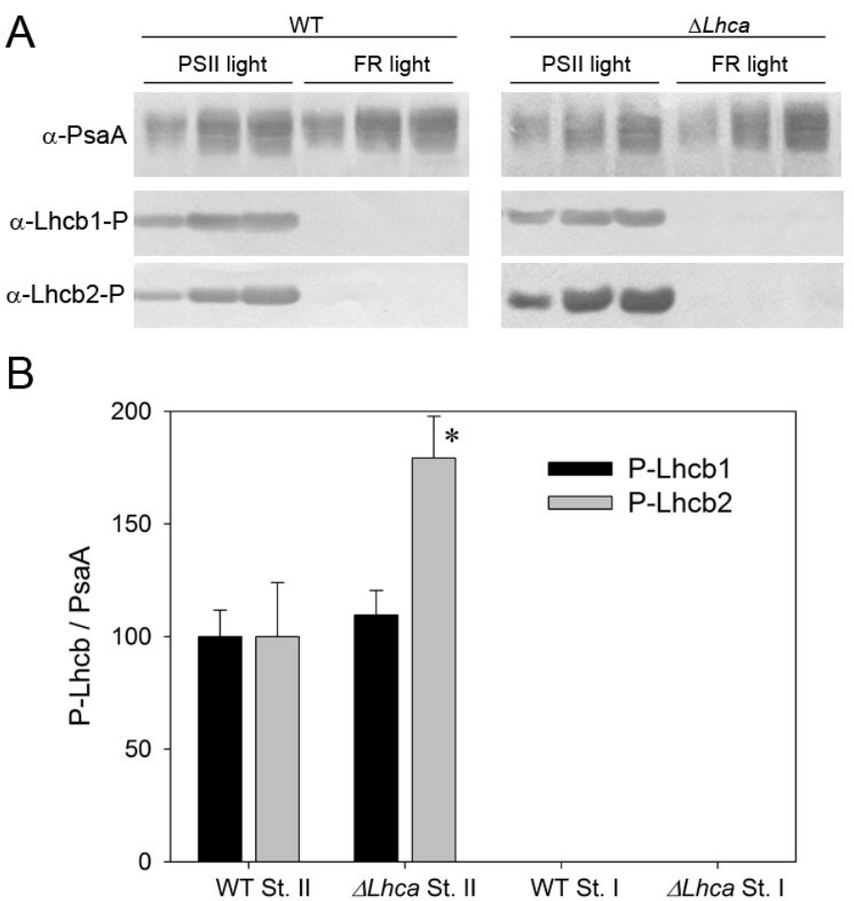

Supplemental Figure S2. Diagonal electrophoresis of PSI-LHCI-LHCII and PSI-LHCII complexes cross-linked with DTSP, immunodetection of PsaH and P-Lhcb2 subunits distribution. The first dimension of the gel was run from left to right, together with a pre-stained molecular weight marker, and the second dimension was run from top to bottom after cleavage of the cross-linker. The cross-linking products containing subunits PsaH (upper panel) and phosphorylated Lhcb2 (P-Lhcb2, lower panel) were identified with specific antibodies. The molecular weight in the first dimension is indicated at the top. Protein spots derived from the different cross-linking products has been labeled with arrows. Products with apparent molecular weight of ~31, 34 and 38 kDa (yellow, rose and white arrows, respectively) were identified in both supercomplexes. See methods for details.

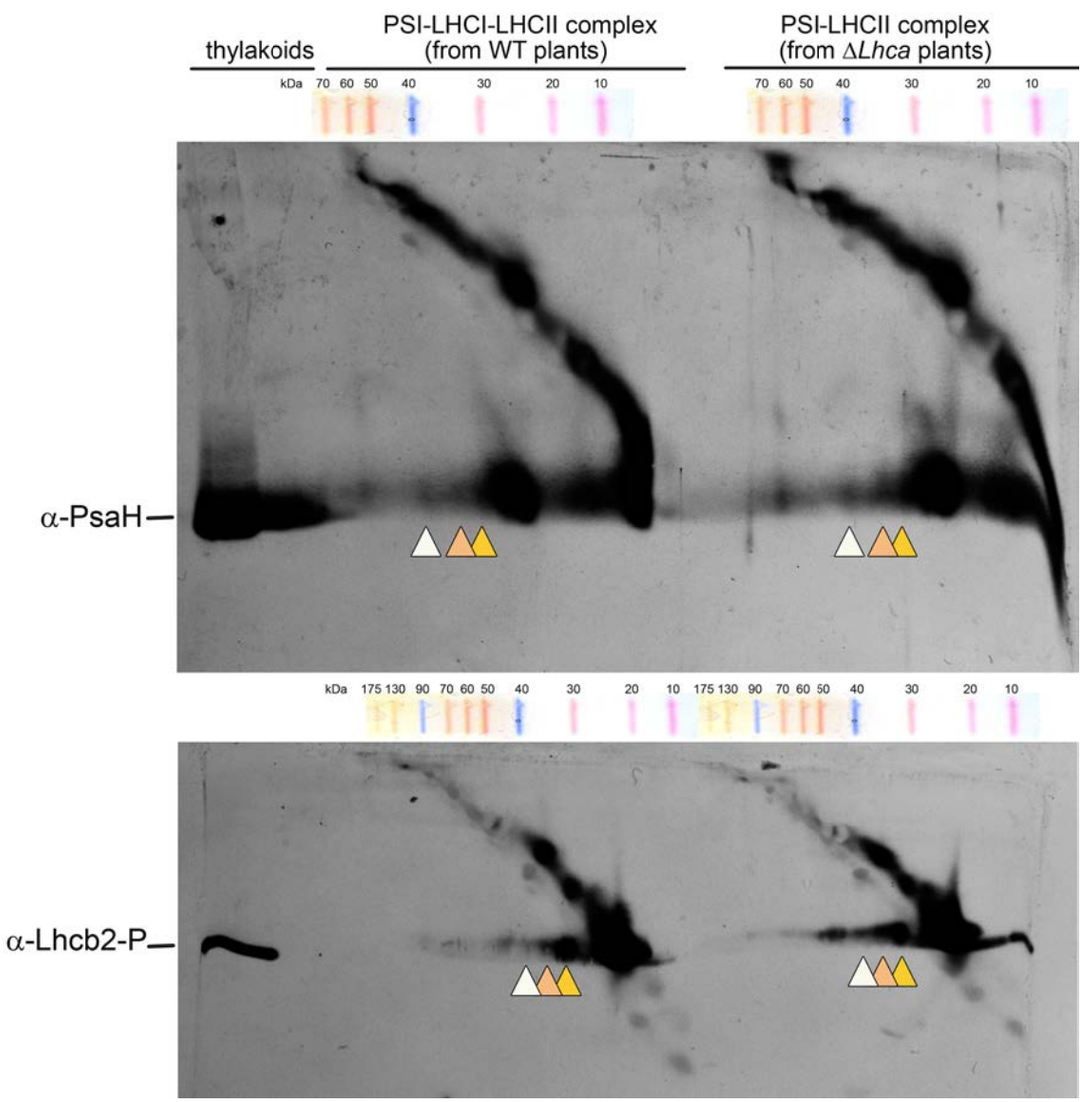

Supplemental Figure S3. Analysis of LHCII distribution into different domains of thylakoids. Thylakoids were isolated from WT and *ΔLhca* plants either grown in PSII or PSI light. Grana, margins and stromatic lamellae were isolated from thylakoids and analyzed by SDS-PAGE and Comassie staining, in order to quantify distribution of the major antenna LHCII among domains upon state I – state II transition. A molecular standard, containing a mix of thylakoid proteins, was loaded to accurately estimate the LHCII content in each preparation.

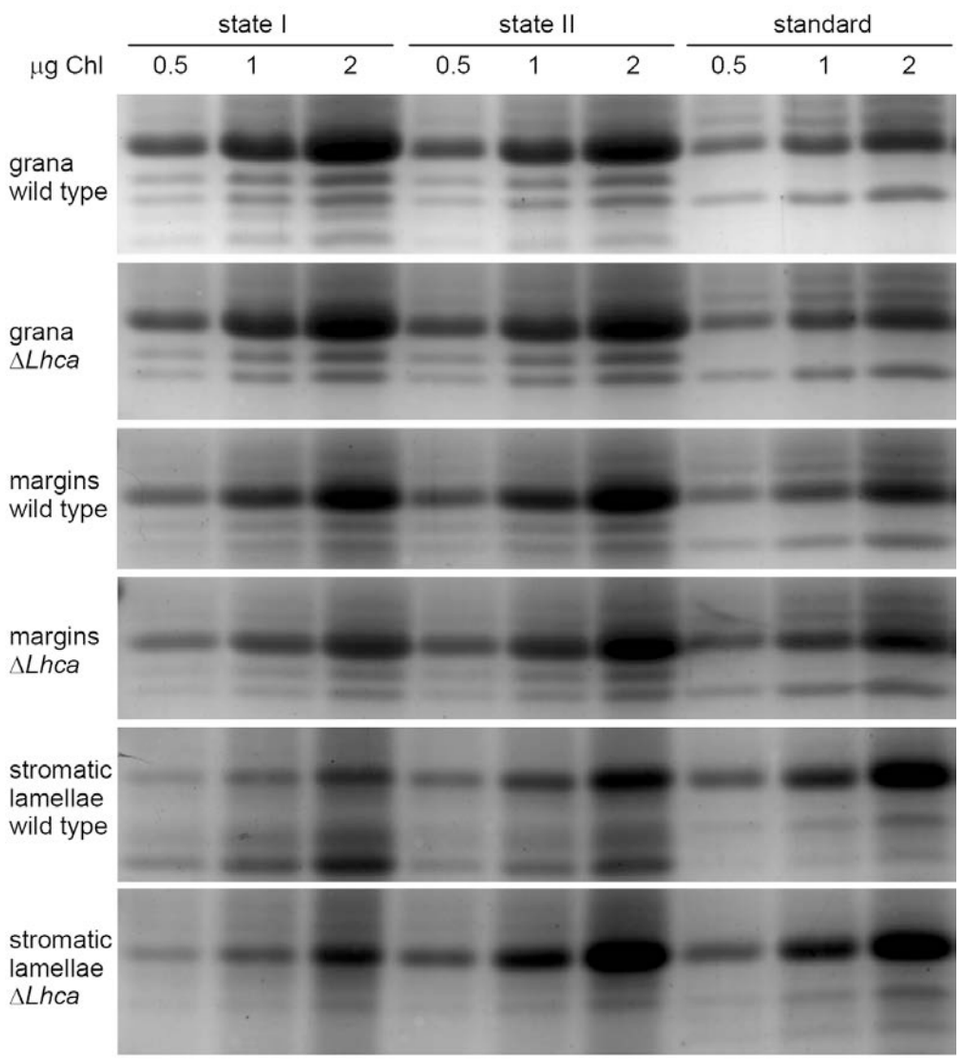

Supplemental Figure S4. Modulation of PSI antenna size in wild type and *ΔLhca*. Stromatic lamellae were isolated from thylakoids, thentheir fluorescence emission yield determined. Spectra were recorded at RT, λexc = 475 nm. Samples were diluted to the same Chl content (0.2 µg/ml), spectra were recorded before and after treatment with 0.05% α-DM, which releases pigment-protein complexes from membranes (Galka et al. 2012). Data are expressed as mean ± SD. Spectra are reported as mean of three independent measurements; each measure is the average of three records.

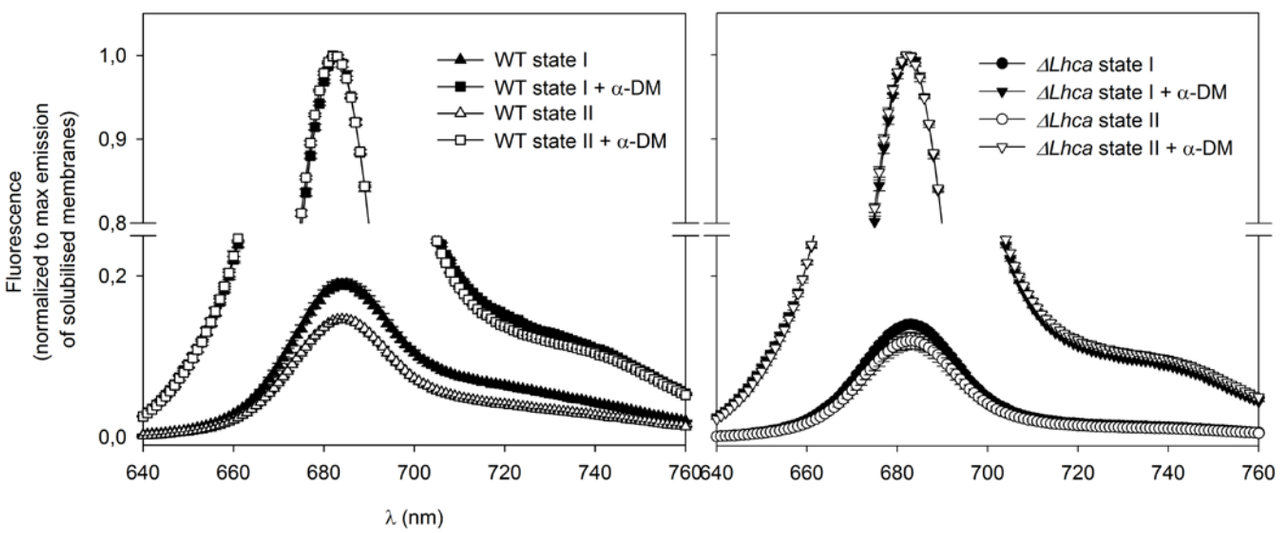

Conclusion

This thesis work was aimed to elucidate the functional role of antenna complexes in higher plants. The chlorophyll a/b-binding complexes (or LHC proteins) belong to a large, highly homologous, protein family. Members of the Lhc family are commonly divided into Lhca or Lhcb depending whether the encoded gene product belongs to PSI or PSII supercomplexes, respectively. In Arabidopsis at least 30 genes encode Lhc proteins, while even higher figures were reported in several crop species.

The main function of these pigment-proteins is light harvesting. However, a regulatory function is also associated with Lhc proteins through their role in state transitions, which balance excitation energy between PSs at moderate irradiances. In excess light conditions, singlet excite states of chlorophyll are thermally dissipated through the process of NPQ (non photochemical quenching), thus limiting ROS release. Accumulation of stress-induced xanthophyll zeaxanthin, and its binding to antenna subunits, has been shown (i) to modulate the yield of potentially dangerous triplet excited state of chlorophyll, and (ii) to induce a high level of quenching in overwintering species. It therefore appears that LHC proteins can be involved in photoprotection mechanisms with lifetime spanning from minutes to months. Although structure and pigment organization are similar among all the members of the LHC family, composition of peripheral antenna systems of both PSs are highly conserved among all higher plants, implying there is strong selective pressure to maintain genes of each protein. A biologist's view of evolution clearly suggests that this genetic redundancy suggests a peculiar role of individual gene products, which has likely been conserved since providing ecological flexibility, that is a precious skill in the highly variable conditions of natural environment. To assess the importance of specific gene products in photosynthesis optimization, we investigated the molecular physiology of abiotic stress response in a set of genetically modified Arabidopsis plants with differing LHC protein contents, by a combined analytical approaches including molecular biology, physiology, biochemistry of membrane proteins and time-resolved spectroscopy.

The features of mutants characterized during this PhD thesis, the major conclusions drawn and other final considerations are listed below.

The NPQ switch: investigation on sites and physical mechanism(s) of the quencher(s). Avoiding photoinhibition in the ever-changing environment is of vital importance for plant: tracking light, maintaining high rates of assimilation and avoiding photoinhibition is clearly beneficial for photosynthesis. This is predicted to affect canopy photosynthesis by up to 30%. NPQ, the major

photoprotective mechanisms of PSII, responds to variations in light intensity, working as a safety valve to reduce the excitation pressure in the photosystem. To identify the site(s) of quenching within the PSII antenna system, the PSBS partners in quenching reactions and the biophysical mechanism(s) by which the quenching reactions are initiated, we constructed and characterize *NoM* mutant, lacking all monomeric LHC proteins while retaining LHCII trimers. PSBS abundance with respect to LHCII and Zea accumulation was similar in *NoM* versus wild type, thus changes in quenching activity are expected to reflect altered efficiency of quenching reactions only. However, lack of monomeric LHC was compensated by over-accumulation (+60%) of the trimeric LHCII antenna in *NoM* plants. Therefore, we cannot completely exclude the possibility that amplitude of NPQ measured in *NoM* could be affected by the higher LHCII content per unit of chlorophylls.

Lack of monomeric antennae delayed substantially the onset of NPQ and changed the xanthophyll-dependence of the residual NPQ activity. In particular, we identified distinct, fast- and slow-activated components contributing to NPQ in wild type, catalyzed respectively by monomeric and trimeric components of the PSII antenna system. In addition, we combined mutations preventing, respectively, Zea and Lut synthesis or PSBS accumulation, on *NoM* genetic background. We further studied the events in the antenna moieties leading to quencher formation on the atomic scale. A carotenoid radical cation signal was detected in wild type chloroplast exposed to high light, while lost in the *NoM*. We conclude that the fastest activated response of NPQ is catalyzed by an independent mechanisms within monomeric LHC proteins, depending on both zeaxanthin and lutein and on a Chl-Zea charge transfer events. The slowly activated quenching component, mediated by trimeric LHCII, does not depend on lutein nor on charge transfer events, while zeaxanthin was essential. 77K fluorescence emission spectroscopy of either high-light-treated or dark-adapted leaves suggest that a process of clustering/aggregation of trimeric LHCII might be associated with the build-up of NPQ in *NoM*.

LHCI, photoprotection and optimization of thylakoid electron flow. A large part of my studies have been devoted to LHCI, chlorophyll-/carotenoid-binding subunits of the PSI outer antenna. Members of these sub-group share similarities in structure and pigment organization with all the members of the LHC family. However, Lhca subunits display peculiar spectroscopic properties, including “red chlorophylls”: since these spectral forms have energy level lower with respect to all other pigments in PSI, 90% of excitation energy is concentrated in these chlorophylls before being transferred to the

reaction centre. It was hypothesized they provide preferential absorption of photons transmitted under a canopy, or catalyze photoprotective reactions by localizing ^{3}Chl* formation and ^{3}Chl*→^{3}Car* quenching reaction far from the reaction center. We first investigated the role of LHCI in the photoprotection of PSI, by focusing on carotenoid-protein interaction.

We compared a panel of Arabidopsis mutants whose biosynthesis of either xanthophylls or carotenes was impaired and analyzed the effect of these depletions on PSI photosensitivity. In particular we studied the szl1 mutant, having both a lower carotene content and an altered xanthophyll composition within LHCI, and npq1, devoid of zeaxanthin. Despite zeaxanthin bound LHCI under excess light, it neither enhanced photoprotection of the supercomplex. On the other hand, szl1 plants displayed a far stronger photoinhibition of PSI than wild type plants and a greater level of ^{3}Chl* originating in the LHCI moiety. We conclude that a crucial mechanism is mediated by carotenes bound to the peripheral antenna system of PSI, which is instrumental in reducing the yield of harmful ^{3}Chl*.

To elucidate the specific function of LHCI, the phenotype of an *Arabidopsis* mutant devoid of the whole LHCI system (*ΔLhca* plants) was studied over a range of conditions, including rapid changes in irradiation. Lack of LHCI could not be compensated by over-accumulation of other LHC gene products, thus showing that PSI-LHCI is a stable system, lacking the dynamic properties of PSII. Capacity of building a trans-thylakoid ΔpH gradient, redox balance of photosynthetic membrane and growth rate were all impaired in the mutant, especially under conditions of rapidly changing light.

When exposed to high light intensity, however, *ΔLhca* plants did not appear to be more sensitive to photooxidative stress than wild type; even, growth rate reduction *vs*. wild type was mitigated under constant light regimes. This represent a striking difference than previous reports on PSII, in which LHC binding is crucial for protecting reaction centre and avoiding photoinhibition. We conclude that PSI photoprotection does not rely on LHCI interaction, indeed P700 activity was fully protected in both wild type and *ΔLhca* plants. Rather completeness of PSI supercomplex, including LHCI, is crucial for balancing PSI *vs.* PSII photosynthetic electron transport under rapidly changing light conditions. It is worth noting that lack of photooxidation of PSI-core under stress condition does not contradict the photoprotection role of pigment-protein interaction within LHCI. Excitation energy transfer and trapping in the PSI core are extremely fast, so that Chl excited states are rapidly quenched both in the presence and absence of LHCI. However, enlargement of PSI cross section by LHCI system can also produce negative effects under increasing light intensity, namely when the photosynthetic reaction

centers become progressively saturated. Thus, differences in the rates of energy absorption and electron transport show that PSI antennas can experience ^{3}Chl* formation and that carotenoid species bound to LHCI play a crucial role in ^{3}Chl* quenching.

The "red absorption forms" of LHCI. From the former results, it emerges that neither is the PSI peripheral antenna necessary *per se* nor does it provide any advantage under sustained over-excitation. Therefore, still open question remains the role of red Chls, a peculiar spectroscopic feature of LCHI system, in the optimization of photosynthetic process. Some hints came from the analysis of compensative mechanisms activated in *ΔLhca* plants. Mutant compensates for decreased antenna size by strongly enhancing LHCII binding to PSI with respect to the wild type, as a strategy aimed at alleviating the imbalance in the excitation energy between PSs. Indeed, by comparing the excitation energy transfer efficiency properties of wild type and mutant PSI-LHCII complexes, we found that LHCII is a very good antenna when bound to PSI core complex, independently on the presence of LHCI. However, particularly under conditions of fluctuating light, the redox unbalance displayed by *ΔLhca* plants reveals that the depletion of LHCI cannot be entirely compensated, despite greatly enhancing the transition to state II. It can be ascribed to the significant reduction in PSI absorption cross-section which comes from the substitution of LHCI with LHCII, the latter being consistent with the different chlorophyll content bound by LHCI (57) and LHCII (42). However, a striking features of the PSI core-bound LHCII is the following: the overall range of wavelengths it absorbs is narrower than that provided by LHCI in wild type plants. LHCII absorbs the same wavelengths when bound to PSI or PSII; therefore, besides lower pigment content, absence of far-red spectral forms further disadvantage light-harvesting capacity of PSI-LHCII, due to the “shading” effect by the abundant PSII-LHCII antenna system. The hypothesis was confirmed by comparing growth of wild type and mutant plants under lamps either enriched or devoid of far-red wavelengths. The highest biomass production was measured in wild type grown under halogen lamps, while fresh weight of *ΔLhca* plants was unaffected by the presence of light enriched in wavelengths above 680 nm. All these results point to a crucial role of the LHCI in optimizing linear electron flow, particularly in limiting light conditions, and in the adaptation of plants to life under ever-changing light conditions, typical of canopies.